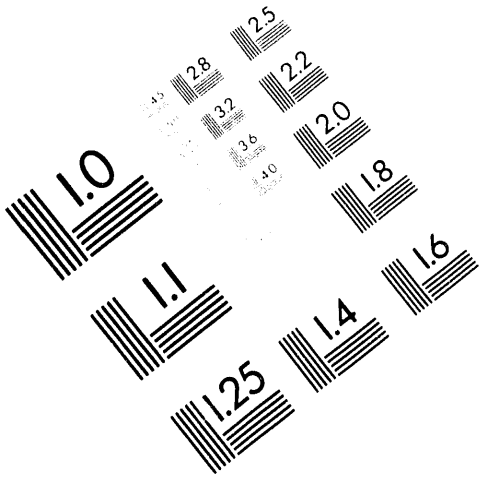

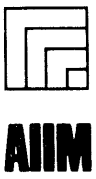

Association for Information and Image Management

1100 Wayne Avenue, Suite 1100
Silver Spring, Maryland 20910

301/587-8202

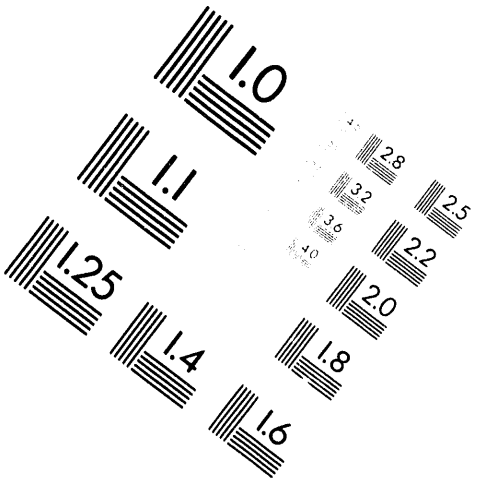

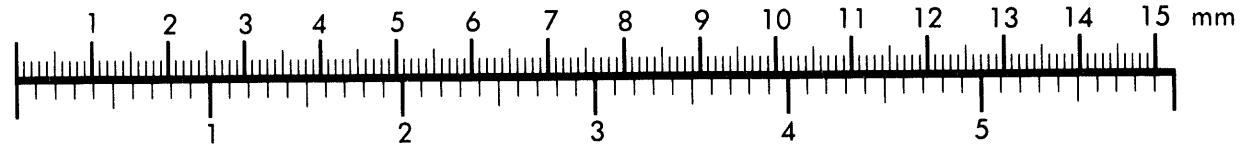

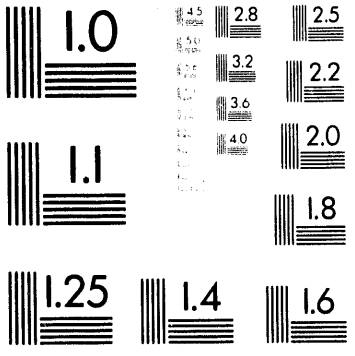

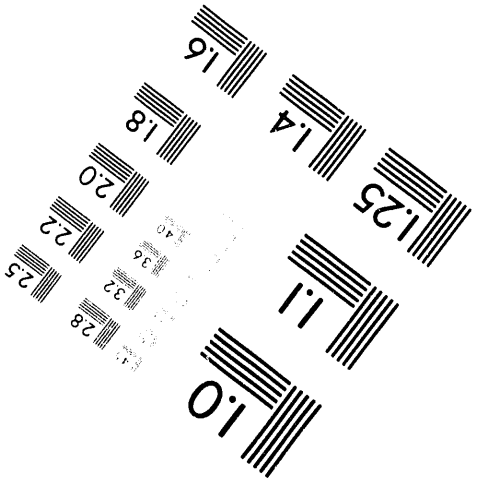

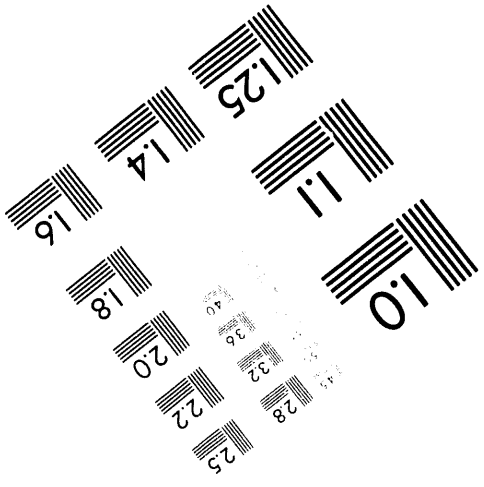

MANUFACTURED TO AIIM STANDARDS
BY APPLIED IMAGE, INC.

1 of 2

DOE/BC/14448--T5

Reservoir Heterogeneity in Carboniferous Sandstone of the Black Warrior Basin

Final Report

By

Ralph L. Kugler

Jack C. Pashin

Richard E. Carroll

G. Daniel Irvin

Henry E. Moore

April 1994

Work Performed Under Contract No. FG22-90BC14448

Prepared for

U.S. Department of Energy

Assistant Secretary for Fossil Energy

Chandra Nautiyal, Project Manager

Bartlesville Project Office

P.O. Box 1398

Bartlesville, OK 74005

Prepared by

Geological Survey of Alabama

420 Hackberry Lane

P.O. Box O

Tuscaloosa, AL 35486-9780

CONTENTS

Page

Executive summary ix
Abstract 1
Introduction 1
Objectives 1
Methods 4
Regional geological framework 10
Structure and tectonics 10
Stratigraphy and sedimentation 12
Chattanooga Shale 12
Maury Shale 15
Fort Payne Chert and Tuscumbia Limestone 15
Pride Mountain Formation and Hartselle Sandstone 17
Lewis cycle 17
Evans and Hartselle cycles 23
Bangor Limestone and Floyd Shale 28
Parkwood Formation 30
Lower Parkwood Formation 30
Middle Parkwood Formation 35
Upper Parkwood Formation 38
Pottsville Formation 41
Summary of depositional history 45
Burial history and source-rock characteristics 46
Thermal maturation 46
Burial history 50
Source-rock geochemistry 52
Oil geochemistry 57
Characterization of heterogeneity in Carter and *Millerella* oil reservoirs 59
Facies heterogeneity in Carter and *Millerella* oil reservoirs 61
Reservoir lithofacies 66
Shale-and-siltstone facies 66
Sandstone facies 66
Variegated facies 69
Reservoir Architecture 69
North Blowhorn Creek oil unit 69
Wayside oil unit 71
South Brush Creek oil unit 71
Blowhorn Creek *Millerella* oil unit 71
Bluff oil field 74
Environmental interpretations 74
Shale-and-siltstone facies: storm-dominated shelf 74
Sandstone facies: shoreface and foreshore 77
Variegated facies: backshore 78
Depositional systems and facies heterogeneity 78
Petrologic characteristics 81
Detrital framework 81
Diagenesis 82
Petrophysical properties 88
Petrographic evidence 88

CONTENTS-CONTINUED

Page

Commercial core analyses 89
High-pressure mercury porosimetry 91
Well-log derived porosity and water saturation 98
Problems in prediction of petrophysical properties in interwell regions 113
Overview of Black Warrior basin oil production 121
Improved-recovery projects in the Black Warrior basin of Alabama 123
Blowhorn Creek *Millerella* oil unit 124
Central and South Fairview Carter Sand oil units 126
Mud Creek *Millerella* oil unit 132
North Blowhorn Creek oil unit 134
South Brush Creek oil unit 148
Wayside oil unit 158
Discussion: heterogeneity in Black Warrior basin oil reservoirs 158
Gigascopic heterogeneity 165
Megascopic heterogeneity 165
Macroscopic heterogeneity 166
Mesoscopic heterogeneity 166
Microscopic heterogeneity 167
Summary and conclusions 167
Acknowledgments 171
References cited 171

ILLUSTRATIONS

Page

Figure 1. Stratigraphic column showing oil reservoirs in the Black Warrior basin of Alabama 2
2. Location and tectonic setting of the Black Warrior basin of Alabama 3
3. Location map of oil fields in the Black Warrior basin of Alabama and Mississippi 5
4. Pie chart showing relative percent of oil production from sandstone reservoir units in the Black Warrior basin of Alabama 6
5. Pie chart showing relative percent oil production from Carter sandstone reservoirs in the Black Warrior basin of Alabama 6
6. Scales of reservoir heterogeneity in the Black Warrior basin 7
7. Structural contour map of the top of the Tuscumbia Limestone 11
8. Measured section of Silurian through basal Chesterian rocks in the Black Warrior basin 13
9. Stratigraphic cross section showing facies relationships from the Chattanooga Shale through the Lewis cycle 14
10. Isopach map of the combined Fort Payne Chert and Tuscumbia Limestone 16
11. Idealized geophysical well log showing stratigraphy of the Pride Mountain Formation and the Hartselle Sandstone 18

ILLUSTRATIONS-CONTINUED

			Page
Figure	12.	Stratigraphic cross section showing facies relationships from the Tuscumbia Limestone through the base of the upper Parkwood Formation	19
	13.	Selected graphic logs of the Lewis cycle in southern Lamar County, Alabama	20
	14.	Isopach map of the Lewis cycle	21
	15.	Net-sandstone isolith map of the Lewis sandstone	22
	16.	Isopach map of the combined Evans and Hartselle cycles	24
	17.	Net-sandstone isolith map of the Hartselle Sandstone	26
	18.	Measured section of the Hartselle Sandstone through the Bangor Limestone	27
	19.	Isopach map of the Bangor Limestone and equivalent strata in the Floyd Shale	29
	20.	Stratigraphic cross section showing facies relationships in the Parkwood Formation	31
	21.	Measured section of the Parkwood Formation	32
	22.	Isopach map of the lower Parkwood Formation	33
	23.	Net-sandstone isolith map of the lower Parkwood Formation	34
	24.	Isopach map of the middle Parkwood Formation	36
	25.	Net-sandstone isolith map of the *Millerella* sandstone	37
	26.	Isopach map of the upper Parkwood Formation	39
	27.	Net-sandstone isolith map of the Gilmer sandstone	40
	28.	Net-sandstone isolith map of the Coats sandstone	41
	29.	Measured section of the Pottsville Formation	42
	30.	Stratigraphic cross section showing facies relationships in the Parkwood and Pottsville formations	43
	31.	Vitrinite reflectance map of the Mary Lee coal group in Alabama, showing the location of wells PN2191 and PN1780	47
	32.	Vitrinite reflectance versus depth profiles	48
	33.	Representative vitrinite reflectance histograms for well PN1780	49
	34.	Burial history curves	51
	35.	Time/temperature index versus time cumulative curves	54
	36.	Plots of hydrogen index versus oxygen index based on Rock-Eval pyrolysis	56
	37.	API gravity distribution of oil from Carter sandstone reservoirs	57
	38.	Plot of API gravity versus depth in Mississippian oils from the Black Warrior basin	58
	39.	Ternary diagram illustrating gross chemical composition of C15+ fraction of crude oils from the Black Warrior basin	59
	40.	Plot of pristane/n-C17 versus heptane for oils from Mississippian reservoirs in the Black Warrior basin and Jurassic and Cretaceous reservoirs in the Gulf Coastal Plain	61
	41.	Index map showing location of wells, oil fields and stratigraphic cross sections in Carter and *Millerella* sandstone, northeastern Lamar and southwestern Fayette Counties, Alabama	63
	42.	Net-sandstone isolith map of the Carter sandstone, northeastern Lamar and southwestern Fayette Counties, Alabama	64
	43.	Net-sandstone isolith map of the *Millerella* sandstone, northeastern Lamar and southwestern Fayette Counties, Alabama	65

ILLUSTRATIONS-CONTINUED

Page

Figure 44. Selected graphic logs of cores of Carter sandstone, North Blowhorn Creek oil unit 67
45. Selected photographs of cores showing characteristics of lithofacies in North Blowhorn Creek oil unit 68
46. Resistivity-log cross sections of the lower Parkwood Formation and associated units, North Blowhorn Creek oil unit 70
47. Resistivity-log cross sections of the lower Parkwood Formation and associated units, Wayside oil unit 72
48. Resistivity-log cross sections of the lower Parkwood Formation and associated units, South Brush Creek oil unit 73
49. Resistivity-log cross sections of the lower Parkwood Formation and associated units, Blowhorn Creek oil unit 75
50. Resistivity-log cross sections of the lower Parkwood Formation and associated units, Bluff oil field 76
51. Depositional model of Carter sandstone showing lateral variation of facies within sandstone lenses and environmental interpretations 77
52. Paleogeographic reconstruction of the North Blowhorn Creek spit system 79
53. Detrital framework composition of Carter sandstone 82
54. Backscattered-electron micrograph showing detrital framework composition of Carter sandstone 83
55. Generalized paragenetic sequence for Carter sandstone in North Blowhorn Creek oil unit 84
56. Ca-Mg-Fe ternary diagram showing composition of authigenic carbonate minerals in Carter sandstone, based on electron microprobe analyses 85
57. Plot of $\delta^{18}O$ versus $\delta^{13}C$ for authigenic carbonate minerals in Carter sandstone in North Blowhorn Creek oil unit 87
58. Influence of clay-mineral distribution on effective porosity 89
59. Plot of porosity versus permeability for all commercial core analyses from North Blowhorn Creek oil unit 90
60. Plot of porosity versus permeability for commercial core analyses from well PN3314, North Blowhorn Creek oil unit 91
61. Plot of permeability and porosity versus depth for well PN3314, North Blowhorn creek oil unit 92
62. Plot of pore-throat radius versus cumulative-intrusion volume and incremental-intrusion volume showing polymodal pore-throat size distribution 93
63. Plot of pore-throat radius versus cumulative intrusion showing typical shapes of cumulative-intrusion curves for Carter sandstone 94
64. Plot of pore-throat radius versus cumulative intrusion as a percent of maximum mercury intrusion volume for all data from well PN3314 95
65. Plots of pore-throat radius versus cumulative-intrusion volume and incremental-intrusion volume for well PN3314 96
66. Plot of differential porosity versus depth for well PN3314 97
67. Comparison of median pore-throat size determined by high-pressure mercury porosimetry with that determined from commercial core analyses by Pittman's method for well PN3150 99

ILLUSTRATIONS-CONTINUED

Page

Figure 68. Comparison of median pore-throat size determined by high-pressure mercury porosimetry with that determined from commercial core analyses by Pittman's method for well PN3160 100
69. Comparison of median pore-throat size determined by high-pressure mercury porosimetry with that determined from commercial core analyses by Pittman's method for well PN3314 101
70. Frequency histogram and cumulative-percent curve of well-log derived effective porosity for Carter sandstone in North Blowhorn Creek oil unit 102
71. Frequency histogram and cumulative-percent curve of core-analysis porosity for Carter sandstone in North Blowhorn Creek oil unit 102
72. Bubble map of mean effective porosity for Carter sandstone, North Blowhorn Creek oil unit 103
73. Bubble map of net pay thickness for Carter sandstone in North Blowhorn Creek oil unit 104
74. Bubble map of pore volume for Carter sandstone in North Blowhorn Creek oil unit 105
75. Bubble map of effective and total water saturation for Carter sandstone, North Blowhorn Creek oil unit 107
76. Bubble map of the product, net pay times effective porosity times oil saturation, for Carter sandstone, North Blowhorn Creek oil unit 108
77. Longitudinal structural cross-section A-A' of effective porosity profiles, Carter sandstone, North Blowhorn Creek oil unit 109
78. Transverse structural cross-section B-B' of effective porosity profiles, Carter sandstone, North Blowhorn Creek oil unit 110
79. Transverse structural cross-section C-C' of effective porosity profiles, Carter sandstone, North Blowhorn Creek oil unit 111
80. Transverse structural cross-section D-D' of effective porosity profiles, Carter sandstone, North Blowhorn Creek oil unit 112
81. Bubble map of coefficient of variation of effective porosity for Carter sandstone, North Blowhorn Creek oil unit 114
82. Zones in Carter sandstone in North Blowhorn Creek oil unit with different reservoir characteristics 115
83. Frequency histogram and cumulative-percent curve of well-log derived effective porosity for *Millerella* sandstone, Blowhorn Creek *Millerella* oil unit 116
84. Frequency histogram and cumulative-percent curve of well-log derived effective porosity for Carter sandstone, Central Fairview Carter sand oil unit 116
85. Frequency histogram and cumulative-percent curve of well-log derived effective porosity for Carter sandstone, South Brush Creek oil unit 117
86. Frequency histogram and cumulative-percent curve of well-log derived effective porosity for Carter sandstone Wayside oil unit 117
87. Plot of effective water saturation versus total water saturation for selected Carter sandstone reservoirs 118
88. Example of a modeled experimental semivariogram for Carter sandstone in North Blowhorn Creek oil unit 119

ILLUSTRATIONS-CONTINUED

Page

Figure 89. Example of an experimental semivariogram for Carter sandstone in North Blowhorn Creek oil unit that could not be modeled 120
90. Bar chart of cumulative oil production for reservoir units in the Black Warrior basin of Alabama, as of July 1992 123
91. Bar chart of cumulative oil production from Carter sandstone fields in the Black Warrior basin of Alabama, as of July 1992 124
92. Bar chart of cumulative oil production from *Millerella* sandstone fields in the Black Warrior basin of Alabama, as of July 1992 125
93. Bar chart of cumulative oil production from Lewis sandstone fields in the Black Warrior basin of Alabama, as of July 1992 126
94. Bar chart showing pre- and post-unitization oil production from unitized fields in the Black Warrior basin of Alabama, as of July 1992 128
95. Production plot for Blowhorn Creek *Millerella* oil unit 130
96. Bubble map of cumulative oil production from Blowhorn Creek *Millerella* oil unit, as of July 1992 131
97. Bubble map of cumulative water production from Blowhorn Creek *Millerella* oil unit, as of July 1992 132
98. Bubble map of net pay thickness for *Millerella* sandstone in Blowhorn Creek *Millerella* oil unit 133
99. Bubble map of effective and total water saturation in *Millerella* sandstone, Blowhorn Creek *Millerella* oil unit 134
100. Bubble map of effective porosity in *Millerella* sandstone, Blowhorn Creek *Millerella* oil unit 135
101. Structural cross-section E-E' of effective porosity profiles, Carter sandstone, Blowhorn Creek *Millerella* oil unit 136
102. Structural cross-section F-F' of effective porosity profiles, Carter sandstone, Blowhorn Creek *Millerella* oil unit 137
103. Production plot for Central Fairview Carter sand oil unit 138
104. Production plot for South Fairview Carter sand oil unit 139
105. Production plot for Mud Creek *Millerella* oil unit 140
106. Production plot for North Blowhorn Creek oil unit 142
107. Bubble map of cumulative oil production from Carter sandstone in North Blowhorn Creek oil unit, as of July 1992 143
108. Bubble map showing cumulative volume of water injected into the Carter sandstone reservoir in North Blowhorn Creek oil unit, as of July 1992 144
109. Bubble map of cumulative water production in North Blowhorn Creek oil unit, as of July 1992 145
110. Bubble map showing water injection radius in North Blowhorn Creek oil unit, as of July 1992 147
111. Production plot for South Brush Creek oil unit 149
112. Bubble map of cumulative oil production in South Brush Creek oil unit, as of July 1992 150
113. Bubble map of cumulative water production in South Brush Creek oil unit, as of July 1992 151
114. Bubble map of net pay thickness in Carter sandstone, South Brush Creek oil unit 152
115. Bubble map of effective porosity in Carter sandstone, South Brush Creek oil unit 153

ILLUSTRATIONS-CONTINUED

Page

Figure 116. Bubble map of effective and total water saturation in Carter sandstone, South Brush Creek oil unit 154
117. Structural cross-section G-G' of effective porosity profiles, Carter sandstone, South Brush Creek oil unit 155
118. Structural cross-section H-H' of effective porosity profiles, Carter sandstone, South Brush Creek oil unit 156
119. Bubble map of cumulative oil production in South Brush Creek oil unit one year after unitization 157
120. Production plot for Wayside oil unit 159
121. Bubble map of cumulative oil production in Wayside oil unit, as of July 1992 160
122. Bubble map of net pay thickness in Carter sandstone, Wayside oil unit 160
123. Bubble map of cumulative water production in Wayside oil unit, as of July 1992 161
124. Bubble map of effective porosity in Carter sandstone, Wayside oil unit 161
125. Structural cross-section I-I' of effective porosity profiles, Carter sandstone, Wayside oil unit 162
126. Structural cross-section J-J' of effective porosity profiles, Carter sandstone, Wayside oil unit 163
127. Bubble map of effective and total water saturation in Carter sandstone, Wayside oil unit 164

TABLES

Page

Table 1. Vitrinite reflectance data for the PN1780 and PN2191 wells 50
2. TTI data for the PN1780 and PN2191 wells 53
3. Rock-Eval pyrolysis for the PN1780 and PN2191 wells 55
4. Gross chemical composition of oils from Mississippian oil fields in the Black Warrior basin 60
5. Pristine/n-C17 and Heptane values for oil from Mississippian, Jurassic, and Cretaceous oil fields 62
6. Stable isotopic composition of carbonate cements in Carter sandstone 86
7. Characteristics of oil fields in the Black Warrior basin of Alabama 122
8. Characteristics of unitized oil fields in the Black Warrior basin of Alabama 127
9. Reservoir fluid properties for selected oil fields in the Black Warrior basin of Alabama 129

EXECUTIVE SUMMARY

Although oil production in the Black Warrior basin of Alabama is declining, additional oil may be produced through improved recovery strategies, such as waterflooding, chemical injection, strategic well placement, and infill drilling. High-quality characterization of reservoirs in the Black Warrior basin is necessary to utilize advanced technology to recover additional oil and to avoid premature abandonment of fields. This report documents controls on the distribution and producibility of oil from heterogeneous Carboniferous reservoirs in the Black Warrior basin of Alabama. This is the final summary report for DOE contract number FG22-90BC14448, entitled "Characterization of Sandstone Heterogeneity in Carboniferous Reservoirs for Increased Recovery of Oil and Gas from Foreland Basins."

The first part of the report summarizes the structural and depositional evolution of the Black Warrior basin and establishes the geochemical characteristics of hydrocarbon source rocks and oil in the basin. This second part characterizes facies heterogeneity and petrologic and petrophysical properties of Carter and *Millerella* sandstone reservoirs. This is followed by a summary of oil production in the Black Warrior basin and an evaluation of seven improved-recovery projects in Alabama. In the final part, controls on the producibility of oil from sandstone reservoirs are discussed in terms of a scale-dependent heterogeneity classification.

The Black Warrior basin is a foreland basin that formed by tectonic loading of the Alabama promontory during late Paleozoic Appalachian-Ouachita orogenesis. The sedimentary sequence in the basin records the tectonic evolution of the Alabama promontory as well as major climatic changes. Hydrocarbon source and reservoir rocks in the basin range in age from Devonian through Pennsylvanian. From Late Devonian through Middle Mississippian time, the Black Warrior basin was part of the passive margin of the Ouachita embayment. During this time, organic-rich Chattanooga Shale, phosphatic and glauconitic Maury Shale, siliceous micrite of the Fort Payne Chert, and skeletal calcarenite of the Tuscumbia Limestone were deposited.

Foreland-basin development began at the start of the Chesterian epoch. As an orogenic forebulge formed, the lowstand wedge of the Lewis cycle was deposited. Deposition of the Lewis was followed by the Evans and Hartselle cycles. These cycles comprise southwest-dipping clinoformal sequences that contain shelf, deltaic, and beach-barrier deposits derived from cratonic sources. The Evans and Hartselle cycles represent the onset of load-related subsidence adjacent to the Ouachita orogen. Deposition of clinoformal parasequences continued after deposition of these cycles, culminating with formation of the prograding Bangor carbonate platform-ramp system. During deposition of the Bangor, starved-basin conditions persisted in the southwestern part of the basin and are represented by the organic-rich Floyd Shale, the major source rock in the basin. The Bangor platform-ramp system significantly influenced localization of the most prolific oil reservoirs in the Black Warrior basin.

As Bangor deposition ended, deep-water deltaic sediment of the lower Parkwood Formation filled the starved basin. This deltaic system ultimately prograded onto the carbonate bank, resulting in deposition of a destructive, shoal water deltaic system, represented by the Carter sandstone. The most productive hydrocarbon reservoirs in the basin are part of this shoal-water delta system, which formed as the receiving basin shallowed along the bank margin. The lower Parkwood Formation records a reversal of the southwest paleoslope that prevailed earlier in basin evolution and thus represents the first succession to enter the basin from sources in the Ouachita orogen.

Marine transgression occurred in middle Parkwood time, following deposition of Carter sandstone, as *Millerella* limestone accumulated in a carbonate platform-ramp system. Deposition of *Millerella* sandstone marked continued destruction of the Carter delta plain. After this phase, the remaining parts of the starved basin filled with deltaic sediment. Subsidence and continued filling of the foreland basin with deltaic sediment continued as the upper Parkwood Formation was deposited. Clinoformal Gilmer sandstone represents highstand progradation of deltaic sediment at the start of upper Parkwood deposition, whereas the aggradational Coats sandstone represents transgressive modification of the deltaic system. The Pottsville Formation unconformably overlies the Parkwood and Bangor Formations and signals the onset of the Alleghanian orogeny. Pottsville deposition was characterized by fluvial and deltaic sedimentation adjacent to the orogenic belts and by mesotidal shelf and beach sedimentation seaward of the fluvial-deltaic systems.

Vitrinite reflectance of the Mary Lee coal group in the lower Pottsville Formation reveals that thermal maturity in the Black Warrior basin increases from northwest to southeast. Vitrinite reflectance values increase from 0.62 percent near the top of the Pottsville Formation to 1.12 percent in the Chattanooga Shale in a well near the margin of the Bangor carbonate platform. Deeper in the basin, to the southwest, vitrinite reflectance values also show an increase with depth, from 0.74 percent in the upper Pottsville Formation to 1.61 percent in Lewis shale. Burial history and time/temperature index modeling indicate that conditions suitable for liquid hydrocarbon generation occurred between 290 and 200 MA. Near the margin of the Bangor carbonate platform, shale beneath the Carter sandstone is within the liquid hydrocarbon window but below peak generation potential. Deeper in the basin, the same units are near the upper limit of liquid hydrocarbon generation.

Results of total organic carbon and Rock-Eval pyrolysis analyses indicate that sufficient quantities of type II kerogen occur in Chattanooga and Floyd shales for these units to serve as oil source rocks. Because of volume considerations and proximity to the most productive Carter and *Millerella* sandstone reservoirs, the Floyd Shale is considered to be the primary source for oil in the basin. API gravity of oil in Carter sandstone increases systematically from northeast to southwest from 22° to 44°, paralleling an increase in depth of burial. Chemical analyses of oil show that most contain a high percent of saturated hydrocarbons relative to aromatic hydrocarbons and asphaltenes, indicating that minimal biodegradation has occurred.

Carter and *Millerella* oil reservoirs present the best opportunity for understanding reservoir heterogeneity in the Black Warrior basin because these units are the most productive in the basin, have the closest well spacing, and have the most available cores. All Carter cores contain the same tripartite sequence of lithofacies, including from bottom to top: (1) shale-and-siltstone facies; (2) sandstone facies; and (3) variegated facies. These facies are interpreted to represent storm-dominated shelf deposits, shoreface and foreshore deposits, and backshore deposits, respectively. Beach deposits of Carter sandstone developed on a muddy strandplain during destruction of the lower Parkwood deltaic system. Although lithofacies vary little among Carter and *Millerella* fields, stratigraphic architecture varies considerably and is a primary source of heterogeneity. This diversity in geometry of beach systems from lobate bodies in the southwest to thin, isolated lenses in the northeast records systematic evolution of the strandplain and exceptional preservation of the paleogeographic framework of the shoal-water delta.

Carter sandstone in North Blowhorn Creek oil unit represents a spit-type beach system, composed of imbricate, clinoformal sandstone lenses that decrease in size and segment toward the southeastern terminus of the reservoir. In contrast to the elongate geometry of the North Blowhorn Creek spit complex, Carter sandstone in Wayside oil unit occurs as a localized, arcuate body that accumulated at the distal edge of the shoal-water delta system. The lobate, coarsening upward Carter sandstone in South Brush Creek oil unit reflects deposition at the distal edge of a constructive, wave-dominated delta complex. The Carter reservoir in Blowhorn Creek oil unit is a continuation of that in South Brush Creek oil unit and was deposited at the distalmost edge of the constructive, wave-dominated delta system. The Carter reservoir in Bluff oil field is part of a string of beach systems that formed after abandonment of the North Blowhorn Creek spit complex and is the most heterogeneous Carter-*Millerella* oil field in the basin, containing several uncontacted or poorly contacted oil compartments.

Millerella sandstone bodies were deposited during the latest stage of delta destruction as carbonate deposition was reestablished. The *Millerella* reservoir in Blowhorn Creek oil unit differs from the other beach systems and represents part of a delta-destructive shoal massif. In Bluff oil unit, *Millerella* sandstone exhibits a backstepping relation relative to Carter sandstone bodies and represents development of a small beach above a tidal inlet as the deltaic strandplain was inundated.

Carter sandstone in North Blowhorn Creek oil unit is dominantly very fine to fine-grained, moderately well-sorted quartzarenite. Despite the quartzose nature of Carter sandstone, reservoirs in North Blowhorn Creek and other fields are heterogeneous, owing not only to imbricate, clinoformal sandstone lenses and associated facies changes, but also to the presence of intrabasinal framework grains and to diagenesis. Volumetrically important authigenic minerals in Carter sandstone are quartz, kaolinite, and a variety of carbonate minerals, including nonferroan and ferroan calcite, ferroan dolomite/ankerite, and siderite. The distribution of diagenetic components in North Blowhorn Creek oil unit is directly related to depositional facies, but the present composition of authigenic minerals, and the nature of compactional features, resulted from burial diagenesis. Carbonate

cemented zones along the margins of the reservoir and in the vicinity of shell accumulations form baffles and barriers to fluid flow. Pressure-solution seams also form effective barriers to flow and mark the lower limit of oil stained sandstone in several cores. Wispy microstylolites associated with small-scale sedimentary structures and deformed rip-up clasts increase tortuosity of fluid flow.

The pore system in Carter sandstone consists of effective macropores between framework grains and ineffective micropores between detrital and authigenic clay particles. The effective pore system was not enhanced significantly by dissolution of aluminosilicate framework grains because products of dissolution are redistributed locally kaolinite. Further, authigenic carbonate minerals occlude all pores only in the vicinity of shell accumulations, suggesting that secondary porosity formed by dissolution of carbonate cement is not widespread. Dispersed and laminated clay have the most detrimental effects on reservoir properties.

Owing to the presence of detrital and authigenic clays, only a weak correlation exists between porosity and permeability ($R^2 = 0.52$) in the Carter reservoir in North Blowhorn Creek oil unit. Moreover, because Carter sandstone was deposited on a muddy strandplain, porosity and permeability are lower than that in beach-barrier sequences that have been used as models for reservoir heterogeneity. Capillary pressure data indicate that pore-throat size distributions typically are polymodal, reflecting the mixture of macropores and micropores in Carter sandstone. Pore-throat size distributions determined by empirical methods that utilize commercial core analysis data are similar to distributions determined by high-pressure mercury porosimetery, suggesting that capillary-pressure data can be derived from routine core analyses of Carter and other Black Warrior basin reservoirs. Local, order-of-magnitude variation in permeability occurs in some wells in upper shoreface and foreshore sandstone due to grain size differences. These grain size variations affect sweep efficiency during waterflood because fluids are channeled through the high-permeability zones.

Because of the scarcity of cores in the Black Warrior basin, porosity and other petrophysical parameters must be determined by well-log analysis. The distribution well-log derived parameters, including mean effective porosity, porosity-feet, total and effective water saturation, and the product, effective porosity times net pay thickness times effective water saturation, demonstrates that the Carter sandstone reservoir in North Blowhorn Creek oil unit is heterogeneous. However, prediction of the distribution of these reservoir properties in interwell regions by routine geostatistical methods is difficult because of the relatively unpredictable distribution of both detrital and authigenic clay.

Based on evaluation of petrophysical parameters, North Blowhorn Creek oil unit can be divided areally into four zones with different reservoir characteristics. The spatial distribution of these zones closely corresponds to the depositional architecture of the reservoir. The highest quality reservoir occurs in the northern part of the unit, where clinoformal sandstone lenses are amalgamated. Fluid flow in this northern zone is favored along the reservoir axis. The southern part of the unit also contains high quality reservoir. Sandstone lenses in this zone, however, are segmented and smaller than those in the northern zone. In addition, the lenses are oriented obliquely to the axis of the sandstone body. Flow patterns are more irregular in this zone than in the northern zone. A transitional zone with lower quality reservoir occurs along the reservoir axis between the northern and southern zones. A fourth zone, with the lowest quality reservoir, occurs in depositionally updip areas. This zone is dominated by backshore deposits. The probability of uncontacted or unconnected compartments is greatest in this zone.

Although depositional modeling indicates that Carter and *Millerella* sandstone reservoirs in other fields also are beach deposits consisting of similar clinoformal sandstone lenses similar to those in North Blowhorn Creek oil unit, these reservoirs were deposited in smaller, muddier, less well-preserved beach systems and contain more detrital and authigenic clay. These differences explain why North Blowhorn Creek oil unit is the most productive field in the basin. These same factors also suggest that, despite similarities in depositional setting, caution should be used in application of the North Blowhorn Creek reservoir as a direct analog for modeling fluid flow and heterogeneity in other reservoirs of the basin.

Oil production in the Black Warrior basin of Alabama declined after reaching a peak in 1985. As of July 1992, the basin produced 9.2 million barrels of oil; 7.5 million barrels of this oil have been extracted from the 26 designated oil fields and units. Seven Mississippian sandstone units produce oil in Alabama, including Carter, Coats, Chandler, Gilmer, Lewis, *Millerella*, and Sanders sandstones. Of these units, the Carter sandstone has produced more than 90 percent of the oil extracted from

designated oil fields and units. Two-thirds of that oil has been extracted from the Carter sandstone reservoir in North Blowhorn Creek oil unit. South Brush Creek oil unit is the only Carter field that has produced more than one million barrels of oil. The second and third most productive reservoir units in the Alabama part of the Black Warrior basin are the *Millerella* and Lewis sandstones.

In order to sustain or increase oil production in the Alabama part of the Black Warrior basin, five Carter and two *Millerella* sandstone oil fields have been unitized for waterflood, gas injection, or a combination of the two processes. No tertiary or enhanced recovery operations currently are active in the basin. Unitized fields, as of July 1992, include Blowhorn Creek *Millerella*, Central Fairview Carter, North Blowhorn Creek, Mud Creek *Millerella*, South Brush Creek, South Fairview Carter, and Wayside oil units. The success of these projects has been variable.

Oil and water production patterns in North Blowhorn Creek oil unit correlate well with the zones determined by depositional modeling and evaluation of petrophysical parameters. Most oil has been extracted along the axis of the reservoir in the northern zone. Patterns of oil production in the southern zone are more variable reflecting both segmentation of sandstone lenses and changes in orientation of the lenses. Although water injection began at approximately the same time throughout the unit, breakthrough is more widespread in the southern zone. Channeling of fluids through high-permeability thief zones or through fractures is likely to have resulted in bypassing of some producible oil in North Blowhorn Creek oil unit, particularly in the southern zone. Similar factors affect the efficiency of improved-recovery projects in other unitized fields. In addition, erosional truncation of part of the upper Carter sandstone in South Brush Creek oil unit resulted in segmentation of the reservoir.

Because the geological processes that form a sandstone reservoir operate at a variety of scales, heterogeneity in petrophysical and other engineering properties in the reservoir also is scale-dependent. Knowledge of controls on reservoir heterogeneity at smaller scales becomes increasingly important as field development progresses. Heterogeneity in the Black Warrior basin is discussed in terms of a scale-dependent classification that acknowledges gigascopic, megascopic, macroscopic, mesoscopic, and microscopic features of reservoirs. Carter and *Millerella* reservoirs do not fit well into existing heterogeneity classifications, such as that used in the TORIS database, or into commonly used reservoir models for beach-barrier systems. Moreover, Carter reservoirs represent diverse beach systems in a small area, so each field needs to be characterized individually. For these reasons, investigators of reservoir heterogeneity need to evaluate carefully the sedimentologic, structural, and diagenetic characteristics of individual sandstone bodies to gain the fullest understanding of controls on oil production and the methods that can best be applied to improve recovery.

ABSTRACT

The Mississippian System of the Black Warrior basin can be characterized as an intricate system of source and reservoir rocks related to foreland-basin tectonism, climate change, and burial history. Oil-prone source rocks accumulated in deep, starved-basin environments under a density-stratified water column. Reservoir sandstone was deposited in deltaic, beach, and shelf environments, and the distribution and internal characteristics of those deposits reflect interacting siliciclastic depositional systems and carbonate banks during an early phase of the Ouachita orogeny. As the Alleghanian orogeny began and the basin drifted from the arid southern tradewind belt into the humid equatorial belt during Pennsylvanian time, development of a major coastal plain favored accumulation of gas-prone source rocks, including coal.

More than 90 percent of oil produced from the Black Warrior basin in Alabama was extracted from Carter sandstone. Most of that production is from a belt of lensoid, quartzarenitic beach deposits, which were part of a shoal-water deltaic complex developed along a carbonate bank margin. The remaining Carter production is from lobate and elongate sandstone bodies deposited in constructive deltaic lobes to the southwest. Reservoirs within the shoal-water deltaic complex consist of imbricate sandstone lenses with variable geometry and distribution. For example, sandstone in North Blowhorn Creek oil unit, which accounts for two-thirds of total oil production was deposited in a spit complex consisting of a series of clinoformal lenses that decrease in size toward the southeastern terminus of the reservoir. Smaller, less productive reservoirs represent a spectrum of delta-destructive beach systems.

Shoreface and foreshore deposits contain the best interconnected pore system, whereas backshore deposits have abundant depositional and diagenetic baffles and barriers to fluid flow, lower effective porosity, and higher water saturation. Pore and pore-throat size distributions in reservoir sandstone are polymodal owing to a mixture of effective intergranular macroporosity and ineffective microporosity in authigenic and detrital clay. The combined effects of variation in grain size and in the abundance of clays result in local order-of-magnitude scale permeability contrasts within shoreface and beach deposits that affect sweep efficiency. Zones cemented with ferroan dolomite formed around shell accumulations are discontinuous barriers to fluid flow. Although the present diagenetic character of Carter reservoirs is the result of late-stage events during burial diagenesis, the distribution of diagenetic features is directly related to depositional components of the reservoirs. Patterns of oil production from individual reservoirs also closely correspond to depositional architecture. Characterization of heterogeneity in Carter reservoirs through integrated sedimentologic, petrologic, and petrophysical modeling provides a valuable supplement to engineering analysis of reservoir performance during planning and evaluation of improved-recovery operations.

INTRODUCTION

OBJECTIVES

Oil production from Carboniferous reservoirs (fig. 1) in the Black Warrior basin of Alabama (fig. 2) reached a peak in 1985 (Masingill, 1991) and has declined in recent years although much additional oil may be producible using improved recovery strategies, such as waterflooding, chemical injection, strategic well placement, and infill drilling. High-quality reservoir characterization and reliable criteria for recognition of the types and scale of reservoir heterogeneity are crucial to development of enhanced recovery strategies, because reservoirs typically contain numerous features at megascopic, macroscopic, mesoscopic, and microscopic levels that affect fluid flow (Weber, 1986; Haldorsen and Damsleth, 1993). Previous investigations concerning the Black Warrior basin have been regional in scope, addressing the large-scale depositional setting of reservoir units (for example, Cleaves and Broussard, 1980; Cleaves, 1983; Thomas, 1988). Bearden and Mancini (1985) and Epsman (1987) established salient features pertinent to hydrocarbon production at the field scale, such as trapping mechanism. Because oil production in the basin is declining, secondary recovery projects have been initiated in several oil fields, and improved recovery utilizing advanced technology is being considered, this report, which documents controls on the occurrence and producibility of oil from heterogeneous Carboniferous reservoirs in the Black Warrior basin, is timely.

Reservoir sandstone evaluated in this investigation was deposited in beach systems that were preserved as part of a muddy, destructive, shoal-water delta complex. This type of reservoir, which consists dominantly of clinoformal sandstone

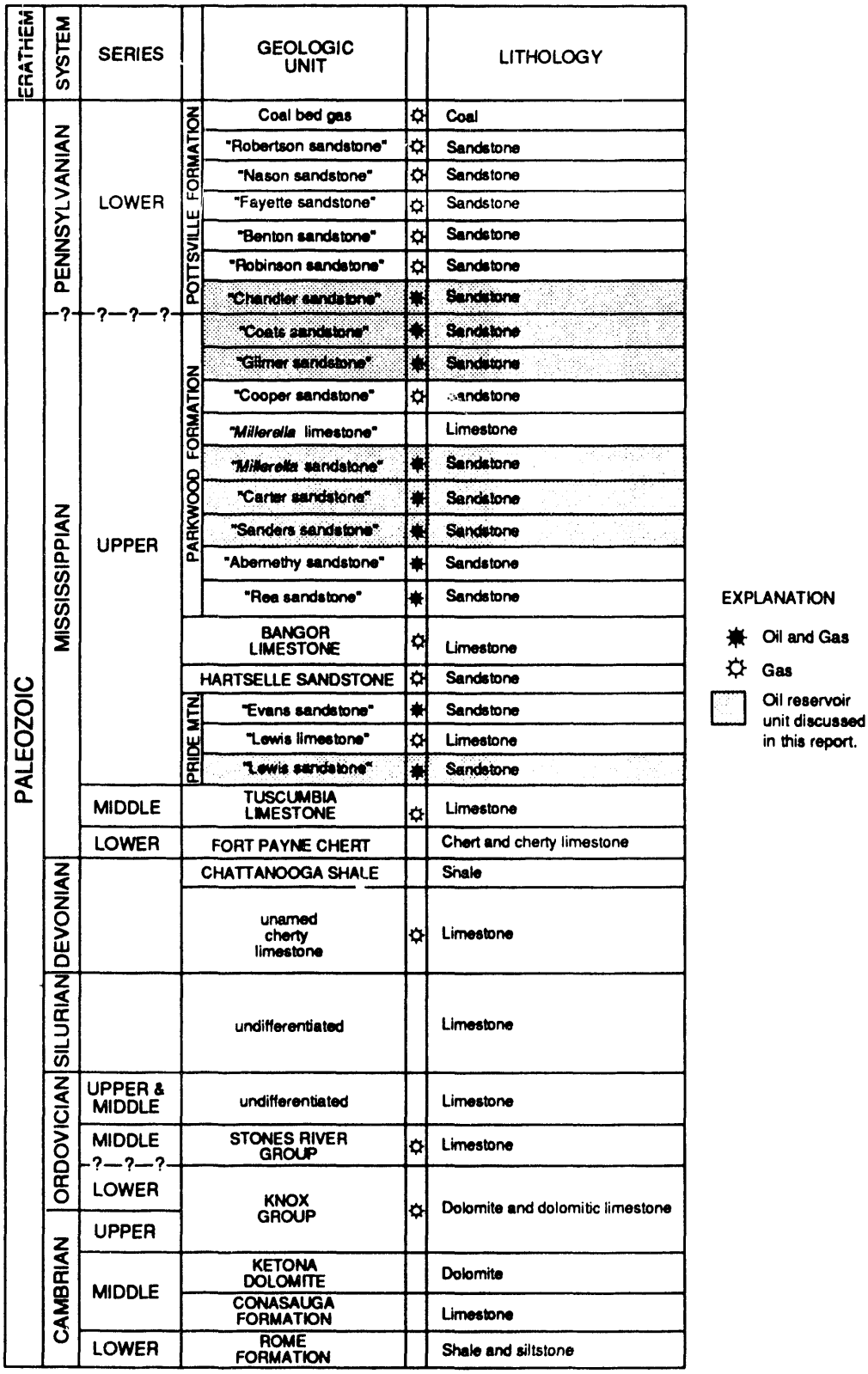

Figure 1.--Stratigraphic column showing oil reservoirs in the Black Warrior basin of Alabama.

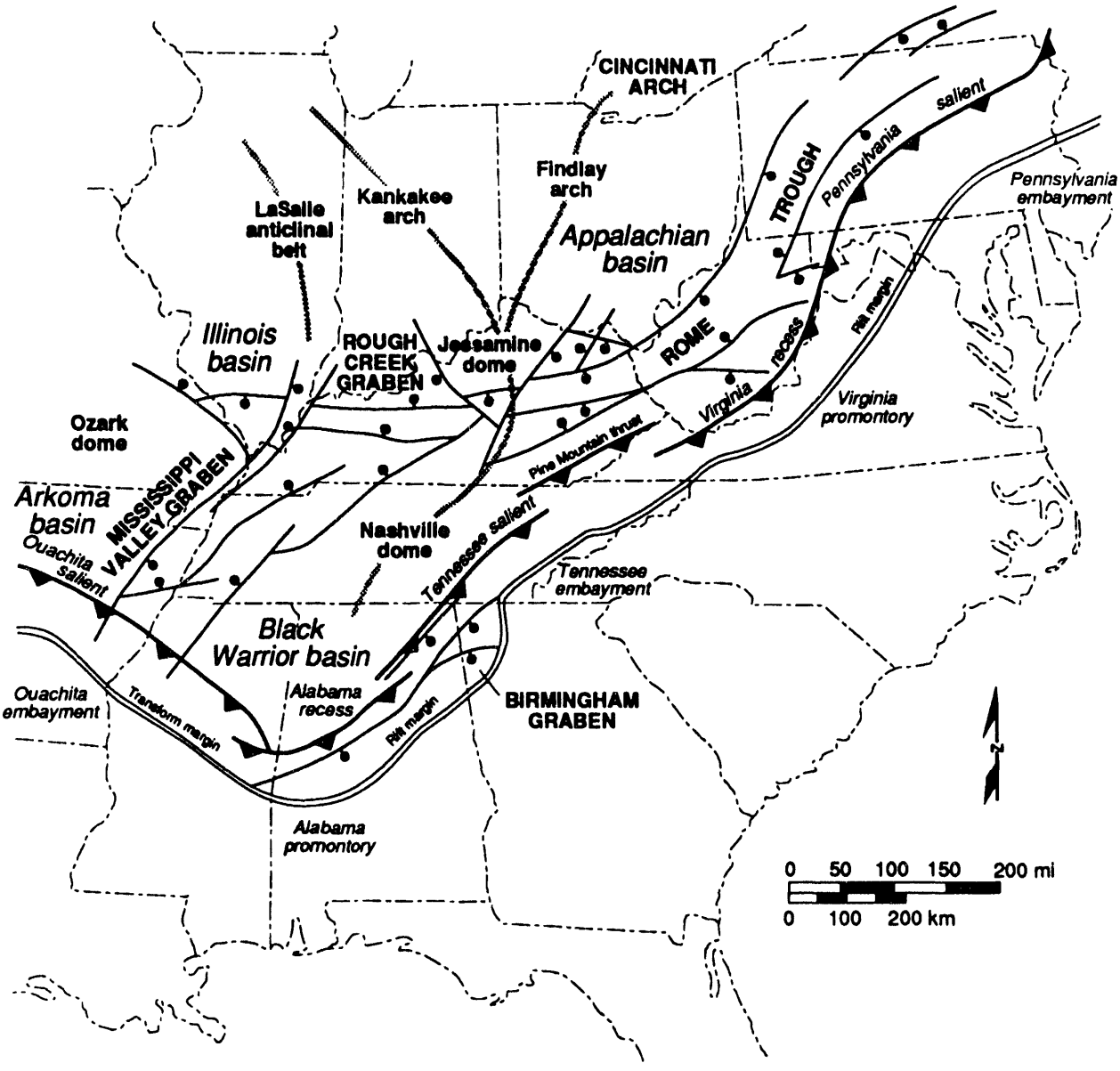

EXPLANATION

Intracratonic arch

Normal basement fault of Iapetan rift

Frontal structures of Appalachian-Ouachita orogen

Early Paleozoic continental margin
(after Sloss, 1988; not palinspastically restored)

Figure 2.--Location and tectonic setting of the Black Warrior basin of Alabama (modified from Thomas, 1988, 1991).

lenses, is poorly documented in the literature and differsgreatly from the beach-barrier deposits that serve as the basis for commonly used reservoir models (Sharma and others, 1990a,b; Szpakiewicz and others, 1991; Schatzinger and others, 1992; Jackson and others, 1993). Thus, results of this investigation are pertinent not only to reservoirs in the Black Warrior basin but to those in other basins as well.

Of 123 fields that produce conventional hydrocarbons and coal-bed methane from Paleozoic sandstone reservoirs in the Black Warrior basin of Alabama, 26 are designated oil fields or units and produce from 33 pools in Carboniferous strata (fig. 3). The basin primarily is a gas basin. Cumulative oil production, as of July 1992, from the 26 designated oil fields and units in the Alabama part of the basin is 8,305,741 stock tank barrels. An additional 932,420 stock tank barrels have been produced from gas fields and from wells that are now abandoned. The Mississippi part of the basin has 17 active oil fields that produced 1,110,747 barrels of oil, as of December 1991, from 29 Mississippian sandstone pools (fig. 3). In Alabama, six Mississippian sandstone units produce oil. The Carter sandstone is the most prolific of these units and has produced 91 percent of the oil extracted from the 26 designated oil fields and units in Alabama (fig. 4). A single unitized field, North Blowhorn Creek oil unit, has produced two-thirds of that oil (fig. 5). Seven oil fields in Alabama have been unitized for waterflood projects. No tertiary recovery projects are active in the Alabama part of the basin, although a pilot project using microbial recovery in the southern part of North Blowhorn Creek oil unit is planned (Gulf Coast Oil World, 1992). Waterflood projects in some unitized oil fields, such as North Blowhorn Creek oil unit, have been successful. However, others have encountered problems or have had disappointing performance.

This report characterizes heterogeneity in Carter and *Millerella* sandstone oil reservoirs in the Black Warrior basin of Alabama. The first part of the report is a regional synthesis of the structural and stratigraphic setting of the Black Warrior basin, as well as of the geochemical characteristics of hydrocarbon source rocks and of oil in the reservoirs. The second part of the report describes depositional facies, petrologic character, and petrophysical properties of reservoirs in North Blowhorn Creek oil unit and other oil fields in order to characterize reservoir heterogeneity. This is followed by a summary of oil production in the Black Warrior basin and an evaluation of seven improved-recovery projects in Alabama.

The final section of the report discusses controls on reservoir heterogeneity, using a modification of the scale-dependent classification of Moore and Kugler (1990) (fig. 6). Scales of heterogeneity include microscopic, macroscopic, mesoscopic, and megascopic features of a reservoir. Microscopic heterogeneity occurs at the scale of pores and pore throats. Mesoscopic heterogeneity represents features that occur at an interwell to borehole scale. Macroscopic heterogeneity represents features that restrict fluid flow and occur among two or more wells. Megascopic heterogeneity is the reservoir, namely a body of permeable reservoir rock surrounded by impermeable nonreservoir rock. In addition to these four commonly utilized scales of heterogeneity (for example, see Lake and others, 1991), an additional category, the gigascopic scale, was found to be particularly useful for explaining variation among reservoirs in the basin. This scale of heterogeneity incorporates those features encompassing several producing fields in a reservoir unit to entire sedimentary basins.

This is the final summary report on DOE contract number FG22-90BC14448, entitled "Characterization of Sandstone Heterogeneity in Carboniferous Reservoirs for Increased Recovery of Oil and Gas From Foreland Basins." This volume consists of the final report for the entire project except for Subtask 4 which will be completed in June of 1993 with the submittal of a computer tape for the TORIS database for oil fields in the Black Warrior basin of Alabama and Mississippi. This report incorporates, and adds to, results of Subtask 1 (outcrop studies; Pashin and others, 1991) and Subtask 3 (characterization of North Blowhorn Creek oil unit; Kugler and Pashin, 1992). In addition to this volume, digital map data and digital well logs used in this investigation are available at the Geological Survey of Alabama for use with a petroleum-oriented geographic information system (GIS).

METHODS

In order to characterize heterogeneity in Carboniferous reservoirs in the Black Warrior basin, this investigation employed a multidisciplinary approach that incorporated stratigraphic, sedimentologic, petrologic, geochemical, petrophysical, and engineering data. Characterization of oil reservoirs in the Black Warrior basin requires collection and analysis of data ranging from basin- to pore-scale.

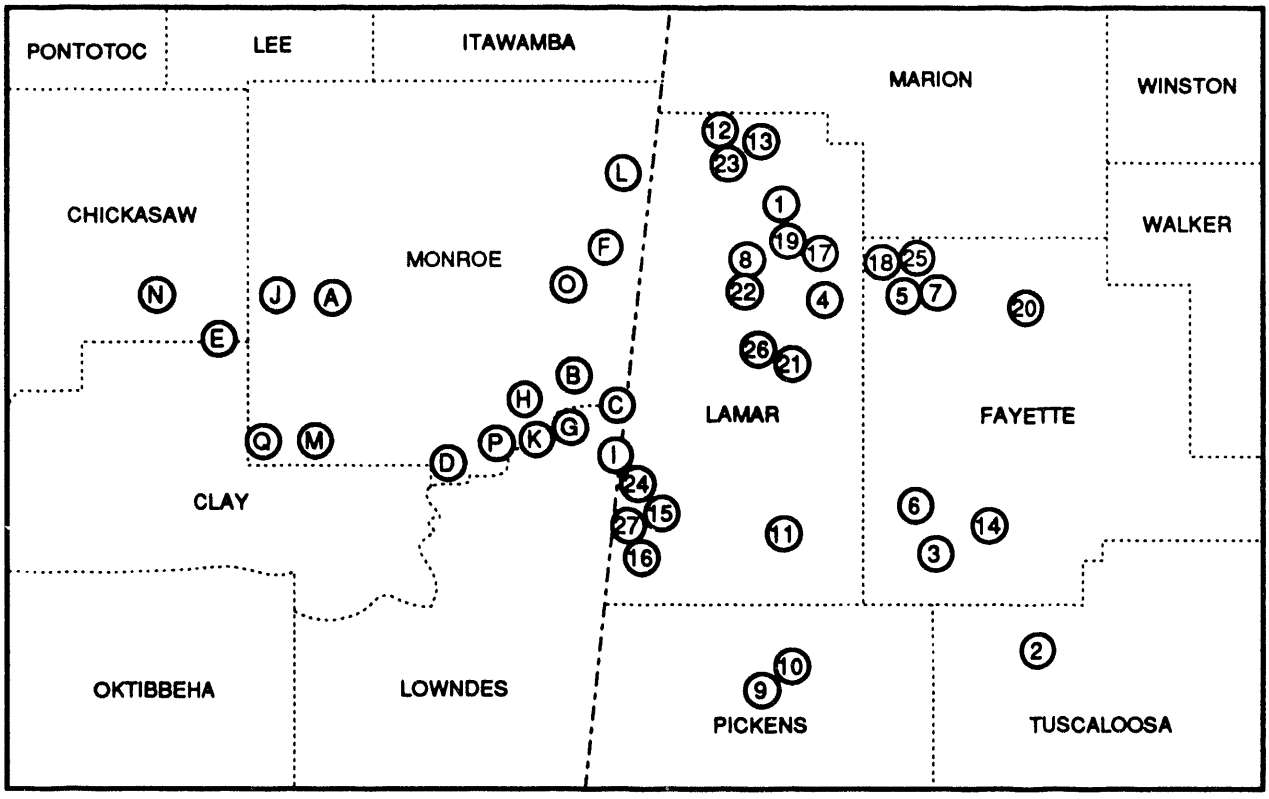

KEY TO MISSISSIPPI OIL AND GAS FIELDS IN THE BLACK WARRIOR BASIN

A. ABERDEEN FIELD
B. BUTTAHATCHIE RIVER FIELD
C. CALEDONIA FIELD
D. CORINNE FIELD
E. GIBSON FIELD
F. GREENWOOD SPRINGS FIELD
G. MAPLE BRANCH FIELD
H. MCKINLEY CREEK FIELD
I. MAYHEW CREEK FIELD
J. PLEASANT GROVE FIELD
K. SOUTH HAMILTON FIELD
L. SOUTH SPLUNGE FIELD
M. STRONG FIELD
N. TREBLOC FIELD
O. WISE GAP FIEL
P. WEST HAMILTON FIELD
Q. WHITES FIELD

KEY TO ALABAMA OIL AND GAS FIELDS IN THE BLACK WARRIOR BASIN

1. BEAVER CREEK FIELD
2. BINION CREEK FIELD
3. BLAKELY CREEK FIELD
4. BLOWHORN CREEK FIELD
5. BLUFF FIELD
6. CAINS RIDGE FIELD
7. CENTRAL BLUFF FIELD
8. CENTRAL FAIRVIEW FIELD
9. CHICKEN SWAMP BRANCH FIELD
10. COAL FIRE CREEK FIELD
11. COOPER CREEK FIELD
12. EAST DETROIT FIELD
13. HENSON SPRINGS FIELD
14. MCCRAKEN MOUNTAIN FIELD
15. MT. ZION FIELD
16. MUD CREEK FIELD
17. NORTH BLOWHORN CREEK FIELD
18. NORTH BLUFF FIELD
19. NORTH FAIRVIEW FIELD
20. SAND SPRINGS FIELD
21. SOUTH BRUSH CREEK FIELD
22. SOUTH FAIRVIEW FIELD
23. SOUTHEAST DETROIT FIELD
24. STAR FIELD
25. WAYSIDE FIELD
26. WEST BRUSH CREEK FIELD
27. YELLOW CREEK FIELD

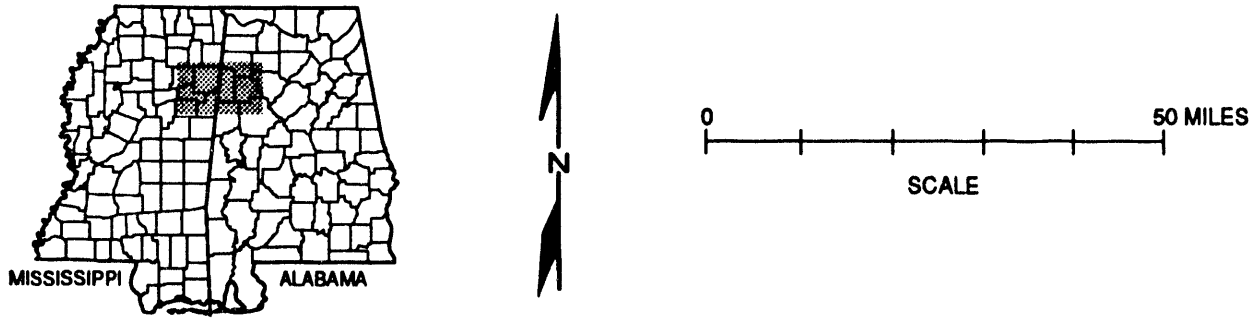

Figure 3.--Location map of oil fields in the Black Warrior basin of Alabama and Mississippi.

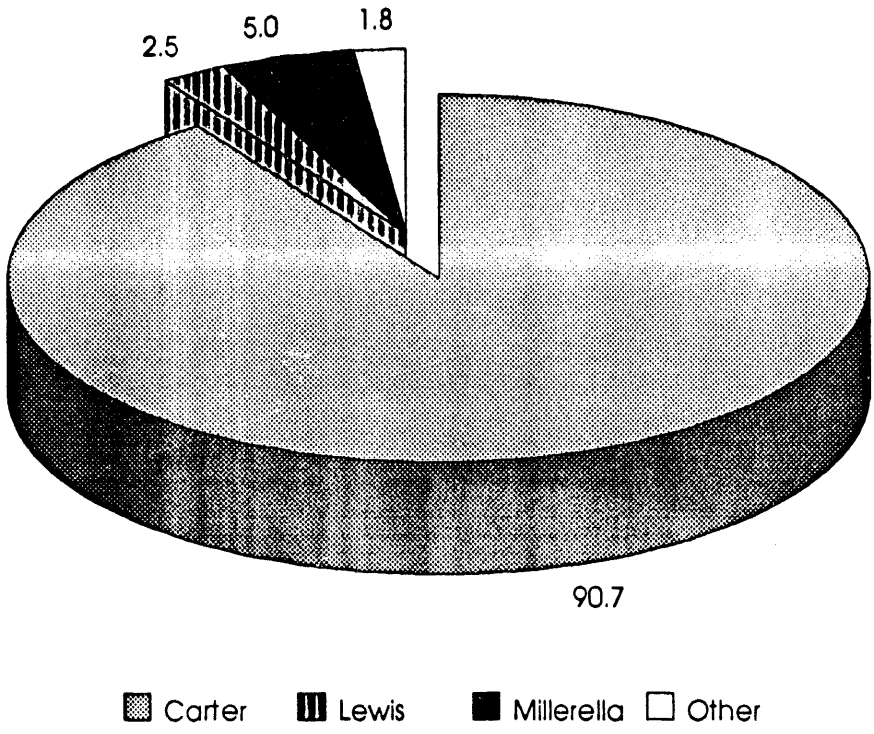

Figure 4.--Pie chart showing relative percent of oil production from sandstone reservoir units in the Black Warrior basin of Alabama. Numbers adjacent to pie slices are percents.

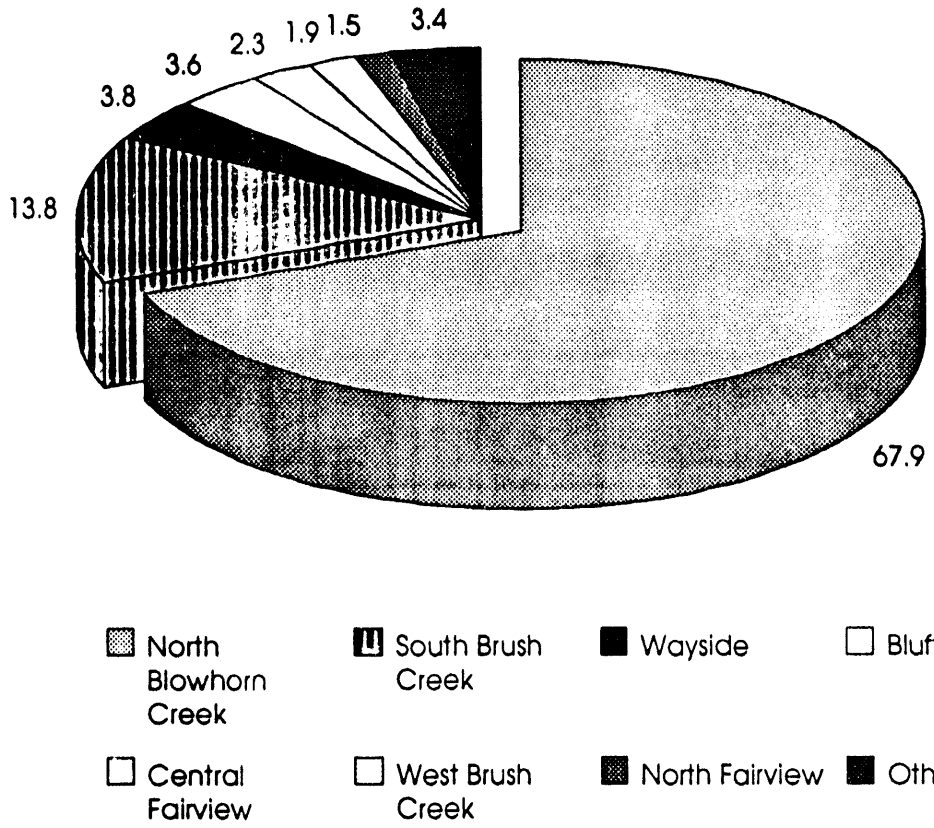

Figure 5.--Pie chart showing relative percent of oil production from Carter sandstone reservoirs in the Black Warrior basin of Alabama. Numbers adjacent to pie slices are percents.

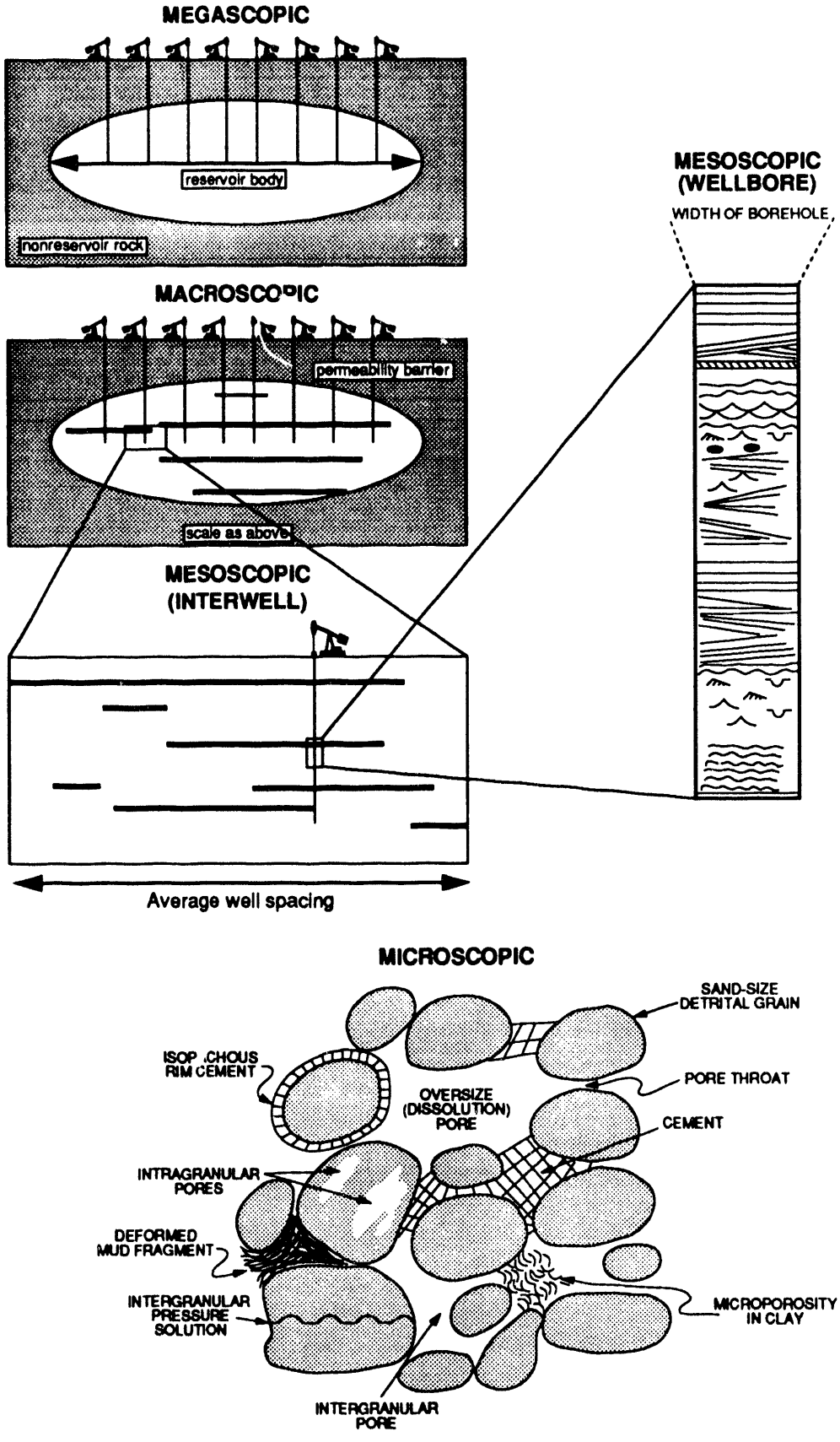

Figure 6.--Scales of reservoir heterogeneity in the Black Warrior basin.

Basin-wide (gigascopic-scale) modeling establishes the spatial distribution of depositional environments and tectonic setting. Organic geochemical data collected for characterization of oil source rocks also requires integration of information at a gigascopic scale. Field-scale (megascopic-scale) data are required to determine the overall architecture of the reservoir. These megascopic scale data also are used to determine the geometry of smaller-scale heterogeneities that affect fluid flow and production. Mesoscopic-scale data are collected to characterize spatial variation in properties within reservoir units, including bedding type, sedimentary structures, sandstone framework composition, and diagenetic character. Microscopic-scale data characterize aspects of the reservoir important to fluid storage and movement, such as pore geometry, pore-throat size, and clay mineral composition and morphology. The diverse scales of reservoir heterogeneity influence production differently at various stages of field development. In general, heterogeneities important to production decrease in size as field development progresses from primary to tertiary recovery (Jackson and others, 1993). Methodologies used in this investigation reflect these differences in the type of data required for the diverse stages of field development.

Stratigraphic and sedimentologic characterization of Carboniferous oil reservoirs in the Black Warrior basin of Alabama employed subsurface techniques. Geophysical well logs are numerous in the Black Warrior basin and, along with cores and cuttings, provide the principal basis for understanding facies heterogeneity. Five major rock types that have distinctive geophysical signatures were identified in the well logs on the basis of bulk density, density porosity, neutron porosity, gamma count, resistivity, and spontaneous potential. These rock types are: (1) coal, (2) shale, (3) limestone, (4) porous (reservoir) sandstone, and (5) tight sandstone. Porous sandstone is distinguished from tight sandstone on the basis of crossing of the neutron- and density-porosity curves. A detailed discussion of log interpretations used in this study is available in Pashin and others (1991).

To provide regional perspective, a network of cross sections based on sample descriptions and interpreted geophysical well logs was made to determine facies patterns and stratal geometry. Log patterns were interpreted and used to make a structural contour map of the top of the Tuscumbia Limestone. Isopach maps and net-sandstone isolith maps of each major stratigraphic interval and reservoir sandstone unit were made to determine depositional history and identify the controls on the distribution and characteristics of Carboniferous oil reservoirs in Alabama.

Having completed regional facies analysis, a detailed sedimentologic study of Carter and *Millerella* sandstone oil reservoirs was conducted in northeastern Lamar and northwestern Fayette Counties, Alabama, where more than 80 percent of the oil from the Black Warrior basin is produced. Lithology, grain-size trends, stratification type, and sedimentary structures were described from 11 cores, and lithofacies were defined. To determine the distribution and internal architecture of Carter and *Millerella* reservoirs, a net-sandstone isolith map was made for each reservoir, and several cross sections using the closest well spacing possible were made. Well-log and core data were then integrated to develop a depositional model for Carter and *Millerella* oil reservoirs.

Two wells, one from near the North Blowhorn Creek Oil Unit (PN2191) and the other from northern Pickens County (PN1780), were selected for study in order to assess differences in thermal maturation and history in shallow (PN2191) and in deep (PN1780) parts of the Black Warrior Basin. Samples of cuttings sets from these wells were used in vitrinite reflectance and Rock-Eval pyrolysis.

Samples for vitrinite reflectance were crushed to minus 20 mesh size and then embedded in epoxy to create a pellet. After polishing, the pellets were allowed to dry in a desiccator for at least 24 hours. Reflectance measurements were made with a Nikon P1 photometer mounted on a Nikon Microphot-FX compound microscope. Data were collected using PHOSCAN 3, a PC compatible program developed by Nikon. Typically, 40 measurements were made for each sample. However, many samples had low organic content which made attaining this level difficult. Vitrinite particles that could be attributed to caving of younger units were not included in either the counts or the histograms. Material identified as reworked vitrinite was not positively encountered. This is probably because the parent rock was most likely either crystalline in nature or was of an age prior to the development of plants with woody tissue.

Lopatin's (Lopatin, 1971; Waples, 1982) method for computing Time/Temperature Indices (TTI) was used to assess the thermal and burial history for the stratigraphic sequence of each of the two wells studied. Decompacted burial curves were generated using compaction constants based on studies by Sclater and Cristie (1980) and Schmoker and Halley (1982).

Sixteen samples from the PN2191 and PN1780 wells, were collected and sent to the U.S. Geological Survey Organic Geochemistry Laboratory in Denver, Colorado, where the samples were analyzed for total organic carbon and kerogen type using Rock-Eval pyrolysis. Twenty-three samples of oil fields also were analyzed by this laboratory for gross chemical composition. API gravity data were compiled from Alabama State Oil and Gas Board records.

Framework-grain composition and diagenetic character of Carter sandstone from North Blowhorn Creek oil unit was determined by modal analysis with a standard petrographic microscope. Approximately 300 points were identified in each of 75 thin sections. Generally, the composition of more than 200 framework grains in each sample was determined using this procedure. Three-hundred thin sections of Carter and Lewis sandstone were examined qualitatively. Particular attention was given to relationships between authigenic minerals and pores. All thin sections were back-pressure impregnated with blue-dyed epoxy to facilitate identification of pore types. Thin sections were stained also with alizarin red-S and potassium ferricyanide, according toe the method of Evamy (1963) to aid identification of carbonate minerals. X-ray diffraction analysis of selected, unoriented whole-rock powders corroborated mineral identification. The morphology, distribution, and composition of authigenic minerals and pores were evaluated with a scanning electron microscope, using secondary-electron images of gold-palladium coated, freshly broken rock surfaces and backscattered-electron images of carbon-coated, polished thin sections. Qualitative energy-dispersive X-ray analysis aided mineral identification. Concentrations of calcium, iron, magnesium, manganese, and strontium in authigenic carbonate minerals were determined by electron-probe microanalysis, using Bence-Albee routines for data reduction. Stable carbon and oxygen isotopic analyses were performed on authigenic siderite, calcite, and ferroan dolomite/ankerite by a commercial laboratory, using standard procedures and multiple-extraction methods for samples containing more than one carbonate phase. Replicate analyses were run for several samples.

Porosity and permeability data from all available commercial core analyses for wells within oil fields were compiled for comparison with core descriptions, petrographic data, and high-pressure mercury porosimetry. Selected data from North Blowhorn Creek oil unit are discussed in this report. Capillary-pressure data obtained from high-pressure mercury porosimetry were used to characterize pore-throat size distributions and their relationships to pore types. A Micromeritics Autopore II 9200 was used for these analyses, following the procedures of Kopaska-Merkel (1991). Mercury intrusion volume was monitored from 1.5 to 20,000 psia. Thin sections were made from the ends of plugs used for porosity measurement. All porosimetry samples were cleaned by refluxing toluene in a Soxhlet extractor. Samples were also cleaned with chloroform as necessary.

A geographic information system (GIS) that incorporates all wells in the Black Warrior basin of Alabama was prepared for this investigation using Geographix Exploration System version 7 software. This GIS system contains a digital land grid encompassing 15 counties and the locations of more than 2,500 conventional oil and gas wells and approximately 5000 coalbed-methane wells, as well as oil and gas field boundaries. Basic header information for each well, including State Oil and Gas Board of Alabama permit number, API number, well name, well status, operator, field name, productive unit, total depth, and available cores, was placed in a database associated with the digital map. Additional information was added to the database for fields examined in more detail in this investigation. These data include fluid production and injection volumes, core analyses, well-log derived porosity and fluid saturations, initial production tests, depths of unit boundaries, and digital well logs. Contour and bubble maps, cross sections, and volumetric determinations utilized information in the GIS database.

Spontaneous potential, gamma ray, caliper, deep, medium, and shallow resistivity, neutron porosity, and density porosity logs were digitized through the appropriate reservoir intervals in approximately 300 wells using Schlumberger/Geographix QLA2 well-log analysis software. Porosity and water saturation were computed using a dual-water model (Clavier and others, 1984; Asquith, 1989). Clay volumes (V_{cl}) were determined from gamma ray curves. R_w values for each field were obtained from Schlumberger and cross checked with water chemical data on file at the State Oil and Gas Board of Alabama and by the method of Elphick (1990). Although it has been shown that R_w can vary significantly within a single reservoir (Szpakiewicz, 1993; Sharma and others, 1993), a single R_w value was used in computations for all wells in each field because of limited data availability.

REGIONAL GEOLOGIC FRAMEWORK

Carboniferous strata of the Black Warrior basin have long been understood to represent interaction of siliciclastic and carbonate depositional systems during an early phase of the Ouachita orogeny (Thomas, 1972a, b, 1974). This Ouachita phase continued into Pennsylvanian time, when Appalachian orogenesis also began affecting the basin (Thomas, 1988; Pashin, 1991). Recent investigators have built on this general theme and have found a distinctive relationship between the characteristics of Carboniferous reservoirs and the evolving tectonic and sedimentologic framework of the basin (Cleaves and Broussard, 1980; Higginbotham, 1986; Pashin and Kugler, 1992). The following sections review the basic characteristics of Carboniferous strata and establish the setting of the principal oil reservoirs with respect to tectonic and sedimentologic events.

STRUCTURE AND TECTONICS

The Black Warrior basin is a late Paleozoic foreland basin formed by tectonic loading of the Alabama continental promontory during Appalachian-Ouachita orogenesis (Thomas, 1977; Beaumont and others, 1987, 1988; Hines, 1988) (fig. 2). Paleozoic rocks are exposed in the eastern part of the basin, and the western part is below as much as 6,000 feet of Mesozoic and Cenozoic overburden of the Mississippi Embayment and the Gulf Coastal Plain. The Black Warrior basin is triangular in plan and formed along the juncture of the Appalachian and Ouachita orogenic belts (Thomas, 1973, 1985a; Hale-Ehrlich and Coleman, 1993). Early Cambrian rifts, which strike northeast, help define the boundaries of the basin (Thomas, 1991). Northwest of the basin is the Mississippi Valley graben, which strikes perpendicular to the Ouachita orogen, and southeast of the basin is the Birmingham graben, which is below and parallels the frontal structures of the Appalachian orogen.

A structural contour map of the top of the Tuscumbia Limestone establishes the major structural relationships in Alabama (fig. 7). The Tuscumbia Limestone dips uniformly southwest in the northern part of the study area, forming a homocline that is transitional from the Nashville dome to the Black Warrior basin. Appalachian folds are present along the southeast margin of the homocline. These folds formed during the Alleghanian orogeny and have been interpreted as detached structures related to decollements that ramp blindly upward from Cambrian shale (Rodgers, 1950; Thomas, 1985b).

Southwest of the homocline, structural dip increases markedly, and strata are displaced by as much as 1,000 feet along normal faults striking northwest to west (fig. 7). Most faults dip and are downthrown to the southwest, but several faults with displacement larger than 300 feet have an antithetic complement that defines long, narrow grabens. Fault length and displacement generally increase southwestward, and major faults contain fault-bound anticlines, or rollover structures, in the hanging wall. These faults generally parallel the Ouachita orogenic belt and are thus interpreted as the result of flexural extension (Bradley, 1991) caused by deformational loading near the southwest margin of the Alabama promontory.

The pre-orogenic continental margin affected profoundly the evolution of the Black Warrior basin (Thomas, 1988) (fig. 2). The southwest edge of the Alabama promontory has been interpreted as a passive margin formed by transform faulting (Thomas, 1991). In Mississippian time, oblique convergence of a microcontinental island arc with the promontory closed the eastern part of the Ouachita trough, thus forming an active margin (Thomas, 1976; Viele and Thomas, 1989). Closure and concomitant collision thrust an accretionary prism onto the former transform margin, thereby helping provide the tectonic load that formed the Black Warrior foreland basin.

Tectonism proceeded differently along the southeast side of the Alabama promontory. The Birmingham graben (fig. 2) is a rifted half graben that localized thrust ramps in the Appalachian orogenic belt (Thomas, 1985b, 1991). The cratonic character of strata in the Appalachian thrust belt contrasts strongly with the oceanic character of those in the Ouachita belt, reflecting the maturity of the Appalachian orogen. Convergence east of the promontory began in Middle Ordovician time during the Blountain phase of the Taconian orogeny (Ettensohn, 1990). Basement faults remained active through Mississippian time (Thomas, 1968; Thomas and Neathery, 1982), and during the Early Pennsylvanian Lackawanna phase of the Alleghanian orogeny, blind thrusts evidently propagated into the sedimentary cover above the rift structures (Pashin, 1991; Pashin and Carroll, 1993). The Black Warrior basin had effectively been protected from Appalachian tectonism by the graben (Thomas, 1974), but during Pennsylvanian time, the Appalachian flexural moat impinged on the basin, and orogenic

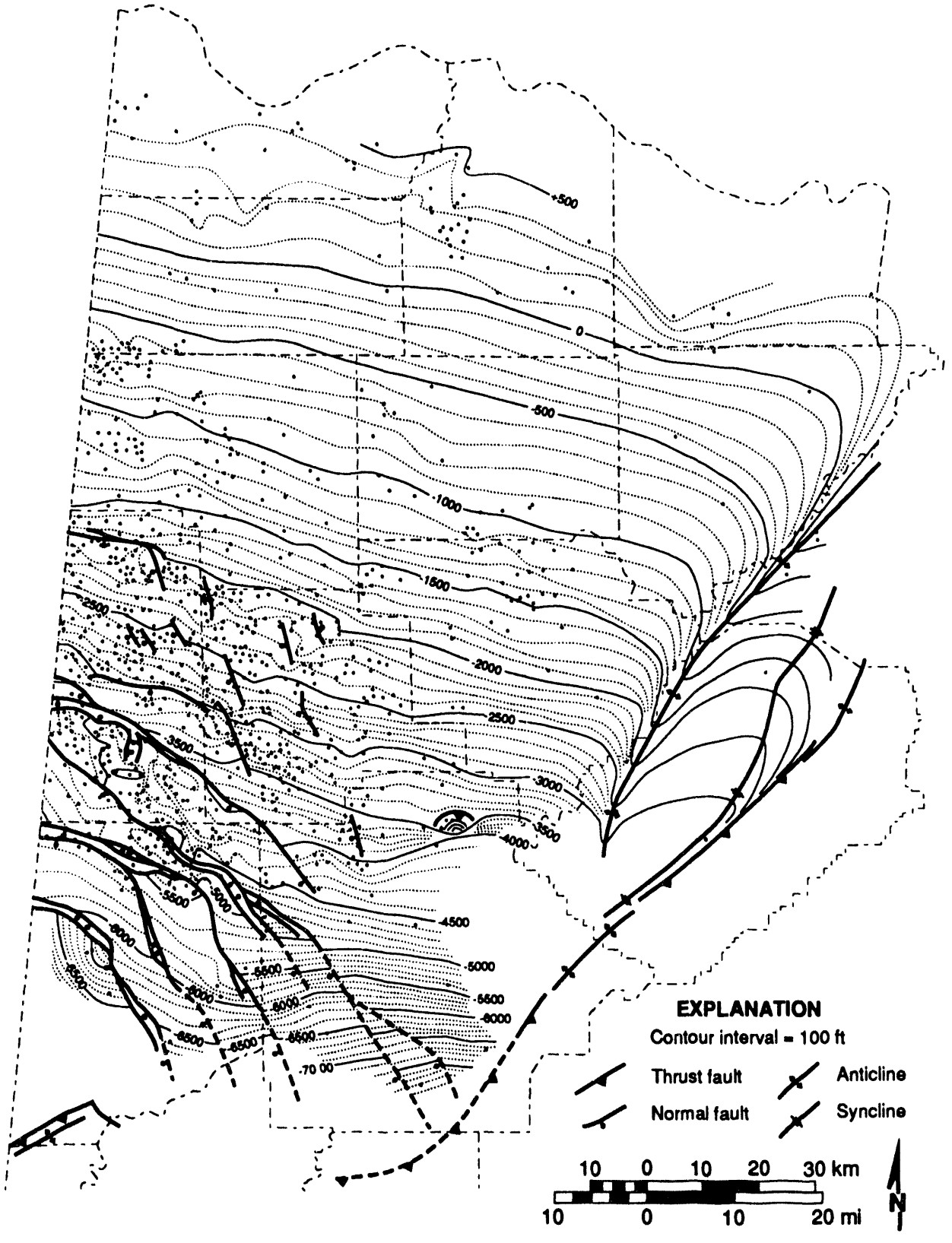

Figure 7.--Structural contour map of the top of the Tuscumbia Limestone.

sediment finally entered the basin from the east (Pashin, 1991).

After the Alleghanian orogeny, the basin was unroofed until the Late Cretaceous, when strata of the Gulf Coastal Plain and the Mississippi embayment began to accumulate. Development of the coastal plain and embayment signal a transition to an extensional tectonic regime related to rifting and opening of the Gulf of Mexico. As Mesozoic and Cenozoic sediment was deposited, the Black Warrior basin was tilted southwestward (Thomas, 1988). An important result of basin tilting was loss of closure within the fault-bound anticlines (fig. 7). Instead, most of these structures now close against faults. Throughout the Black Warrior basin, fault closure acts in concert with stratigraphic and diagenetic factors to make the principal hydrocarbon traps (Bearden and Mancini, 1985).

STRATIGRAPHY AND SEDIMENTATION

The major hydrocarbon source and reservoir rocks in the Black Warrior basin range in age from Devonian through Pennsylvanian and are parts of the Kaskaskia and Absaroka cratonic sequences of Sloss (1963). These sequences record the tectonic evolution of the Alabama promontory as well as major climatic changes. According to paleogeographic reconstructions, the Black Warrior basin was in the southern tradewind belt at an approximate paleolatitude of 30° S. during Upper Devonian time (Scotese, 1990). By the Early Pennsylvanian, however, the Pangaea supercontinent was assembling, and the Appalachian region had drifted northward into the equatorial belt as causing a shift from arid carbonate banks and coastal plains to humid coastal plains with major coal-forming peat swamps (Cecil, 1990). The following section discusses the basic characteristics of Devonian through Pennsylvanian rocks in the Black Warrior basin of Alabama and shows how interwoven tectonic and climatic variables produced an intricate system of source and reservoir rocks.

CHATTANOOGA SHALE

The Upper Devonian (Chataquan) Chattanooga Shale (fig. 8) forms the base of the Kaskaskia sequence in the Black Warrior basin and is composed mainly of black, fissile, pyritic shale. The Chattanooga disconformably overlies Upper Ordovician through Middle Devonian carbonate and siliciclastic rocks (Conant and Swanson, 1961; Rheams and Neathery, 1988). The shale is easily identified in gamma-ray logs because of extremely high radioactivity. The radioactive signature of the Chattanooga and equivalent strata has provided a basis for subdividing and correlating homogeneous black shale throughout the Appalachian region (Ettensohn and others, 1979), but a detailed internal radioactive stratigraphy has yet to be developed for the Black Warrior basin.

An isopach map of the Chattanooga Shale in Alabama is available in Rheams and Neathery (1988). The shale is generally thinner than 40 feet and is locally absent (fig. 9). In the northern part of the study area, however, the shale is locally thicker than 40 feet, and in southern Tuscaloosa County the shale reaches a maximum thickness of more than 80 feet. Nearly all oil from the Black Warrior basin is produced from areas where the shale is thinner than 15 feet.

The Brooks core is the only available continuous core of the Chattanooga Shale in the Black Warrior basin (fig. 8). The shale overlies disconformably an unnamed Middle Silurian carbonate unit containing abundant specimens of the pentamerid brachiopod, *Chonchidium* sp. The Chattanooga consists of black, fissile shale with wavy, graded siltstone beds containing current ripples, horizontal laminae, and feeding burrows. Fossils in black shale are dominated by the alga, *Tasmanites*, and some siltstone beds contain sand-size crinoid ossicles.

Rich (1951a, b) recognized the continuity of Chataquan black shale which is now thought to have extended from Hudson Bay through Alabama to Arizona (Heckel and Witzke, 1979). He was among the first to argue cogently in favor of a deep-water origin for the shale and recognized that coarse clastic sediment in the Appalachian basin prograded into the black-shale environment. Indeed, the shale was deposited on an euxinic foreland basin floor that formed in response to the Acadian orogeny (Byers, 1977; Ettensohn and Barron, 1981; Ettensohn, 1985a, b).

Anoxia and low sedimentation rate are considered the principal factors that favored preservation of black, fissile shale that is enriched in oil-prone kerogen, including *Tasmanites*. In the Black Warrior basin, the Chattanooga represents accumulation of less than 80 feet of black shale in approximately 7 million years. The graded siltstone beds are typical of storm-generated turbidites in Devonian black shale (Ettensohn and Barron, 1981; Pashin and Ettensohn, 1987), and feeding burrows suggest that most of the shale was deposited in the dysaerobic

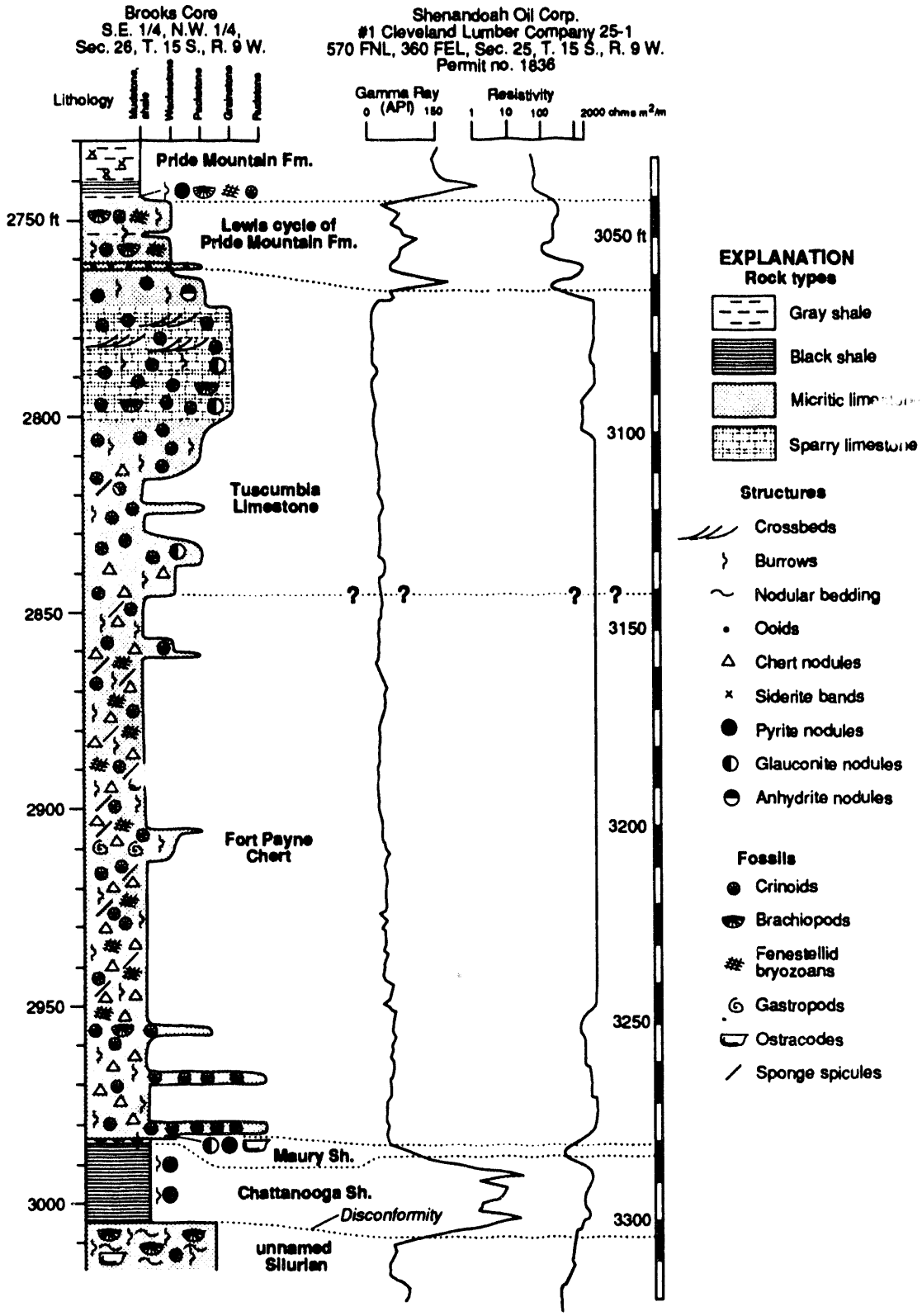

Figure 8.--Measured section of Silurian through basal Chesterian rocks in the Black Warrior basin.

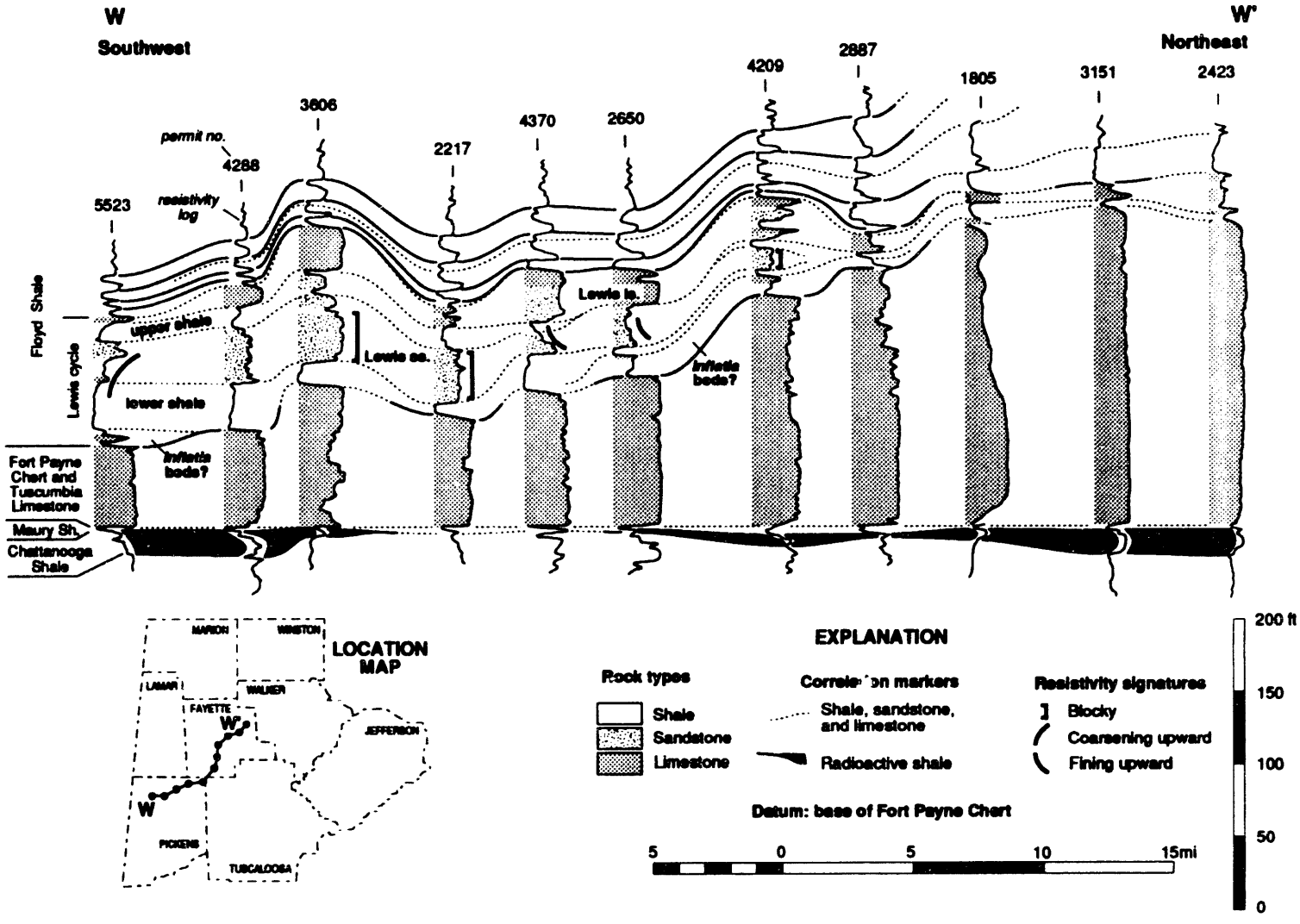

Figure 9.--Stratigraphic cross section showing facies relationships from the Chattanooga Shale through the Lewis cycle.

zone. The sand-size echinoderm ossicles in some siltstone beds may represent stunted crinoid faunas reworked by storm-induced flows.

A dysphotic to aphotic depth favors preservation of organic matter in an open-marine environment with extremely slow sedimentation, and therefore, clear water. Proximity to the passive margin of the Ouachita embayment (fig. 2), moreover, indicates that the Chattanooga of the Black Warrior basin accumulated on a shelfal extension of the Acadian foreland basin floor. Perhaps the shale represents sedimentation within a continental extension of an oceanic oxygen-minimum zone that may have existed in the Ouachita trough during Late Devonian time.

MAURY SHALE

The Maury Shale sharply overlies the Chattanooga Shale and is the basal Mississippian unit in the Black Warrior basin. The Maury contains a late Kinderhookian to early Osagian conodont fauna (Drahovzal, 1967); early Kinderhookian strata have not been identified definitively in the Black Warrior basin. Indeed, the Chattanooga-Maury contact may be disconformable in places (Conant and Swanson, 1961), and disconformities have been identified on the basis of biostratigraphic data within the Maury Shale as well as equivalent strata in the southern midcontinent (Ham and Wilson, 1967).

Maury Shale is composed of greenish-gray, glauconitic shale with phosphate nodules and separates the Chattanooga Shale from the Fort Payne Chert (Conant and Swanson, 1961; Thomas, 1972a; Welch, 1978) (figs. 8, 9). The shale is generally 2 to 3 feet thick, is locally absent (Thomas, 1972a; Rheams and Neathery, 1988), and is thus difficult to identify in the subsurface (fig. 9). In the Brooks core (fig. 8), the Maury Shale contains 12 inches of poorly fissile, medium gray shale with sharp contacts and abundant feeding burrows. Some burrows are filled with phosphate, and the contact with the Fort Payne Chert is glauconitic.

The Maury Shale represents a transition from the euxinic basin of the Chattanooga Shale to the carbonate banks that dominated Mississippian sedimentation in the Black Warrior basin. Presence of organic-poor Maury shale above the black Chattanooga Shale suggests that the basin floor was reasonably oxygenated, perhaps partly by shallowing, and abundant phosphate nodules suggest that upwelling currents traversed the basin floor. Concentration of phosphate and glauconite in the Maury also indicates slow sedimentation. Regional oxygenation of the basin floor is interpreted to have been the preliminary stage in developing substrates suitable for habitation by the calcareous benthos that built the Mississippian carbonate banks of north Alabama.

Development of regional unconformities during Maury deposition also indicates a change from a passive margin to an active one along the Ouachita embayment. Tectonism along the western side of the embayment may have begun in the Middle Devonian, but the major collision took place near the Devonian-Mississippian transition and continued into Kinderhookian time in that area (Johnson, 1971). Cratonward bulge migration or continental braking (Dickinson, 1977) may have been responsible for the unconformities during Maury deposition. Hence, the Maury Shale signifies far-field effects of the start of the Ouachita orogeny.

FORT PAYNE CHERT AND TUSCUMBIA LIMESTONE

The Fort Payne Chert is composed dominantly of dark brownish-gray siliceous micrite and bluish-gray nodular chert containing abundant fenestrate bryozoans, crinoid ossicles, and articulate brachiopods (Butts, 1926; Thomas, 1972a; Thomas and others, 1979) (fig. 8). Siliceous sponge spicules also are common in Fort Payne micrite. Conodonts indicate that the Fort Payne is Osagian in age (Ruppel, 1979). The Tuscumbia Limestone gradationally overlies the Fort Payne, is composed dominantly of light gray skeletal calcarenite, and contains fewer chert nodules than the Fort Payne (Thomas, 1972a; Fisher, 1987). Caliche zones have also been identified in the Tuscumbia (Fisher, 1987). Faunas in the Tuscumbia Limestone are diverse and include echinoderms, corals, bryozoans, and brachiopods. Conodonts indicate a Meramecian age for the Tuscumbia (Ruppel, 1979).

Fort Payne Chert and Tuscumbia Limestone are difficult to separate using geophysical well logs and were thus mapped together in the subsurface (figs. 8, 9, 10). In the northeasternmost part of the study area, the isopach interval also includes the Meramecian-Genevievian Monteagle Limestone. These formations have a combined maximum thickness of more than 450 feet in the northeast and thin southwestward to less than 25 feet (fig. 10).

As these units thin southwestward, Tuscumbia calcarenite grades into a chert facies that cannot be distinguished from the Fort Payne Formation (Thomas, 1972a; 1988; Thomas and others, 1979). Spacing of isopach contours northeast of the 250-

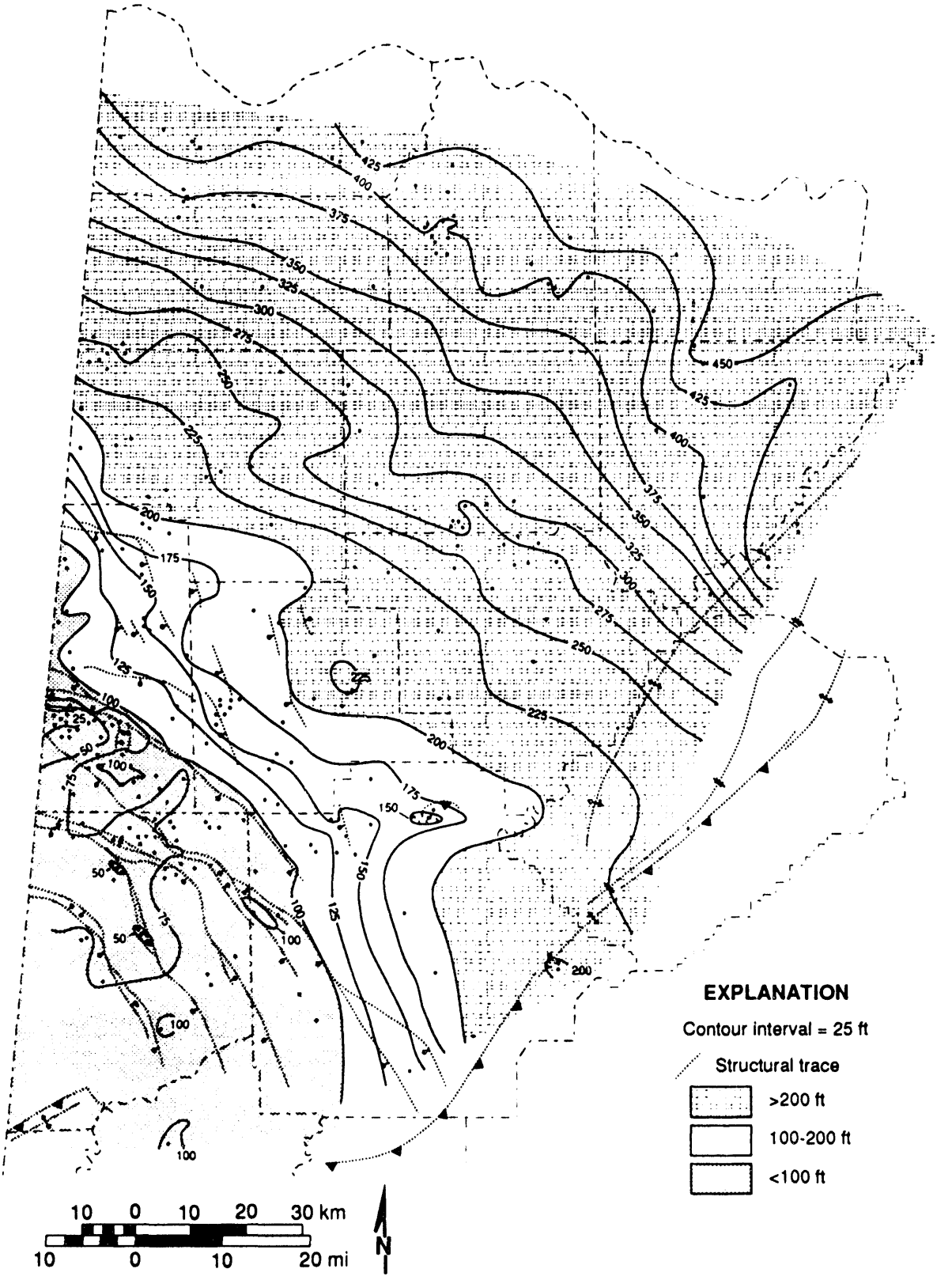

Figure 10.--Isopach map of the combined Fort Payne Chert and Tuscumbia Limestone.

foot contour is generally uniform (fig. 10). The 200- through 250-foot contours are widely spaced, but southwest of the 200-feet contour, strata thin markedly. The 100-foot contour follows the trace of a major fault, and southwest of that fault, contour patterns are irregular. Across the northwest part of the fault trace, the combined Fort Payne and Tuscumbia Formations thin by more than 75 feet.

The Fort Payne and Tuscumbia Formations accumulated on a carbonate ramp with three major parts. The principal region of calcarenite accumulation is northeast of the 200-feet contour and is thus considered the upper ramp, and wide spacing of the 200- through 250-feet contours suggests that the base of the upper ramp formed a ledge (fig. 10). Calcarenite interfingers with micritic rocks in the belt where the formations thin from 200 to 100 feet, thereby defining the middle ramp, whereas predominance of micritic rocks in the fault-bound area southwest of the 100-ft contour defines the lower ramp.

Skeletal calcarenite with some caliche in the northeast indicates that the upper ramp was an extensive carbonate sand bank with islands (Thomas, 1972a, 1974, 1988; Fisher, 1987). By contrast, siliceous micrite with sponge spicules in the southwest indicates the lower ramp was characterized by deeper, open-marine environments where cool water prevailed throughout Fort Payne-Tuscumbia deposition (Thomas, 1976; Pashin and others, 1991). The abundant crinoids, bryozoans, and brachiopods in the chert-rich facies, moreover, indicate that the lower ramp was rich in oxygen and nutrients. Upwelling of oceanic water from the Ouachita trough is thought to be a primary source of silica in the Fort Payne Formation (Gutschick and Sandberg, 1983) and fostered nutrient-rich habitats across the ramp.

Uniform spacing of contours in the northern part of the study area (fig. 10) indicates that, by the end of Tuscumbia deposition, the upper ramp dipped homoclinally southwest and that depositional topography was largely the product of sedimentary rather than tectonic processes. Conversely, the irregular isopach pattern southwest of a major fault trace suggests that faulting was a key factor that differentiated the middle and lower ramp at that time. Oliver (1988) suggested that, although most normal faults in the Black Warrior basin formed during Ouachita orogenesis, some major faults may have been inherited from Early Cambrian extension. Evidence for local fault control in pre-orogenic strata of the Fort Payne Chert and the Tuscumbia Limestone supports this hypothesis.

PRIDE MOUNTAIN FORMATION AND HARTSELLE SANDSTONE

The Pride Mountain Formation and Hartselle Sandstone are Chesterian (Genevievian-Hombergian) in age (Drahovzal, 1967; Burdick and Strimple, 1982) and comprise three coarsening-upward shale-sandstone-limestone cycles that are named in ascending order the (1) Lewis cycle, (2) Evans cycle, and (3) Hartselle cycle (figs. 11, 12). Southwest of where the Hartselle Sandstone pinches out, strata equivalent to the Pride Mountain and Hartselle Formations are included in the Floyd Shale. The shale, sandstone, and limestone of the Lewis cycle are extremely widespread, whereas the two upper cycles comprise clinoformal parasequence sets that pass southwestward from more than 350 feet of shale, sandstone, and limestone into less than 50 feet of black shale that is included in the Floyd (Neal) Shale and contains radioactive zones (fig. 12).

LEWIS CYCLE

The Lewis cycle contains the Lewis sandstone, one of the principal hydrocarbon reservoirs in the Black Warrior basin (Epsman, 1987), and is assigned to the Genevievian and Gasperian stages of the Chesterian Series (Drahovzal, 1967; Thomas and others, 1979; Maples and Waters, 1987). The vertical sequence of the Lewis cycle is typical of Chesterian rocks in northwest Alabama, but carbonate and sandstone units in the cycle are unusually widespread, forming a veneer of sedimentary rock less than 150 feet thick that extends across the study area (figs. 9, 13, 14). Internally, that veneer is quite heterogeneous (figs. 9, 13) and contains diverse carbonate and siliciclastic lithofacies, which have been discussed in detail by Pashin and others (1991).

Thickness of the Lewis cycle is related to the Fort Payne-Tuscumbia ramp in three major ways. In the eastern part of the study area, the cycle is less than 50 feet thick, and the Lewis isopach pattern has no relationship to the Fort Payne-Tuscumbia pattern (figs. 10, 14). The Lewis cycle thickens to more than 75 feet in the northwest part of the study area, where isopach contours cut squarely across those on the Fort Payne-Tuscumbia map. In the southwest part of the study area, the Lewis cycle thickens to more than 100 feet across the upper part of the middle ramp (figs. 9, 10, 14). However, thickness of the Lewis cycle is not related to the major fault trace that affected Fort Payne-Tuscumbia sedimentation.

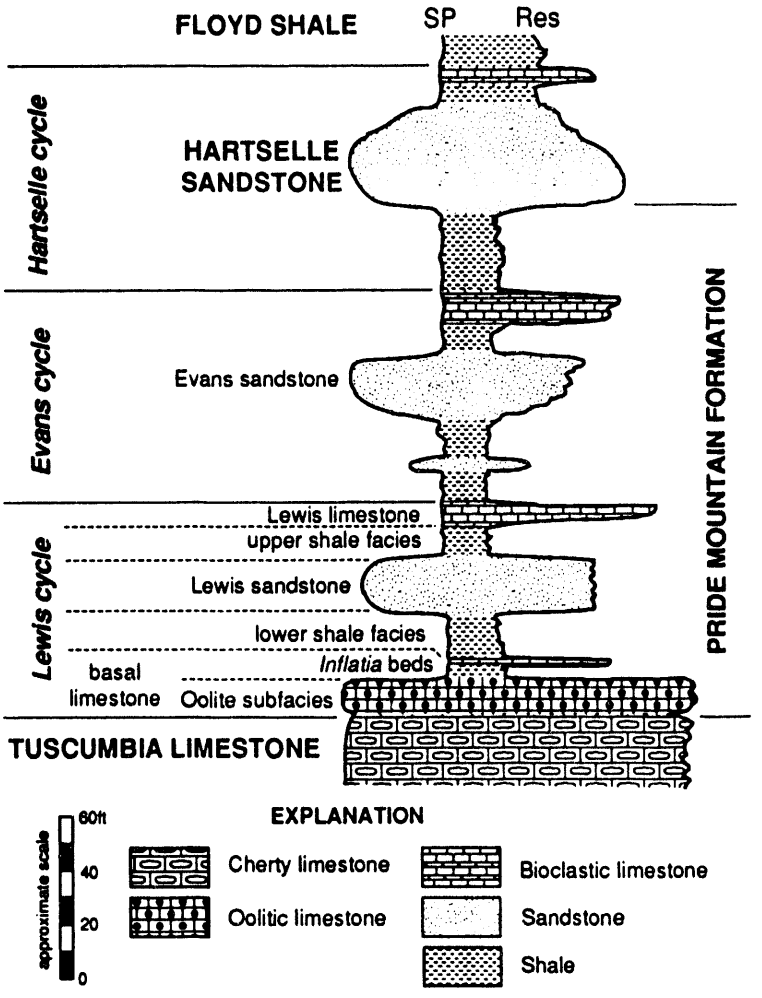

Figure 11.--Idealized geophysical well log showing stratigraphy of the Pride Mountain Formation and the Hartselle Sandstone.

Although the Lewis cycle is widespread, sandstone is present only in the western part of the study area (fig. 15). In Alabama, the sandstone is quartzarenite and is restricted to two main areas. The first corresponds with thickening of the Lewis cycle in the northwest part of the study area (figs. 14, 15), where Lewis sandstone is thinner than 25 feet. The second is in the western part of the map area, where the sandstone is typically 25 to 75 feet thick and is locally thicker than 100 feet. Isolith contours define irregular, lobate patterns of sandstone distribution in western Marion and northern Lamar Counties and define increasingly elongate patterns as the sandstone thins toward the southeast. In the southeast, the Lewis sandstone is developed mainly on the middle and lower ramp (fig. 9), and the elongate sandstone bodies parallel strike of the ramp (figs. 10, 15).

The transition from the upwelling-dominated ramp of the Fort Payne Chert and Tuscumbia Limestone to the cyclic succession of the Pride Mountain Formation represents a major change in depositional style. Predominance of black shale with radioactive zones in the southwestern part of the study area (fig. 12) indicates that circulation had become restricted from the ocean and that tectonic closure along the southwestern part of the Alabama promontory, and perhaps obduction of the accretionary prism, had begun. The widespread nature of Lewis sandstone and carbonate contrasts sharply with the

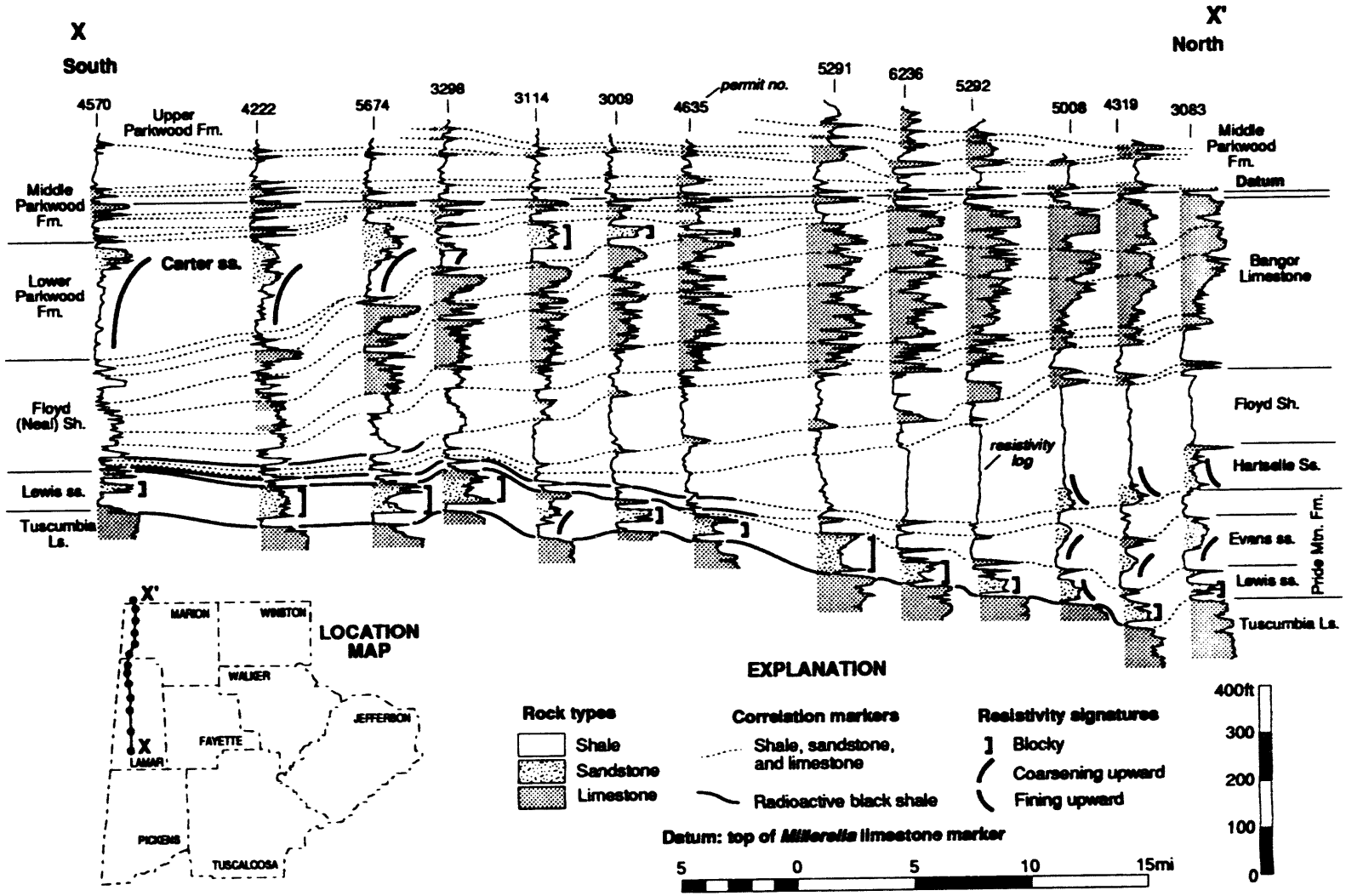

Figure 12.--Stratigraphic cross section showing facies relationships from the Tuscumbia Limestone through the base of the upper Parkwood Formation.

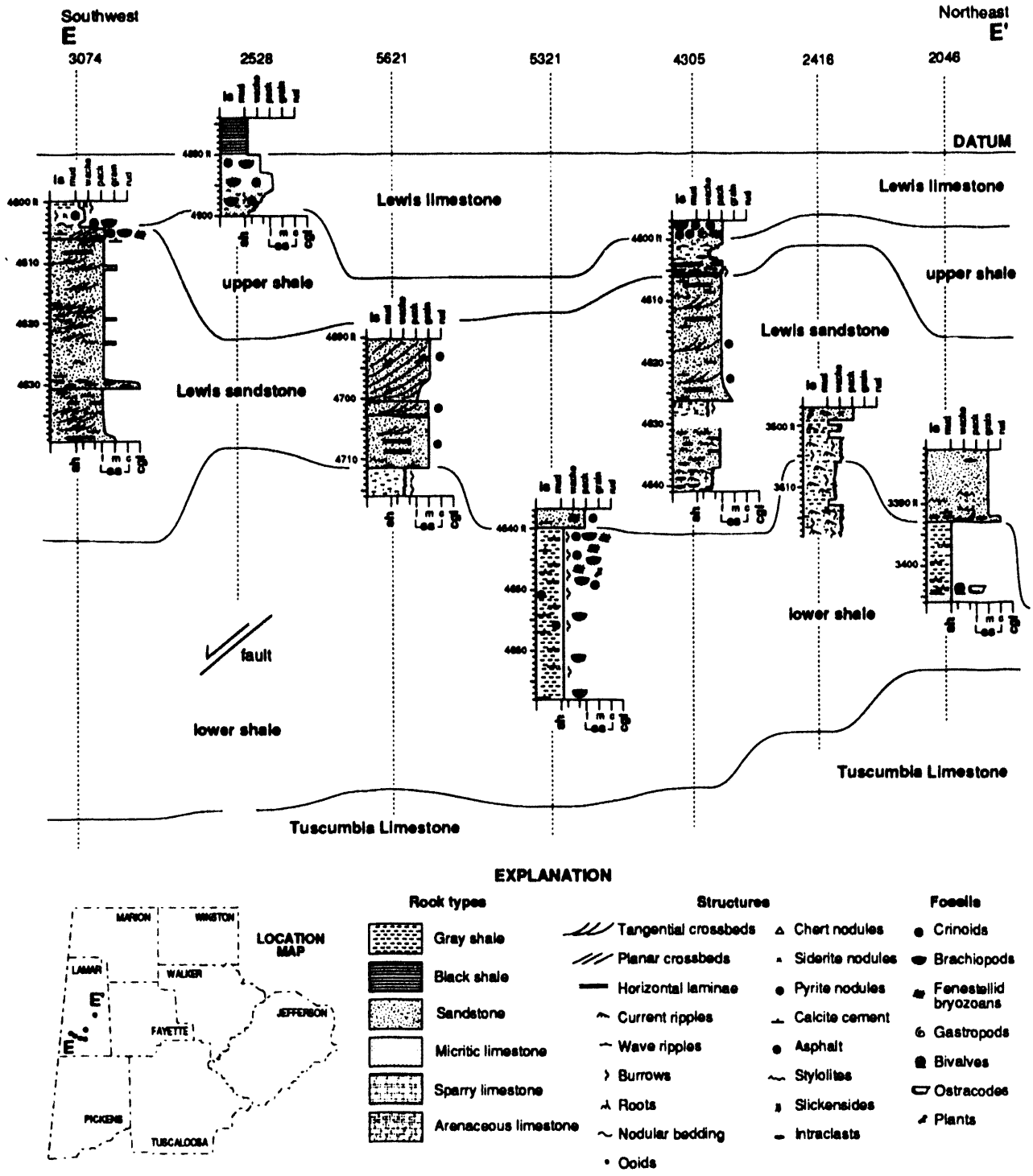

Figure 13.--Selected graphic logs of the Lewis cycle in southern Lamar County, Alabama.

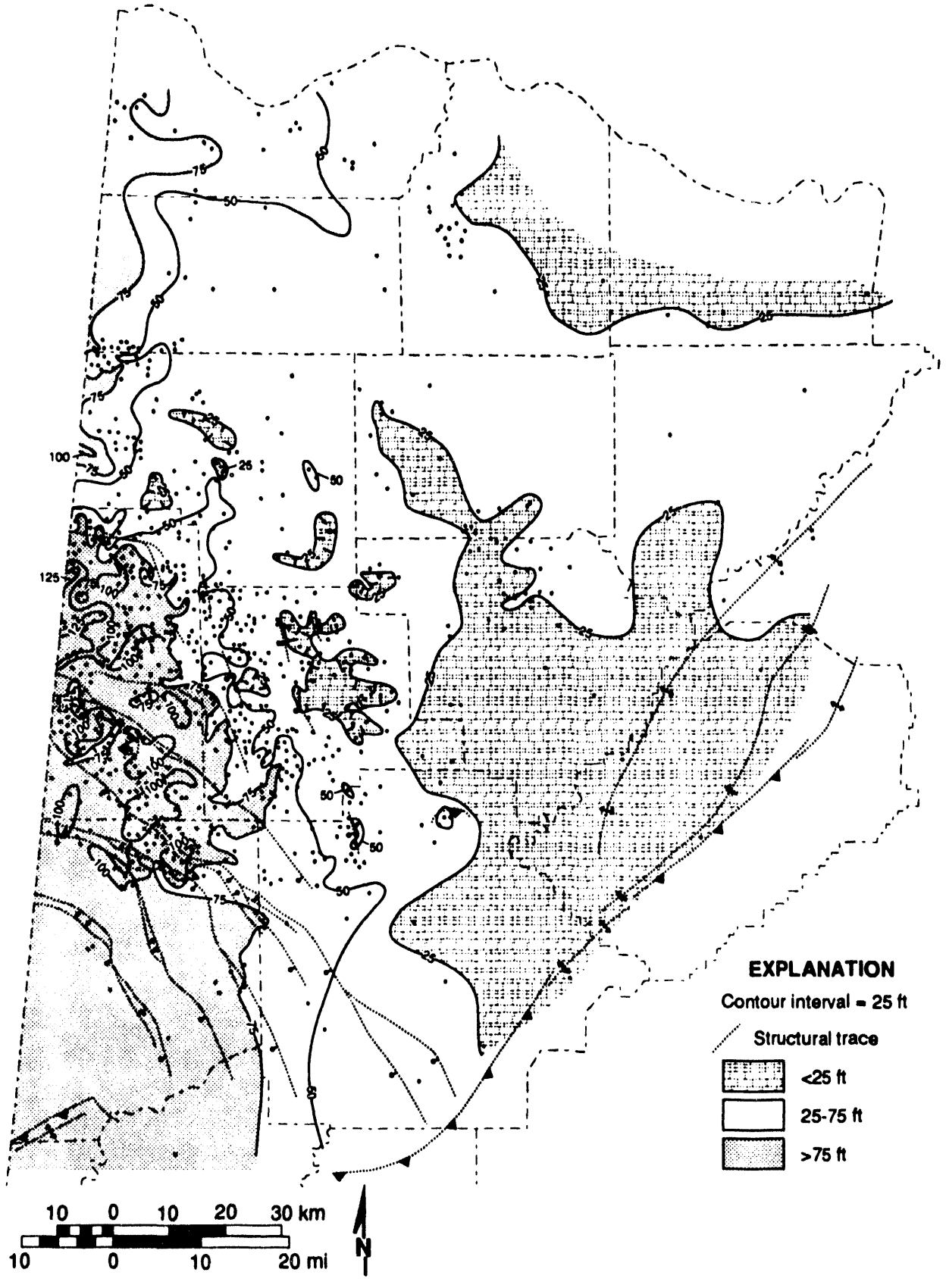

Figure 14.--Isopach map of the Lewis cycle.

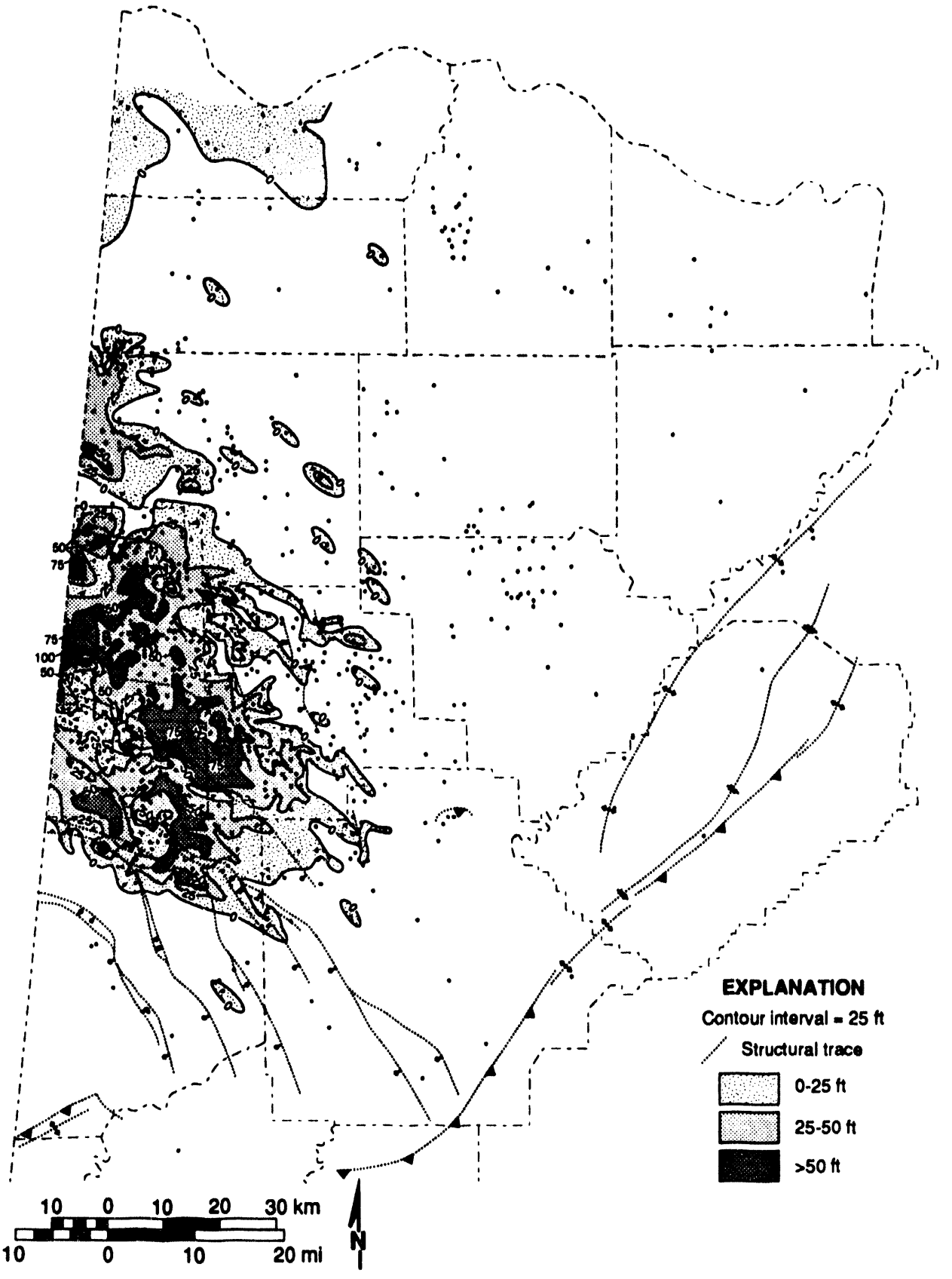

Figure 15.--Net sandstone isolith map of the Lewis sandstone.

clinoformal parasequence sets of overlying strata, which indicate progressive development of a prograding carbonate bank in the northeast (Bangor Limestone) and a starved basin in the southwest (Floyd Shale) (Scott, 1978; Pashin and Kugler, 1992).

Development of strike-parallel sandstone bodies and thickening of the Lewis cycle across the middle ramp in Fayette County (figs. 10, 14, 15) indicates that some topography developed during Fort Payne-Tuscumbia deposition remained effective into Chesterian time. As discussed by Stapor and Cleaves (1992), the Lewis sandstone resembles part of a lowstand wedge that is onlapped by the Lewis limestone (fig. 9). Flexural upwarping by formation of a forebulge in the Black Warrior basin may have been effective as a forcing agent that favored accumulation of the Lewis lowstand wedge on the lower ramp. Carbonate units of the Lewis cycle have been interpreted as transgressive units spanning intertidal to deeper, open-marine environments (DiGiovanni, 1984; Pashin and others, 1991). The Lewis sandstone, by contrast, has been interpreted to include regressive deltaic (Cleaves and Broussard, 1980; Cleaves and Bat, 1988; Thomas, 1988), shelf (Holmes, 1981; DiGiovanni, 1984), and beach deposits (Pashin and others, 1991).

Although the southwest margin of the Alabama promontory had changed from a passive margin to an active margin, pre-orogenic sea-floor topography remained an effective control on facies distribution. Pashin and others (1991) found that paleotopography atop the Fort Payne-Tuscumbia carbonate bank had a strong effect on Lewis sedimentation and regulated the distribution of unconformities, beaches, and carbonate shoals. On the lower ramp of southwest Lamar County, by contrast, the Lewis cycle lacks exposure features (fig. 13) and was deposited in exclusively subtidal environments. Maintenance of a southwestward paleoslope favors transport of siliciclastic Lewis sediment into the Black Warrior basin from a cratonic source, as proposed by Cleaves and Broussard (1980).

EVANS AND HARTSELLE CYCLES

The Evans and Hartselle cycles contain two reservoir sandstone units, the Evans sandstone and the Hartselle Sandstone (fig. 10), which have produced primarily gas. The Evans sandstone is productive primarily in Mississippi, where modest oil production also has been reported. By contrast, the Hartselle Sandstone is productive only in Alabama and contains the bulk of the state's tar-sandstone resources (Wilson, 1987).

The Evans and Hartselle cycles have a combined thickness of more than 375 feet in the northwest part of the study area and are thickest in an elongate area that trends southeast from Colbert County to Jefferson County (fig. 16) along the base of the upper ramp of the Fort Payne-Tuscumbia carbonate bank. The isopach interval is generally thicker than 200 feet in the northern part of the study area and thins gradually toward the east to less than 50 feet where it overlaps the Monteagle Limestone. Southwest of where the isopach interval is thickest, the Evans and Hartselle cycles thin in a distance of approximately 20 miles to less than 25 feet as they pass into Floyd black shale (figs. 12, 16).

The Evans sandstone consists mainly of fine- to medium-grained quartzarenite and is most widespread in Mississippi (Cleaves, 1983; Higginbotham, 1986; Cleaves and Bat, 1988). Butts (1926) suggested that strata assigned to the Evans cycle be included in the Gasperian stage. Evans sandstone is distinctive in well logs because it typically has a coarsening-upward resistivity signature (figs. 11, 12). Sandstone and limestone bodies assignable to the Evans cycle descend stratigraphically toward the southeast where they sit less than 20 feet above the Lewis limestone.

In Mississippi, the Evans sandstone is locally thicker than 150 feet and has a dominant northeast trend (Higginbotham, 1986; Cleaves and Bat, 1988), whereas in Alabama, the sandstone is thin, discontinuous, and has a generalized northwest-southeast trend (Cleaves and Bat, 1988). In Alabama, Evans sandstone bodies are distributed sporadically along the base of the upper ramp of the Fort Payne-Tuscumbia carbonate bank. Cores of Evans sandstone are lacking in Alabama, but in Mississippi, Bat (1987) established that the sandstone is dominantly medium grained quartzarenite. Sedimentary structures in the sandstone include current ripples, horizontal laminae, and low-angle, planar crossbeds. Near the top of the cycle are sandstone and mudstone units containing plant fossils and root structures.

According to Butts (1926), the Hartselle sandstone separates beds containing Gasperian and Hombergian faunas. Fossils in the Hartselle are similar to those in the overlying Hombergian strata, so the Gasperian-Hombergian boundary indeed appears to be near the base of the sandstone (Pashin and others, 1991). In the northwestern part of the study area, where the Evans cycle is thick, the Hartselle typically forms a single sandstone unit with a

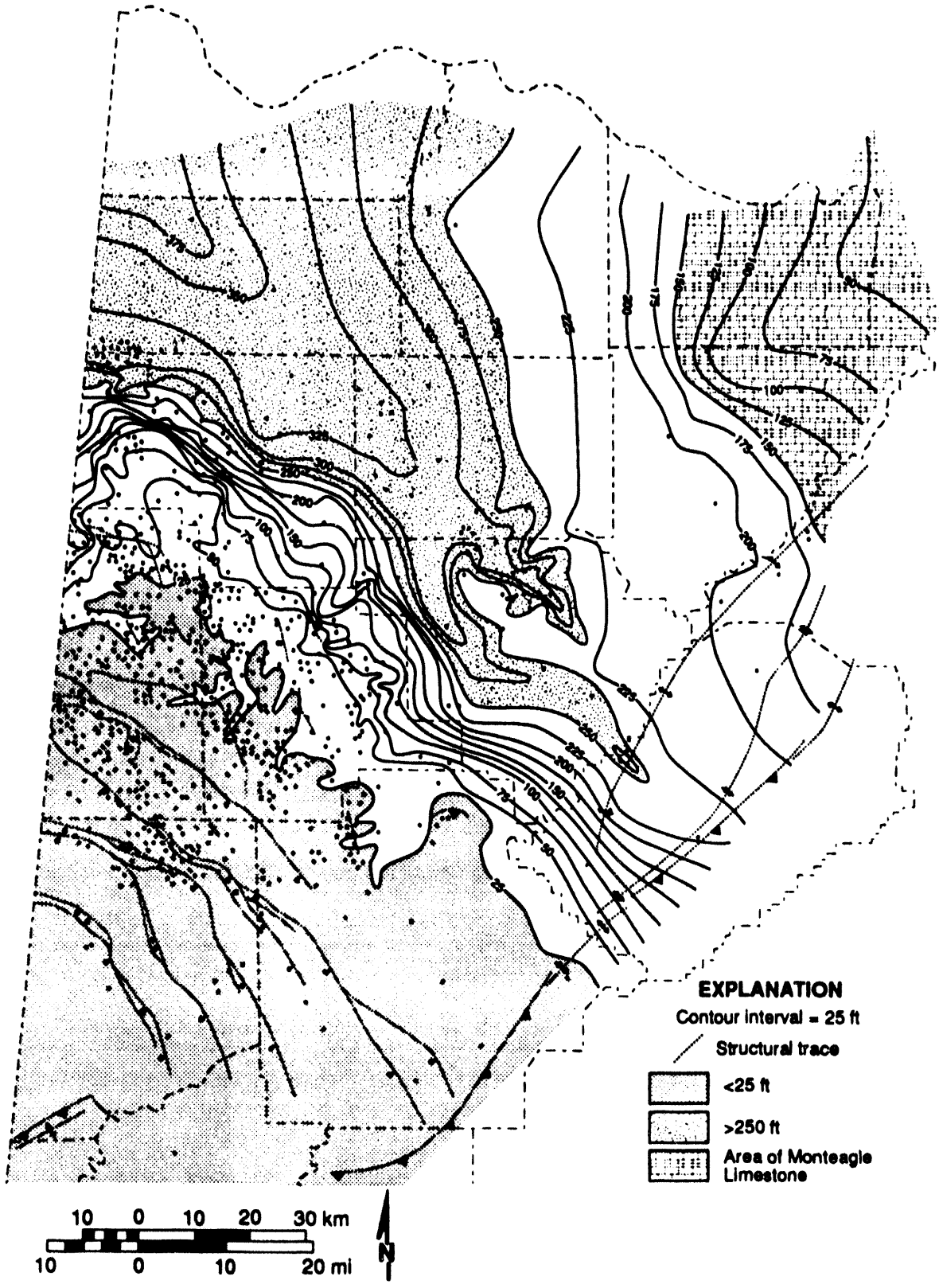

Figure 16.--Isopach map of the combined Evans and Hartselle cycles.

fining-upward resistivity signature (fig. 12). As the Evans cycle thins eastward, however, the Hartselle typically contains two stacked sandstone bodies, each commonly having a coarsening-upward resistivity signature. The Hartselle sandstone is thickest in the northwest part of the study area and is present in a series of elongate bodies that, westward from the Monteagle carbonate bank, extend progressively farther southeast (fig. 17). The sandstone thins northeastward as it overlaps the Monteagle Limestone. Southeast of the elongate sandstone bodies, sandstone thickness is irregular. The Hartselle Sandstone pinches out toward the southwest as the Evans and Hartselle cycles pass into Floyd Shale.

The Hartselle Sandstone is well exposed in northwest Alabama and contains distinctive lithofacies that have been described by Thomas and Mack (1982) and Pashin and others (1991). The base of the sandstone is sharp in the western part of the outcrop belt and is typically gradational in the eastern part. Near the base of the sandstone, horizontal laminae and low-angle, wedge-planar crossbeds are common. Where the sandstone is thickest, horizontal laminae are accompanied by scour fills with trough to planar-tabular crossbeds. The middle part of the Hartselle is dominated by sandstone and shale with wavy bedding, current ripples, and solitary crossbeds, many with reverse-reactivation structures. Wavy-bedded sandstone generally crops out between the elongate isopach maxima (fig. 17). Biogenic structures in wavy-bedded sandstone and shale include invertebrate traces, plants, and roots. The upper part of the sandstone is calcareous and is abundantly fossiliferous with brachiopods, fenestrate bryozoans, and crinoids. Eastward, horizontally laminated sandstone becomes less common, and marine fossils become increasingly abundant in all parts of the sandstone.

The Brooks core provides the only detailed record of the Hartselle Sandstone in the subsurface (fig. 18). The core penetrated the Hartselle near the southwest fringe of the formation and consists of very fine- to fine-grained sandstone that coarsens upward from Pride Mountain Shale. The lower part of the sandstone contains wavy- and flaser-bedded sandstone and shale with ripple-drift cross laminae, feeding burrows, and siderite. The upper part of the sandstone resembles the lower part but lacks shale. At the top of the sandstone is 3 inches of biopelsparite with abundant crinoid ossicles and pyrite nodules.

Thomas (1972a) was first to recognize beach deposits in the Evans cycle. Bat (1987) confirmed this hypothesis by documenting a coarsening-upward sequence with sandstone containing horizontal laminae and low-angle, planar crossbeds in the lower part and containing plants and roots in the upper part. However, the orientation of the beach systems and the source of the coarse siliciclastic sediment is a matter of controversy. Higginbotham (1986) and Thomas (1988) suggested that the Evans cycle contains deltaic deposits and associated beach and shelf-bar deposits that were fed from the Ouachita orogen. Alternatively, Cleaves (1983) and Cleaves and Bat (1988) suggested that the Evans represents a wave-dominated deltaic system that prograded southeast and was fed from a cratonic source.

Thomas and Mack (1982) recognized beach deposits in the Hartselle Sandstone on the basis of horizontal laminae and low-angle, wedge-planar crossbeds. They also interpreted the wavy-bedded sandstone and shale to represent backshore and offshore deposits. Pashin and others (1991) noted that backshore and offshore deposits can be distinguished readily on the basis of fossil content and further suggested that wavy-bedded sandstone with reverse-reactivation structures indicates development of Hartselle beach systems in an area with a significant tidal range. Burrowing in most of the Hartselle Sandstone in the Brooks core (fig. 18) suggests that the sandstone accumulated along the distal fringe of the shoreface.

As with the Evans cycle, virtually all workers agree that beach deposits are present, but controversy exists regarding the nature of Hartselle beach systems and the location of sediment sources. Thomas and Mack (1982) and Higginbotham (1986) interpreted the Hartselle as a series of shelf bars and barrier islands that prograded northeast from the Ouachita orogen onto the carbonate bank represented by the Monteagle Limestone. By contrast, Cleaves and Broussard (1980), Cleaves (1983), and Stapor and Cleaves (1992) interpreted the Hartselle as an elongate, wave-dominated deltaic complex that, like the Evans cycle, was fed from cratonic sources.

The clinoformal nature of the Evans and Hartselle cycles, which pass southwestward into fondoformal black shale (fig. 12), indicates development of prograding beach systems in the northern part of the study area and establishment of a starved basin in the southern part. Therefore, regional facies relationships support a cratonic source for Evans and Hartselle sandstone, and development of a starved basin reflects loading of the continental margin before the orogen gained relief sufficient to supply

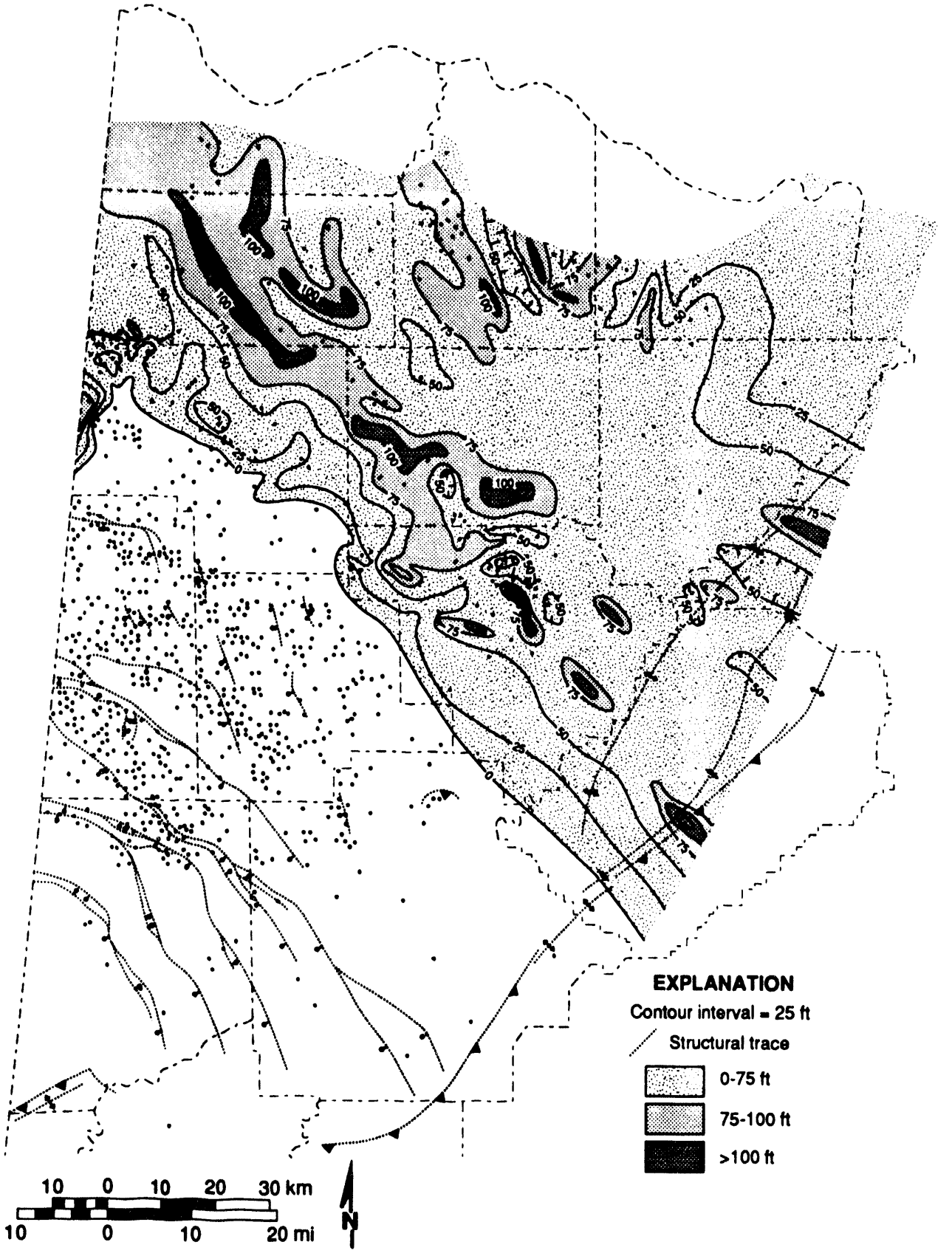

Figure 17.--Net sandstone isolith map of the Hartselle sandstone.

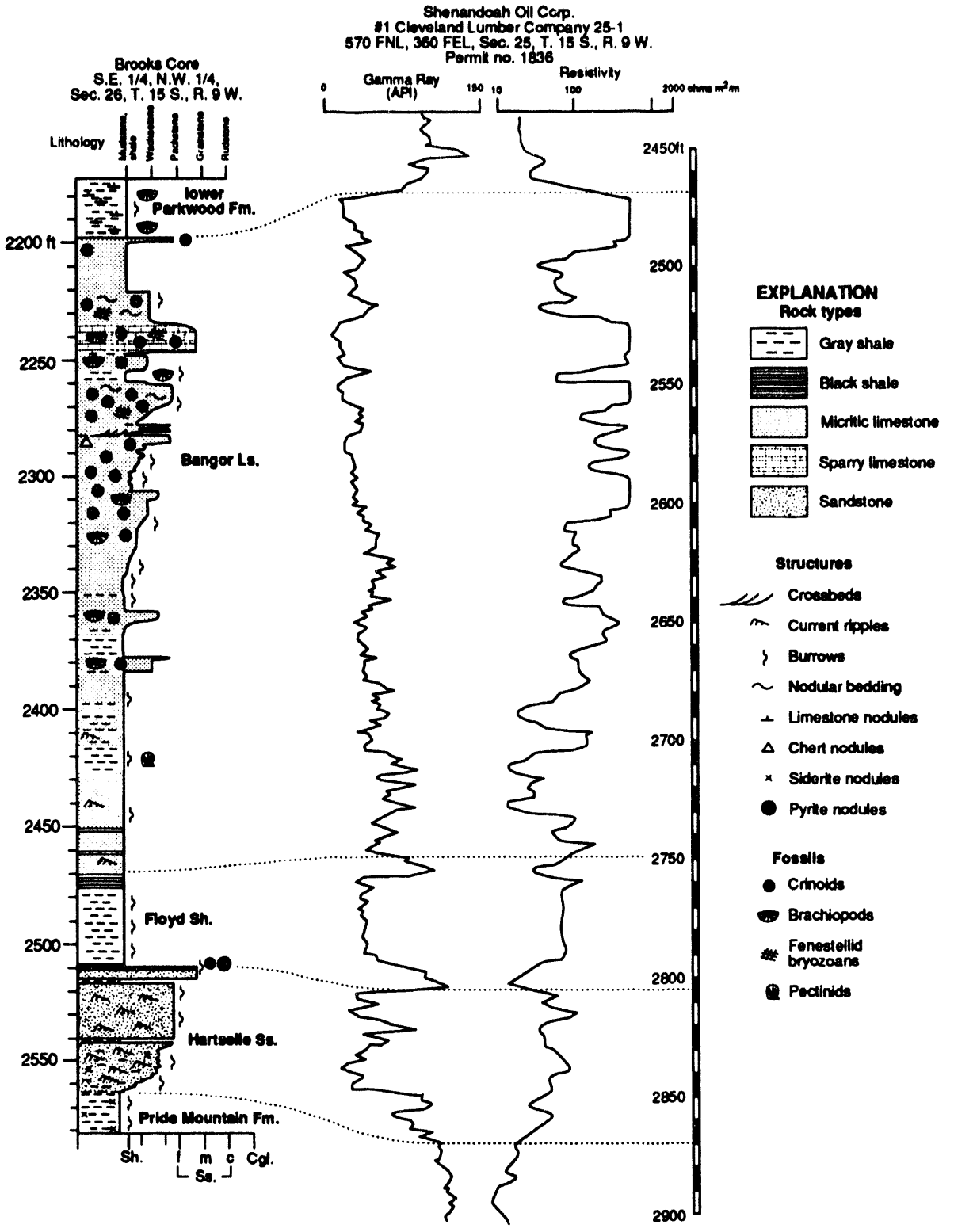

Figure 18.--Measured section of the Hartselle Sandstone through the Bangor Limestone.

sediment to the basin. The coarsening-upward signature of the Evans sandstone has been interpreted to represent highstand progradation of a wave-dominated delta (Cleaves and Bat, 1988; Stapor and Cleaves, 1992). One possibility is that the Evans represents the eastern half of a cuspate delta system that was fed through the Mississippi Valley graben.

In the northwest part of the study area, the fining-upward signature of the Hartselle Sandstone, not to mention a vertical transition from beach to open-marine facies, supports a transgressive origin, as proposed by Stapor and Cleaves (1992). A southeastward transition to coarsening-upward successions, however, indicates that as relative sea level rose, the Hartselle strandplain-barrier system prograded basinward and extended progressively farther southeast. An unusual aspect of Hartselle deposition is formation of barrier axes perpendicular to those in the Evans cycle and parallel to strike of the Fort Payne-Tuscumbia carbonate bank. One interpretation is that the Hartselle represents a delta-destructive strandplain that formed by transgressive reworking of the Evans deltaic system. As the deltaic system was reworked, sediment apparently was transported along strike of the Fort Payne-Tuscumbia ramp, thereby forming a siliciclastic rim that skirted the southern end of the Monteagle carbonate bank.

BANGOR LIMESTONE AND FLOYD SHALE

The Bangor Limestone contains a spectrum of carbonate rock types ranging from oolitic calcarenite to calcilutite (Thomas, 1972a; Scott, 1978; Andronaco, 1986) but has produced only a modest amount of hydrocarbons. In this study, the Bangor Limestone is synonymous with that of Welch (1958, 1959) and with the lower Bangor of Thomas (1988). A rich echinoderm fauna indicates that the lower part of the Bangor Limestone correlates with the Glen Dean Limestone of the Illinois basin and thus is near the top of the Hombergian stage (Butts, 1926; Drahovzal, 1967; Burdick and Strimple, 1982). Foraminifera confirm this interpretation and establish that the limestone extends into the Elviran stage (Rich, 1982).

The Bangor Limestone is composed of numerous shoaling-upward cycles (Andronaco, 1986), or parasequence sets, with a distinctive progradational stacking pattern (fig. 12). The parasequence sets contain limestone and gray shale in the northern part of the study area and, like the Evans and Hartselle cycles, pass southwestward into the black Floyd Shale. Thickness of the Bangor Limestone is fairly uniform in the northeastern part of the study area, typically ranging from 350 to 400 feet (fig. 19). A depocenter outlined by the 450-foot contour is in the northwest part of the study area and is developed just basinward of the Evans-Hartselle depoaxis (figs. 12, 19). Thomas (1972a) and Thomas and others (1979) indicated that major accumulations of oolitic grainstone are present in the northern part of the study area. According to Scott (1978), grainstone-dominated facies pass laterally into wackestone- and shale-dominated facies as the limestone thins. Well logs and sample sets further indicate that limestone is absent south of the 150-foot contour.

The Floyd Shale is distinctive because it is dark in color, brittle, and is rich in organic matter, including marine algae and other oil-prone kerogen. The shale is also distinctive because it is highly resistive and maintains the signature of the Bangor Limestone throughout the study area (fig. 12). Fossils are few in the resistive black-shale facies but include pectinids, brachiopods, and microgastropods. A tongue of the Floyd Shale extends into north Alabama and separates the Hartselle cycle from the Bangor Limestone; this shale has been mapped with the Bangor Limestone in outcrop (Szabo and others, 1988). This Floyd tongue crops out as poorly fissile, gray shale that contains a diverse assemblage of Hombergian fossils including colonial corals, crinoids, brachiopods, and bryozoans (Butts, 1926; Drahovzal, 1967). In the subsurface of Franklin and Marion Counties, the shale is commonly thicker than 200 feet, but the shale thins eastward and is locally absent.

As with other Mississippian units in the Black Warrior basin, the Brooks core contains the only detailed record of the Floyd Shale and the Bangor Limestone (fig. 18). The Floyd is composed mainly of bioturbated gray shale with intervals of black shale that are fissile, resistive, and radioactive. The contact with the Bangor Limestone is gradational, and fissile black-shale beds are present in the lower 20 feet of the limestone. The lower part of the Bangor is composed mainly of dark gray, argillaceous micrite interbedded with gray shale; graded beds, current ripples, and burrows are common. The middle part of the limestone is composed largely of medium-gray, bioturbated biomicrite, or more specifically, wackestone and packstone. The biomicrite forms stacked shoaling-upward cycles up to 40 feet thick and contains abundant crinoids and some productid brachiopods. In addition to biomicrite, the upper 50 feet of the limestone includes fossiliferous biosparite and light gray micrite.

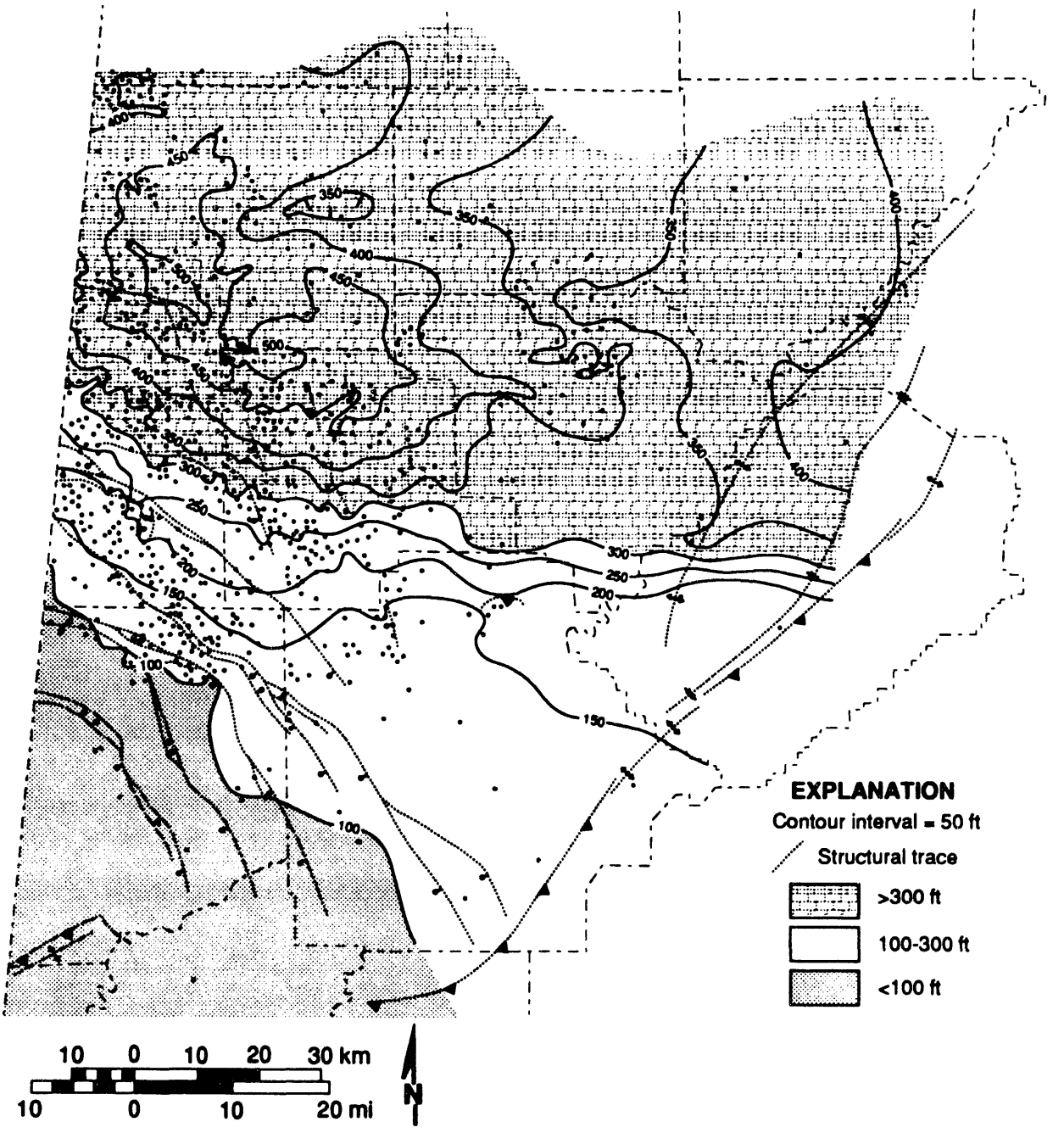

Figure 19.--Isopach map of the Bangor Limestone and equivalent strata in the Floyd Shale.

The Bangor Limestone represents establishment of a carbonate platform in the Black Warrior basin (Thomas, 1972a; Scott, 1978; Miesfeldt, 1985; Andronaco, 1986). Southwestward thinning of the Bangor and passage of oolitic grainstone into wackestone and shale suggests that agitated environments of the platform were bordered on the southwest by a carbonate ramp where deposition of lower-energy biomicrite and shale prevailed (Scott, 1978). Major accumulations of ooid grainstone near the southwest edge of the platform facies (Thomas, 1972a; Thomas and others, 1979) indicate

development of a shoaled bank rim like that which exists today on the leeward side of the Bahama Platform (Hine and others, 1981).

The resistive facies of the Floyd has been interpreted as a deep-water, basinal facies on the basis of dark color and fondoformal stratal geometry (Scott, 1978; Pashin and Kugler, 1992). High organic content and limited biotas suggest development of an oxygen-deficient basin. Indeed, equivalence of the resistive black shale to the Evans cycle through the top of the Bangor Limestone (fig. 12) indicates that starved-basin conditions persisted in the southern part of the study area from Gasperian to Elviran time. The richly fossiliferous tongue of Floyd Shale that extends northward into outcrop establishes that the Floyd also contains clinoformal and undaformal deposits. Clinoformal shale accumulated on the lower ramp. By contrast, undaformal shale in the northern part of the study area is interpreted to represent a muddy shelf transitional between the beach deposits of the Hartselle cycle and the carbonate platform deposits of the Bangor Limestone.

The clinoformal nature of strata from the Evans cycle through the Bangor limestone (fig. 12) suggests that the siliciclastic and carbonate units are more closely related than generally realized. Moreover, the Evans and Hartselle cycles apparently represent units of rank equal to the shoaling-upward cycles of the Bangor Limestone and Floyd Shale, which are interpreted as third-order parasequence sets. Progradation of the Bangor carbonate bank established a clinoformal slope well southwest of that which persisted from Fort Payne deposition through Hartselle deposition (figs. 10, 16, 19). This progradation further accentuated that slope as the starved basin was differentiated from the Bangor carbonate bank. Development of the Bangor bank had a profound effect on subsequent sedimentation and determined the distribution and quality of sandstone reservoirs in the Parkwood Formation, which account for more than 85 percent of the oil produced to date from the Black Warrior basin.

PARKWOOD FORMATION

The Parkwood Formation is a thick succession of shale, sandstone, and limestone that is divided into three major parts called the lower, middle, and upper Parkwood (figs. 12, 20, 21). The lower Parkwood Formation contains the Carter sandstone, the most prolific hydrocarbon reservoir in the Black Warrior basin. The middle Parkwood Formation contains the *Millerella* limestone, an important subsurface marker, but lacks major petroleum reservoirs. The upper Parkwood Formation is a thick, siliciclastic-dominated interval that spans the Mississippian-Pennsylvanian boundary and contains two important petroleum reservoirs called the Gilmer sandstone and the Coats sandstone.

LOWER PARKWOOD FORMATION

The lower Parkwood Formation is a thick, progradational interval that has been identified only in the subsurface of the Black Warrior basin. In the northern part of the basin, the lower Parkwood Formation overlies the Bangor Limestone, whereas in the southern part, the formation overlies the resistive facies of the Floyd Shale (fig. 12). Throughout the Black Warrior basin, the lower Parkwood Formation is overlain by limestone and shale of the middle Parkwood Formation. Biostratigraphic data are not available for the lower Parkwood Formation, but the position between the Bangor Limestone and the middle Parkwood Formation places it in the Elviran stage.

In Alabama, the lower Parkwood Formation has a maximum thickness of nearly 400 feet and thins markedly toward the northeast (figs. 12, 22). In Mississippi, the lower Parkwood is locally thicker than 1,000 feet (Mellen, 1947; Cleaves, 1981, 1983). Reservoir sandstone is absent in the northern part of the study area, where the lower Parkwood was identified as a shale marker that is commonly thinner than 10 feet. The Brooks core penetrated the lower Parkwood Formation northeast of the limit of reservoir sandstone and contains calcareous shale that is bioturbated and contains brachiopods (fig. 21).

The lower Parkwood contains four named reservoir sandstone units; these are, in ascending order, (1) Rea, (2) Abernathy, (3) Sanders, and (4) Carter (Cleaves, 1981, 1983; Nix, 1986; Thomas, 1988). Rea and Abernathy sandstone is present only in Mississippi and is equivalent to the shale forming the base of the upper two shoaling-upward cycles of the Bangor Limestone (Nix, 1991). Carter and Sanders reservoirs are widespread in Mississippi and Alabama (fig. 1), and because these units are closely related, they are designated only as Carter in regional cross sections. A net-sandstone isolith map of the lower Parkwood Formation shows that, in the former starved basin, the sandstone forms lobate to elongate bodies up to 200 feet thick that trend northeast (fig. 23). Along the margin of the carbonate bank, however, the sandstone is generally less than 50 feet thick and forms elongate bodies that trend southeast.

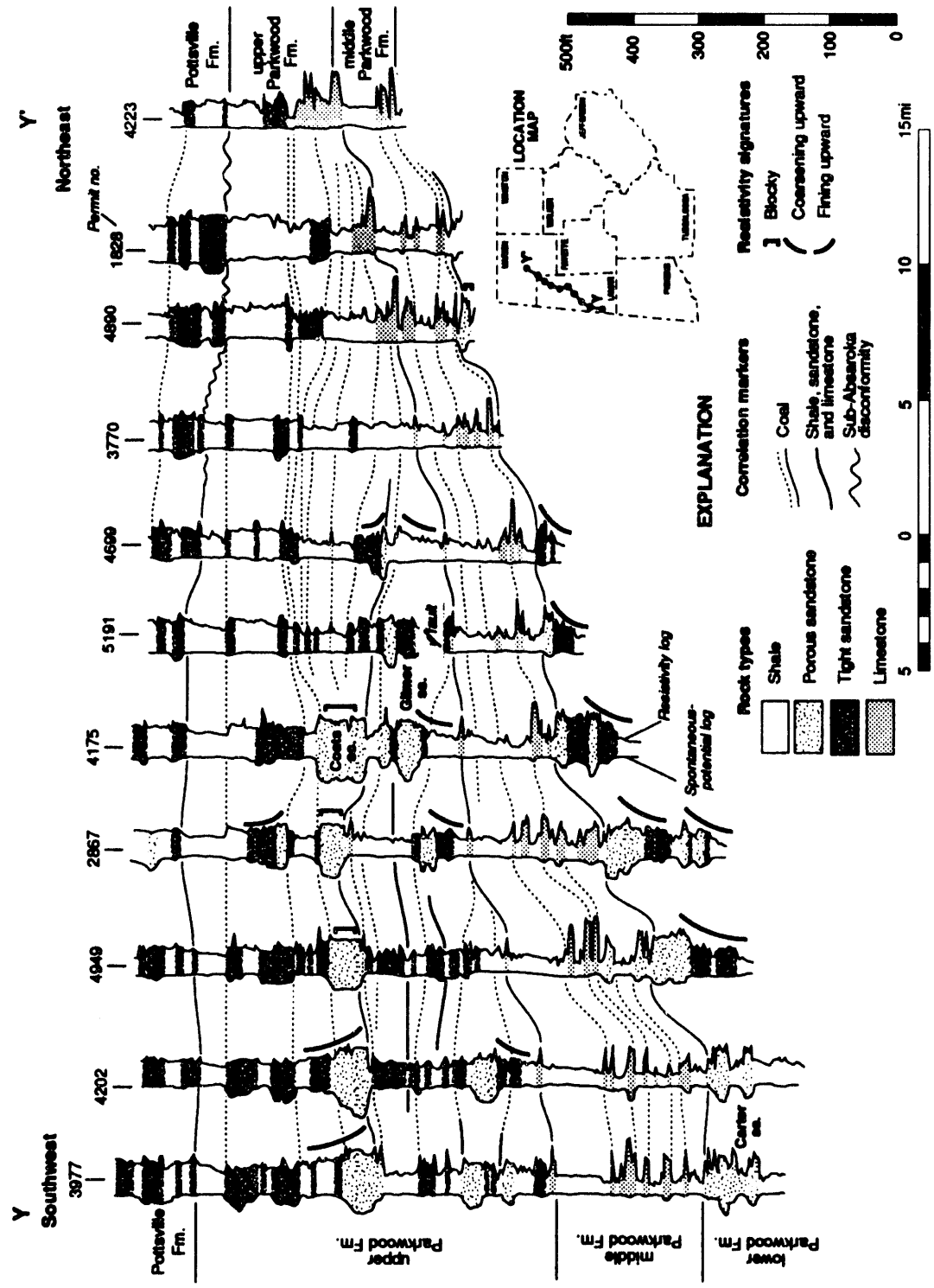

Figure 20.--Stratigraphic cross section showing facies relationships in the Parkwood Formation.

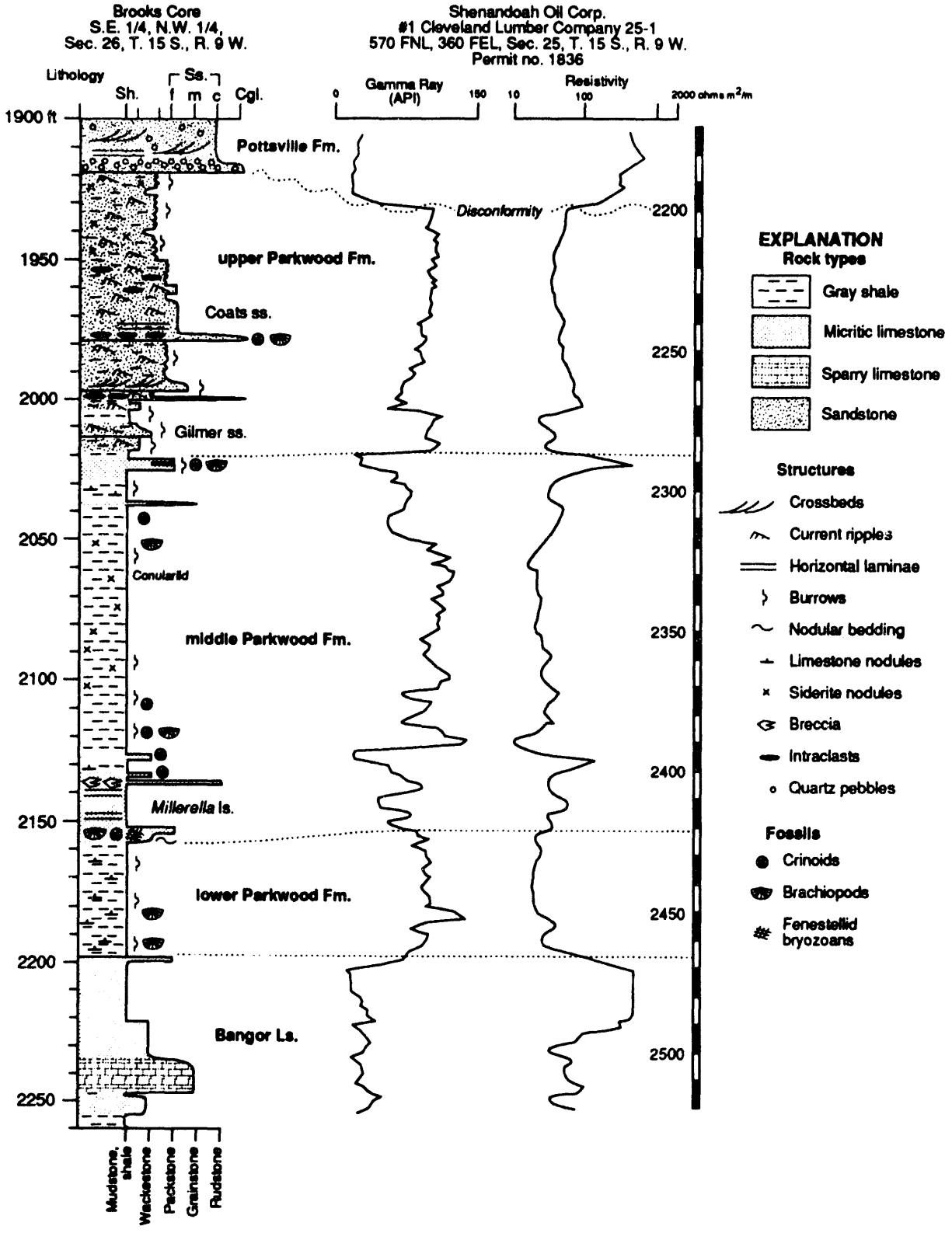

Figure 21.--Measured section of the Parkwood Formation.

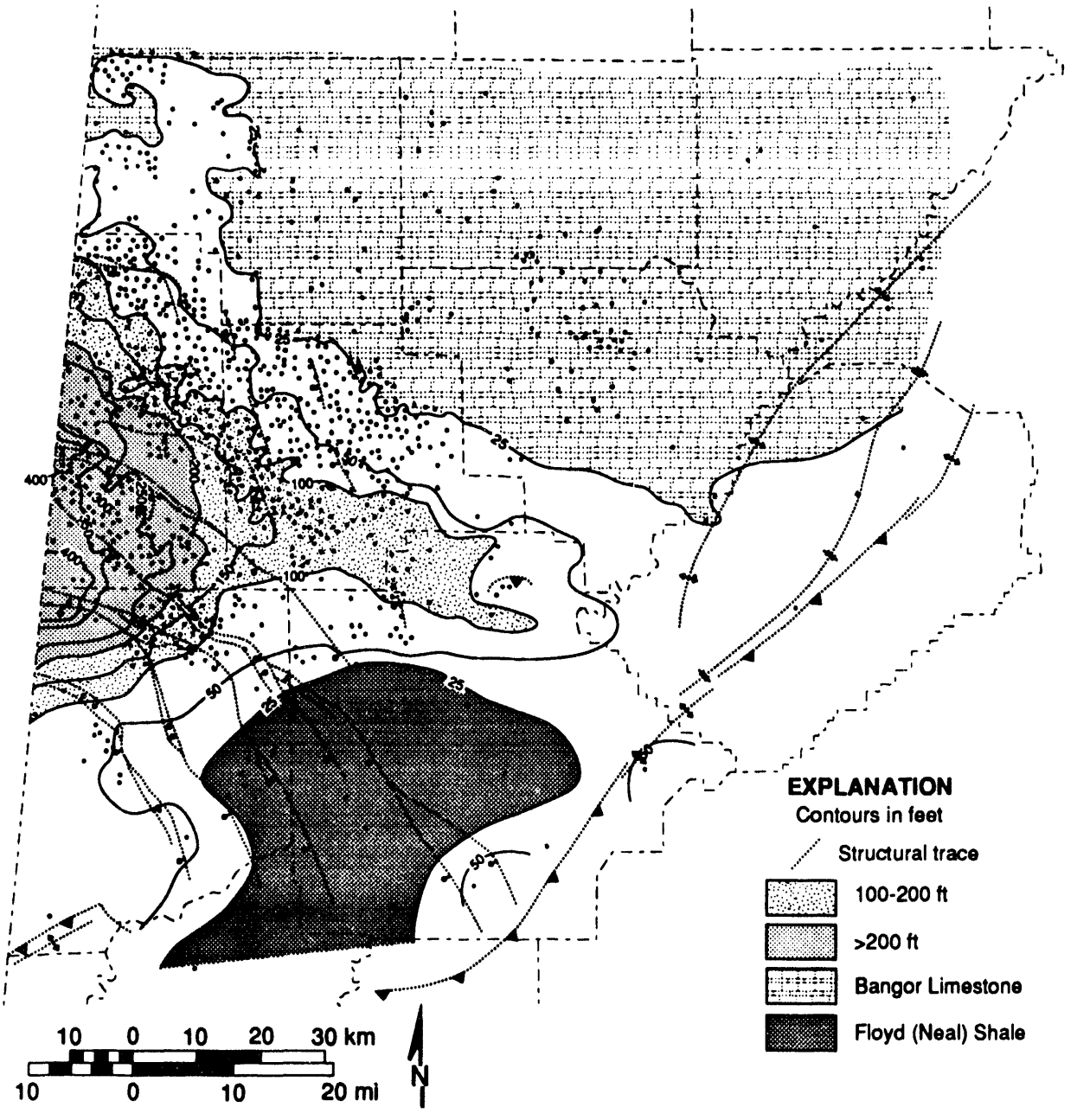

Figure 22.--Isopach map of the lower Parkwood Formation (modified from Pashin and Kugler, 1992).

In well logs, characteristics of the lower Parkwood Formation change markedly with respect to the Floyd starved basin and the Bangor carbonate bank (fig. 12). In the basinal area to the southwest, Carter sandstone typically has an irregular, coarsening-upward resistivity signature. In this area, the sandstone is locally thicker than 250 feet and forms east- to northeast-trending lobate to elongate bodies outlined by the 25-foot contour (fig. 23). Atop the carbonate bank, the Carter sandstone commonly has a blocky signature and is thinner than 50 feet. Isolith contours establish that most sandstone bodies in this area are elongate toward the southeast; many are connected to east- to northeast-oriented lobate

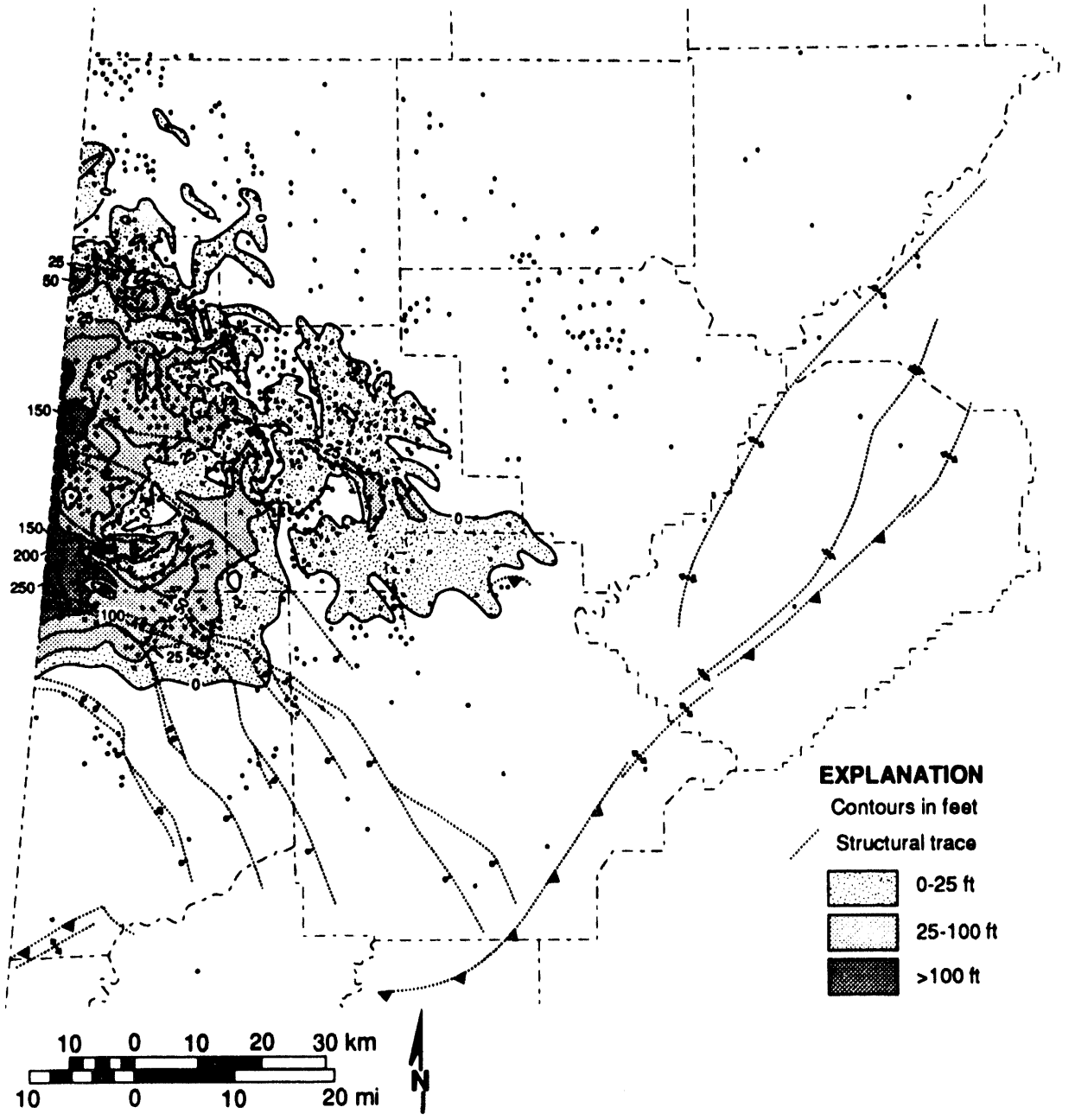

Figure 23.--Net-sandstone isolith map of the lower Parkwood Formation (modified from Pashin and Kugler, 1992).

and elongate bodies. Most Carter oil production is from sandstone with a blocky well-log signature (Pashin and Kugler, 1992). Numerous cores of this sandstone are available and are described in a later section on facies heterogeneity in the Carter sandstone.

The lower Parkwood Formation has been interpreted to include delta, beach, and shelf deposits (Shepard, 1979; Cleaves and Broussard, 1980; Cleaves, 1981, 1983; Bearden and Mancini, 1985; Nix, 1986, 1991; Thomas, 1988), but sediment sources are controversial. One school of thought favors a southwestern source in the Ouachita orogen (Thomas, 1988; Nix, 1986, 1991). The other school, alternatively, favors a cratonic source in the north or northwest (Welch, 1978; Shepard, 1979; Cleaves

and Broussard, 1980; Cleaves, 1981, 1983; Bearden and Mancini, 1985). Most researchers have emphasized depositional systems and sediment source areas, but the importance of pre-Parkwood depositional topography on Carter sedimentation and reservoir characteristics has been overlooked.

Following progradation of the Bangor carbonate bank, siliciclastic sediment of the lower Parkwood Formation began prograding. The lower Parkwood Formation represents partial filling of the starved basin and progradation of deltaic clastics onto the Bangor carbonate bank from the southwest, thereby reversing regional paleoslope (Pashin and Kugler, 1992), suggesting that the lower Parkwood represents the earliest infilling of the basin with orogenic sediment. The isopach map demonstrates that part of the starved basin remained unfilled after lower Parkwood progradation (fig. 22). An elongate body of sediment thicker than 100 feet extends into northern Tuscaloosa County and is interpreted to represent distal deltaic sediment that accumulated along the bank margin.

The major lobate and elongate sandstone bodies in Lamar and Pickens Counties are interpreted to represent constructive, deep-water delta lobes on the basis of thickness, geometry, log signature, and location in the former starved basin. Previous investigators established that much of the blocky sandstone is quartzarenite that accumulated in beach environments (Nix, 1986, 1991; Kugler and Pashin, 1992; Pashin and Kugler, 1992). The apparent downlapping relationship of blocky beach sandstone to the coarsening-upward, deep-water delta deposits (fig. 12) indicates that beaches formed by delta destruction during or shortly after relative lowstand. Another factor contributing to delta destruction was simply progradation onto the carbonate bank where a shallow receiving basin contributed to marine reworking and beach formation. In short, the best Carter oil reservoirs are interpreted as a part of a destructive, wave-influenced, shoal-water delta complex.

MIDDLE PARKWOOD FORMATION

In contrast to the lower Parkwood Formation, the middle Parkwood is composed mainly of limestone and shale with a lesser amount of sandstone (figs. 12, 20, 21). With the exception of the Fort Payne Chert and Tuscumbia Limestone, limestone units in the middle Parkwood Formation are the most widespread carbonate markers in the Mississippian System of Alabama (Welch, 1958; Miesfeldt, 1985; Thomas, 1988). Welch (1958, 1959) recognized red shale within and above the middle Parkwood and thus correlated the limestone with similar limestone and red shale in the Pennington Formation which crops out above the Bangor in northeastern Alabama and extends into Virginia. Foraminifera in the *Millerella* limestone are similar to those identified by Rich (1980) in the Pennington Formation, thus supporting this interpretation.

The *Millerella* limestone marker is near the base of the middle Parkwood and is associated with numerous other limestone markers less than 20 feet thick (figs. 12, 20, 21). Among these markers are localized sandstone bodies that are significant oil reservoirs in Alabama (Cleaves, 1983; Nix, 1991). These limestone and sandstone units have an aggradational stacking pattern and are overlain by a widespread shale unit that has a coarsening-upward log signature and passes northeastward into a limestone facies (fig. 12). The Cooper sandstone (fig. 1), which has produced only a minor amount of gas, is within this shale unit and is present only in Pickens and Tuscaloosa Counties. The top of the middle Parkwood Formation is marked by thin, widespread limestone beds that form distinctive resistivity markers. These limestone markers have a weak, progradational stacking pattern, reflecting intertonguing with the upper Parkwood Formation (fig. 12).

The middle Parkwood Formation is thicker than 700 feet in the southern part of the study area and is locally absent in the northern part (fig. 24). Thickness of the middle Parkwood is generally uniform northeast of the 100-foot contour and is less than 250 feet where it overlies the Bangor Limestone and the Carter sandstone (fig. 24). The middle Parkwood thickens dramatically south of this area and is thicker than 500 feet where it overlies the Floyd Shale. The *Millerella* sandstone is present only in the west-central part of the study area where the Carter sandstone also is present (figs. 23, 25). The *Millerella* sandstone is generally thinner than 25 feet but is locally thicker than 50 feet. The sandstone is thickest and most widespread in the area containing thick, lobate sandstone bodies in the lower Parkwood Formation. Farther northeast, the *Millerella* sandstone forms elongate bodies that parallel those in the Carter sandstone.

In the northern part of the study area, the *Millerella* limestone includes grainstone with abundant endothyrid foraminifera (Welch, 1958) and also contains oolitic grainstone similar to that in the Bangor Limestone (Miesfeldt, 1985). As the middle Parkwood thickens southward, the *Millerella* limestone contains dominantly micritic carbonate and also contains radioactive black shale. No cores of

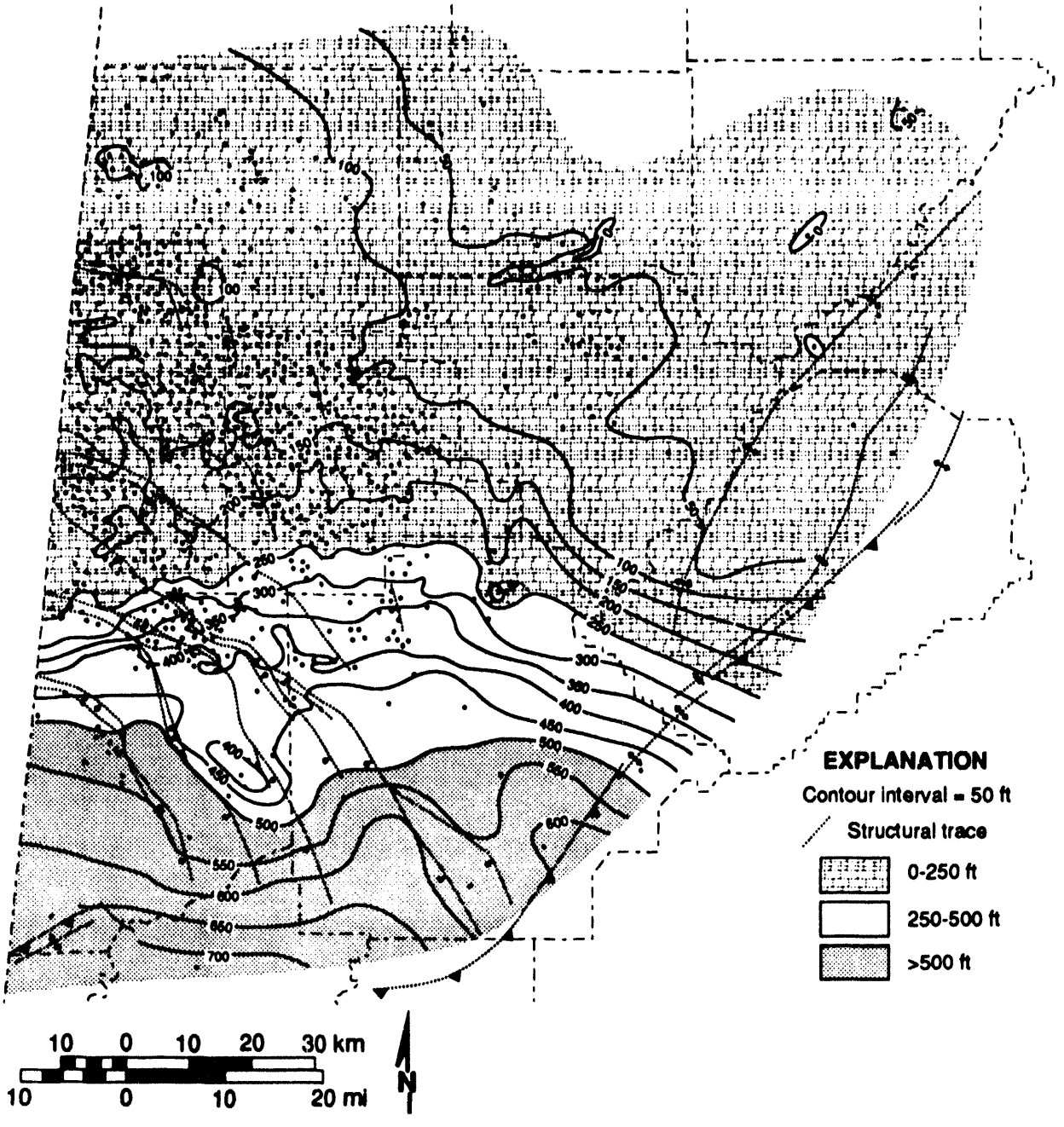

Figure 24.--Isopach map of the middle Parkwood Formation.

Millerella sandstone are available, but the Brooks core contains a complete section of the middle Parkwood Formation (fig. 21). At the base of the middle Parkwood, the *Millerella* limestone contains mostly laminated micrite and fossiliferous biomicrite, or wackestone and packstone. Also within the limestone is a brecciated layer containing hematitic fracture fills and clasts with bleached cutans. The shale above the *Millerella* limestone contains numerous siderite nodules and is fossiliferous and bioturbated, whereas the limestone beds that mark the top of the Middle Parkwood Formation are composed of biomicrite resembling that in the Bangor Limestone.

The onlapping relationship of the middle Parkwood Formation to the lower Parkwood Formation

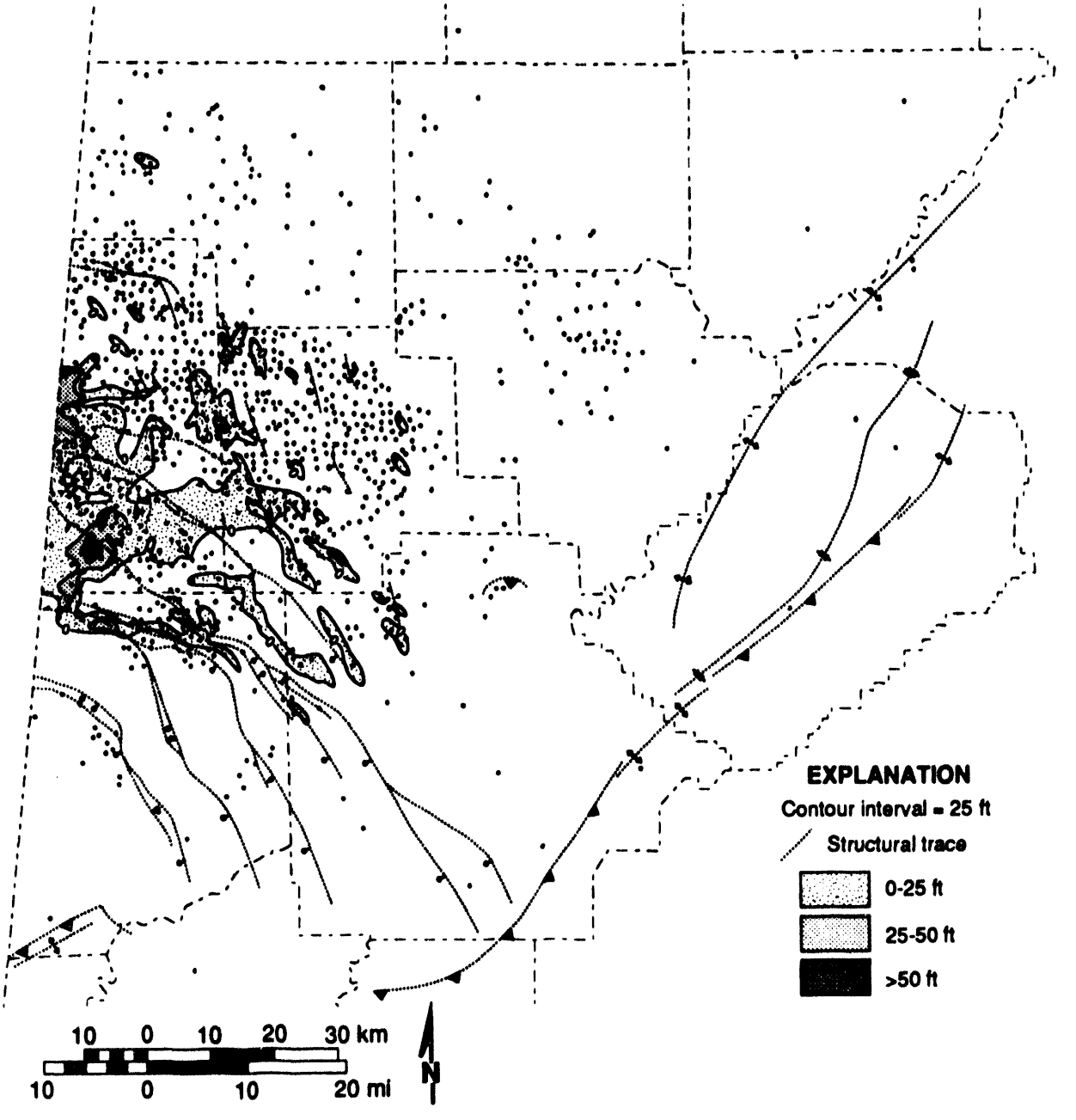

Figure 25.--Net-sandstone isolith map of the *Millerella* sandstone.

and the aggradational nature of the *Millerella* limestone (fig. 12) indicate deposition during marine transgression. The close relationship of the *Millerella* sandstone to the Carter sandstone suggests that the *Millerella* formed during the late stages of delta destruction, recording inundation and reworking of much of the Carter delta plain, as already suggested by Cleaves (1983) and Nix (1986, 1991). The precise depositional environment of the *Millerella* sandstone is unclear because of a lack of core, but the close relationship to the Carter sandstone suggests that the *Millerella* represents beach and shallow-shelf sandstone bodies.

Thickening of the middle Parkwood Formation south of the Bangor carbonate bank and the Carter deltaic system (figs. 19, 22, 24) indicates that mid-

die Parkwood sediment filled the remaining part of the starved basin. Oolitic grainstone indicates that shallow-water, platformal carbonate deposition prevailed in the northern part of the study area, and the breccia zone with bleached cutans (fig. 21) indicates that parts of the platform were exposed. Predominance of micritic limestone and black shale in the southern part of the study area suggests development of a lower-energy carbonate ramp in the former starved basin.

The shale interval containing the Cooper sandstone is interpreted to represent highstand progradation of deltaic systems that provided sediment sufficient to finally fill the starved basin. The onlapping relationship of the limestone markers at the top of the middle Parkwood Formation to the underlying shale indicates that, as the basin was filled, a minor transgression interrupted deltaic progradation, resulting in renewed carbonate deposition across the study area. However, the weakly clinoformal nature of the carbonate markers (fig. 12) signifies renewed progradation of siliciclastic sediment into the Black Warrior basin during deposition of the upper Parkwood Formation.

UPPER PARKWOOD FORMATION

The upper Parkwood Formation (figs. 20, 21) is a thick siliciclastic succession that contains shale, sandstone, and thin, discontinuous coal beds (Butts, 1926; Thomas, 1972a; Miesfeldt, 1985) and forms the top of the Kaskaskia sequence in the Black Warrior basin. Red shale and discontinuous limestone beds are most abundant near the base of the upper Parkwood. In outcrops of the Appalachian fold-and-thrust belt in Alabama, invertebrate fossils indicate that the lowermost part of the succession is of Elviran age, whereas foraminifera, plant fossils and palynomorphs indicate that the upper Parkwood is of Pocahontasian (earliest Pennsylvanian) age (Butts, 1926; Moore, 1944; Wanless, 1975; Rich, 1980; Jennings and Thomas, 1987). Hence, the Mississippian-Pennsylvanian boundary has been interpreted to be conformable in these outcrops.

The upper Parkwood Formation is thicker than 950 feet in the southwest part of the study area and thins markedly toward the northeast where it is locally absent (figs. 20, 26). As the upper Parkwood thins, siliciclastic rocks become finer grained and interfinger with carbonate rocks. Two reservoir sandstone units, the Gilmer sandstone and the Coats sandstone, are thickest in the southwestern part of the study area and range in composition from quartzarenite (porous sandstone) to litharenite (tight sandstone). These sandstone units can be distinguished readily in geophysical well logs on the basis of stratigraphic position and resistivity signature (fig. 20). The Chandler sandstone, which is typically included in the Pottsville Formation (fig. 1), is in reality equivalent to the Coats sandstone and was accordingly mapped with the Coats.

The Gilmer sandstone has a characteristic coarsening-upward log signature and is interpreted to be a clinoformal unit that thins northeast and merges with the limestone facies (fig. 20). The sandstone is locally thicker than 100 feet, and isolith contours outline numerous lobate to elongate sandstone bodies that trend northeast (fig. 27). The Coats sandstone, by contrast, has a characteristic fining-upward to blocky log signature and is equivalent to clinoformal parasequence sets that step backward relative to those associated with the Gilmer (fig. 20). Like the Coats sandstone, the Gilmer has a northeast-trending, lobate to elongate geometry (fig. 28). In Pickens County, the Coats sandstone is thickest in two linear axes where Gilmer sandstone is absent (figs. 27, 28). Above the Coats sandstone, the upper Parkwood formation contains dominantly tight sandstone and shale that are not productive of hydrocarbons (fig. 20). This uppermost siliciclastic interval extends northeast above the upper Parkwood limestone units and is truncated below the Pottsville Formation.

Gilmer and Coats sandstone are present in the Brooks core and are composed of litharenite and shale with siderite nodules (fig. 21). The Gilmer is represented by 18 feet of interbedded sandstone and shale with wavy, flaser, and lenticular bedding as well as feeding and dwelling burrows. The Coats sandstone, by contrast, comprises three stacked, fining-upward cycles with intraclastic conglomerate near the base and interbedded sandstone and shale wavy, flaser, and lenticular bedding near the top. The conglomerate beds contain mainly shale and siderite pebbles, and one layer contains crinoids and brachiopods. Unfortunately, cores are not available where the Gilmer and Coats are producing reservoirs.

Most investigators have characterized the upper Parkwood as a major deltaic sequence that prograded northeastward (Thomas, 1972a, 1988; Cleaves, 1983; Miesfeldt, 1985), and the immature, lithic nature of upper Parkwood sandstone has been interpreted to represent unroofing of volcanic and metamorphic terranes in the Ouachita orogen (Mack and others, 1981, 1983). Because the starved basin was full with sediment prior to upper Parkwood deposition, southwestward thickening of the

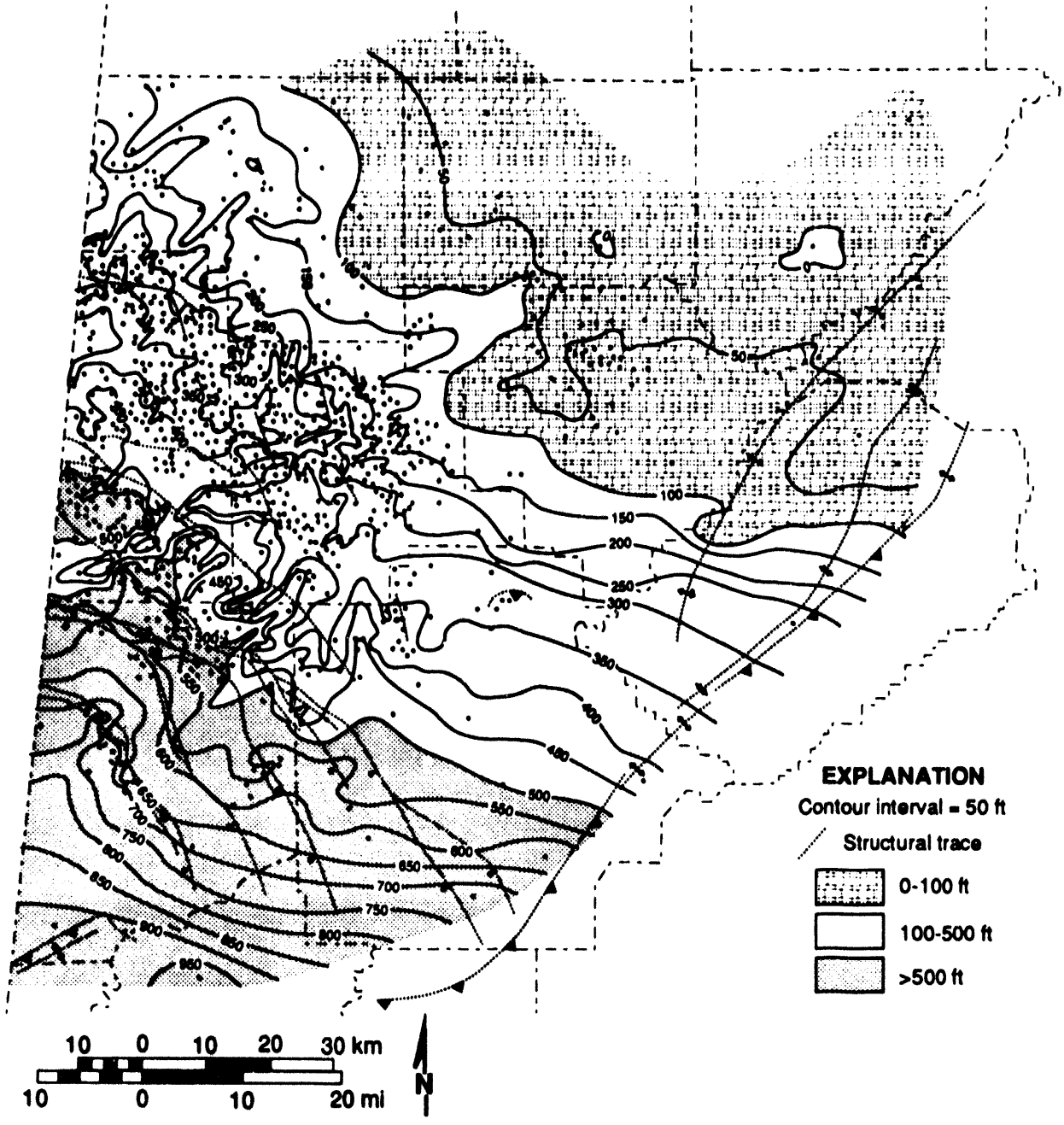

Figure 26.--Isopach map of the upper Parkwood Formation.

upper Parkwood is interpreted to be more the product of tectonic subsidence than depositional topography and differential compaction, which controlled sediment thickness and facies distribution so strongly during Chesterian time. Furthermore, the transition from carbonate rocks to siliciclastic, coal-bearing rocks during upper Parkwood deposition signifies development of a more humid coastal plain as the Appalachian region drifted toward the equatorial rainy belt.

The lobate to elongate geometry of Gilmer and Coats sandstone and the association of these units with clinoformal strata (figs. 20, 27, 28) support a deltaic origin. The stacked, fining-upward cycles in the Brooks core (fig. 21) are typical of tidal-flat deposits (van Beek and Koster, 1972), and similar cy-

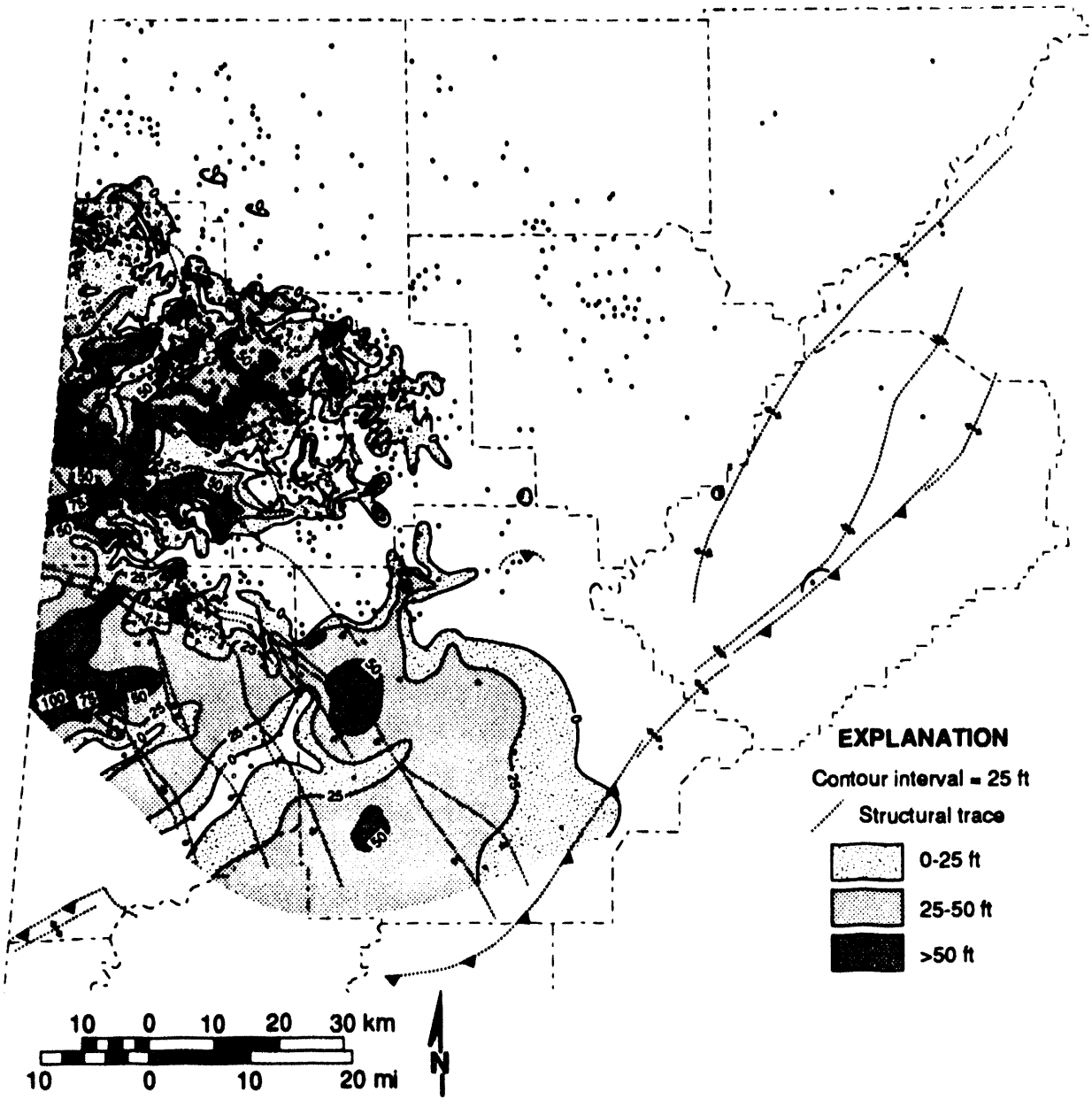

Figure 27.--Net-sandstone isolith map of the Gilmer sandstone.

cles are common in other Pennsylvanian rocks in Alabama (Pashin and Carroll, 1993). In the absence of other cores, however, classifying upper Parkwood deltas in terms of wave, tide, and fluvial energy is difficult, and most interpretations have to be based on geophysical well logs.

The coarsening-upward signature of the Gilmer sandstone (fig. 20) is interpreted to represent renewed highstand progradation of a constructive delta system following regional marine transgression at the close of middle Parkwood deposition. The sharp base of the Coats sandstone (figs. 20, 21), by contrast, is interpreted as a lowstand surface of erosion. This interpretation is supported by the absence of Gilmer sandstone below the thick, axial Coats sandstone bodies in Pickens County (figs. 27,

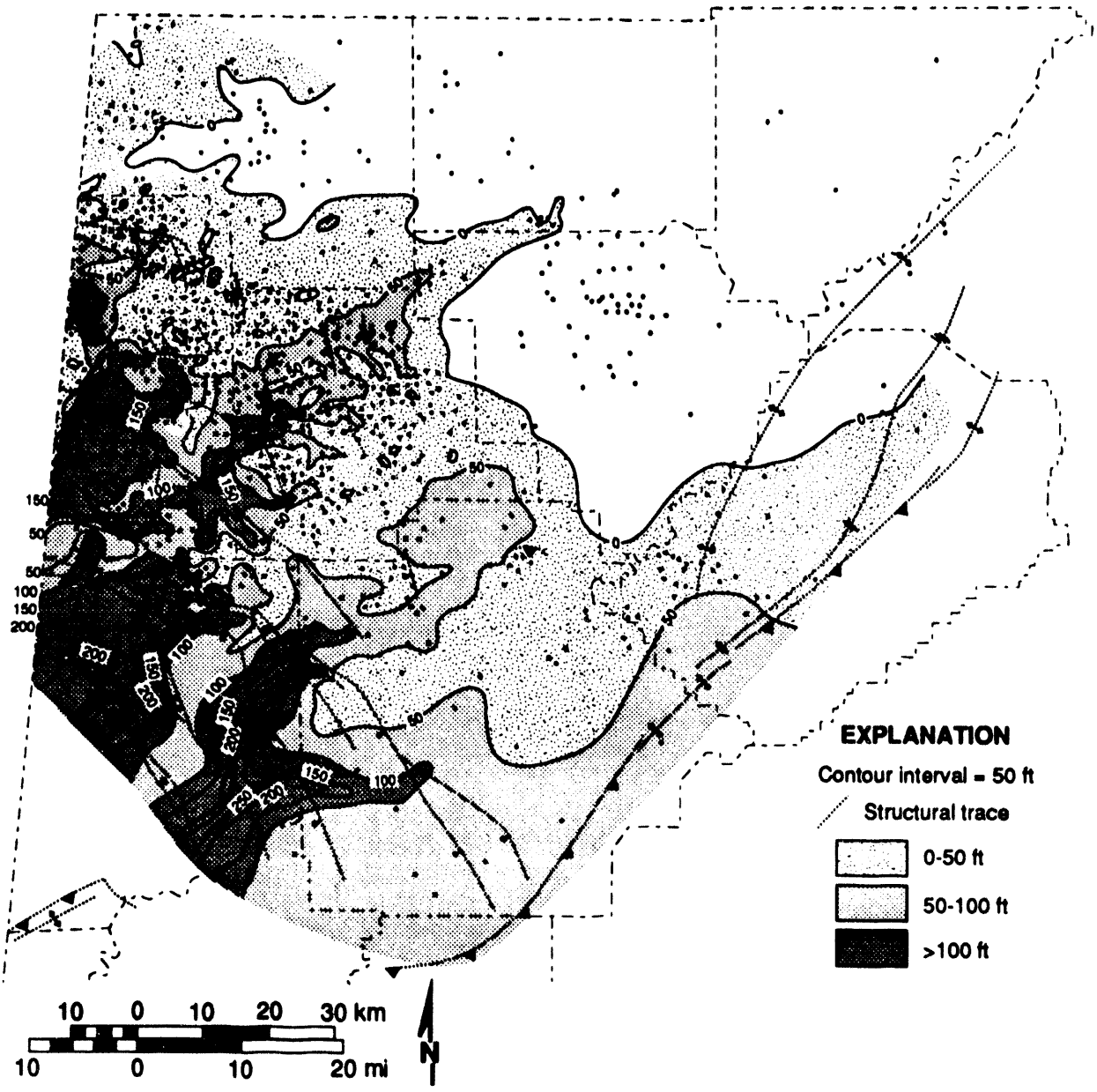

Figure 28.--Net-sandstone isolith map of the Coats sandstone.

28). The backstepping nature of correlative clinoformal parasequence sets (fig. 20) indicates marine transgression and formation of a destructive deltaic complex late in upper Parkwood deposition. However, high sediment flux from the evolving Ouachita orogenic belt apparently caused siliciclastic sediment to overstep the remnants of the carbonate bank in the northeast, setting the stage for the coal-bearing Pottsville Formation.

POTTSVILLE FORMATION

The Lower Pennsylvanian Pottsville Formation composes all of the Absaroka sequence in the Black Warrior basin and is composed of shale, sandstone, and coal (figs. 29, 30). The Pottsville has been divided into two parts, the lower Pottsville and the upper Pottsville (McCalley, 1900) and contains numerous coarsening-upward cycles (Pashin, 1991).

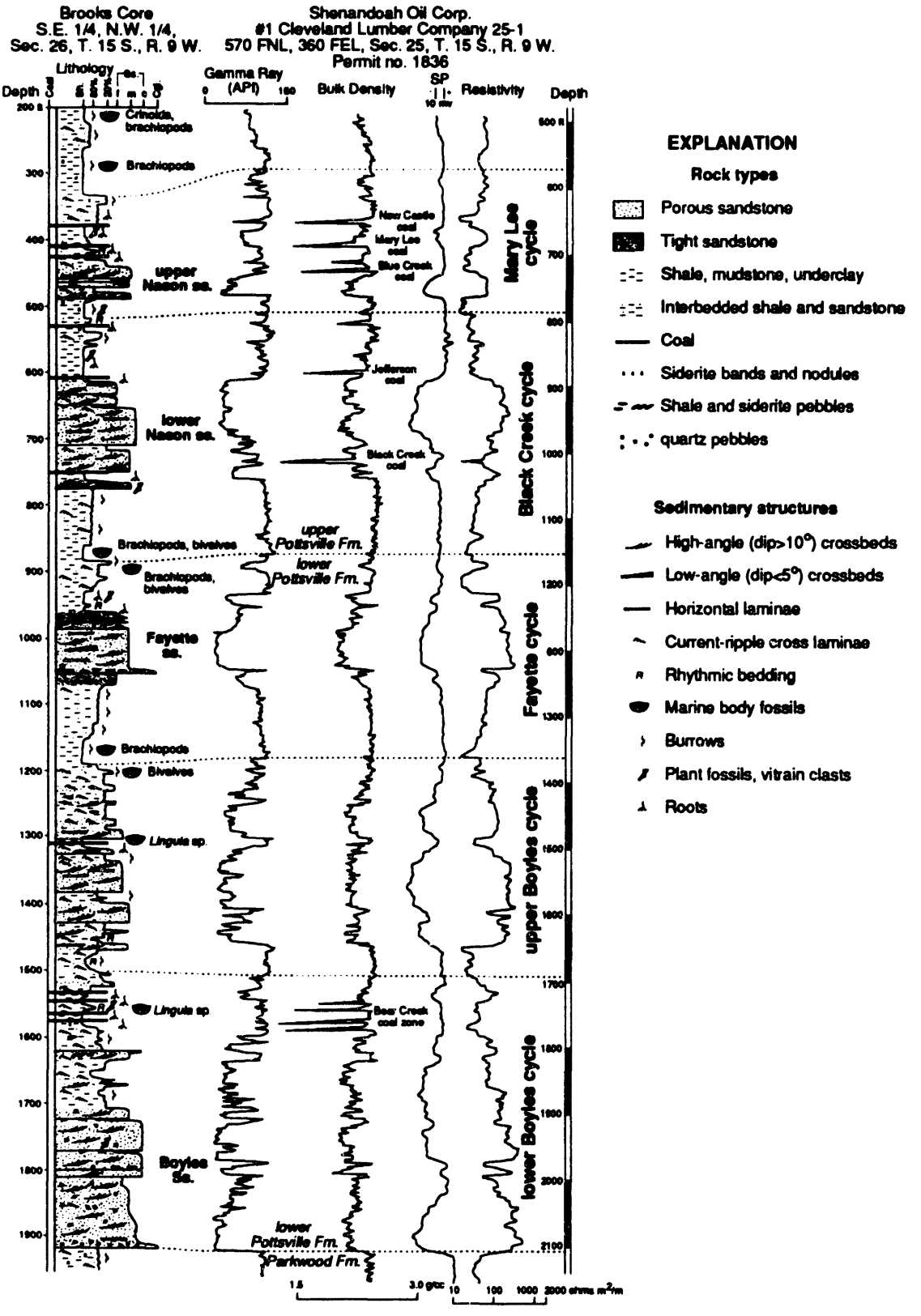

Figure 29.--Measured section of the Pottsville Formation.

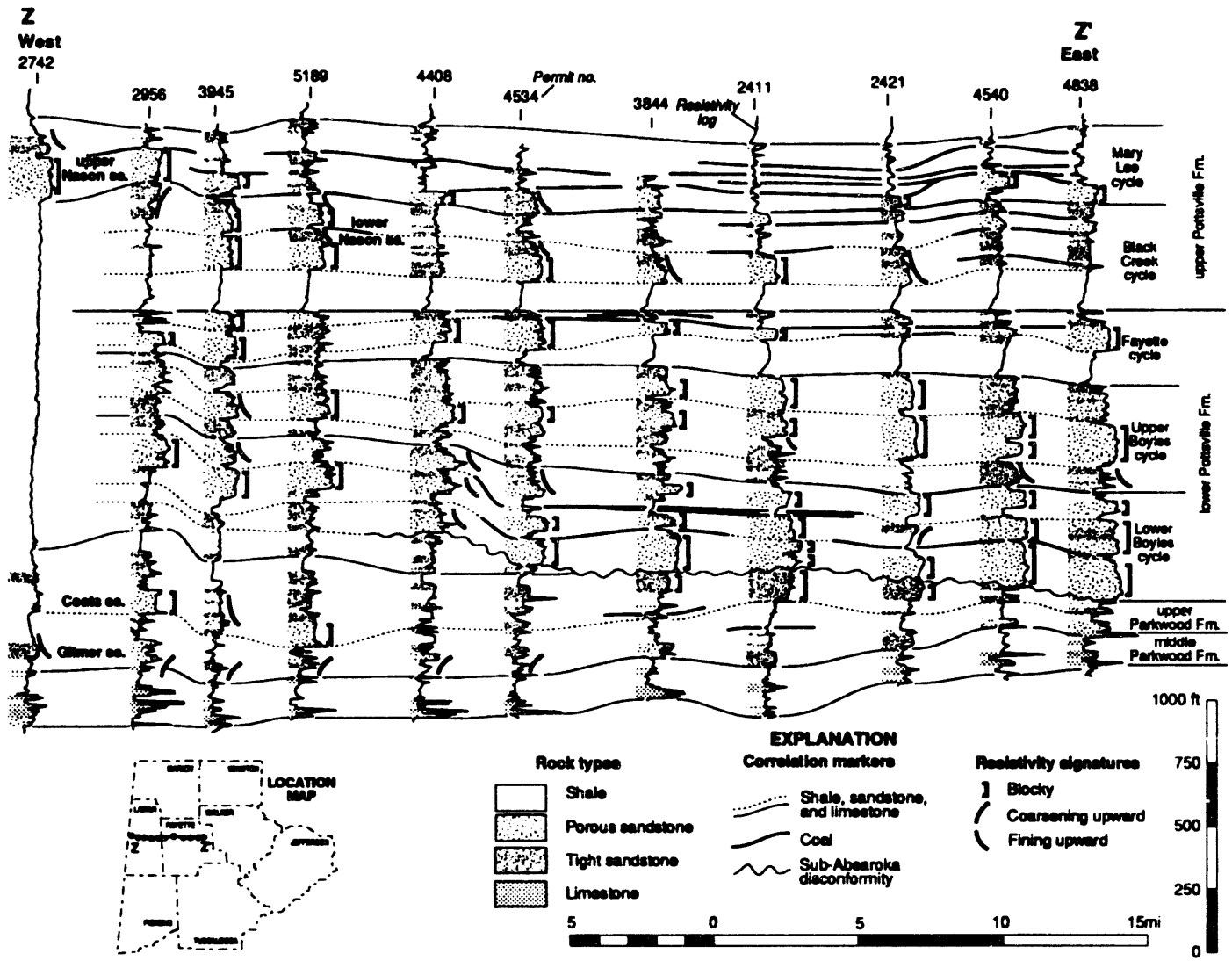

Figure 30.--Stratigraphic cross section showing facies relationships in the Parkwood and Pottsville formations.

The lower Pottsville contains the lower Boyles through Fayette cycles, whereas the upper Pottsville includes the Black Creek and Mary Lee cycles. Cycles above the Mary Lee lack reservoir sandstone and are therefore not considered in this investigation. Palynomorphs indicate that the Pottsville Formation is mainly Newriverian in age and that the Pocahontasian-Newriverian boundary is at the base or within the lowermost part of the Pottsville Formation (Eble and Gillespie, 1989; Eble and others, 1991).

The lower Pottsville Formation is dominated by quartzarenite and sublitharenite containing quartz pebbles (porous sandstone) and contains subordinate litharenite (tight sandstone), shale, and thin, discontinuous coal beds (figs. 29, 30). In contrast, the upper Pottsville is dominated by litharenite and shale and contains less quartzarenite than the lower Pottsville; most minable coal bodies are in the upper Pottsville (Ferm and others, 1967; Weisenfluh, 1979; Horsey, 1981; Mack and others, 1981, 1983). Each Pottsville cycle from the lower Boyles through the Mary Lee contains quartzarenitic reservoir sandstone, and most named reservoirs (fig. 1) are localized sandstone bodies in the Boyles Member. Although a significant amount of gas has been produced from Pottsville sandstone, oil production has been minimal. In addition to reservoir sandstone, the Mary Lee cycle contains the most important coalbed-methane reservoirs in the Black Warrior basin.

The Pottsville Formation sharply overlies the upper Parkwood Formation throughout most of the study area (figs. 29, 30). Early definition of the base of the Pottsville was based on the lowest conglomeratic quartzarenite (McCalley, 1896; Butts, 1926), but Engman (1985) reported that resistivity signatures can be used to distinguish Pottsville from upper Parkwood strata in many places (figs. 20, 30). The base of the Pottsville is sharp in the northeastern part of the study area and is marked by an extensive quartzarenite unit that locally truncates the upper and middle Parkwood Formation. The base of the sandstone rises stratigraphically toward the southwest where it is within the Pottsville (figs. 20, 30).

The continuous, stacked cycles, or parasequence sets, of the Pottsville Formation stand out in strong contrast to the steep, clinoformal parasequence sets of the Chesterian Series. However, stacking patterns are apparent in vertical trends in the distribution of quartzarenite, litharenite, and coal. Upward in section, quartzarenite units migrate northwestward and are replaced by coal, litharenite, and shale (Pashin, 1991). Hence, Pottsville cycles have a net progradational stacking pattern. Thickness patterns in the Pottsville Formation vary considerably from those in the Mississippian System. Cycles generally thicken toward the southeast, forming an arcuate depoaxis adjacent to the Appalachian-Ouachita orogen.

Pottsville sedimentation represents a major change in the configuration of the Black Warrior basin, reflecting the effects of Appalachian tectonism (Pashin, 1991). The combined effect of Appalachian tectonsim was a near doubling of subsidence rate throughout the basin (Thomas and others, 1991). Moreover, deposition of major coal-bearing sequences indicates fully equatorial, ever-wet conditions. Quartzarenite (porous sandstone), which forms the major conventional petroleum reservoirs in the Pottsville, has been interpreted to represent mesotidal barrier-island, shelf, and tidal-flat deposits (Hobday, 1974; Pashin, 1991; Pashin and Carroll, 1993). Sequences dominated by coal and litharenite (tight sandstone), by contrast, have been interpreted to represent fluvial, deltaic, and estuarine deposits (Ferm and others, 1967; Ferm and Weisenfluh, 1989; Gastaldo and others, 1991; Pashin, 1991).

Existence of a major unconformity separating the Kaskaskia and Absaroka sequences is one of the most contentious topics in Appalachian stratigraphy (Ettensohn, 1980, 1986; Ferm and Weisenfluh, 1989). Early investigators favored an unconformity at the base of the Pottsville Formation in Alabama (Butts, 1926; Welch, 1958, 1959), whereas recent investigators favored a conformable basal contact (Ferm and others, 1967; Thomas, 1972a, 1988; Ferm and Weisenfluh, 1989). Cross sections demonstrate progressive truncation of the Parkwood Formation toward the northeast (figs. 20, 30), confirming development of a sub-Absaroka unconformity. This unconformity is most pronounced in the northeastern part of the study area, where locally, the full thickness of the Parkwood Formation has been truncated. By contrast, the unconformity that rises southwestward into the Pottsville Formation is absent near the Ouachita orogen, reflecting continuation of an upper Parkwood-style coastal plain into Pottsville time.

The unconformity apparently had limited relief (approximately 200 feet) at the time of formation as demonstrated by the continuity of the lower Boyles cycle (fig. 30). This configuration stands out in strong contrast to the high-relief unconformity in the Appalachian basin that reflects incision of deep alluvial valleys (Rice, 1984; Chesnut, 1988).

Therefore, low relief and widespread mesotidal beach, shelf, and tidal-flat deposits in the lower Pottsville indicate that the unconformity formed in response to transgressive shoreface erosion rather than alluvial valley incision. Indeed, Pashin and Carroll (1993) characterized the unconformity in the Appalachian fold-and-thrust belt as a transgressive surface of erosion with limited time value.

As Pottsville deposition began, fluvial-deltaic deposits were restricted to the southwest part of the Black Warrior basin near the Ouachita orogen, where the Kaskaskia-Absaroka boundary is conformable. At this time, beach, shelf, and tidal-flat deposits were widespread in the northeastern part of the basin, where carbonate banks prevailed during Mississippian time (Engman, 1985; Thomas, 1988). As Pottsville sedimentation progressed, however, fluvial-deltaic systems, where thick peat (coal) accumulated, formed in the southeastern part of the basin adjacent to the Appalachian orogen, indicating that the basin was no longer protected from Appalachian sediment sources by the Birmingham graben. Associated beach and shelf deposits formed northwest of those systems and migrated northwest with the evolving coastal plain (Pashin, 1991). Therefore, the Pottsville Formation recorded progressive foreland basin evolution and the increasing influence of Appalachian tectonism related to orogenesis in the eastern part of the Alabama promontory.

SUMMARY OF DEPOSITIONAL HISTORY

During Late Devonian time, when deposition of the Kaskaskia sequence began, the Black Warrior basin was part of the passive margin of the Ouachita embayment, which was situated in the arid southern tradewind belt. At this time the organic-rich Chattanooga Shale accumulated slowly below an oxygen-deficient, density-stratified water column where an oceanic oxygen-minimum zone apparently impinged on the shelf. At the start of Mississippian time, regional shallowing and upwelling currents oxygenated the basin floor and resulted in deposition of the phosphatic and glauconitic Maury Shale. Cool, basinal water persisted well into Mississippian time, and as the sea continued to shallow, sedimentation rate increased, and siliceous carbonate ramp deposits of the Fort Payne Chert formed. As the ramp matured, calcarenite of the Tuscumbia Limestone prograded into the Black Warrior basin, thereby restricting cool-water chert facies to the southwestern part of the basin.

The initial stage of foreland-basin development followed deposition of the Tuscumbia Limestone and reflects loading of the westernmost part of the Alabama promontory at the start of the Chesterian epoch. The basin apparently became isolated from upwelling, oceanic water at this time, and as an orogenic forebulge formed, the Fort Payne-Tuscumbia ramp was uplifted, and the lowstand wedge of the Lewis cycle was deposited. The Evans and Hartselle cycles comprise southwest-dipping, clinoformal parasequence sets containing shelf, deltaic, and beach-barrier deposits. These cycles record differentiation of a coastal plain in the northeastern part of the basin from an oxygen-deficient starved basin in the southwestern part. Differentiation of the coastal plain and starved basin is interpreted to represent the onset of load-related subsidence adjacent to the Ouachita orogen. Sediment apparently entered the basin from cratonic sources, perhaps through the Mississippi Valley graben, forming the cuspate, wave-dominated delta of the Evans cycle. Transgressive reworking of the deltaic system during Hartselle deposition culminated in transport of sediment along the Fort Payne-Tuscumbia ramp, forming a barrier-rimmed carbonate bank.

Deposition of clinoformal parasequence sets continued after Hartselle deposition and culminated in formation of the prograding Bangor carbonate platform. Starved-basin conditions persisted in the southwestern part of the study area and are represented by the organic-rich, resistive facies of the Floyd Shale. Establishment of the Bangor platform-ramp system had a marked effect on subsequent sedimentation and development of the most prolific oil reservoirs in the Black Warrior basin. Late in Bangor progradation, the starved basin began filling with the deltaic sediment of the lower Parkwood Formation. Constructive, deep-water deltaic lobes filled the starved basin, and as the deltaic system prograded onto the carbonate bank and the receiving basin shallowed, a destructive, shoal-water deltaic system represented by the Carter sandstone formed. The most productive hydrocarbon reservoirs in the basin are part of the Carter shoal-water delta system.

The lower Parkwood Formation marks initial reversal of the southwest paleoslope that prevailed throughout earlier deposition. For this reason, the lower Parkwood is interpreted as the first flysch-type succession to enter the basin from sources in the Ouachita orogen. After lower Parkwood deposition, the transgressive *Millerella* limestone accumulated, renewing the carbonate platform-ramp system. Delta destruction continued during this time,

and *Millerella* sandstone reservoirs accumulated as the Carter deltaic plain was reworked. Following this early episode of transgressive limestone deposition, deltaic clastics filled the remaining part of the starved basin. Progradation of deltaic clastics was punctuated by deposition of the transgressive limestone marker at the top of the middle Parkwood Formation.

The upper Parkwood Formation spans the Mississippian-Pennsylvanian boundary and represents continued subsidence and filling of the foreland basin with deltaic clastics. The lithic nature of upper Parkwood sandstone indicates that the metamorphic and volcanic core of the Ouachita orogen was uplifted and contributing sediment to the distal foreland. Peat accumulation on the upper Parkwood coastal plain further indicates a more humid climate as the Black Warrior basin drifted toward the equatorial belt. The clinoformal Gilmer sandstone represents highstand progradation of deltaic clastics at the start of upper Parkwood sedimentation, whereas the aggradational Coats sandstone is associated with backstepping clinoformal markers and represents transgressive modification of the deltaic system. Near the end of upper Parkwood deposition, however, continued influx of orogenic sediment caused the Parkwood coastal plain to overstep remnants of the carbonate bank in the northeast, terminating limestone deposition in the Black Warrior basin.

The sub-Absaroka unconformity is within the Pocahontas stage of the Pennsylvanian System or at the Pocahontasian-Newriverian boundary and progressively truncates the Parkwood Formation toward the northeast and was formed mainly by shoreface erosion. The unconformity is most pronounced in the northeast where the Pottsville Formation locally overlies the Bangor Limestone and is least pronounced in the southwest where the Ouachita coastal plain continued to prograde. Pottsville deposition was characterized by fluvial and deltaic sedimentation adjacent to the orogenic belts and mesotidal shelf and beach sedimentation seaward of the fluvial-deltaic systems. At the start of lower Pottsville deposition, fluvial-deltaic deposits were restricted to the southwest part of the Black Warrior basin adjacent to the Ouachita orogen. By the start of upper Pottsville deposition, however, thick peat (coal) accumulated upon equatorial fluvial-deltaic platforms in the southeastern part of the basin, indicating that the basin was no longer isolated from Appalachian tectonism and sediment sources by the Birmingham graben.

BURIAL HISTORY AND SOURCE-ROCK CHARACTERISTICS

The distribution of production from Mississippian oil reservoirs in the Black Warrior basin may be explained, in part, by variability in quantity and quality of the source rock, and by the burial and thermal evolution of the basin. However, the source, or sources, of the hydrocarbons produced in the Black Warrior basin remains uncertain. The Devonian Chattanooga Shale, Mississippian Floyd Shale and shales in the lower Parkwood Formation, and shales within the Pennsylvanian Pottsville Formation have been identified as possible sources of Mississippian oil. To help resolve the origin of hydrocarbons in the basin, the quantity, quality, and thermal maturity of organic matter of upper Paleozoic rocks from the North Blowhorn Creek oil unit and other localities within the Black Warrior basin were investigated. The three general parameters were used in evaluation of the hydrocarbon generation potential of each unit, including abundance of total organic carbon, source of organic carbon or kerogen type, and degree of maturation of the kerogen.

THERMAL MATURATION

Regional trends of thermal maturity within the Black Warrior basin, based on vitrinite reflectance of the Mary Lee coal group of the lower Pennsylvanian Pottsville Formation (fig. 31), show a general increase from northwest to southeast. Vitrinite reflectance values for this unit range from 0.6 to over 1.6 percent. However, most higher rank (1.1 to 1.6 percent) rocks are associated with an elliptical high-rank anomaly along the southeast margin of the basin in Jefferson and Tuscaloosa Counties. In Lamar and Pickens Counties, the Mary Lee coal group ranges from 0.6 to 1.0 percent reflectance, and generally increases in rank from north to south. Plots of percent vitrinite reflectance versus depth for the PN2191 and PN1780 wells (fig. 32) show an irregular but distinct increase in reflectance with increased depth. Vitrinite reflectance histograms from the PN2191 well (fig. 33) illustrate typical data from several units. Sample standard deviation ranges between 0.045 and 0.150, with the lowest values occurring in the terrestrial Pottsville and upper Parkwood formations, and the highest in the marine Floyd, Lewis, and Chattanooga shales (table 1).

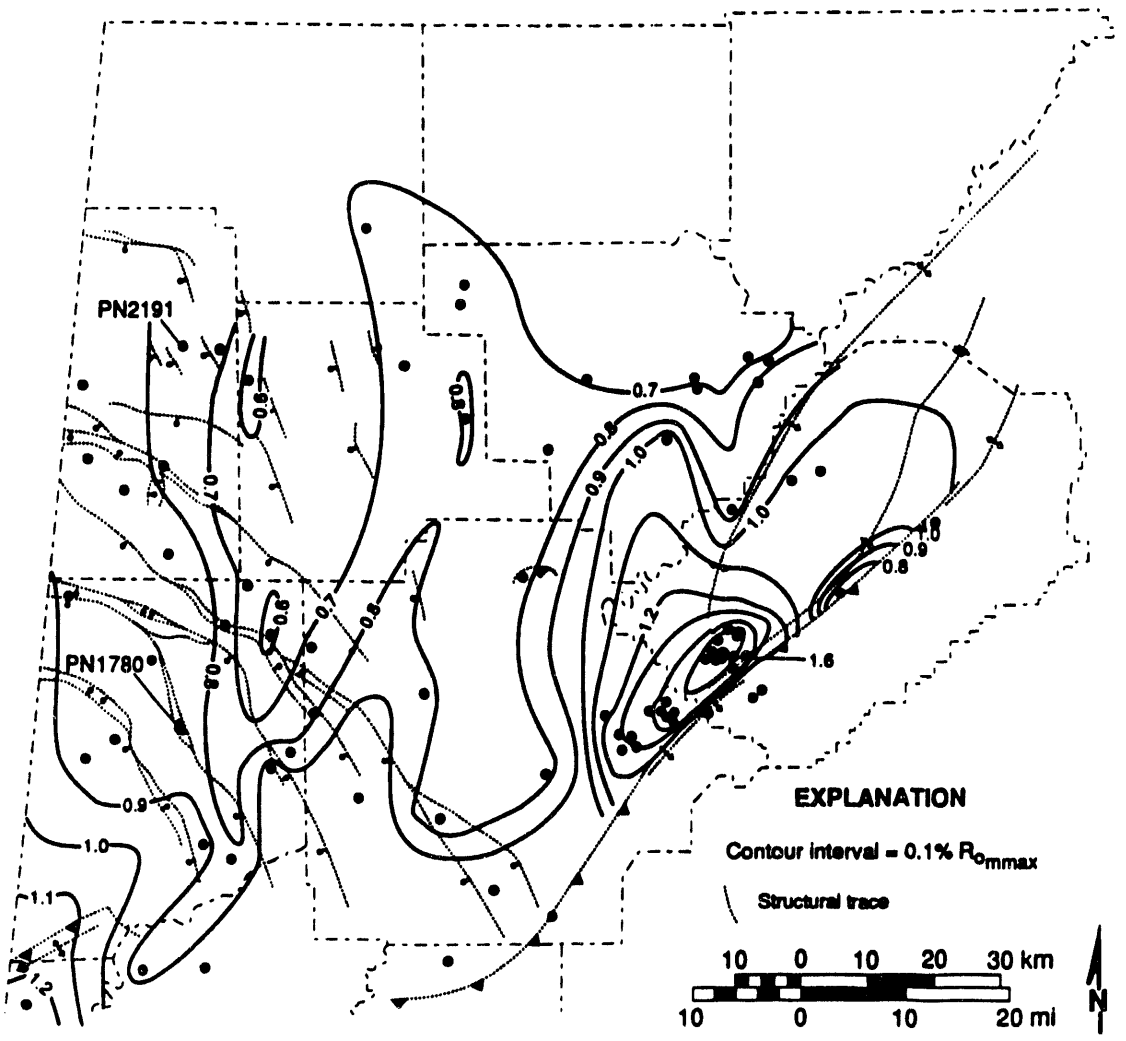

Figure 31.--Vitrinite reflectance map of the Mary Lee coal group in Alabama, showing the location of wells PN2191 and PN1780 (modified from Winston, 1990).

Reflectance values from the PN2191 well range from 0.62 to 1.12 percent. These values correspond to High Volatile C Bituminous and Medium Volatile Bituminous in the coal rank series. The lower value, from near the top of the Pottsville Formation, is above the oil window, and therefore, is thermally immature with respect to the generation of oil. The higher value, from the Chattanooga Shale, is near the value associated with peak oil generation. Projection of the regression line back to 0.2 percent reflectance (that of peat) gives an estimate of the total depth of burial. Based on this projection, the amount of stratigraphic section that was removed by erosion is estimated to be about 5,600 ft (±1,650 feet at 0.95 confidence).

Reflectance values for the PN1780 well range from 0.74 percent in the upper part of the Pottsville Formation to 1.61 percent in the Lewis shale. These values correspond to High Volatile Bituminous to Low Volatile Bituminous in the coal rank series. The lower value falls within the oil window, while the higher value is overmature, and out of the oil window. Total stratigraphic section removed by erosion is estimated to be about 5,950 feet (±2,300 feet at 0.95 confidence) in this well.

Vitrinite reflectance profiles from three wells in the vicinity of the PN1780 (PN2571, PN3097, and PN4141), produced by Robertson Research (U.S.), Inc. (1985) show comparable ranges in reflectance values. However, lost section estimates made from

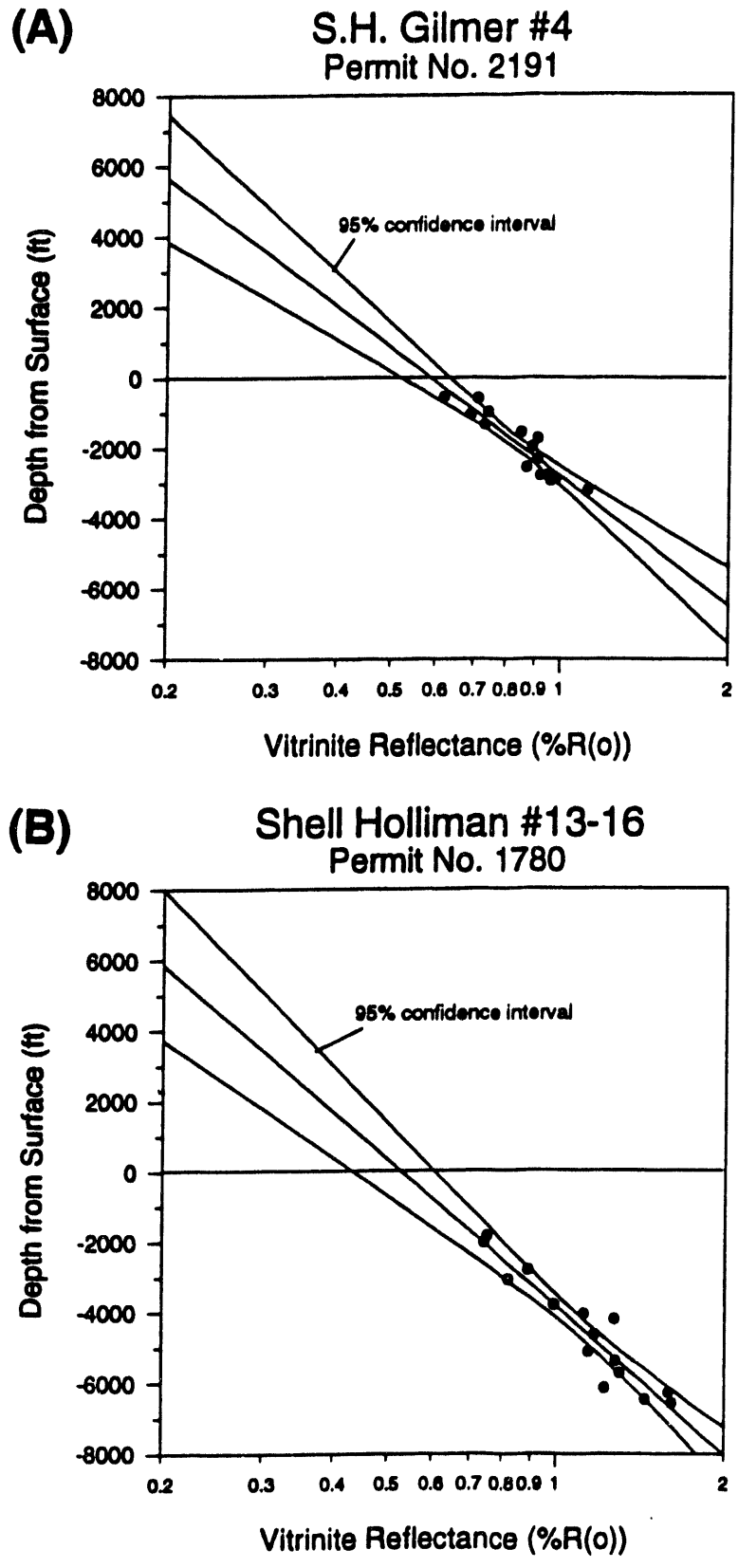

Figure 32.--Vitrinite reflectance versus depth profiles. (A) Well PN2191, (B) Well PN1780.

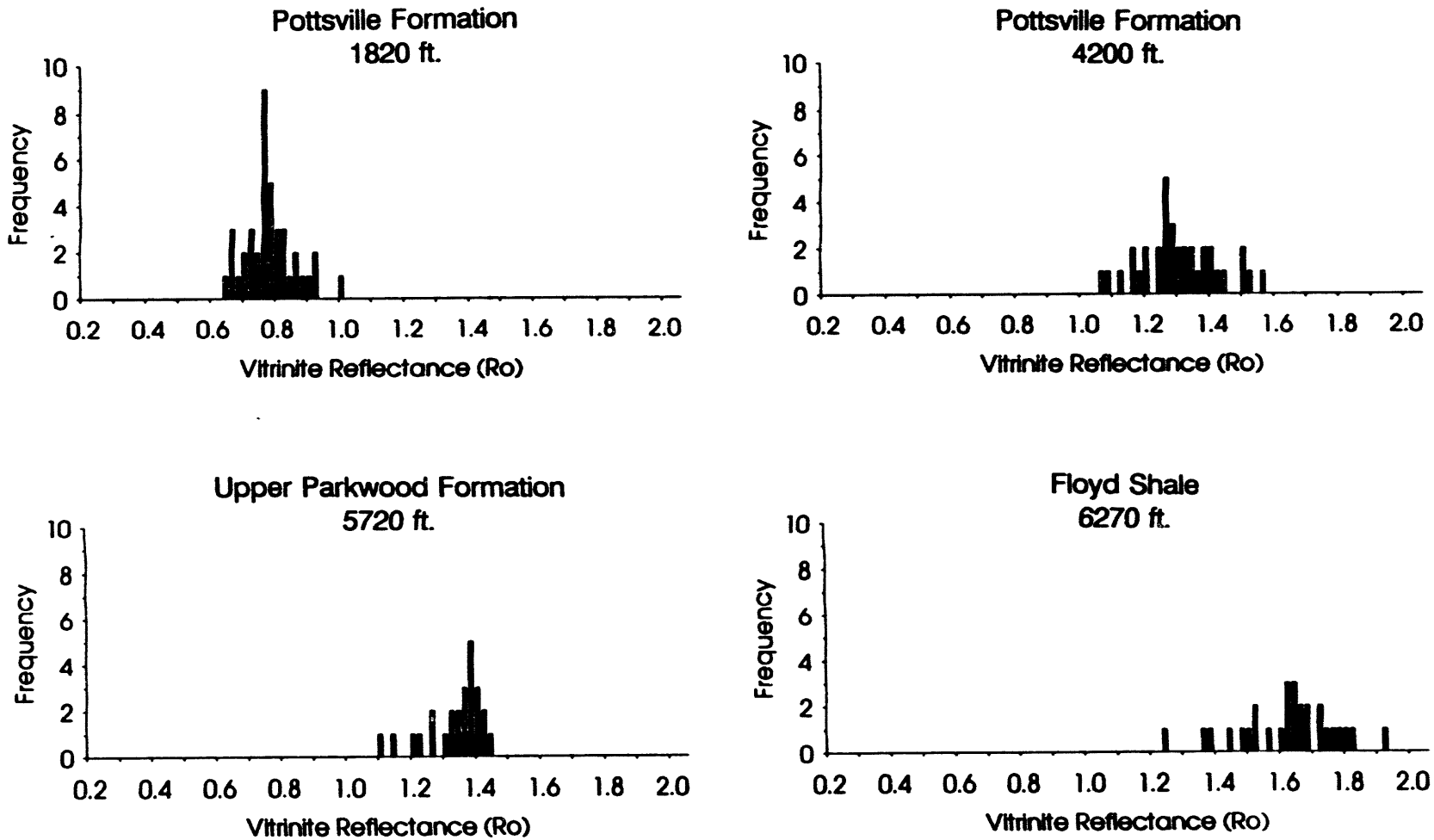

Figure 33.--Representative vitrinite reflectance histograms for well PN1780.

Table 1. Vitrinite reflectance data for wells PN1780 and PN2191.

Well	Depth (ft)	Formation	Mean %R(o)	Min.	Max.	Stand. Dev.	Count
PN1780	1,820	Pottsville	0.75	0.61	0.97	0.078	40
PN1780	2,010	Pottsville	0.74	0.59	0.89	0.063	40
PN1780	2,790	Pottsville	0.89	0.72	1.11	0.086	40
PN1780	3,070	Pottsville	0.82	0.69	1.02	0.066	36
PN1780	3,790	Pottsville	0.99	0.84	1.14	0.072	40
PN1780	4,050	Pottsville	1.12	0.93	1.36	0.099	40
PN1780	4,200	Pottsville	1.27	1.03	1.53	0.120	35
PN1780	4,630	Upper Boyles	1.17	1.00	1.40	0.084	40
PN1780	5,110	Lower Boyles	1.14	0.93	1.33	0.096	33
PN1780	5,380	Lower Boyles	1.28	1.01	1.49	0.110	29
PN1780	5,720	Upper Parkwood	1.30	1.07	1.40	0.089	25
PN1780	6,140	Upper Parkwood	1.22	0.95	1.53	0.132	36
PN1780	6,270	Floyd	1.59	1.20	1.89	0.150	28
PN1780	6,470	Floyd	1.44	1.22	1.70	0.121	23
PN1780	6,560	Lewis	1.61	1.27	1.86	0.148	37
PN2191	520	Pottsville	0.62	0.52	0.77	0.050	40
PN2191	570	Pottsville	0.71	0.58	0.81	0.048	40
PN2191	960	Pottsville	0.74	0.62	0.91	0.061	40
PN2191	1,020	Pottsville	0.69	0.55	0.84	0.064	40
PN2191	1,320	Pottsville	0.73	0.56	0.95	0.094	35
PN2191	1,550	Pottsville	0.85	0.69	1.05	0.090	40
PN2191	1,730	Pottsville	0.91	0.75	1.10	0.088	40
PN2191	1,950	Pottsville	0.89	0.76	1.09	0.627	33
PN2191	2,310	Parkwood	0.91	0.72	1.18	0.110	40
PN2191	2,540	Carter	0.87	0.79	1.02	0.051	40
PN2191	2,740	Floyd	0.95	0.76	1.14	0.087	35
PN2191	2,780	Floyd	0.92	0.80	1.09	0.067	21
PN2191	2,855	Floyd	0.98	0.77	1.19	0.097	35
PN2191	2,920	Lewis	0.96	0.79	1.10	0.806	32
PN2191	3,180	Chattanooga	1.12	0.88	1.33	0.113	25

these profiles tend to be higher and range from 8,580 to 12,500 feet.

BURIAL HISTORY

Burial history curves for the PN2191 and PN1780 wells (fig. 34) are based on unit thicknesses picked from well logs, ages based on Harland and others (1982), and estimated lost section from vitrinite reflectance profiles. The burial and tectonic histories of the geologic section represented by the two wells are quite similar. Their main difference consists of thicker upper Pennsylvanian and Cretaceous section found in the PN1780 well.

In order to assess the thermal history of kerogen contained within each unit, Lopatin's (Lopatin, 1971; Waples, 1982) method for computing Time/Temperature Indices (TTI) was used. The objective was to develop a model for the history of kerogen maturation that would result in TTI values for several horizons in each section that would be equivalent to actual vitrinite reflectance values observed for these horizons.

The two variables that were varied to produce the most reasonable model were thickness of section lost to erosion and geothermal gradient. The thickness of lost section used in these calculations is based on the vitrinite reflection profiles produced

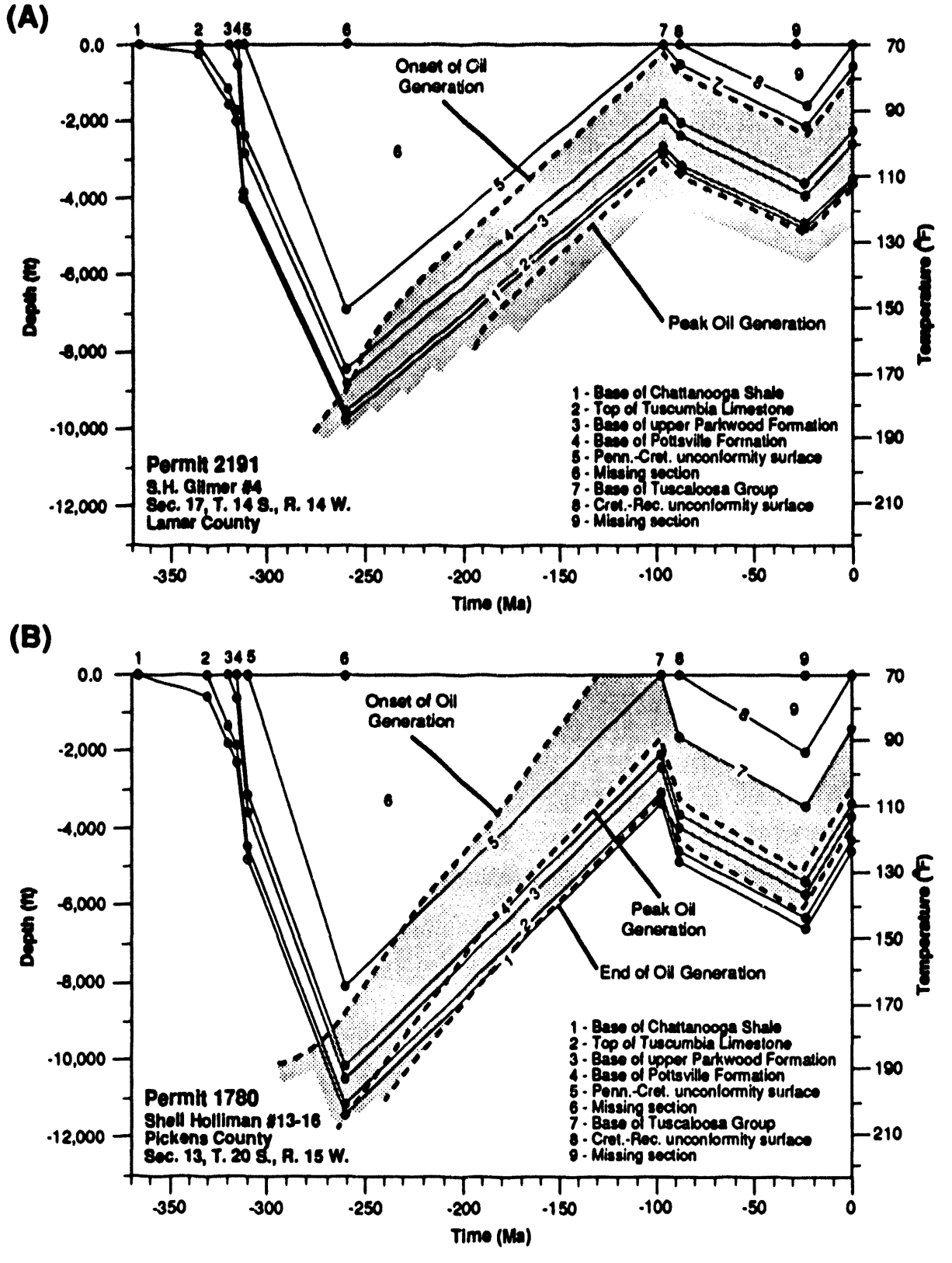

Figure 34.--Burial history curves. (A) Well PN2191, (B) Well PN1780.

during this study (fig. 33). These thicknesses are somewhat lower than those used by other investigators (Telle and others, 1987; Levine and Telle, 1991; Robertson Research (U.S.), Inc., 1985), but do not fall outside the range of realistic values.

The present-day geothermal gradient in the area of the wells studied ranges from 1.1 to 2.0°F/100 feet (U.S.G.S. and AAPG, 1976). A value of 1.6°F/100 feet was chosen as an average value for the model. Gradients less than this seem unlikely, especially during the time of rapid burial and eventual uplift and erosion of the Pottsville Formation. Geothermal gradients from the analogous Western Canadian Sedimentary Basin range from 1.6 to greater than 2.7°F/100 feet (Majorowicz and Jessop, 1981; Hitchon, 1984). However, using a gradient significantly greater than 1.6°F/100 feet would require that the thickness of lost section be reduced, which seems unlikely taking into account the range of values from other sources that would indicate that the thickness of lost section is actually greater.

The results of the TTI calculations (table 2) are presented in the form of cumulative TTI-through-time curves for several horizons in each well (fig. 35). Two trends are apparent from these curves. The first is that kerogen maturation occurred fairly rapidly with maximum maturation occurring between 290 and 200 MA. The second is that, except for the deepest units in the PN1780 well, reburial of Paleozoic rocks by Cretaceous sedimentation added little, if any, to the thermal maturation of the kerogen in the Paleozoic rocks. Liquid-hydrocarbon generation occurs between TTI values of 15 and 160, with peak generation occurring at a TTI of 75 (Waples, 1982). In the PN2191 well Mississippian rocks above the Tuscumbia Limestone and below the upper Parkwood Formation, which includes the Carter sandstone, attained TTI values from 42 to 68 which indicates these rocks have been heated to the extent of oil generation, but not to the point of peak generation potential. This same interval in the PN1780 well attained TTI values of between 108 and 169 indicating a higher degree of maturation to the point where they are nearly overmature. Shepard (1985) calculated TTI values for a well in the Plateau region of the Black Warrior basin and found values ranging from 58 for Mississippian rocks to 91 for Ordovician rocks. The data from these three wells show a trend of generally increasing TTI values for Mississippian rocks from north to south, or from the shallower part of the basin to the deeper.

Based on these cumulative TTI-through-time curves, and graphically depicted in figure 35, Parkwood Formation, in the PN2191 well, entered the oil window (TTI = 15) between 240 and 260 MA, but never reached peak oil generation (TTI = 75). In the PN1780 well, the Parkwood Formation entered the oil window between 260 and 270 MA, and reached peak oil generation between 200 and 250 MA. Based on these calculated dates, geothermal maturation of the Parkwood Formation occurred earlier to the south in the deeper part of the basin.

SOURCE-ROCK GEOCHEMISTRY

Sixteen samples from the PN2191 well and 16 samples from the PN1780 well, in addition to others, were submitted to the U.S. Geological Survey organic geochemistry lab for analysis using Rock-Eval pyrolysis to determine total organic carbon and kerogen type (table 3). All samples from these two wells contained total organic carbon values in excess of 0.5% indicating that all units were capable of generating hydrocarbons. However, samples from the Floyd and Chattanooga typically had values greater than 2.0 percent.

A plot of the Hydrogen Index (HI) versus Oxygen Index (OI) for these samples is illustrated in figure 36 (also see table 3). The plot for the PN2191 well shows that organic matter from the Carter, Pottsville, and Upper Parkwood is dominated by type III or gas-prone kerogen. However, kerogen in the Floyd and Chattanooga shales is primarily type II or oil prone. Subjective visual examination of kerogen from whole-rock polished pellets in reflected light and kerogen concentrates by transmitted light verify that the samples from the Pottsville, and Parkwood, including the shales below the Carter, are dominated by terrestrial plant material such as vitrain and degraded woody material (type III kerogen). Floyd and Chattanooga samples were dominated by amorphous organic material, which has been attributed to degraded marine sources (type II kerogen) but is mixed with varying amounts of terrestrial plant material.

The HI versus OI plot for the PN1780 well shows that all units, including those for the Floyd and Chattanooga shales, fall in or very near type III kerogen. Additionally, samples from the Pottsville and Parkwood which are typically type III, have, in general, lower OI values than those from the PN2191 well. Lower HI values from samples that typically have type II kerogen and lower OI values from samples that typically have type III kerogen indicate raised thermal maturation.

The potential for the Chattanooga Shale to produce large amounts of hydrocarbons is limited,

Table 2. TTI data for wells PN1780 and PN2191.

	PN1780		PN2191	
	TTI Value	MA	TTI Value	MA
Top of Remaining Cretaceous Section				
Initial	0	91	0	91
Onset of Oil Generation	--	--	--	--
Peak Generation	--	--	--	--
End of Oil Generation	--	--	--	--
Final	0.5	0	0.5	0
Top of Remaining Pottsville Formation				
Initial	0	309	0	309
Onset of Oil Generation	15	231	--	--
Peak Generation	--	--	--	--
End of Oil Generation	--	--	--	--
Final	23	0	6	0
Base of Pottsville Formation				
Initial	0	315	0	315
Onset of Oil Generation	15	266	15	211
Peak Generation	75	198	--	--
End of Oil Generation	--	--	--	--
Final	87	0	18	0
Base of Upper Parkwood Formation				
Initial	0	320	0	320
Onset of Oil Generation	15	268	15	254
Peak Generation	75	228	--	--
End of Oil Generation	--	--	--	--
Final	108	0	23	0
Top of Tuscumbia Limestone				
Initial	0	336	0	336
Onset of Oil Generation	15	272	15	275
Peak Generation	75	254	--	--
End of Oil Generation	160	112	--	--
Final	170	0	39	0
Base of Chattanooga Shale				
Initial	0	267	0	367
Onset of Oil Generation	15	274	15	281
Peak Generation	75	256	--	--
End of Oil Generation	160	214	--	--
Final	202	0	43	0

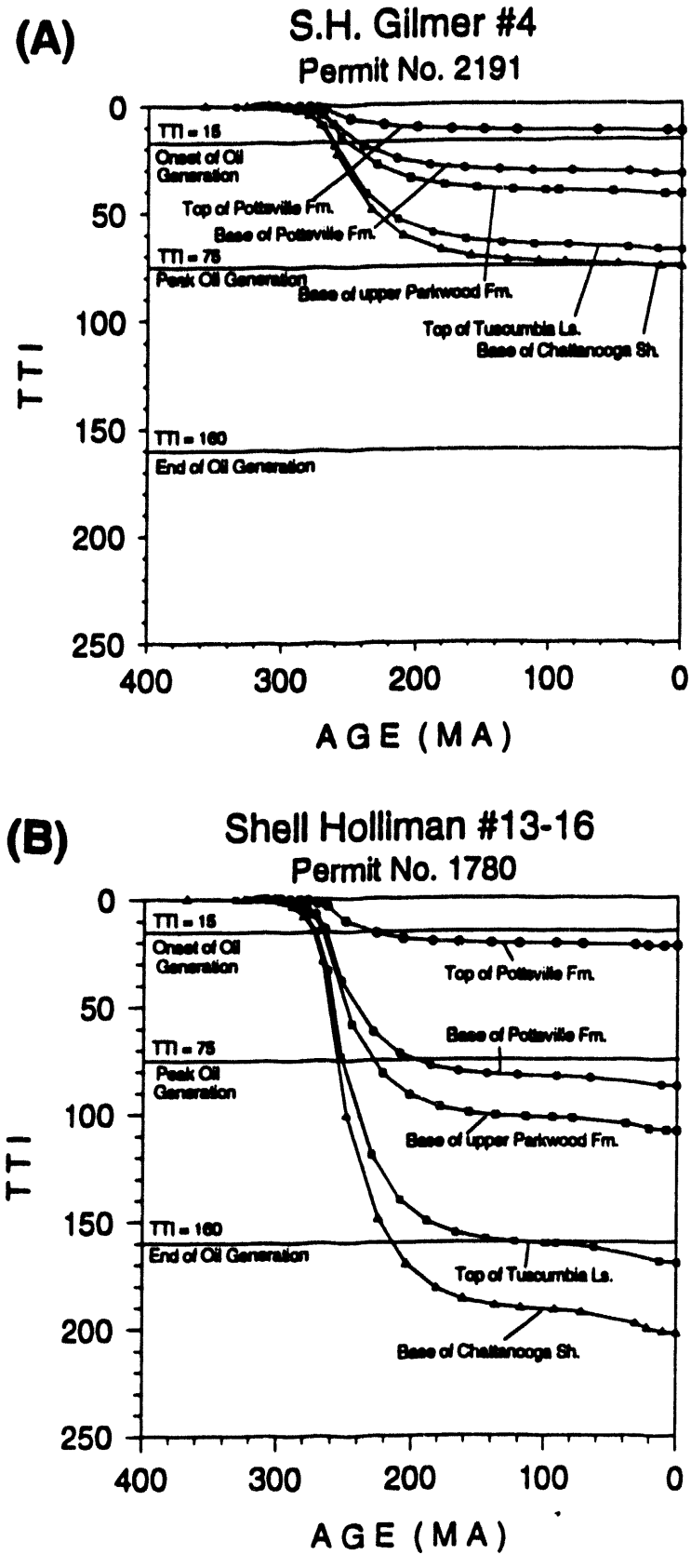

Figure 35.--Time/temperature index versus time cumulative curves. (A) Well PN2191, (B) Well PN1780.

Table 3. Rock-eval pyrolysis data for the PN1780 and PN2191 wells.

Well	Depth (ft)	Formation	Sample Weight	Tmax oC	S1	S2	S3	PI	S2/S3	TOC (wt%)	HI	OI
PN1780	1,690	Pottsville	205.1	467	0.04	0.25	1.2	0.14	0.2	0.53	47	226
PN1780	2,440	Pottsville	185.9	450	0.06	0.41	0.69	0.13	0.59	0.54	75	127
PN1780	2,570	Pottsville	197.5	458	0.05	0.33	1.07	0.13	0.3	0.67	49	159
PN1780	3,670	Pottsville	216.8	454	0.03	0.28	1.29	0.1	0.21	0.7	40	184
PN1780	3,680	Pottsville	212.5	458	0.02	0.27	1.18	0.07	0.22	0.67	40	176
PN1780	4,050	Pottsville	224.1	464	0.04	0.32	0.83	0.11	0.38	0.73	43	113
PN1780	4,480	Fayette	194.1	471	0.02	0.31	1.36	0.06	0.22	1.09	28	124
PN1780	4,610	Upper Boyles	185.2	461	0.02	0.24	0.73	0.08	0.32	0.73	32	100
PN1780	4,910	Lower Boyles	168.9	445	0.06	0.77	0.69	0.07	1.11	1.28	60	53
PN1780	5,430	Parkwood	190	467	0.05	0.27	0.78	0.16	0.34	0.53	50	147
PN1780	5,690	Parkwood	224.9	464	0.02	0.13	0.78	0.14	0.16	0.44	29	177
PN1780	5,880	Parkwood	189.2	470	0.02	0.18	0.78	0.1	0.23	0.55	32	141
PN1780	5,980	Parkwood	159.3	459	0.04	0.26	0.47	0.13	0.55	0.66	39	71
PN1780	6,450	Floyd	214.9	450	0.31	1.35	1	0.19	1.35	2.22	60	45
PN1780	6,560	Lewis	209.4	459	0.07	0.59	1.16	0.11	0.5	1.12	52	103
PN1780	6,600	Chattanooga	185.8	454	0.07	0.31	0.74	0.18	0.41	0.5	62	148
PN2191	570	Pottsville	182	447	0.03	0.58	2.72	0.05	0.21	1.09	53	249
PN2191	700	Pottsville	211	438	0.07	1.68	1.81	0.04	0.92	1.43	117	126
PN2191	1,020	Pottsville	175.2	456	0.02	0.34	2.87	0.06	0.11	1.06	32	270
PN2191	1,540	Lower Boyles	178.6	461	0.04	0.39	1.76	0.1	0.22	0.92	42	191
PN2191	1,730	Lower Boyles	196.3	445	0.03	0.39	2.28	0.07	0.17	1.07	36	213
PN2191	1,950	Lower Boyles	177.6	442	0.04	0.48	1.98	0.08	0.24	1.23	39	160
PN2191	2,140	Upper Parkwood	186.6	439	0.04	0.38	2.27	0.1	0.16	0.88	43	257
PN2191	2,310	Upper Parkwood	211.7	445	0.02	0.24	0.92	0.08	0.26	0.56	42	164
PN2191	2,490	Carter	238.5	443	0.03	0.37	1.71	0.07	0.21	0.76	48	225
PN2191	2,740	Floyd	145.6	437	0.53	3.84	1.92	0.12	2	1.6	240	120
PN2191	4,770	Floyd	230.2	439	0.6	8.41	1.66	0.07	5.06	2.45	343	67
PN2191	2,820	Floyd	210.3	438	0.29	5.78	1.36	0.05	4.25	1.74	332	78
PN2191	2,855	Floyd	23.3	443	0.68	4.89	0.9	0.12	5.43	2.36	207	38
PN2191	2,920	Floyd	19.1	446	1.15	9.1	2.46	0.11	3.69	3.94	230	62
PN2191	3,010	Floyd	239	432	0.04	0.4	0.95	0.09	0.42	0.47	85	202
PN2191	3,180	Chattanooga	166.1	433	0.54	7.41	1.37	0.07	5.4	3.05	242	44

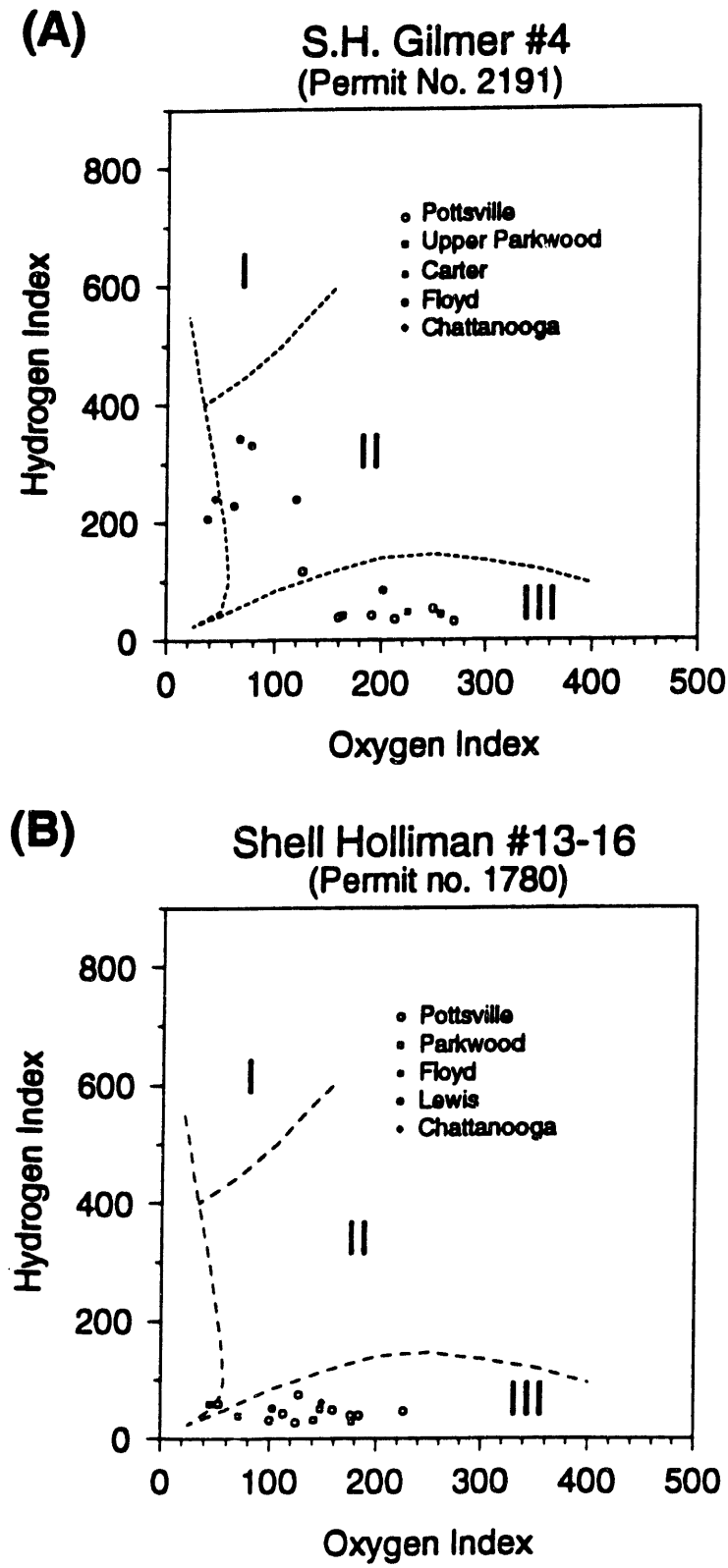

Figure 36.--Plots of hydrogen index versus oxygen index based on Rock-Eval pyrolysis. (A) Well PN2191, (B) Well PN1780.

however, because it is generally less than 10 feet thick in the study area. The Floyd, while having typically lower total organic content than the Chattanooga, is in excess of 200 feet in thickness. In samples from the PN2191 well, the Floyd Shale had an average TOC value of 2.1 percent, while the Chattanooga Shale had a TOC value of 3.1 percent. Given the relative thicknesses of these two units in the North Blowhorn Creek area, the potential volume of generated hydrocarbons for the Floyd Shale is at least 15 times greater than that of the Chattanooga Shale.

OIL GEOCHEMISTRY

The distributions of oil and gas fields in the Carter sandstone and of API gravity were mapped based on information in Masingill (1989) and Alabama State Oil and Gas Board files (fig. 37). Cumulative oil production as of March 1990, was also mapped. In some cases, overlapping oil and gas fields have the same name but may not have identical boundaries. In such cases, the overlapping fields have been mapped as one field. API gravity of oil in Carter sandstone increases systematically toward the southwest from 22° to 44° (fig. 37). This

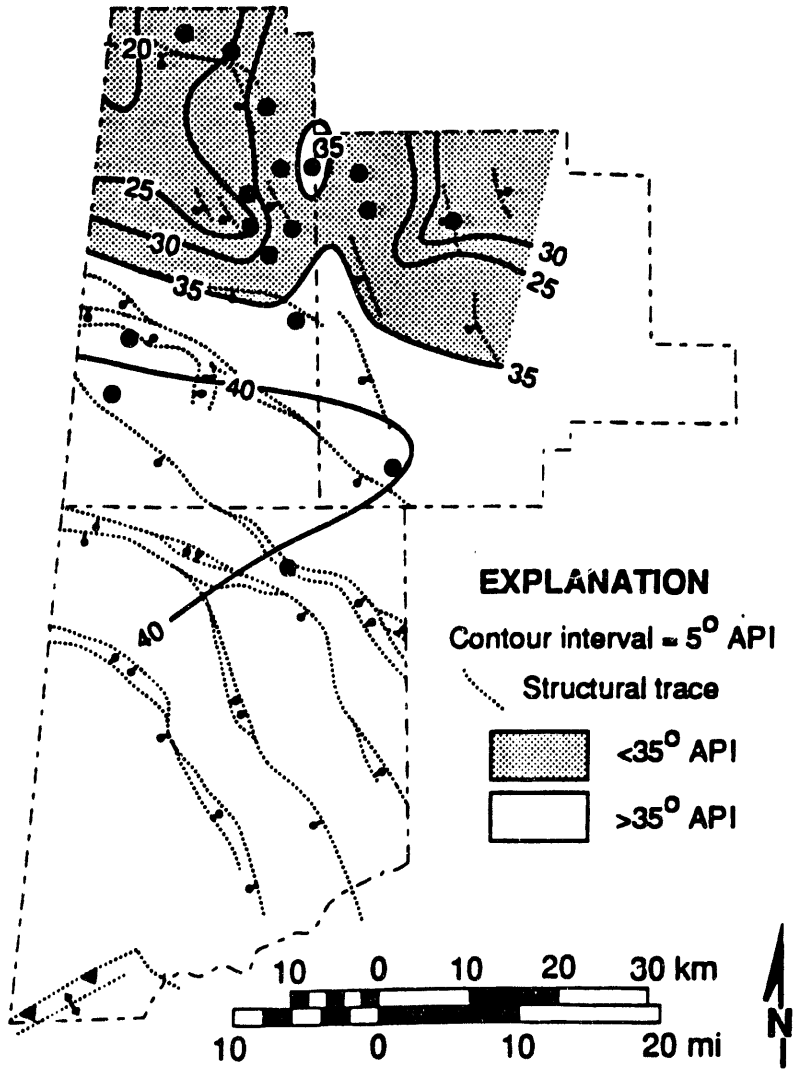

Figure 37.--API gravity distribution of oil from Carter sandtone reservoirs.

increase in API gravity parallels an increase in depth of burial of Carter sandstone. API gravity also parallels the rank of coal in the overlying Pottsville Formation (see fig. 31). One exception is the Blakely Creek field which occurs in an area of low coal rank but which has an API gravity of 40°.

A plot of API gravity versus depth (fig. 38) shows a general increase of API gravity with increasing depth. Because API gravity values tend to increase with increasing hydrocarbon maturation, the range of API gravity values can be explained solely on the basis of increasing thermal maturation of the hydrocarbons with increasing depth of the reservoir, which has been shown to be the case based on vitrinite reflectance. However, there is a clustering of API gravity values between 22° and 34° for reservoir depths between 1,500 and 3,000 feet, and between 39° and 41° for reservoir depths greater than 3,000 feet. This may be due to slight differences in timing, rock characteristics and migrational pathways from source rock to reservoir between the shallower and deeper parts of the basin.

Analysis of the gross chemical composition of Mississippian oils found in the Black Warrior basin

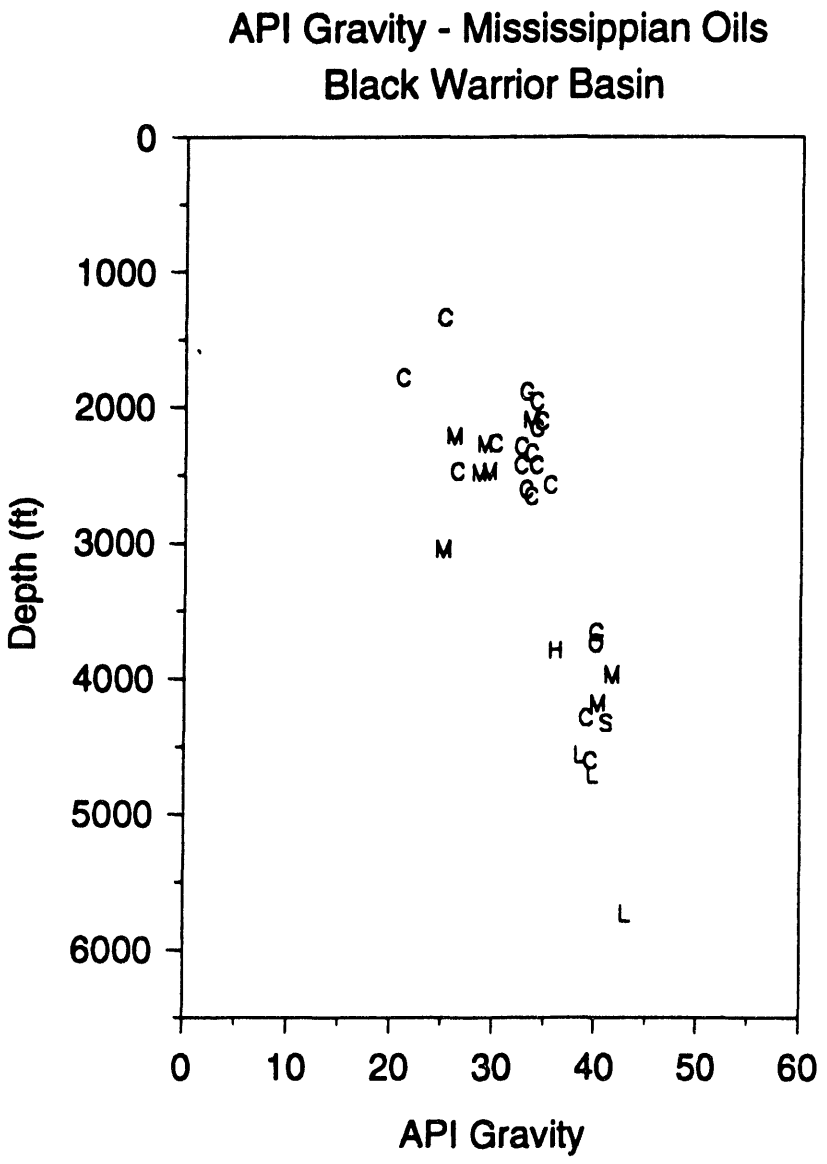

Figure 38.--Plot of API gravity versus depth in Mississippian oils from the Black Warrior basin. (C = Carter sandstone, H = Chandler sandstone, O = coats sandstone, G = Gilmer sandstone, L = Lewis sandtone, M = *Millerella* sandstone, S = Sanders and Carter sandstones.)

(fig. 39, table 4) shows that most tend to contain a high percent saturated hydrocarbons in relation to aromatic hydrocarbons and asphaltenes. This indicates that little biodegradation of the oil has taken place. Gas chromatograms from these oil samples also do not reveal evidence of extensive biodegradation.

Carbon isotope data are very consistent among the oil fields. $\delta^{13}C$ values for the saturate hydrocarbon fraction range from -30.1 to -31.3‰ for a difference of 1.2‰. For the aromatic hydrocarbon fraction, $\delta^{13}C$ values range from -29.3 to -30.6‰ for a difference of 1.1‰. Differences of $\delta^{13}C$ values between the saturate and aromatic hydrocarbon fractions range from 0.1 to 1.2‰. The differences in these values is within the acceptable range attributable to maturity transformation only (Waples, 1982). Therefore, based on these data, API gravity, and gross chemical composition, there are no conclusive reasons to indicate that oil produced from the various Mississippian oil fields in the Black Warrior basin are unrelated.

Figure 40 is a plot of pristane/n-C_{17} versus heptane that compares samples of Mississippian oils from the Black Warrior basin with those from the Jurassic and Cretaceous of the Gulf Coastal Plain. In both plots, the Mississippian oils are shown to be less mature than oils occurring in Jurassic or Cretaceous reservoirs. Data used to construct figure 40 are listed in table 5.

CHARACTERIZATION OF HETEROGENEITY IN CARTER AND *MILLERELLA* OIL RESERVOIRS

Carter and *Millerella* oil reservoirs make up the largest oil fields with the closest well spacing and thus provide the best basis for characterizing reservoir heterogeneity in the Black Warrior basin. This

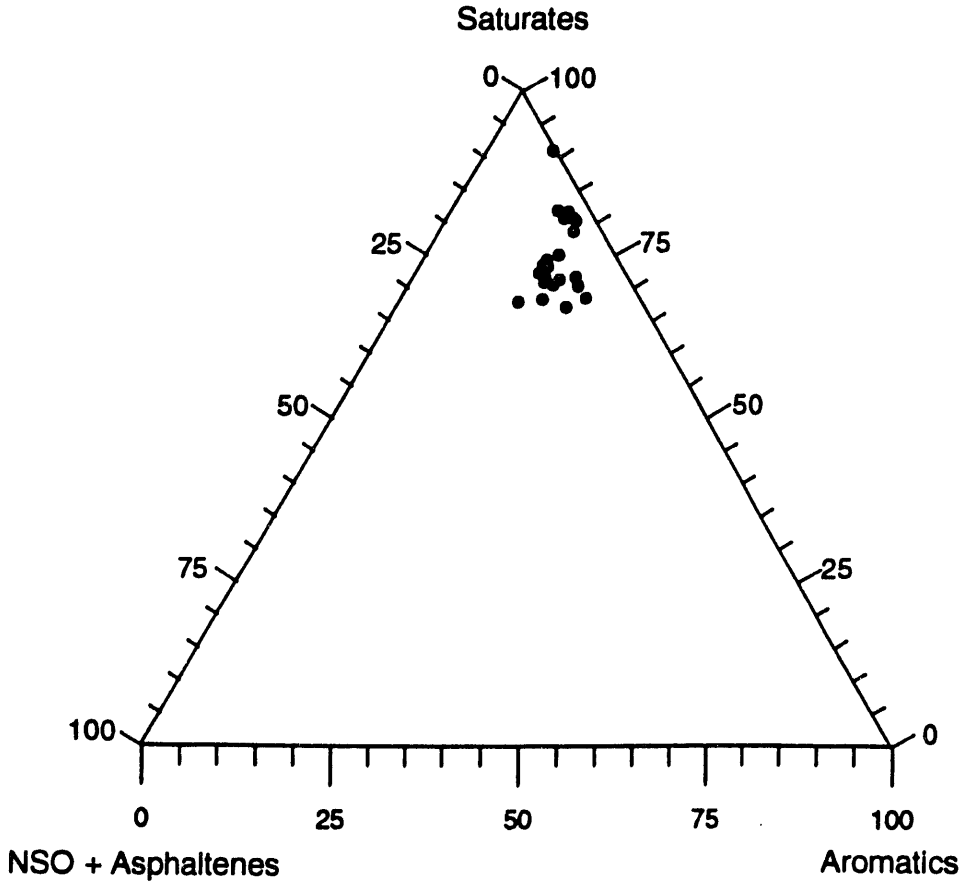

Figure 39.--Ternary diagram illustrating gross chemical composition of C15+ fraction of crude oils from the Black Warrior basin.

Table 4. Gross chemical composition of oils from Mississippian oil fields in the Black Warrior basin.

Oil Field	Age	Permit No.	Unit	Depth (ft)	Sat. (%)	Arom. (%)	NSO (%)	Asph. (%)	NSO + Asph. (%)	API Gravity
Binyon Creek	Mississippian	3769	Lewis Ss.	4,570	--	--	--	--	--	39
Blakely Creek	Mississippian	6863	Carter Ss.	3,666	80.5	16.5	3.0	0.0	3.0	40
Blowhorn Creek	Mississippian	2878	Carter Ss.	2,580	--	--	--	--	--	35.4
Blowhorn Creek	Mississippian	4510	Millerella Ss.	2,480	71.5	21.3	6.5	0.8	7.3	29
Blowhorn Creek	Mississippian	2878	Millerella Ss.	2,495	68.4	24.3	6.9	0.5	7.4	29
Bluff	Mississippian	4609	Gilmer Ss.	1,896	70.8	17.6	9.1	2.5	11.6	33
Bluff	Mississippian	4517	Lower Carter Ss.	2,110	68.2	18.7	11.7	1.4	3.1	34
Bluff	Mississippian	4609	Millerella Ss.	2,098	70.1	22.3	7.3	0.3	7.6	34
Bluff	Mississippian	4469	Upper Carter Ss.	2,348	71.1	19.4	9.3	0.2	9.5	33
Cains Ridge	Mississippian	5941	Millerella Ss.	3,190	74.0	16.3	9.7	0.0	9.7	--
Central Bluff	Mississippian	3905	Millerella Ss.	2,220	--	--	--	--	--	26
Central Fairview	Mississippian	1968	Carter Ss.	2,435	--	--	--	--	--	34
Chicken Swamp Branch	Mississippian	6524	Lewis Ss.	5,741	90.8	8.5	0.7	0.0	0.7	43
Coal Fire Creek	Mississippian	5080	Carter Ss.	4,615	--	--	--	--	--	39
Cooper Creek	Mississippian	4775	Millerella Ss.	3,984	80.0	17.1	2.6	0.2	2.8	41.6
East Detroit	Mississippian	1565	Carter Ss.	1,790	--	--	--	--	--	21
Fairview	Mississippian	3026	Carter Ss.	2,435	71.5	17.3	9.7	1.4	11.1	33
Henson Springs	Mississippian	1623	Carter Ss.	1,345	--	--	--	--	--	25
McCracken Mountain	Mississippian	4667	Millerella Ss.	3,051	74.8	17.5	7.8	0.0	7.8	25
Mount Zion	Mississippian	5454	Lewis Ss.	4,719	81.6	13.8	3.3	1.3	4.6	39.8
Mud Creek	Mississippian	5249	Millerella Ss.	4,190	78.4	17.6	3.9	0.0	3.9	40.2
North Blowhorn Creek	Mississippian	4322	Carter Ss.	2,297	72.1	16.2	10.8	0.9	11.7	33
North Bluff	Mississippian	4321	Millerella Ss.	2,276	67.8	15.6	14.7	1.9	16.6	29
North Bluff	Mississippian	3777	Millerella Ss.	2,278	--	--	--	--	--	29
North Fairview	Mississippian	3832	Carter Ss.	2,275	67.0	22.3	10.2	0.5	10.7	30
South Brush Creek	Mississippian	4322	Carter Ss.	2,612	73.0	17.0	9.7	0.4	10.1	33
South Fairview	Mississippian	2337	Carter Ss.	2,481	--	--	--	--	--	26.3
Star	Mississippian	3569	Carter Ss.	4,298	81.4	15.3	3.3	0.0	3.3	39
Star	Mississippian	3740	Chandler Ss.	3,800	--	--	--	--	--	36
Wayside	Mississippian	4465	Carter Ss.	2,159	73.2	16.2	9.4	1.1	10.5	34
West Brush Creek	Mississippian	5277	Carter Ss.	2,665	70.4	19.0	10.0	0.6	10.6	33
Yellow Creek	Mississippian	3940	Carter and Sanders Ss.	4,335	80.4	15.4	3.2	1.0	4.2	41

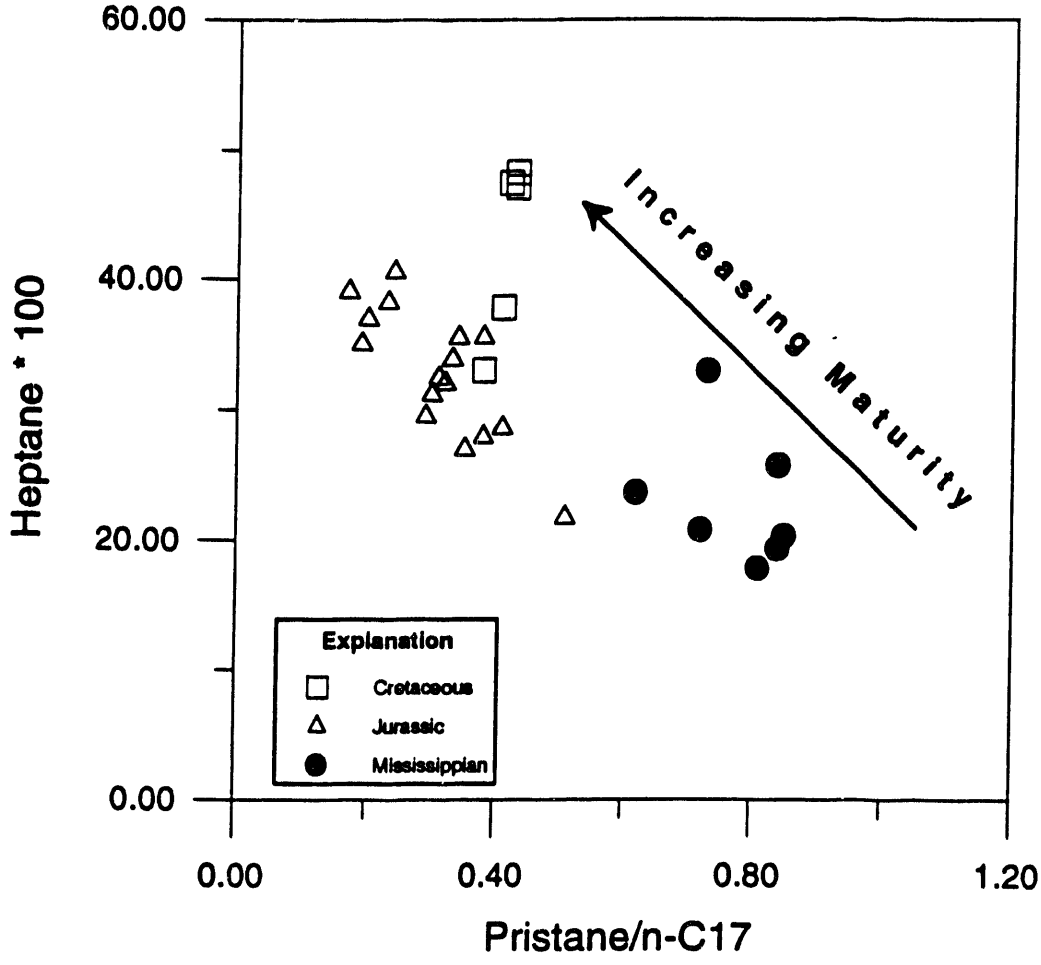

Figure 40.--Plot of pristante/n-C_{17} versus heptane for oils from Mississippian reservoirs in the Black Warrior basin and Jurassic and Cretaceous reservoirs in the Gulf Coastal Plain.

section discusses heterogeneity in these reservoirs using sedimentologic, petrologic, and petrophysical parameters.

FACIES HETEROGENEITY IN CARTER AND *MILLERELLA* OIL RESERVOIRS

Carter and *Millerella* oil reservoirs present the best opportunity to understand facies heterogeneity in the Black Warrior basin because these units are the most productive and make up the largest oil fields with the closest well spacing. Furthermore, cores of Carter sandstone are available from several fields and thus provide the best basis for developing models of sedimentation and reservoir heterogeneity. This section discusses facies heterogeneity in Carter and *Millerella* oil reservoirs by defining reservoir lithofacies, describing facies variation within the most productive fields, and developing depositional models to explain that variation.

Nine fields and oil units are present in the area containing the most productive Carter and *Millerella* oil pools, which were chosen for detailed study (fig. 41). A net-sandstone isolith map of the Carter sandstone shows marked variation of sandstone-body geometry (fig. 42). Isolith patterns in the southwest part of the map area delimit a series of thick, lobate sandstone bodies, which extend into South Brush Creek, West Brush Creek, Blowhorn

Table 5. Pristane/n-C17 and heptane values for oil from Mississippian, Jurassic, and Cretaceous oil fields in Alabama.

Oil Field	Age	Permit No.	Unit	Depth (ft)	Pristane/ n-C17	Heptane
Hubbard's Landing	Cretaceous	4675	Wash-Fred	8,236	0.41	37.89
Latham	Cretaceous	4522	Wash-Fred	8,046	0.38	33.10
Osaka	Cretaceous	6285	Cogle Sand	6,207	0.42	47.44
Osaka	Cretaceous	6285	Pilot Sand	6,083	0.43	48.28
West Foshee	Cretaceous	5325	Pilot Sand	6,168	0.43	47.15
Broken Leg Creek	Jurassic	6153	Smackover Ls.	14,035	0.41	28.61
East Barnett	Jurassic	5739	Smackover Ls.	13,600	0.34	35.56
Gin Creek	Jurassic	4546	Smackover Ls.	13,582	0.19	35.10
Gulf Crest	Jurassic	5226	Smackover Ls.	18,634	0.17	39.07
Hanberry Church	Jurassic	5178	Smackover Ls.	13,627	0.31	32.45
North Smiths Church	Jurassic	6943	Smackover Ls.	14,238	0.38	27.93
Northeast Barnett	Jurassic	6303	Smackover Ls.	13,449	0.33	33.91
Pace Creek	Jurassic	5058	Smackover Ls.	11,194	0.20	36.97
Palmers Crossroads	Jurassic	5584	Smackover Ls.	14,375	0.51	21.75
South Burnt Corn Creek	Jurassic	5272	Smackover Ls.	13,485	0.38	35.63
South Vocation	Jurassic	4225	Smackover Ls.	13,456	0.24	40.63
South Wild Fork Creek	Jurassic	5869	Smackover Ls.	14,287	0.35	26.99
Turnerville	Jurassic	4412	Smackover Ls.	18,407	0.23	38.26
Wallace	Jurassic	6752	Smackover Ls.	13,486	0.29	29.52
West Falco	Jurassic	6239	Smackover Ls.	13,034	0.32	32.03
Wildcat	Jurassic	5930	Smackover Ls.	13,170	0.30	31.20
Bluff	Mississippian	4517	Lower Carter Ss.	2,110	0.84	25.73
Bluff	Mississippian	4609	Millerella Ss.	2,098	0.85	20.31
Bluff	Mississippian	4469	Upper Carter Ss.	2,348	0.84	19.40
Chicken Swamp Branch	Mississippian	6524	Lewis Ss.	5,741	0.62	23.68
Mud Creek	Mississippian	5249	Millerella Ss.	4,190	0.73	32.96
Star	Mississippian	3569	Carter Ss.	4,298	0.81	17.81
Yellow Creek	Mississippian	3940	Carter and Sanders Ss.	4,335	0.72	20.80

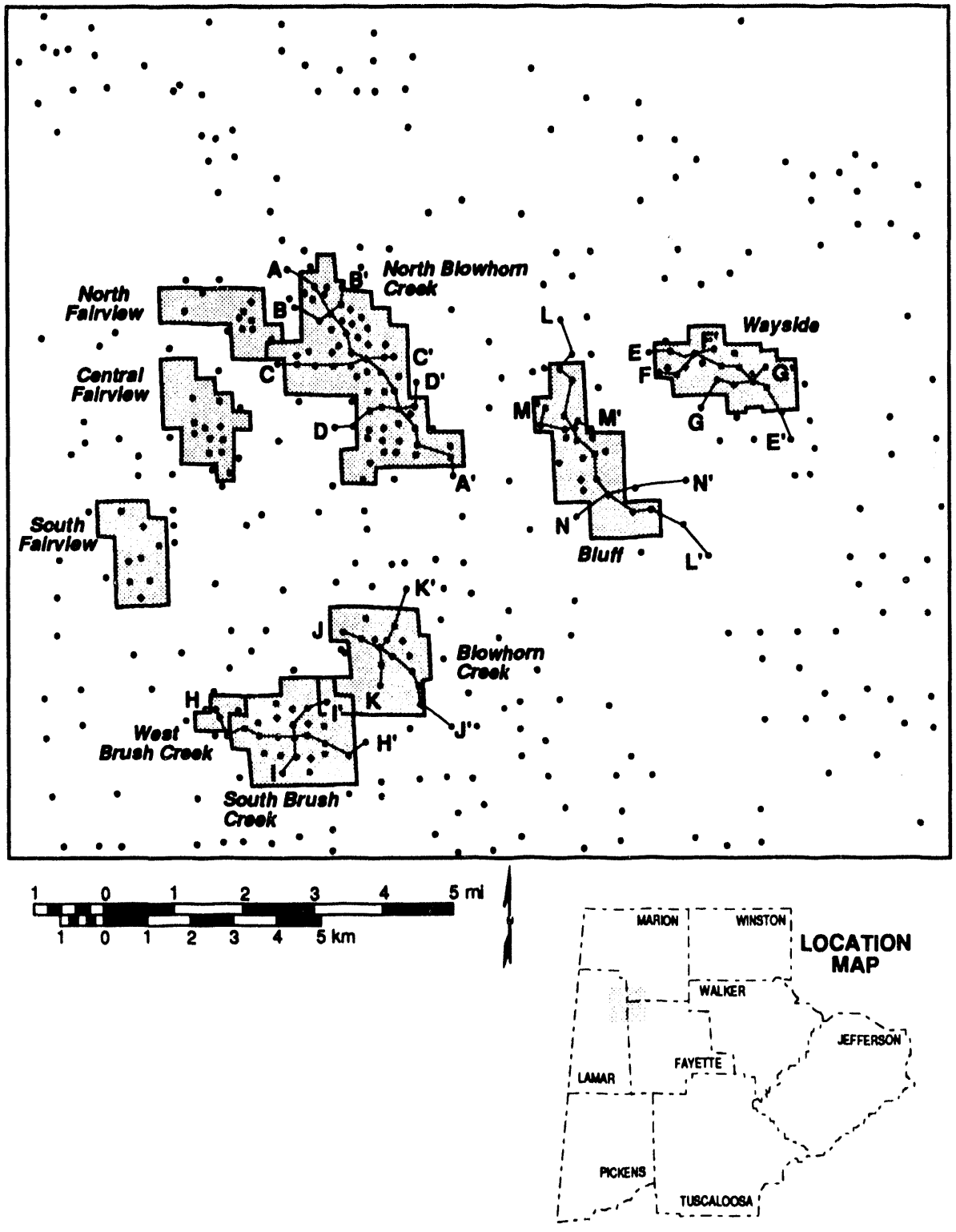

Figure.41.--Index map showing location of wells, oil fields and stratigraphic cross sections in Carter and *Millerella* sandstone, northeastern Lamar and southwestern Fayette Counties, Alabama.

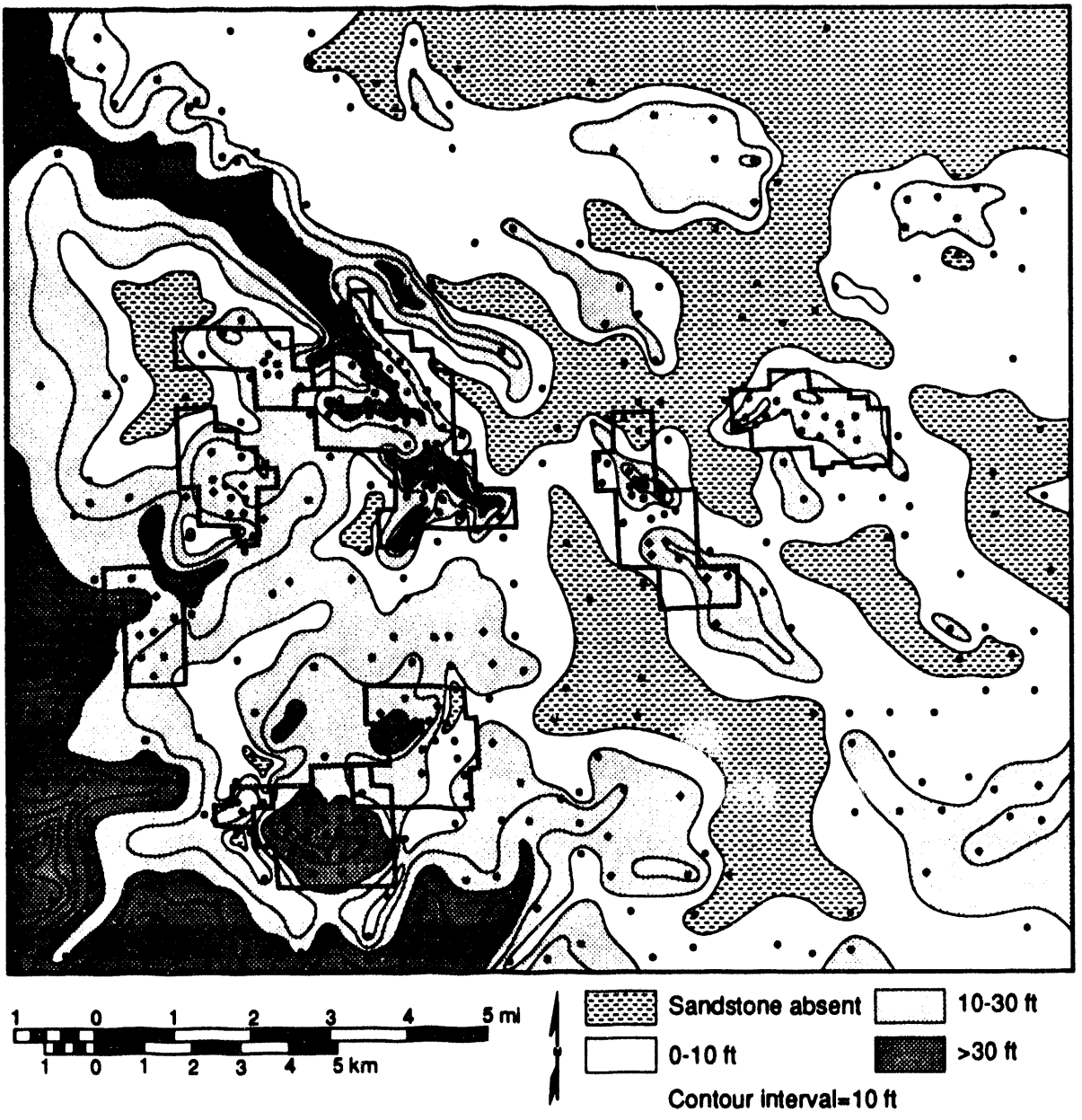

Figure 42.--Net-sandstone isolith map of the Carter sandstone, northeastern Lamar and southwestern Fayette Counties, Alabama.

Creek, South Fairview, and Central Fairview oil units. These lobate bodies represent the distal edge of the constructive deltaic system discussed earlier.

Northeast of the sandstone lobes, isolith patterns define a series of southeast-elongate sandstone bodies (fig. 42). The largest of these sandstone bodies is in North Blowhorn Creek oil unit, and the sandstone bodies become thinner and less continuous toward the northeast and southeast. Oil is produced from these smaller bodies in Bluff oil field and Wayside oil unit. The southeast-elongate sandstone bodies represent beaches of the destructive, shoal-water deltaic system (Kugler and Pashin, 1992; Pashin and Kugler, 1992).

The *Millerella* sandstone is much less continuous than the Carter and forms a series of sandstone lenses which are dispersed throughout the map area (fig. 43). The *Millerella* sandstone is thinner than 40 feet in this area, and sandstone-body geometry and orientation varies markedly. The largest lenses are in the south-central part of the map area, and one of these lenses produces oil in Blowhorn Creek oil unit. The only other lens that produces oil has a curvilinear geometry and is in Bluff oil field. The *Millerella* sandstone was interpreted earlier as a series of delta-destructive beaches and shoals that formed as a transgressing sea inundated the Carter delta plain.

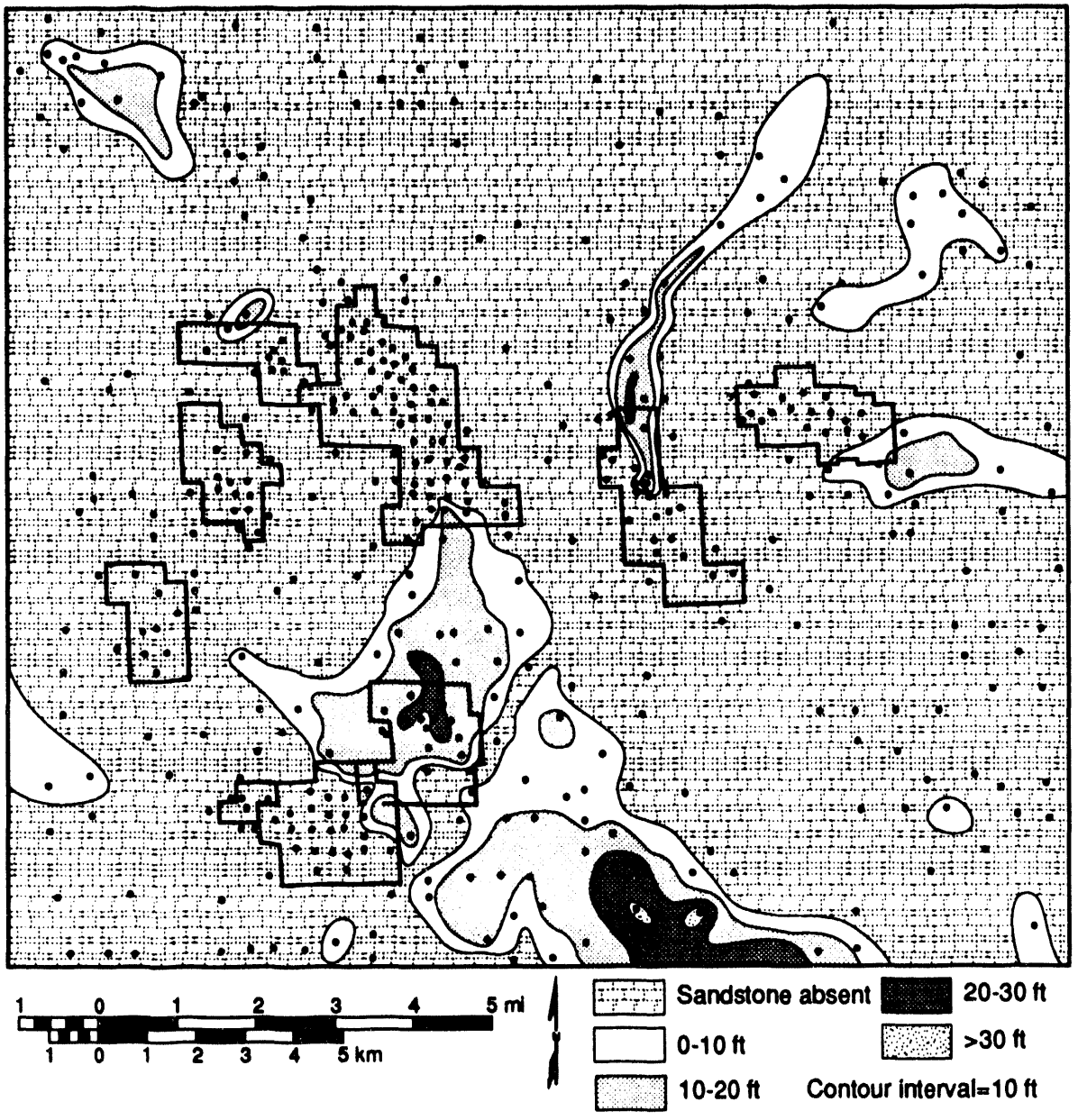

Figure 43.--Net-sandstone isolith map of the *Millerella* sandstone, northeastern Lamar and southwestern Fayette Counties, Alabama.

RESERVOIR LITHOFACIES

Cores of Carter sandstone are available in several oil fields in Alabama and were described from North Blowhorn Creek, Wayside, South Brush Creek, and South Fairview oil units. The cores provide the best control for characterizing the lithofacies of the lower Parkwood formation, which contain a diverse suite of rock types, sedimentary structures, and biogenic structures. All Carter cores contain the same tripartite lithofacies sequence, including from bottom to top, (1) shale-and-siltstone facies, (2) sandstone facies, and (3) variegated facies (fig. 44).

SHALE-AND-SILTSTONE FACIES

The shale-and-siltstone facies forms the base of the lower Parkwood Formation and is composed of medium gray to very dark gray, organic-rich shale and light gray siltstone (fig. 45a). In well logs, the facies has low resistivity and an irregular signature; facies thickness typically ranges from 20 to 75 feet. In core, the facies contains several bedding styles and sedimentary structures. The contact with the Bangor Limestone was not observed in core, but the contact with the overlying Carter sandstone is sharp to gradational (fig. 44).

Wavy, lenticular, and flaser bedding predominate in the shale-and-siltstone facies; shale is generally silty and poorly fissile, whereas siltstone most commonly occurs in laminae to thin beds with sharp upper and lower contacts (fig. 45a). Siltstone beds generally define a thickening- and coarsening-upward sequence (fig. 44). Sideritic concretions are present in all cores and generally form discoid to oblate masses ranging in size from pebbles to cobbles. The concretions commonly displace laminae in the host strata and locally contain septaria. Moreover, discoid to irregular, sand- to pebble-size pyrite nodules occur in some cores. Load casts and associated convolute laminae are abundant at the base of the siltstone layers, particularly the thickest beds (fig. 45a), and wave ripples and horizontal laminae abound within the layers. Current-ripple cross laminae occur in many siltstone beds (fig. 44), and the thinnest siltstone laminae are commonly graded. Horizontal feeding burrows are locally common in the siltstone, and some resting traces also are present.

SANDSTONE FACIES

The sandstone facies consists dominantly of very fine- to fine-grained sandstone that is yellowish-brown, thickly bedded, and moderate- to well-sorted (figs. 45b, c). In well logs, this facies typically has a blocky pattern and the highest resistivity of any part of the Carter sandstone (fig. 44). Furthermore, the sandstone facies contains the most porous and permeable strata in the Carter interval and is thus the principal reservoir rock; much of the sandstone is stained with oil.

The contact of the sandstone with the underlying shale-and-siltstone facies is distinct but gradational, whereas the contact with the overlying variegated facies, which is discussed later, is sharp to gradational (fig. 44). Pressure-solution seams along shale laminae in the lower 3 to 6 inches of the sandstone define the base of the oil-saturated zone. Unsaturated siltstone and sandstone between pressure-solution seams contains abundant interstitial clay and is cemented by ferroan dolomite/ankerite. Hence, the base of the reservoir is not a simple depositional contact, but a diagenetic contact as well.

In many cores, sedimentary structures are readily apparent because dark, clay-rich layers define laminae. The lower part of the sandstone contains abundant small-scale trough crossbeds, or more specifically, lunate-ripple cross laminae (fig. 45b). In a core from North Fairview oil unit, lunate-ripple cross laminae are defined by asphaltic hydrocarbons. Wave ripples also are present locally near the lower contact. Clay drapes are common in some of the ripple-laminated sandstone. The dominant sedimentary structures in the upper part of the sandstone are gently inclined laminae (fig. 45c) that define low-angle (dip<10°), planar crossbeds (fig. 44). Within the low-angle crossbedded sandstone, however, are intervals of lunate-ripple cross laminae and high-angle (dip>10°) planar and large-scale trough crossbeds. In most cores, cross-stratified units within low-angle-crossbedded sandstone are thinner than 0.5 ft. Many of the high-angle crossbeds are coarser grained than the adjacent low-angle-crossbedded and ripple-laminated sandstone.

A few thin to medium beds of shale and siltstone, some of which resemble the shale-and-siltstone facies, are within the sandstone facies. Platy, sand- to pebble-size shale clasts and irregular clay laminae thinner than 0.05 inch are dispersed throughout the facies. Isolated shale clasts are present in most of the reservoir, and locally, the clasts are abundant enough to form sandstone-supported conglomerate. Clay laminae occur singly or in parallel to anasto-

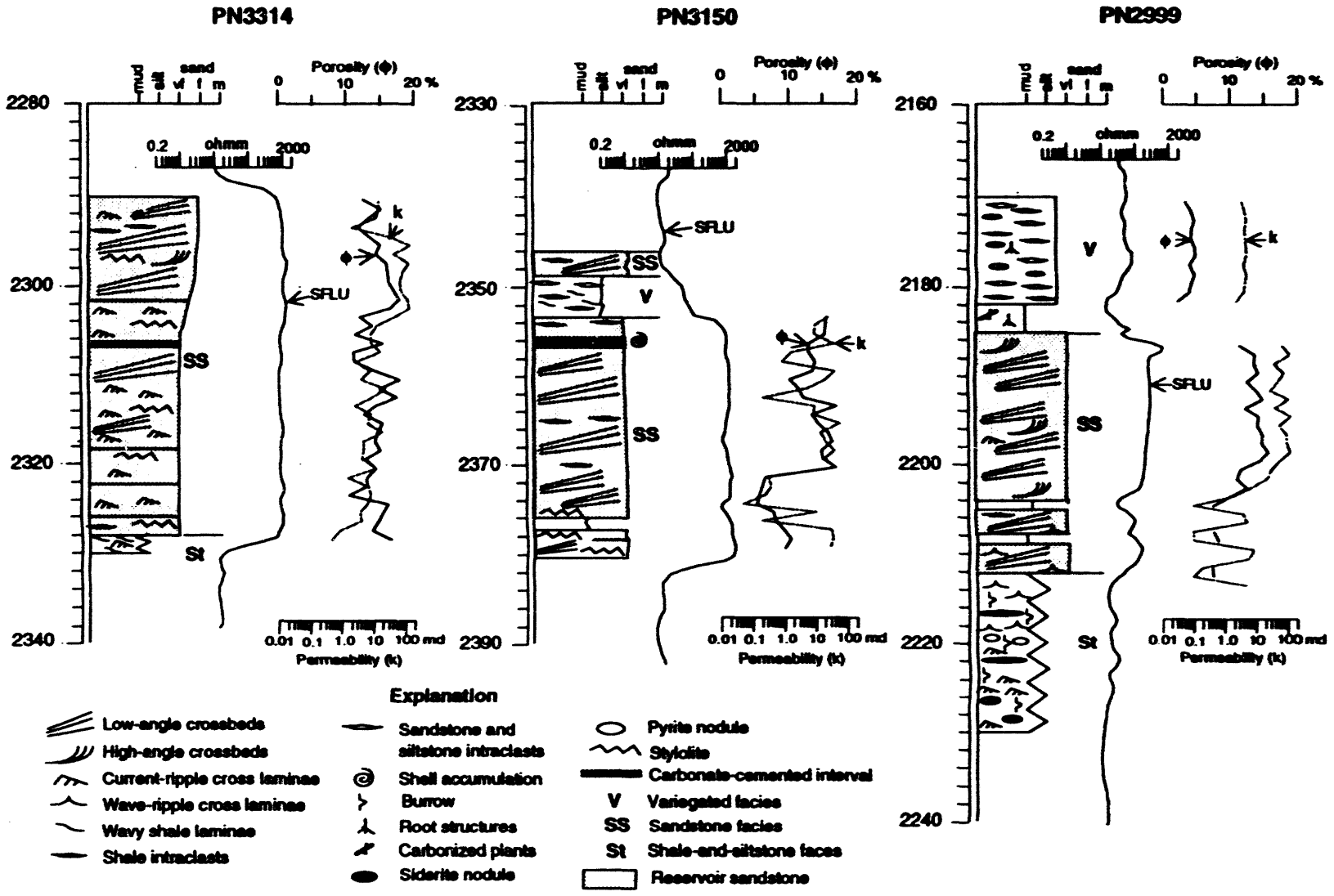

Figure 44.--Selected graphic logs of cores of Carter sandstone, North Blowhorn Creek oil unit (modified from Pashin and Kugler, 1992).

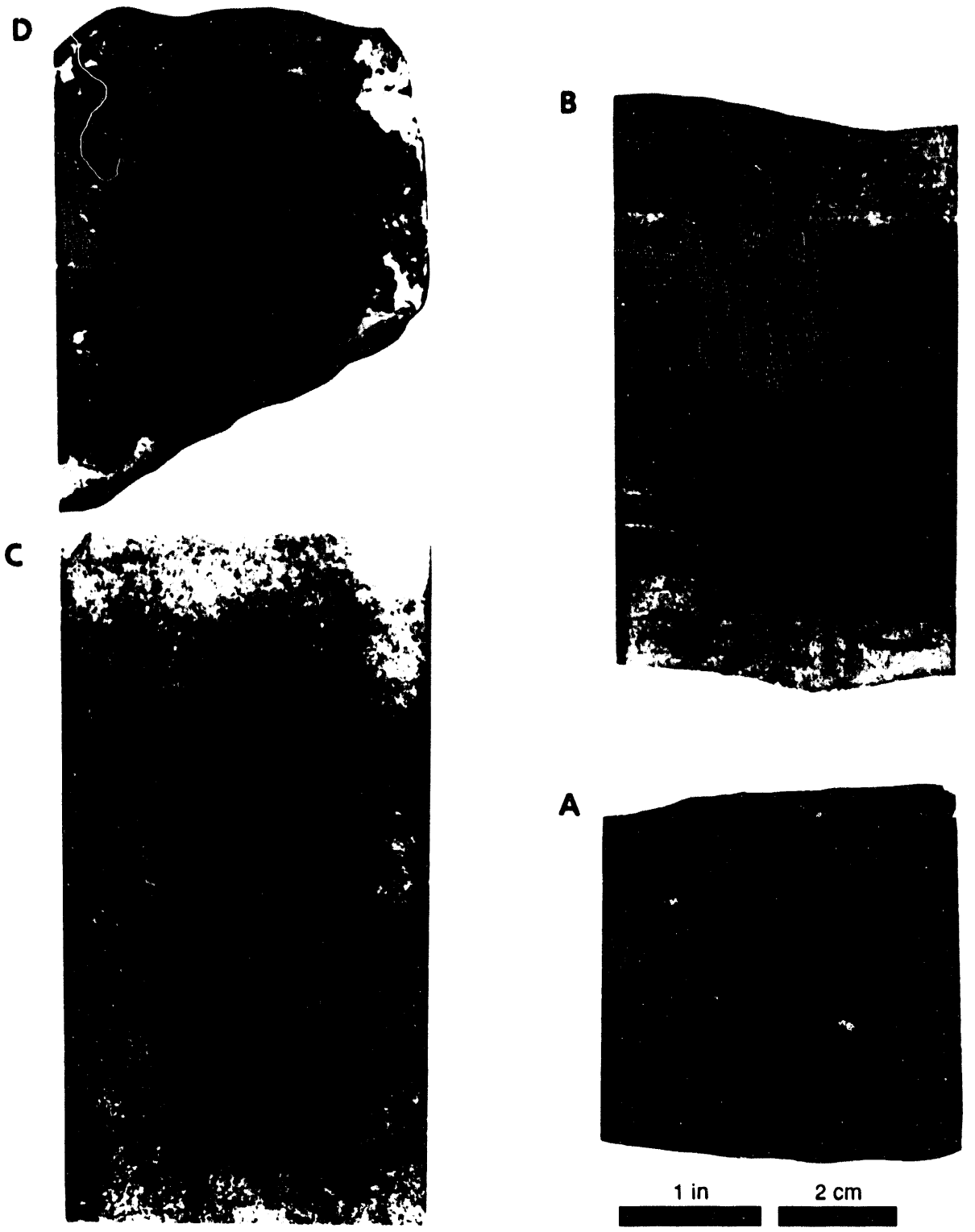

Figure 45.--Selected photographs of cores showing characteristics of lithofacies in North Blowhorn Creek oil unit. (A) Thin siltstone bed with wave-ripple cross laminae and syndepositional load structure, shale-and-siltstone facies (well PN3236, 2,253 ft). (B) Very fine-grained sandstone with current-ripple cross laminae, sandstone facies, (well PN3314, 2,321). (C) Very fine-grained sandstone with gently dipping laminae, sandstone facies (well PN3204, 2,237 ft). (D) Red mudstone with rhizoids and pisoidal caliche nodules, variegated facies (well PN3160, 2,286). Modified from Pashin and Kugler (1992).

mosing groups up to 0.5 feet thick and have variable lateral extent. Stylolites and pressure-solution seams commonly are distributed along laminae. Kaolinite-cemented sandstone with abundant clay laminae and shale clasts is most abundant along the margins of the sandstone lenses.

Disarticulated skeletal material, mainly brachiopod shells, crinoid ossicles, bryozoans, and gastropods, is concentrated in laminae to thick beds. Locally, shell accumulations are as thick as 4.0 feet. Brachiopod shells generally are poorly oriented but are most commonly preserved convex-side up. Concentrations of skeletal debris localize zones of pervasive concretionary calcite and ferroan dolomite/ankerite cement within the sandstone facies. Aside from skeletal material, biogenic structures in the sandstone facies are few, save for isolated feeding, resting, and escape burrows.

VARIEGATED FACIES

The variegated facies is lithologically diverse and is so named because these strata contain the most diverse colors in the lower Parkwood Formation (fig. 44). The facies has a serrate to blocky log signature with resistivity intermediate between that of the shale-and-siltstone and sandstone facies. Cores establish that the variegated facies generally occurs in the upper part of the Carter sandstone. Within the lenses, the sandstone facies grades depositionally updip into lenticular sandstone, siltstone, and shale, which, in turn, grade into medium gray siltstone and dark gray to brownish-gray shale and mudstone.

Lenticular-bedded sandstone, siltstone, and shale predominate in the variegated facies (fig. 44). Sandstone and siltstone occur as irregular, yellowish-brown, calcareous lenticles that typically range in thickness from 0.5 to 4.0 inches and are separated by anastomosing clay laminae. Most of the lenticles appear structureless, but some sandstone and siltstone contains deformed ripple cross laminae which reveal that the lenticles represent pebble- to cobble-size, intraclastic flat pebbles. The lenticles contain few biogenic structures, although branching, dark reddish-brown siderite rhizoids, or root structures, are locally abundant. Sandstone in the variegated facies is cemented pervasively with kaolinite, siderite, and ferroan dolomite/ankerite, which impart a yellowish- to reddish-brown color mottling to much of the facies.

Some cores contain relatively homogeneous medium- to thick-bedded shale and siltstone. The siltstone contains laminae that are disrupted by abundant feeding and escape burrows as well as sideritic rhizoids. Dark gray shale, in contrast, is locally laminated and contains plant fragments. Most of the shale is root mottled or contains abundant slickensides. Sand- to granule-size limestone nodules are also present in the shale. Medium to thick beds of red (brownish-gray) shale have gradational contacts with the dark gray shale and are also root mottled; some red mudstone has a pisoidal texture (fig. 45d).

RESERVOIR ARCHITECTURE

Although lithofacies characteristics vary little among fields, stratigraphic architecture varies considerably and is a primary source of heterogeneity that should be considered when developing strategies for improved oil recovery. This section discusses stratigraphic variation within and among Carter and *Millerella* oil reservoirs on the basis of isolith patterns and resistivity-log cross sections. In each field, reservoir lithofacies vary predictably with respect to reservoir architecture and are readily identified by characteristic well-log signatures.

NORTH BLOWHORN CREEK OIL UNIT

The Carter sandstone in North Blowhorn oil unit, the most productive oil unit in the basin, is a northwest-southeast trending body that extends northwest of the oil unit and terminates in the southeast part of the unit (fig. 42) . The sandstone body has a sublinear northeast margin and an irregular southwest margin. Sandstone is locally thicker than 40 feet along the axis of the body, which is close to the northeast margin of the reservoir. Isolith patterns become increasingly irregular toward the southeast, and the thickest sandstone defines a series of hook-like forms that project westward from the main axis of the sandstone body.

Resistivity-log cross sections from North Blowhorn Creek oil unit establish that reservoir architecture is internally complex but varies systematically along the length of the reservoir sandstone body (fig. 46). The top of the Bangor Limestone is sharp and is readily correlated throughout the oil unit, and above the Bangor is a shale unit that is assignable to the shale-and-siltstone lithofacies and extends throughout the oil unit. Although the basal contact of the shale is sharp and continuous, the upper part of the shale intertongues with Carter sandstone.

The North Blowhorn Creek oil reservoir comprises numerous sandstone lenses (fig. 46). The longitudinal cross section, A-A', reveals a series of imbricate, clinoformal lenses that dip depositionally

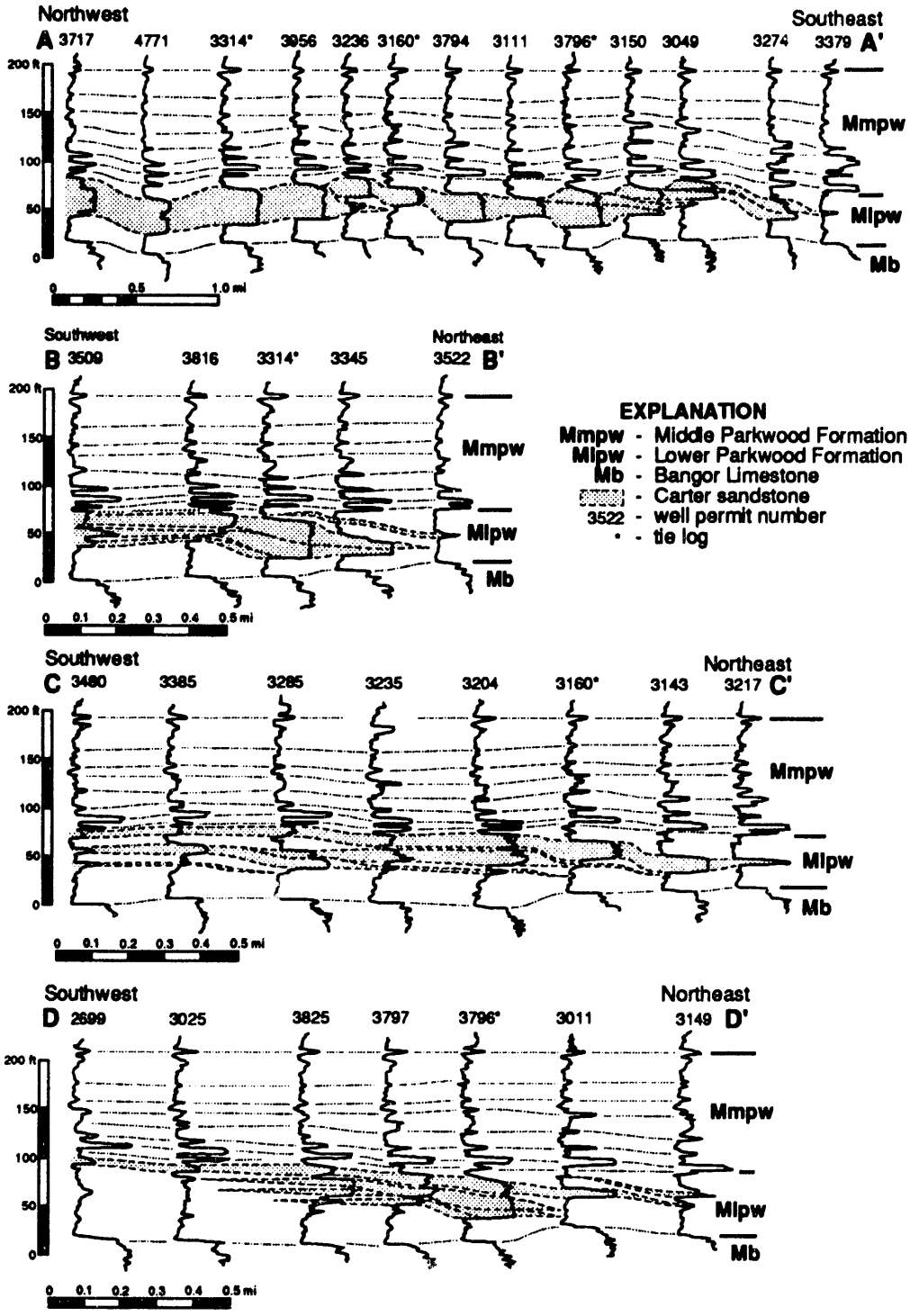

Figure 46.--Resistivity-log cross sections of the lower Parkwood Formation and associated units, North Blowhorn Creek oil unit. See figure 41 for location (modified from Pashin and Kugler, 1992).

southeast and decrease in size toward the terminus of the sandstone body. Similarly, the transverse cross sections, B-B', C-C', and D-D', depict imbricate, clinoformal lenses that dip depositionally northeast. Within the transverse sections, however, the sandstone lenses contain distinctive changes in log signature, and hence, internal facies architecture.

Depositionally downdip parts of the lenses tend to have a blocky log signature with high resistivity, reflecting the best reservoir quality, although a serrate pattern is locally apparent (fig. 46). Lenses are typically amalgamated along the sandstone-body axis, forming a single, blocky unit of reservoir sandstone that is the sandstone facies. In contrast, the depositionally updip parts of the lenses tend to have a serrate log pattern, and resistivity decreases toward the southwest, reflecting decreased reservoir quality. Sandstone with a serrate pattern includes strata of the sandstone and variegated lithofacies.

The middle Parkwood Formation contains many resistive carbonate and shale markers (fig. 46). In general, limestone units thin upward, and carbonate content increases slightly toward the northeast and markedly toward the southeast. Moreover, limestone markers tend to follow irregularities in the upper contact of the sandstone, descending depositionally northeast across the reservoir.

WAYSIDE OIL UNIT

Wayside oil unit was developed in one of the smallest lensoid sandstone bodies in the map area (fig. 42). The sandstone is generally thinner than 25 feet and pinches out abruptly west of the oil unit (fig. 47). Toward the southeast, however, the sandstone thins by intertonguing with lower Parkwood shale siltstone, which belongs to the shale-and-siltstone lithofacies.

As in North Blowhorn Creek oil unit, the Carter reservoir in Wayside oil unit is composed of imbricate, clinoformal sandstone lenses (fig. 47). By contrast, depositional dip of the lenses is much gentler in Wayside oil unit. The sandstone has the blocky resistivity signature of the sandstone lithofacies only in the northwestern part of the reservoir. In most of the reservoir, however, the sandstone has the serrate signature of the sandstone and variegated lithofacies.

The *Millerella* sandstone is present southeast of the oil unit and is generally thinner than 10 feet (figs. 43, 47). The sandstone has a blocky to serrate resistivity signature and passes northwestward into limestone. Resistive markers in the middle Parkwood Formation are continuous and evenly spaced throughout Wayside oil unit, reflecting the limited stratigraphic relief of the top of the Carter sandstone.

SOUTH BRUSH CREEK OIL UNIT

The Carter sandstone in South Brush Creek oil unit has a distinctive, subcircular isolith pattern that contrasts markedly with that of the other oil reservoirs (fig. 42). Like other Carter reservoirs, the sandstone is composed of gently dipping clinoformal sandstone units that dip toward the north and east (fig. 48). A unique characteristic of the Carter reservoir in the South Brush Creek area is truncation of the top of the sandstone below the shale that forms the top of the lower Parkwood Formation.

Well logs in the South Brush Creek area have a serrate, coarsening-upward log signature, and many logs contain a blocky sandstone unit at the top (fig. 48). Cores contain intercalated strata of the shale-and-siltstone and sandstone facies. These cores reflect intertonguing of these lithofacies, with the sandstone lithofacies thickening upward at the expense of the shale-and-sandstone lithofacies. The shale that seals the reservoir belongs to the variegated lithofacies and is composed of silty, rooted mudstone.

The *Millerella* sandstone is preserved in the northeasternmost part of cross-section I-I' (fig. 48) and has a serrate log signature. As in Wayside oil unit, the *Millerella* passes northwestward into limestone. The sandstone is included in the *Millerella* pool of Blowhorn Creek oil unit, which is discussed in detail in the next section. Although considerable stratigraphic relief is at the top of the Carter sandstone, the resistive limestone markers of the middle Parkwood Formation are evenly spaced and have limited stratigraphic relief. However, at the eastern end of cross-section H-H', markers near the base of the middle Parkwood diverge sharply, and the *Millerella* limestone rests directly on the Carter sandstone.

BLOWHORN CREEK *MILLERELLA* OIL UNIT

Blowhorn Creek oil unit contains the most productive *Millerella* sandstone reservoir in the Black Warrior basin and brings to light characteristics of Carter and *Millerella* sandstone that are not apparent in other fields. The isolith pattern of the Carter sandstone in the northwest part of Blowhorn Creek oil unit resembles that in South Brush Creek oil unit

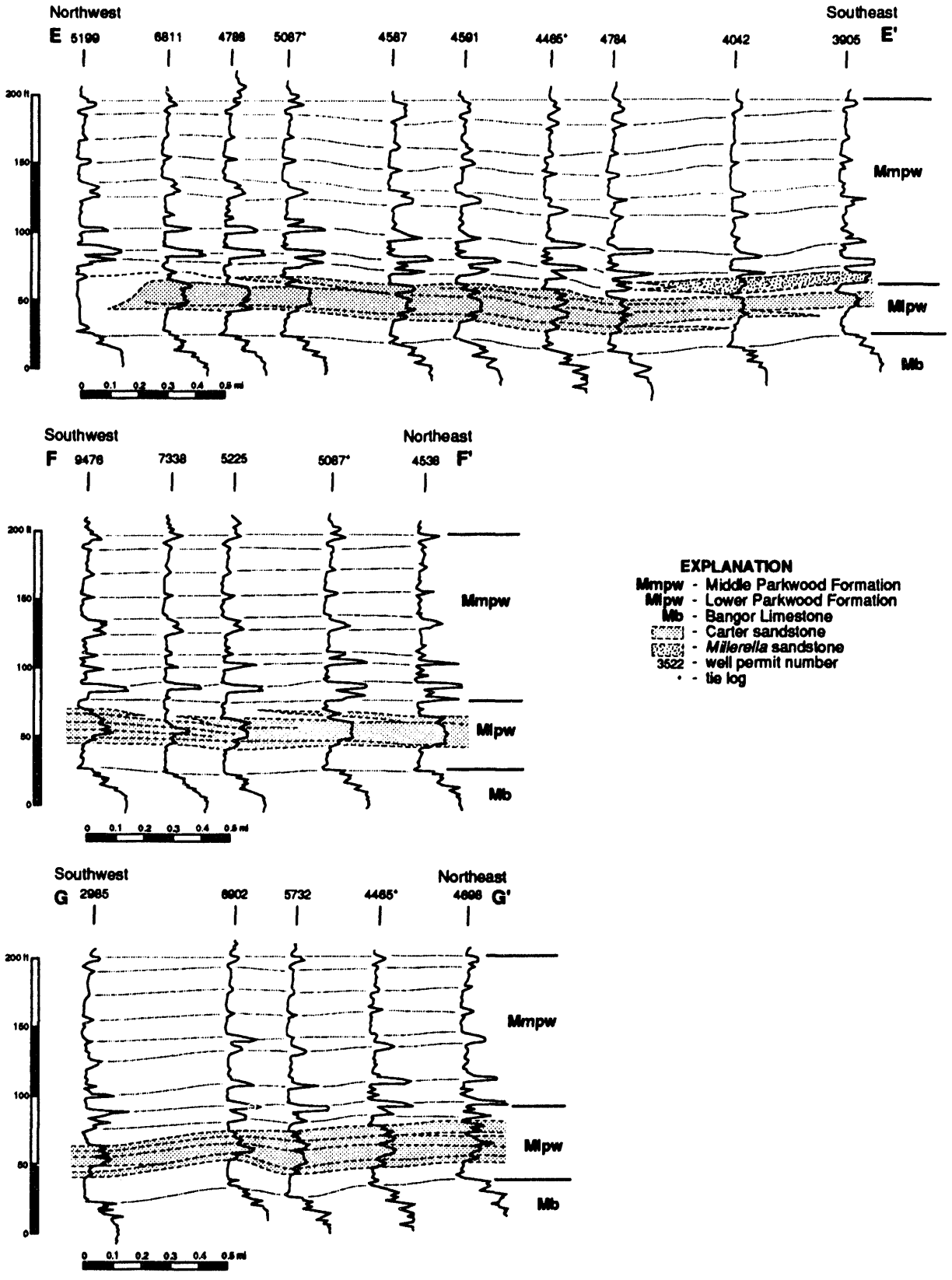

Figure 47.--Resistivity-log cross sections of the Lower Parkwood Formation and associated units, Wayside oil unit. See figure 41 for location.

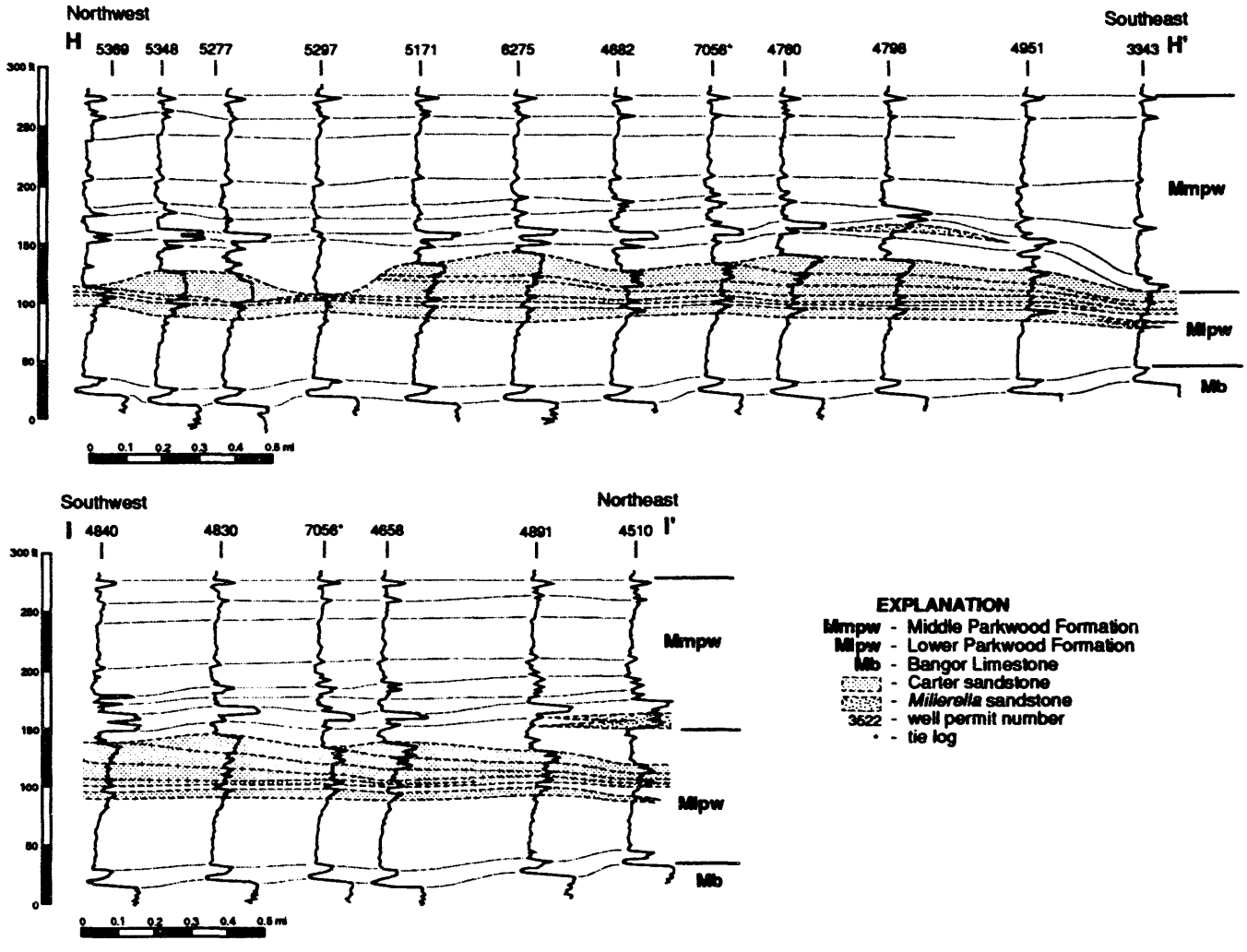

Figure 48.--Resistivity-log cross sections of the lower Parkwood Formation and associated units, South Brush Creek oil unit. See figure 41 for location.

(fig. 42). In the eastern part, by contrast, the Carter reservoir is thin or absent.

As in the South Brush Creek area, the Carter sandstone in Blowhorn Creek oil unit has a serrate to blocky, coarsening-upward resistivity signature (fig. 49). Gently dipping, clinoformal sandstone lenses are readily apparent in the cross sections, and the Carter reservoir is simply a continuation of that in South Brush Creek. Therefore, although cores are lacking, reservoir lithofacies ostensibly are the same as those in South Brush Creek oil unit. In parts of Blowhorn Creek oil unit, however, the Carter sandstone is truncated by shale-filled scours, which locally truncate the full thickness of the sandstone.

The *Millerella* sandstone is present in most of Blowhorn Creek oil unit and generally ranges from 10 to 25 feet in thickness (fig. 43). Thickness is fairly uniform in much of the field, but the sandstone is absent in a northeast-trending belt. Well logs establish that the sandstone has a highly resistive, blocky to serrate log signature with no evidence of a consistent vertical grain-size trend (fig. 49). In the eastern part of the field, where the sandstone is absent, the sandstone is apparently truncated by a shale filled scour similar to the one truncating the Carter sandstone. Resistive markers in the middle Parkwood Formation have considerably more stratigraphic relief than in most other areas. Moreover, the *Millerella* limestone is typically absent in wells that penetrate shale-filled scours that truncate the *Millerella* sandstone.

BLUFF OIL FIELD

Bluff oil field contains the most heterogeneous Carter and *Millerella* sandstone reservoirs discussed in this report. Furthermore, the field contains three oil units, North Bluff, Central Bluff, and South Bluff. The Carter sandstone in Bluff field has two depocenters, and thickness ranges from 0 to more than 30 feet (fig. 42). Overall, the sandstone-isolith pattern resembles that in Wayside oil unit.

As in the other fields, the Carter sandstone in Bluff field has a serrate to blocky, coarsening-upward resistivity pattern and is composed of imbricate, clinoformal sandstone lenses. What separates Bluff field from the other oil units, however, is that together, Carter and *Millerella* reservoirs comprise six uncontacted or poorly contacted oil compartments (fig. 50). The lowermost Carter compartment is restricted to a few wells in the middle of the field and locally rests directly on the Bangor limestone. With the exception of a thin sandstone lens in the northern part of the field, the other Carter compartments have an imbricate aspect, each dipping and stepping toward the southeast.

The *Millerella* sandstone is present only in the northwestern part of the oil field and is locally thicker than 30 feet (fig. 43). The linear nature of the sandstone body contrasts sharply with other *Millerella* sandstone bodies, which have an irregular, patch-like geometry. The resistivity pattern of the sandstone is serrate to blocky and thus resembles that in Blowhorn Creek oil unit (fig. 50). Stratigraphically, the *Millerella* sandstone is the youngest reservoir compartment in Bluff field and represents a reversal of the southeast-stepping trend in the Carter sandstone (fig. 50). Middle Parkwood limestone units conform closely to the upper surface of the sandstone, and thus resemble most closely those in North Blowhorn Creek oil unit. In addition, the *Millerella* limestone thickens markedly as Carter sandstone lenses step clinoformally toward the southeast.

ENVIRONMENTAL INTERPRETATIONS

SHALE-AND-SILTSTONE FACIES: STORM-DOMINATED SHELF

The shale-and-siltstone facies is interpreted to represent a storm-dominated shelf mud blanket that prograded across the Bangor carbonate bank (fig. 51). Presence of thin siltstone beds with wave ripples indicates that mud deposition was interrupted by episodic wave events. Wavy, lenticular, and flaser-bedded siltstone with abundant load casts and wave ripples (fig. 45a) are widespread in the Appalachian region and have been interpreted to represent shelf storm deposits (Pashin and Ettensohn, 1987). Similar sand-rich deposits are now forming on the storm-dominated shelf of the North Sea (Aigner and Reineck, 1982) and have been recognized in the Lewis sandstone of the Black Warrior basin (Holmes, 1981; DiGiovanni, 1984; Pashin and others, 1991). Graded siltstone laminae may represent simple fallout from suspension after storms or alternatively, river-mouth sediment plumes that episodically extended into the shelf area.

Abundant load casts, some of which are syndepositional (fig. 45a), indicate that the muddy substrate was soft, fluid and could be deformed with only minimal accumulation of quartz-rich sediment. Lack of body fossils and presence of pyrite nodules in the facies suggests that the substrate was too fluid and too foul to accommodate a diverse fauna. However, feeding burrows and resting traces indicate

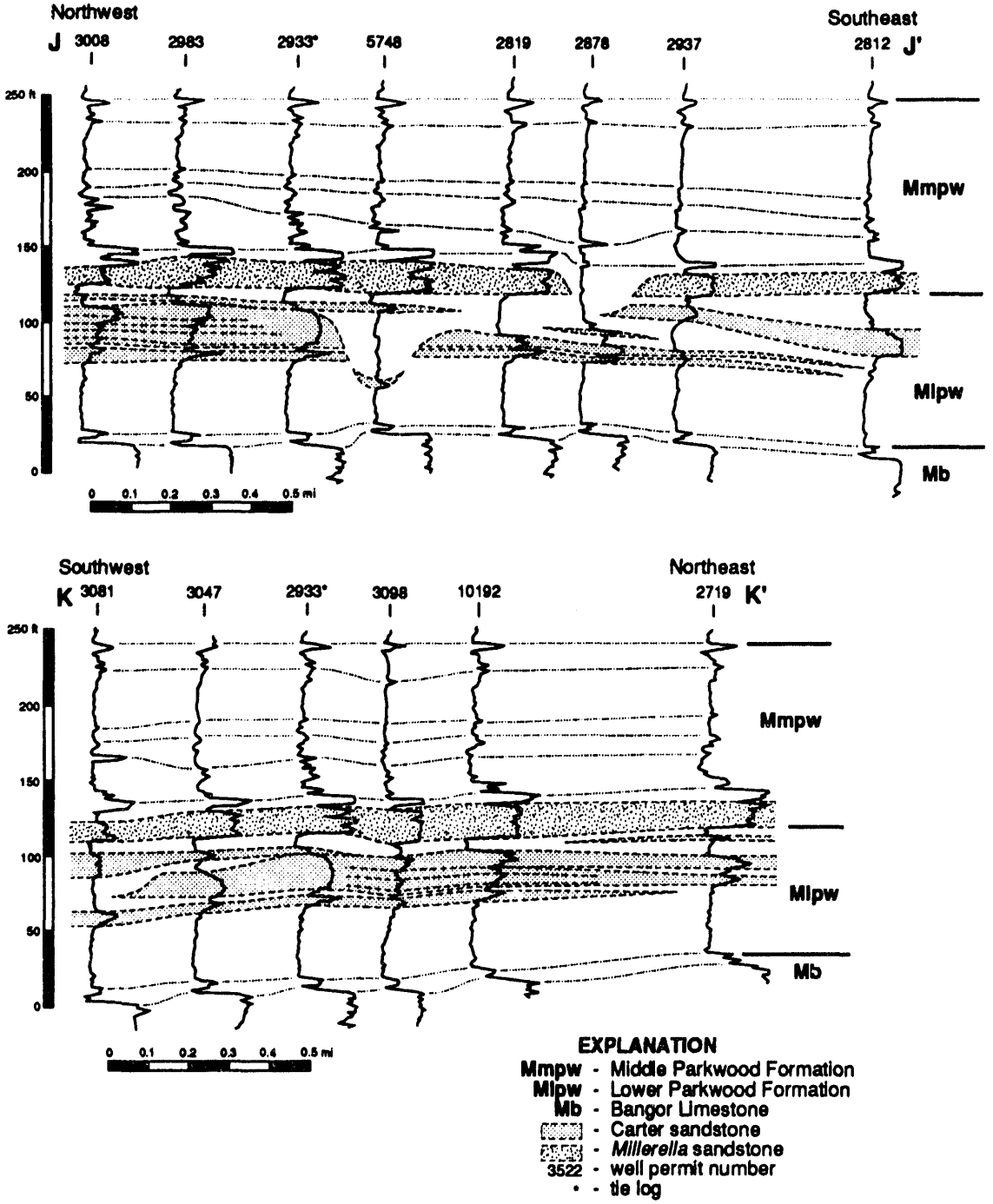

Figure 49.--Resistivity-log cross sections of the lower Parkwood Formation and associated units, Blowhorn Creek oil unit. See figure 41 for location.

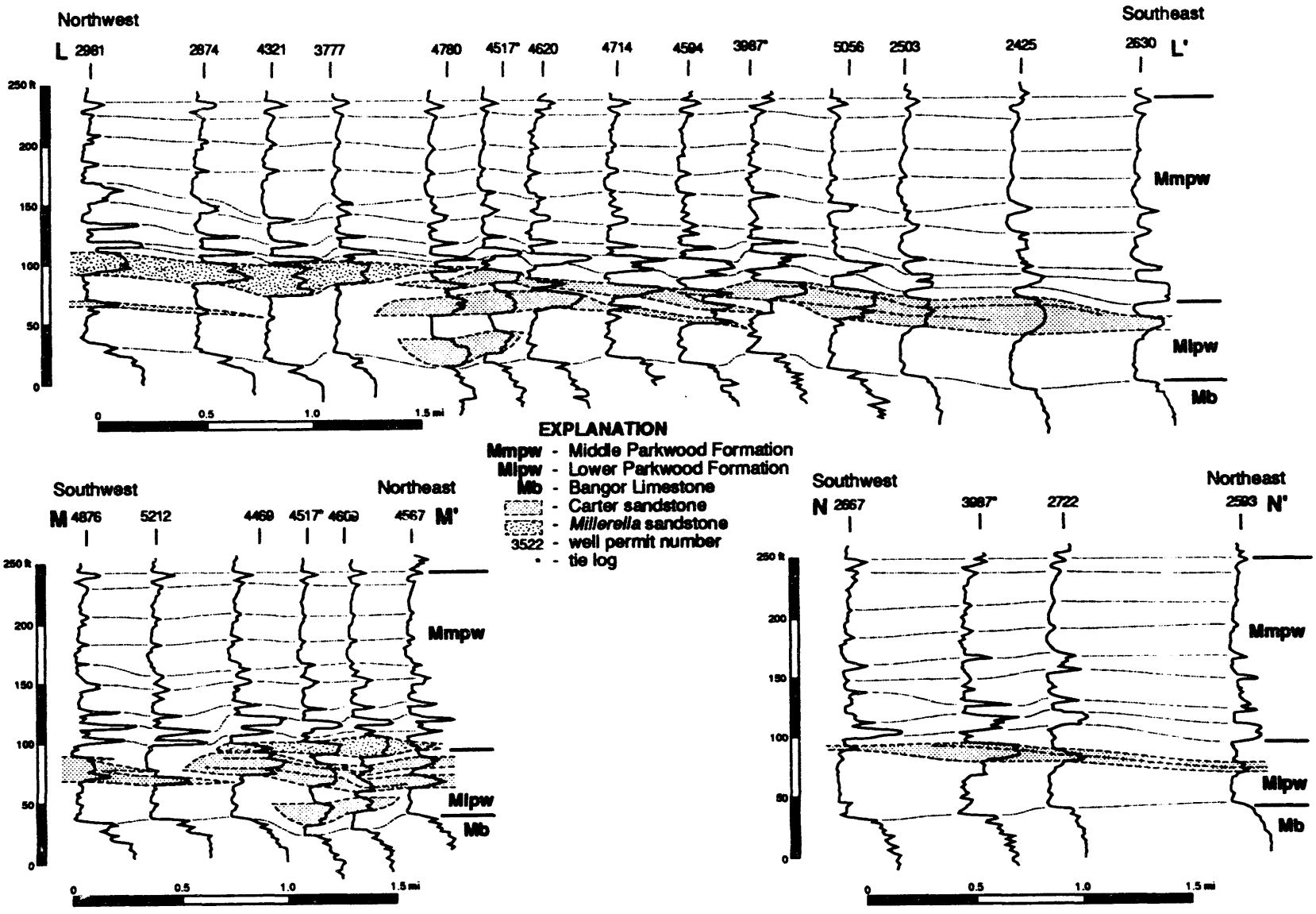

Figure 50.--Resistivity-log cross sections of the lower Parkwood Formation and associated units, Bluff oil field. See figure 41 for location.

that the organic-rich substrate provided food and refuge for some organisms. The general thickening- and coarsening-upward sequence of the shale-and-siltstone facies signifies that these strata are progradational and are genetically related to the shore-zone deposits of the sandstone facies.

SANDSTONE FACIES: SHOREFACE AND FORESHORE

The sandstone facies is interpreted to represent sedimentation in a spectrum of beach and shoreface environments (fig. 51). Similar beach and shoreface deposits are common in other Chesterian reservoirs of the Black Warrior basin (Pashin and others, 1991). The thin zone of gradation from the shale-and-siltstone facies into the sandstone facies indicates that the transition from shelf to shoreface was well defined. The general sequence of sedimentary structures in the sandstone lithofacies, specifically (1) lunate-ripple cross laminae (fig. 45b), (2) high-angle planar and tangential crossbeds, and (3) low-angle, planar crossbeds (fig. 45c), is characteristic of shoreface-beach systems and reflects progressive deformation of waves approaching shore (Clifton, 1976).

Dominance of lunate-ripple cross laminae (fig. 45b) over wave ripples suggests that waves were supplanted by unidirectional currents in the lower shoreface, perhaps in response to geostrophic flows and rip currents that may have at times been affected by high river-mouth discharge. Thin intervals of high-angle crossbedding are characteristic of shoreface bars and ridge-and-runnel systems, which occur in the breaker zone and the lower foreshore of modern beach systems (Davis and others, 1972; Davidson-Arnott and Greenwood, 1976). Low-angle, planar crossbedding (fig. 44), furthermore, is the characteristic sedimentary structure of the breaker, surf and swash zones of beaches (Thompson, 1937; Clifton, 1976). Deviation of sequences in the sandstone facies from an idealized

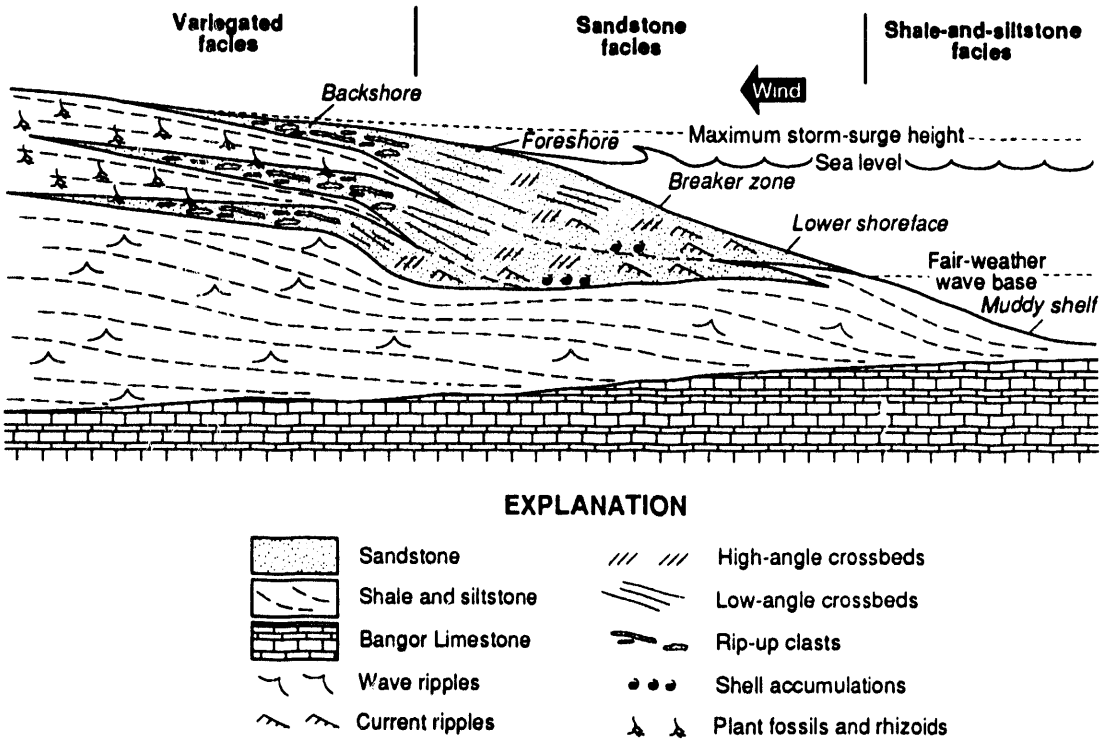

Figure 51.--Depositional model of Carter sandstone showing lateral variation of facies within sandstone lenses and environmental interpretations (modified from Pashin and Kugler, 1992).

succession of sedimentary structures owes to several sources including amalgamation of sandstone lenses (fig. 46), reworking during storm surges (fig. 51), multiple shoreface-bar systems, and instability of the beach-shoreface system caused by tides and variations in river-mouth discharge.

Shale-clast conglomerate layers indicate that shoreface erosion was a significant process. Some conglomeratic intervals apparently signify episodes when muddy intervals were reworked as amalgamated sandstone lenses formed along the reservoir axis. Shale clasts may have also been eroded from the innermost shelf, transported by geostrophic flows, and deposited on the shoreface. Isolated shale clasts, moreover, may simply represent mud drapes reworked from shoreface sediment.

Scarce bioturbation indicates that the sandy substrate was, in contrast to the organic-rich mud of the shale-and-siltstone facies, a poor food source for soft-bodied infauna. Poor orientation and disarticulation of crinoids and brachiopods indicates transport, but it is doubtful that the skeletal material was transported from the adjacent shelf which lacked calcified faunas or from backshore environments which probably had reduced salinity. Perhaps these organisms lived in protected areas at the foot of the shoreface where substrate and other environmental conditions were most stable.

As with shale clasts, shell accumulations apparently formed in more than one manner. Some thin accumulations, particularly those in low-angle crossbedded sandstone, are interpreted to represent shells washed up on the beach, whereas other accumulations, particularly those in rippled sandstone, were concentrated by shoreface currents. The thickest shell accumulations ostensibly formed in rip channels or are thick lower-shoreface storm deposits.

VARIEGATED FACIES: BACKSHORE

The variegated facies is interpreted to represent a suite of backshore environments in which sedimentation was dominated by storm surges and soil formation (fig. 51). The depositionally updip position of the serrate, moderately resistive variegated facies relative to the blocky, highly resistive sandstone facies (figs. 44, 46) indicates that beach topography sloped gently offshore and that eolian dune ridges, which are so prevalent in modern beach-barrier systems (McCubbin, 1982; Elliott, 1986), were not present. Some beach systems in southwestern Florida lack eolian dune ridges and are instead composed of low-relief ridges containing swash deposits (Stapor and others, 1991). Analysis of cores further suggests that washover fans, which develop as dune ridges are breached by a surging sea, also were not developed. Instead, structures herein designated as storm-surge aprons are interpreted to have been the major lower backshore deposit (fig. 52).

Root structures and abundant intraclastic flat pebbles immediately landward of the foreshore indicate episodes of high-energy sedimentation in the supratidal zone. Although no clear analogs for these deposits have been identified, intermittent flooding of the supratidal zone occurs on wind-tidal flats (Miller, 1975; Reineck and Singh, 1980). However, modern wind-tidal flats form in protected lagoons and embayments and are thus dominated by fine-grained deposits with low-energy sedimentary structures. In contrast, the Carter intraclasts formed immediately behind an unprotected foreshore and are thus interpreted to have been deposited by major storm surges, although seasonal tidal variations may have played some role in forming these deposits. Along modern shorelines, hurricane-related surges can raise water level more than 20 feet (Hayes, 1967).

Although sedimentation in the lower backshore was dominated by vigorous, storm-induced flows, low-energy processes prevailed in the upper backshore. Rooting and pisoidal structures (fig. 45d) provide evidence for exposure in an evaporative setting. Gray paleosols probably formed in marshy areas that favored reduction and preservation of organic matter, whereas red paleosols probably formed on topographic highs that favored oxidation and nodule formation. Deposits of laminated or burrowed shale and siltstone are interpreted to have formed in lagoonal environments, and some of these deposits may even represent saline ponds filled with slackwater from storm surges.

DEPOSITIONAL SYSTEMS AND FACIES HETEROGENEITY

The beach deposits of the Carter sandstone indicate development of a muddy strandplain system during destruction of the lower Parkwood deltaic system. The variety of isolith patterns and stratigraphic architecture in Carter and *Millerella* oil reservoirs (figs. 42, 46-50) demonstrates that those beach systems were diverse. Moreover, the change of sandstone-body geometry from the lobate bodies in the southeast to the thin, isolated lenses in the northeast records systematic evolution of the strandplain and exceptional preservation of the paleogeographic framework of the shoal-water delta.

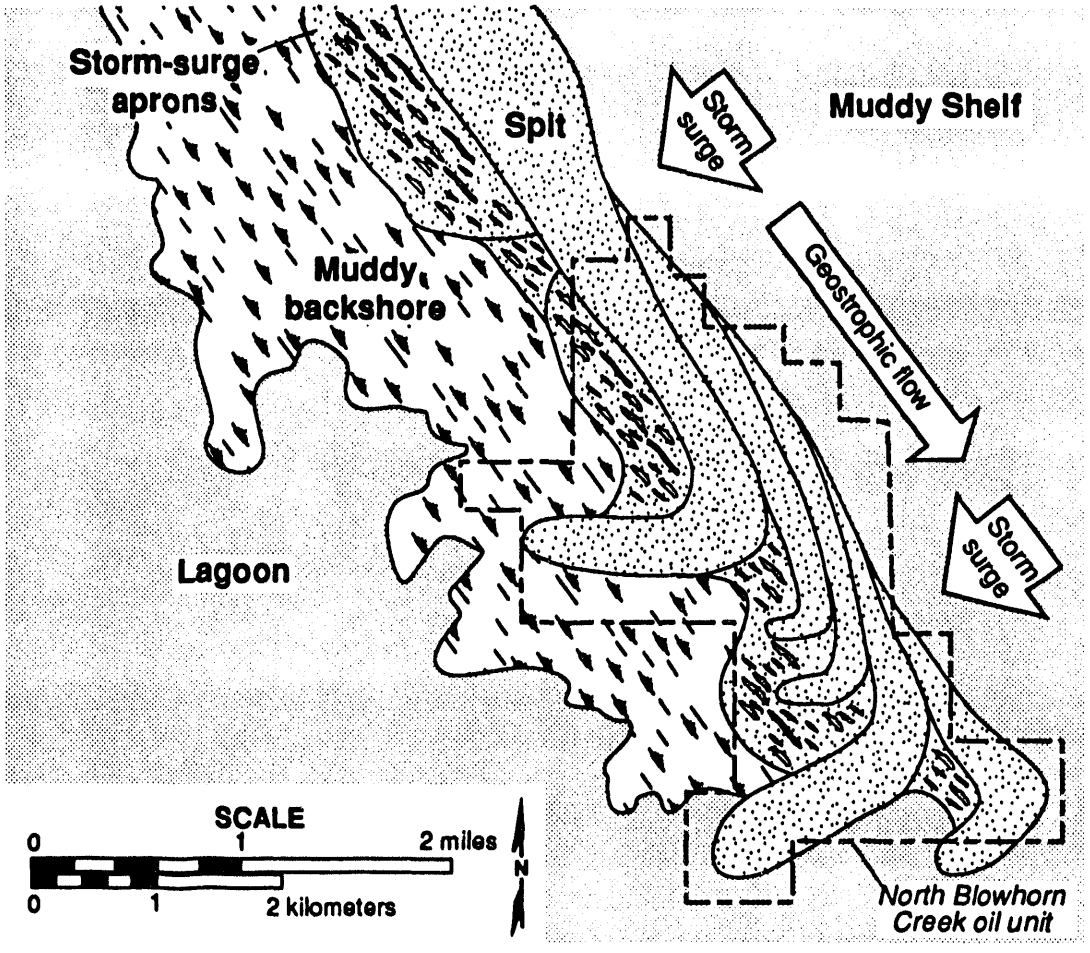

Figure 52.--Paleogeographic reconstruction of the North Blowhorn Creek spit system (modified from Pashin and Kugler, 1992).

The Carter sandstone in North Blowhorn Creek oil unit has been interpreted to represent a spit-type beach system (Pashin and Kugler, 1992) (fig. 52). Spits form at the down-drift ends of beaches and are characterized by a fan-like arrangement of ridges that curve landward and accrete in the direction of geostrophic flow. Spit-style beach systems form in several depositional settings, including tidal inlets (Boothroyd, 1985), estuary mouths (Fairbridge, 1980), and even chenier plains (Gould and McFarlan, 1959). Considering the North Blowhorn Creek reservoir part of a shoal-water delta complex, the best modern analog is in southern France where a spit-style beach complex is fed directly by the Grand Rhône distributary (van Andel and Curray, 1960). Similar distributary-mouth beach systems formed on ancient shoal-water lobes of the Mississippi Delta (Penland and Boyd, 1985) and may be more widespread in the geologic record than commonly thought.

The sublinear northwest boundary of the sandstone body marks the seaward spit margin, whereas the irregular southeast margin delineates spit arms (figs. 42, 52). The most compelling evidence for a spit complex in North Blowhorn Creek is imbrication of successively smaller sandstone lenses toward the southeast terminus of the sandstone body (fig. 46). Each sandstone lens is interpreted to include a spit arm, and the largest arms are in the west-central and southeastern parts of the oil unit. Evidence

for storm surges in a northeast-facing beach system establishes that the dominant wind had a major northerly to easterly, onshore component (figs. 51, 52), and southeastward spit accretion indicates that geostrophic flows were directed southeast. Blocky beach-shoreface sandstone occurs farther above the Bangor Limestone in each successive sandstone lens. This configuration suggests that spit deposition occurred as soft, fluid shelf mud compacted and also provides confirming evidence that delta destruction and beach formation occurred partly in response to a net relative rise of sea level.

The localized, arcuate geometry of the Carter reservoir in Wayside oil unit contrasts with the elongate geometry of that in North Blowhorn Creek oil unit (fig. 42). The gentle dip of the clinoformal sandstone lenses in this area (fig. 47) further indicates that a different style of beach system formed at the distal edge of the shoal-water deltaic system. Small, arcuate barriers commonly form in areas of high tidal range (Hayes, 1979), and similar intertidal beach deposits were documented in the Lewis sandstone by Pashin and others (1991). Abrupt pinchout of the sandstone in the northwesternmost part of the oil unit is suggestive of truncation by an inlet or tidal channel. Indeed, the small, arcuate sandstone bodies in the northeastern part of the map area are separated by an area lacking sandstone that is dendritic in plan (fig. 42). Accordingly, this area is interpreted to represent an estuarine tidal embayment.

The lobate geometry and serrate, coarsening-upward resistivity signature of the Carter sandstone in South Brush Creek oil unit and adjacent areas (figs. 42, 48) reflects sedimentation at the distal edge of the constructive deltaic complex. Beach deposits indicate that this part of the delta was a wave-dominated system with an original cuspate geometry. Truncation of the top of the sandstone below the shale of the variegated facies, however, suggests degradation of the constructive deltaic lobes as the shoal-water deltaic system prograded farther seaward. Hence, the truncation surface is interpreted as a lowstand surface of erosion and the sealing shale is interpreted as a transgressive deposit formed by terrestrial backfilling of the erosional topography. Similar degraded beach sandstone bodies are common in modern wave-dominated deltaic systems and are especially well documented in the Doce Delta of South America (Dominguez and Wanless, 1991).

The Carter reservoir in Blowhorn Creek oil unit is essentially a continuation of that in South Brush Creek oil unit (figs. 42, 49) and is thus interpreted as the distalmost fringe of the constructive, wave-dominated deltaic system. Blowhorn Creek oil unit differs, however, by the presence of shale-filled scours that truncate the full thickness of Carter and *Millerella* reservoirs (fig. 49). These scours differ in origin from the erosional surface that truncates the top of the South Brush Creek reservoir, because sandstone lenses extend above the structures in the Carter sandstone. For this reason, the scour-and-fill structures are interpreted to represent ephemeral tidal channels that were abandoned and filled with mud. Once full, beach environments were again established above the channels. A similar process is active in modern beach systems, where beach systems heal after being incised by inlets (Morton and Donaldson, 1973; Davis and others, 1989).

In Bluff field, the Carter sandstone is part of a string of sandstone lenses that is attached in the northwest to the axial sandstone of the North Blowhorn Creek reservoir (fig. 42). Therefore, the Carter reservoir in Bluff field is interpreted as part of a string of beach systems that formed after abandonment of the North Blowhorn Creek spit system. The southeast-stepping pattern of sandstone bodies resembles that in North Blowhorn Creek oil unit (fig. 50), but sandstone-isolith patterns resemble those in the vicinity of Wayside oil unit (fig. 42), suggesting development of a delta-destructive beach system intermediate between the spit and the arcuate, tide-influenced barriers. The result of this configuration was development of the most heterogeneous Carter-*Millerella* field in the basin, which contains six uncontacted or poorly contacted oil compartments.

Extension of *Millerella* sandstone bodies laterally into limestone (figs. 43, 47, 48) indicates deposition in the latest stages of delta destruction as a carbonate bank was again established in the map area. The highly resistive, blocky to serrate log signature of the *Millerella* (figs. 49, 50), which lacks evidence for systematic vertical grain-size variation, reflects reworking of deltaic by a transgressing sea and formation of the least heterogeneous oil reservoirs analyzed. Preservation of *Millerella* sandstone below the grainstone-bearing *Millerella* limestone indicates deposition in extremely shallow water, and differing isolith patterns indicates deposition in diverse environments.

The widespread, uniformly thick nature of the *Millerella* sandstone in Blowhorn Creek oil unit (fig. 43) differs from all beach deposits described herein and is accordingly interpreted to represent part of a delta-destructive shoal massif. The linear scour-and-fill structure that truncates the sandstone

body (figs. 43, 49) is interpreted as a tidal channel, which islolated the Blowhorn Creek reservoir from the larger sandstone body in the southeast. In Bluff oil field, the linear isolith pattern and close association with Carter beach deposits suggests that it is essentially part of the linear string of beaches that is attached to the North Blowhorn Creek spit (fig. 43). For this reason, the backstepping relationship of the *Millerella* sandstone to the Carter sandstone bodies (fig. 50) is interpreted to represent development of a small beach or shoal massif above a tidal inlet as the deltaic strandplain was inundated.

To summarize, Carter and *Millerella* sandstone reservoirs in the map area represent systematic evolution of a delta-destructive strandplain. Initial formation of a constructive, wave-dominated delta is represented by Carter reservoirs in South Brush Creek and Blowhorn Creek oil units. As the strandplain continued to prograde, the abandoned wave-dominated delta was exposed and eroded, isolating these reservoirs from the main part of the delta system. As the main delta was abandoned, the North Blowhorn Creek spit, which composes the most productive oil reservoir in the Black Warrior basin, accreted in response to southeastward geostrophic flows.

Following spit accretion, a string of tide-influenced beaches developed that is attached to the North Blowhorn Creek beach axis. Among these beach deposits are the Carter reservoirs in Bluff field, which compose multiple uncontacted or poorly contacted oil compartments. The final stage of strandplain progradation was development of small, arcuate barriers and associated tidal inlets, which are preserved in Wayside oil unit. After this event, the strandplain was inundated, and the *Millerella* sandstone, which makes up the least heterogeneous reservoirs examined, was deposited in shoal massifs and possibly beaches as platform carbonate deposition began.

Beach deposits in Carter sandstone are markedly different from those that have been investigated in terms of reservoir heterogeneity. Previous studies (Sharma and others, 1990a, b; Schatzinger and others, 1992; Schatzinger and Sharma, 1993) have focused on widespread, interdeltaic barrier-island deposits that are much less heterogeneous than the localized, muddy, delta-destructive strandplain deposits of the Carter. Imbricate sandstone lenses present a heterogeneity that is common to all Carter reservoirs characterized in this report. However, the size and arrangement of those lenses differ greatly among the oil fields, reflecting the diverse beach systems of an evolving delta-destructive strandplain. Moreover, the arrangement of lenses has been modified in places by channelization related to tidal inlets and subaerial exposure, and reservoir quality changes from best in foreshore parts of the lenses to poor in the backshore parts. For these reasons, each Carter reservoir has a unique pattern of facies heterogeneity, and in order for improved recovery operations to be implemented most effectively, plans need to be tailored to that heterogeneity on a field-by-field basis.

PETROLOGIC CHARACTERISTICS

DETRITAL FRAMEWORK

Carter sandstone in North Blowhorn Creek oil unit is dominantly very fine to fine-grained, moderately well sorted quartzarenite, using the classification of Folk (1980) and excluding intrabasinally derived rock fragments from the detrital framework for classification (figs. 53, 54). Carter and Lewis reservoirs in other parts of the basin have a similar framework composition (Shepard, 1979; Bearden, 1984; Bearden and Mancini, 1985; Bat, 1987; Hughes and Meylan, 1988). A more detailed description of petrologic aspects of Carter sandstone reservoirs in North Blowhorn Creek oil unit is in Kugler and Pashin (1992). Despite the quartzose nature of the sandstone, reservoirs in North Blowhorn Creek oil unit and other fields in the Black Warrior basin are heterogeneous, owing not only to the imbricate sandstone lenses and associated internal facies changes, but also to the presence of intrabasinal framework grains and to diagenesis.

Quartz composes more than 97 percent of the detrital framework of most Carter sandstone in North Blowhorn Creek oil unit. More than 90 percent of detrital quartz is monocrystalline, and more than 95 percent of this quartz has nonundulose to slightly undulose extinction. Polycrystalline quartz generally composes less than 10 percent of total quartz and contains both stable and unstable textures (e.g., Young, 1976), including textures indicative of a metamorphic provenance. Feldspar is scarce and includes orthoclase, microcline, plagioclase, and perthite; it typically composes less than one percent of rock volume. The present feldspar composition of Carter sandstone is not representative of feldspar composition at the time of deposition because of framework grain dissolution and replacement by kaolinite.

Rock fragments are both extrabasinal and intrabasinal and together may account for more than 20

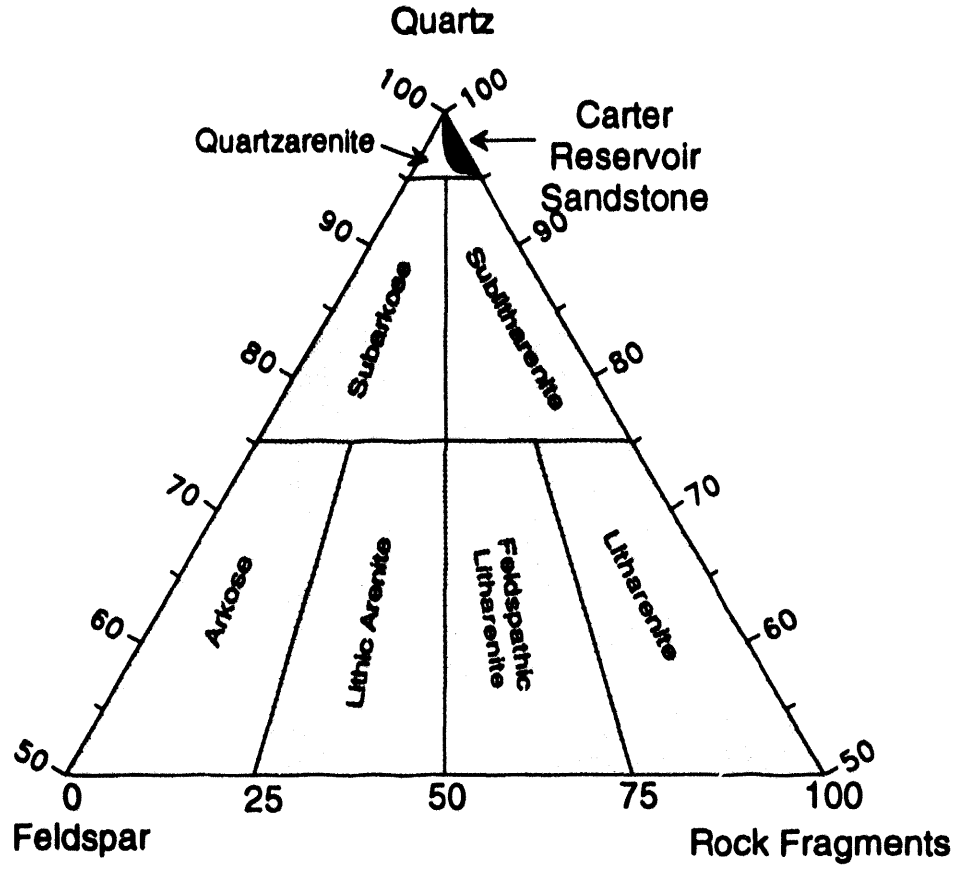

Figure 53.--Detrital framework composition of Carter sandstone (classification diagram of Folk, 1980).

percent of total rock volume. However, extrabasinally derived rock fragments are only a minor component of Carter sandstone and account at most for only a few percent of the total detrital framework. The most common extrabasinally derived rock fragment, composing up to 3 percent of the framework, is chert. Phyllitic rock fragments from low-grade metamorphic sources are present but scarce. Some foliated, clay-rich rock fragments have equivocal textures, suggesting derivation either from shale or from slate. Intrabasinal rock fragments typically are muddy intraclasts. These clasts range in size from the average grain size of the sandstone to clasts several times larger than average grain size. Most intraclasts are clay-mineral rich but some consist of sideritic mud; the dominant clay mineral in these fragments is kaolinite. Shale fragments rich in clay minerals have a detrimental effect on the quality of Carter reservoirs because they deform plastically during compaction to form pseudomatrix that occludes porosity. These clasts further provided sites for pressure solution.

Fossil fragments, micas, and heavy minerals, mostly zircon and tourmaline, are minor detrital framework components in Carter sandstone. Fossil fragments locally account for more than 20 percent of total rock volume. These fragments typically have lost their original internal structure and have been replaced by ferroan calcite, ferroan dolomite/ankerite, or kaolinite. some have dissolved completely or partially to form moldic pores. Although fossil fragments are abundant, they are an important control on reservoir heterogeneity because they serve as nucleation sites for pore-filling carbonate cement.

DIAGENESIS

Volumetrically important authigenic minerals in Carter sandstone are quartz, kaolinite, and a variety

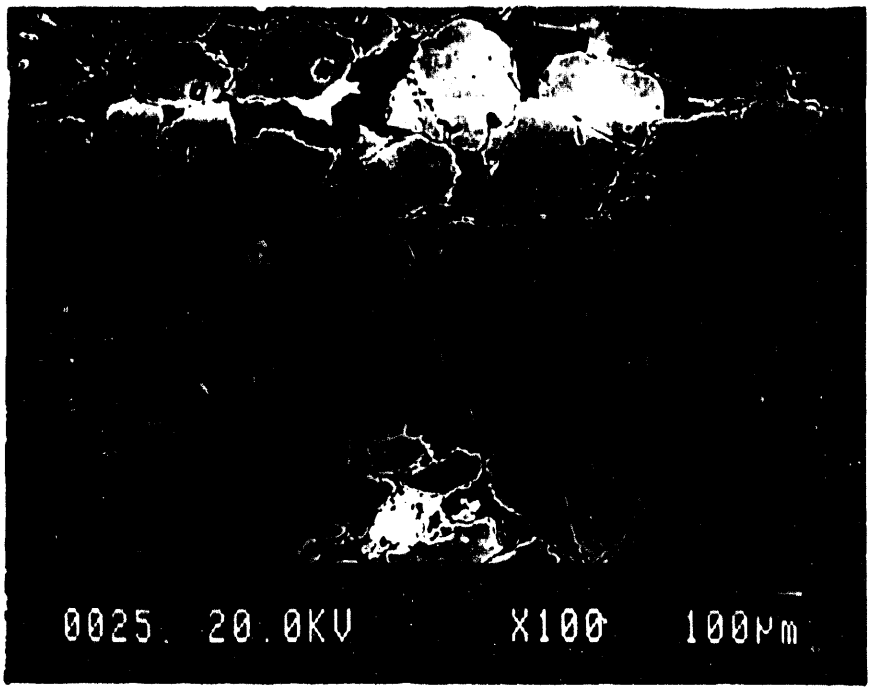

Figure 54.--Backscattered-electron micrograph showing detrital framework composition of Carter sandstone. All detrital grains in the field of view are quartz (medium gray areas). Kaolinite (dark gray) occupies two grain-size areas in the center of the micrograph. White areas are authigenic ferroan dolomite/ankerite and siderite. Black areas are pores (PN2999, 2194 ft, scale is on micrograph.).

of carbonate minerals, including siderite, nonferroan and ferroan calcite, and ferroan dolomite/ankerite (fig. 55). The distribution of diagenetic components in North Blowhorn Creek oil unit is directly related to depositional facies in the spit complex. However, the present composition of authigenic minerals and the nature of compactional features are results of burial diagenesis. For a more complete description of the diagenetic character of Carter sandstone in North Blowhorn Creek oil unit, refer to Kugler and Pashin (1992).

Of the authigenic carbonate minerals in Carter sandstone, siderite and nonferroan calcite precipitated first (fig. 55). Siderite occurs in several forms, including pervasive, pore-occluding microcrystalline mosaics of 10 to 20 µm subhedral crystals, concretionary patches, and layers up to several centimeters in thickness. Siderite also occurs as spherulitic patches up to 0.5 mm in diameter, as thin isopachous coats on sand-size detrital grains, and as dispersed "flattened" rhombic crystals ("wheatseed" siderite) up to 50 µm in length. Concretions and spherulites are most abundant in the nonreservoir shelf and backshore deposits in the North Blowhorn Creek reservoir (shale-and-siltstone and variegated facies). Burrowing and rooting localized siderite and resulted in color mottling in backshore deposits. Deflection of laminae around siderite concretions, open framework-grain packing, and high minus-cement porosity (in excess of 40 percent) establish that siderite precipitated prior to significant burial and compaction.

In reservoir sandstone in North Blowhorn Creek oil unit (sandstone facies), siderite locally occurs as isopachous framework-grain coats and as dispersed rhombic ("wheatseed") crystals. Howard (1990) described isopachous siderite rims similar to those in Carter sandstone in Holocene and Pleistocene beach or nearshore environments on the Mississippi-Alabama-Florida Continental shelf. Ultraviolet-light induced epifluorescence and backscattered-electron microscopy show that rhombic crystals are

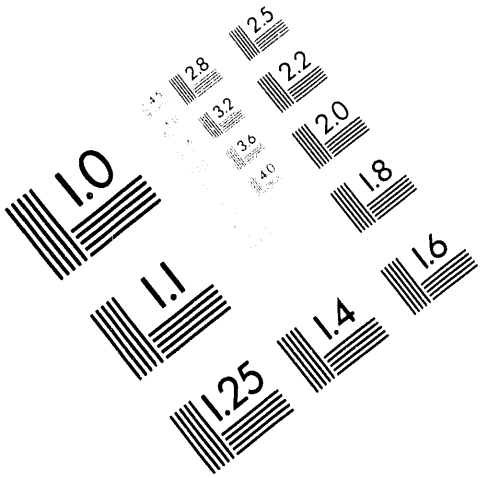

Association for Information and Image Management

1100 Wayne Avenue, Suite 1100
Silver Spring, Maryland 20910

301/587-8202

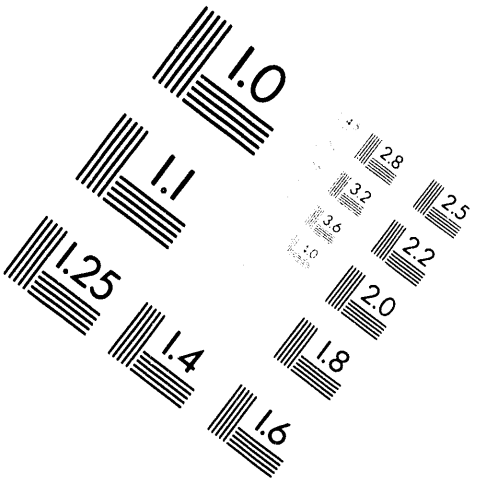

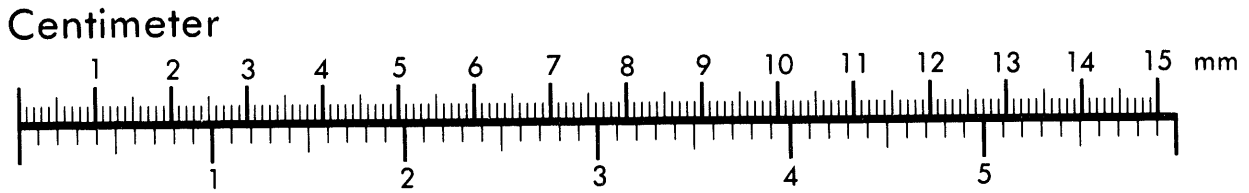

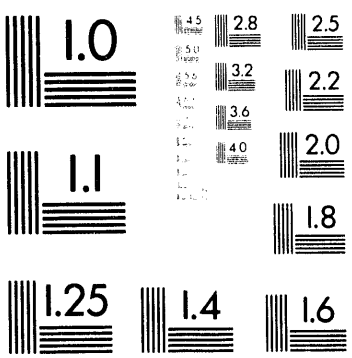

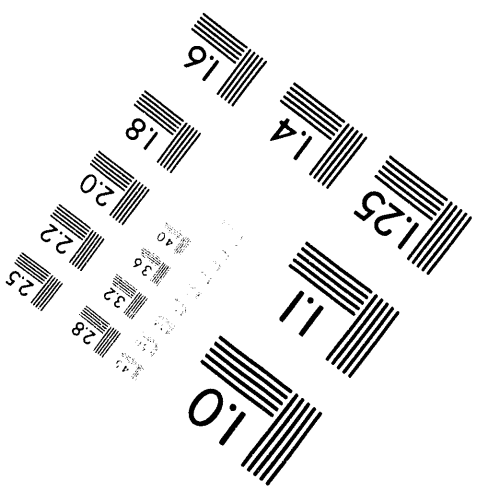

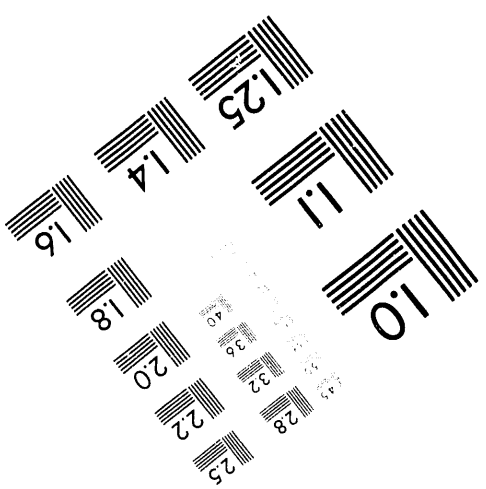

MANUFACTURED TO AIIM STANDARDS
BY APPLIED IMAGE, INC.

2 of 2

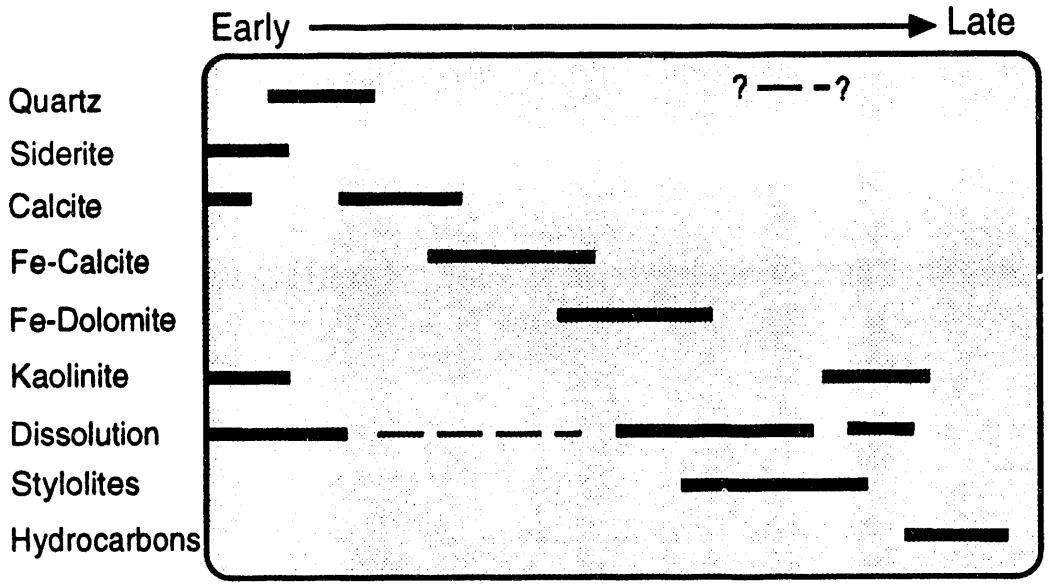

Figure 55.--Generalized paragenetic sequence for Carter sandstone in North Blowhorn Creek oil unit.

complexly zoned, reflecting variations in Fe/(Ca+Mg) ratios, generally with rims that are enriched in iron relative to cores. Electron microprobe analyses reveal the impure nature of the siderite (fig. 56), which results from extensive substitution of magnesium and calcium for iron in the crystal lattice. Both forms of siderite in reservoir sandstone precipitated early in the paragenetic sequence, but cement-stratigraphic relationships show that the dispersed rhombic crystals precipitated after the isopachous grain coats. Siderite precipitates in reducing, anaerobic, sulfide free environments, corresponding to zones of methanogenesis (Berner, 1981). The methanogenic zone is located below the oxic and sulfate-reduction zones. Pore water in the methanogenic zone is sulfide-free due to sulfate-reducing bacteria and enriched in Fe^{++} due to decomposition of organic matter.

Authigenic nonferroan and ferroan calcite are confined to intervals in shoreface and foreshore deposits that contain abundant fossil fragments. Both minerals have the same occurrence and typically are replaced partially by ferroan dolomite/ankerite. Calcite occurs as mosaics of crystals between detrital framework grains and as poikilotopic crystals that encompass several grains. Loose packing of detrital grains and high minus-cement porosity indicate that calcite precipitated prior to significant compaction. Intervals with pervasive calcite cement range in thickness from centimeters to decimeters. The lateral extent of the cemented zones ranges from less than the width of a core to more extensive horizons that probably do not extend from well to well. Thus, calcite-cemented zones form discontinuous baffles and barriers to vertical fluid flow that are most abundant in shelly parts of the sandstone facies.

Ferroan dolomite/ankerite is the most abundant authigenic carbonate mineral in Carter sandstone and occupies in excess of 40 percent of total rock volume in some sandstone with concentrations of fossil debris and in nonreservoir siltstone and very fine-grained sandstone Ferroan dolomite/ankerite partially to completely replaces calcite and siderite. Ferroan dolomite/ankerite cement forms permeability barriers within the reservoir and partially to completely seals the margins of the reservoir. Ferroan dolomite/ankerite is present throughout the reservoir interval, but typically accounts for less than 5 percent of total rock volume. In reservoir sandstone, ferroan dolomite ankerite occurs as isolated rhombic crystals or as clusters of crystals that partially fill pores or partially to completely replace shale clasts and fossil fragments. Ferroan dolo-

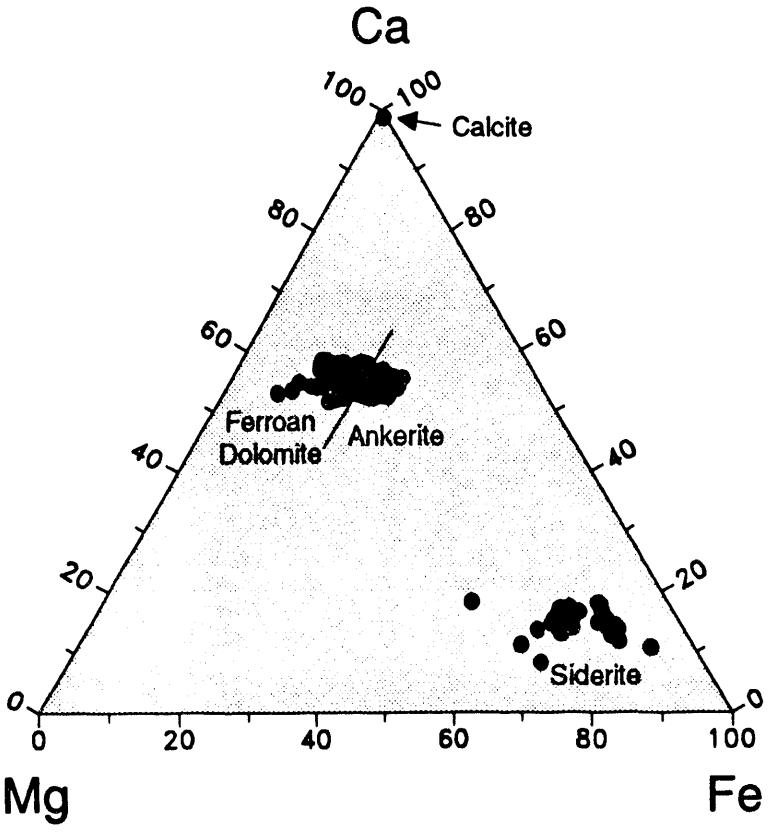

Figure 56.--Ca-Mg-Fe ternary diagram showing composition of authigenic carbonate minerals in Carter sandstone, based on electron microprobe analyses.

mite/ankerite is a late-stage diagenetic mineral that postdates precipitation of all other authigenic carbonate minerals and quartz (fig. 55).

Stable isotopic data (table 6, fig. 57) support the sequence of precipitation of carbonate mineral cements. Calcite, siderite, and ferroan dolomite/ankerite occur in distinct but overlapping fields on a plot of $\delta^{18}O$ versus $\delta^{13}C$ (fig. 57). Siderite is the most depleted of the three minerals in ^{18}O but is similar to calcite in carbon isotopic composition. Calcite and ferroan dolomite/ankerite have similar oxygen isotopic compositions, but calcite is more depleted in ^{13}C and less depleted in ^{18}O. Most $\delta^{13}C$ values for siderite in Carter sandstone are negative (fig. 57), which is typical of siderite precipitated in marine environments (Mozley and Wersin, 1992). The $\delta^{13}C$ and $\delta^{18}O$ values for Carter siderites fall within the zone of overlap for isotopic values for marine and continental environments on the plot of Mozley and Wersin (1992; their figure 4). However, the chemical impurity of Carter siderite (fig. 56) also is indicative of precipitation in a marine environment (*cf.* Mozley, 1989). Although petrographic evidence indicates that Carter siderite formed very early in the diagenetic history of the sandstone, there is a large amount of variation in $\delta^{18}O$ values. Even the heaviest values are too depleted in ^{18}O to be compatible with precipitation from seawater at low temperature. Explanations for this depletion of ^{18}O in early pore waters include mixing with meteoric water or water-sediment interaction (*cf.* Mozley and Carothers, 1992).

Authigenic quartz occurs as euhedral, syntaxial overgrowths on detrital quartz grains that partially fill pores in reservoir sandstone and locally occlude

Table 6..--Stable isotopic composition of carbonate cements in Carter sandstone.

Permit #	Depth (feet)	Calcite del13C PDB (o/oo)	Calcite del18O PDB (o/oo)	Fe-Dolo. del13C PDB (o/oo)	Fe-Dolo. del18O PDB (o/oo)	Siderite del13C PDB (o/oo)	Siderite del18O PDB (o/oo)
PN3049	2348.5	-0.3	-8.4	1.3	-7.9		
PN3049	2349.5	-3.0	-8.2	-1.1	-8.8		
PN3049	2352			-1.2	-9.4		
PN3049	2354.8	-1.9	-9.4	-1.9	-9.4		
PN3049	2356.2			-1.6	-9.7		
PN3049	2358.5			-2.0	-9.7		
PN3069	2263	2.5	-6.3	8.4	-7.4		
PN3069	2263	2.3	-6.3	8.1	-7.2		
PN3069	2263.5	-5.0	-7.1	-8.2	-6.8		
PN3069	2263.5	-4.9	-7.3	-7.9	-6.5		
PN3069	2265.5			-0.7	-8.0		
PN3069	2266			2.4	-7.7	-3.2	-14.1
PN3069	2267			4.6	-7.1	5.7	-9.9
PN3069	2267			4.6	-8.6		
PN3069	2270			3.0	-8.9		
PN3150	2356			4.7	-8.9		
PN3150	2373			-0.9	-9.4		
PN3150	2378			0.9	-8.6		
PN3150	2378.5			3.2	-8.5		
PN3160	2297.5			2.4	-9.5		
PN3160	2299.2			0.1	-8.4	-5.6	-12.3
PN3160	2299.2			0.1	-8.3		
PN3160	2302.5			0.3	-8.4	-3.8	-13.3
PN3160	2303.7			1.1	-9.0		
PN3160	2304.7			1.2	-9.2		
PN3160	2312.5			3.1	-7.8	0.6	-16.1
PN3204	2213	0.3	-8.5	-0.5	-3.3		
PN3204	2214	-1.8	-1.8	-0.5	-9.0		
PN3204	2215	-1.9	-1.9	-0.6	-8.9		
PN3204	2228			0.6	-9.7	-2.2	-8.7
PN3236	2216.3			0.7	-8.1	0.1	-9.5
PN3236	2216.3			0.7	-8.0	-6.2	-8.8
PN3236	2220.1			3.6	-7.8		
PN3236	2221.5			2.0	-7.6		
PN3236	2226.5			1.0	-8.3		
PN3236	2229.4			0.8	-9.3	6.9	
PN3236	2229.4			0.8	-9.4	-12.6	
PN3236	2230	-0.9	-7.9	2.9	-9.0		
PN3236	2231.5	-3.7	-6.0				
PN3236	2232.5	-3.2	-6.9	0.5	-8.8		
PN3236	2294.5			0.6	-9.1		
PN3314	2302			1.6	-9.4		
PN3314	2316			1.4	-8.6		
PN3314	2325			1.8	-8.5	0.7	-13.5
PN3717	2173.3			1.0	-8.9	-19.0	-19.4
PN3717	2173.3			1.2	-8.8		
PN3717	2197.1			0.1	-5.8	-2.4	-9.5
PN3717	2199.1			-2.5	-3.8	-5.2	-10.4
PN3717	2199.1			-2.6	-4.0	-5.4	-10.7

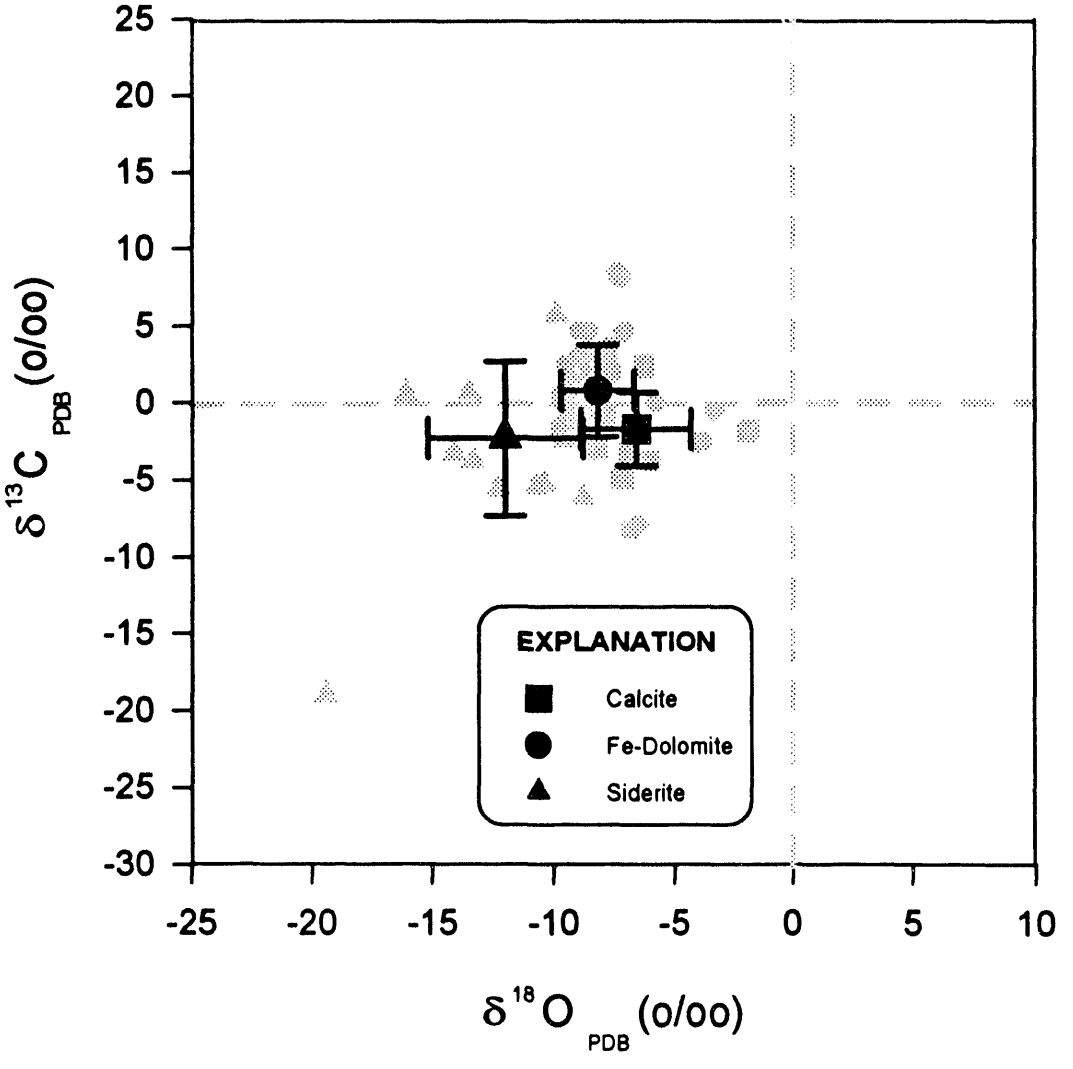

Figure 57.--Plot of $\delta^{18}O$ versus $\delta^{13}C$ for authigenic carbonate minerals in Carter sandstone in North Blowhorn Creek oil unit. Gray symbols are data for individual samples. Black symbols represent the mean value for each mineral. Black lines extend one standard deviation horizontally and vertically away from the mean.

pores in nonreservoir siltstone and sandstone. In reservoir sandstone, quartz overgrowths occupy up to 10 percent, but typically less than 7 percent, of total rock volume. Although quartz overgrowths are ubiquitous in Carter sandstone reservoirs, an effective, interconnected pore system remains intact.

Kaolinite occurs throughout Carter sandstone in minor amounts but is volumetrically significant in some horizons within high-quality reservoir zones where almost all intergranular space is filled by the mineral. Kaolinite most commonly occurs as vermicular stacks of pseudohexagonal platelets that fill grain-size and grain-shape areas between detrital quartz grains (fig. 54). Individual platelets common are less than 10 μm in diameter. Less abundant kaolinite with similar morphology partially to completely fills intergranular pores and dissolution voids within fossil fragments. Although an authigenic origin for kaolinite in primary intergranular pores and in dissolution voids within fossil fragments is evident, the origin of kaolinite in detrital grain-size areas is less clear.

Some kaolinite occupies rectangular areas similar in shape to detrital feldspar grains and contains stacks of perfectly hexagonal platelets. This kaolinite probably precipitated in areas once occupied by detrital feldspar. However, other kaolinite that occupies grain-size areas appears murky in plane-polarized light. Scanning electron microscopy reveals that some of this kaolinite has texture indicative of detrital kaolinite and is intermixed with other clay minerals, such as illite or chlorite. This kaolinite most likely is a component of intrabasinal shale fragments or fecal pellets.

An origin for kaolinite as a component of intrabasinal shale clasts or as fecal pellets is clear in many cases because of the geometry of the grains. However, where these fragments have partially dissolved, distinction between detrital and authigenic origins is difficult. Formation of most authigenic kaolinite in Carter sandstone postdates precipitation of quartz and ferroan dolomite/ankerite, but predates migration of hydrocarbons into the reservoir. Most kaolinite in Carter sandstone does not form permeability barriers but fills grain size volumes that enhance microporosity and increase tortuosity of fluid flow. However, in intervals with concentrations of clay laminae, particularly laminae spaced on the order of a centimeter apart and thicker than one or 2 mm, kaolinite occupies all intergranular space, resulting in sandstone with only microporosity. These laminae are effective barriers to vertical fluid flow but probably do not extend between adjacent wells. Micropores in kaolinite additionally contain irreducible water that affects interpretation of porosity, water saturation, and hydrocarbon reserves from well logs.

Mechanical and chemical compaction contributed to reservoir heterogeneity in Carter sandstone. The major detrimental effect of mechanical compaction was loss of porosity due to ductile deformation of intrabasinal shale clasts during shallow burial to form pseudomatrix. Porosity lost by ductile-grain deformation, moreover, cannot be regenerated by subsequent diagenetic events (McBride, 1984). Chemical compaction occurred by pressure solution in Carter sandstone. At the scale of an individual core, the most significant type of chemical compaction was development of stylolites or pressure solution seams along individual or anastomosing clay laminae.

The effectiveness of pressure-solution seams as permeability barriers is demonstrated in several wells. The base of the oil-stained interval in the cores is generally a pressure-solution seam formed along a clay lamina. At a smaller scale, wispy microstylolites formed along disrupted clay laminae associated with small-scale sedimentary structures, such as ripples, and along deformed rip-up clasts. These microstytlolites range from less than 1 mm to several millimeters in length. Thus, these microstylolites do not form extensive barriers to fluid flow, but increase tortuosity. Additionally, the presence of these small-scale clay laminae and microstylolites contributes to reduction of permeability in intervals containing these structures. The presence of stylolites suggests that the maximum depth of burial was much greater than the present burial depth of 2,100 to 2,400 feet in North Blowhorn Creek oil unit. This contention is confirmed by burial history reconstructions presented elsewhere in this report.

PETROPHYSICAL PROPERTIES

PETROGRAPHIC EVIDENCE

Petrographic evidence for the nature of the pore system in Carter sandstone is discussed in this section to emphasize the importance of integrating petrographic data with standard petrophysical analysis. Petrographic evidence combined with petrophysical data indicate that the pore system in Carter sandstone consists of effective macropores between framework grains and ineffective micropores between detrital and authigenic clay particles. The effective pore system consists mainly of primary pores

modified by compaction and precipitation of quartz overgrowths and ferroan dolomite/ankerite cement. Although secondary pores are present, the effective pore system was not enhanced significantly by dissolution of aluminosilicate framework grains. Instead, products of dissolution were redistributed as kaolinite. Within Carter sandstone reservoirs, authigenic carbonate minerals occlude all pores only in the vicinity of shell accumulations, and early formed calcite is restricted to these accumulations, suggesting that carbonate-dissolution porosity is not widespread in the reservoirs.

Micropores occur within clay laminae, fragmented clay drapes on ripple foresets (microstylolites), intrabasinal shale clasts, and authigenic kaolinite that occurs in volumes formerly occupied by detrital grains and in pores. The effects of both detrital and authigenic clay in Carter quartzarenite reservoirs merit further consideration. Methods such as X-ray diffraction are inadequate to quantify the effects of clay minerals on reservoir properties because the distribution must be known. The textural distribution of clays in reservoir sandstone commonly is described in terms of dispersed, structural, and laminated types (Frost and Fertl, 1981; Hurst and Archer, 1986) (fig. 58). Dispersed clay typically is authigenic and occurs as discrete particles in pores, coats detrital grains, or bridgespore throats. Structural clay occurs in clay-mineral rich detrital clasts or as authigenic clay that fill areas formerly occupied by detrital grains. Laminated clay occurs in clay-mineral rich or micaceous laminae. Of these three types, dispersed clay has the most detrimental effect on reservoir properties (fig. 58).

COMMERCIAL CORE ANALYSES

Based on all available data from commercial core analyses, the arithmetic mean porosity of reservoir

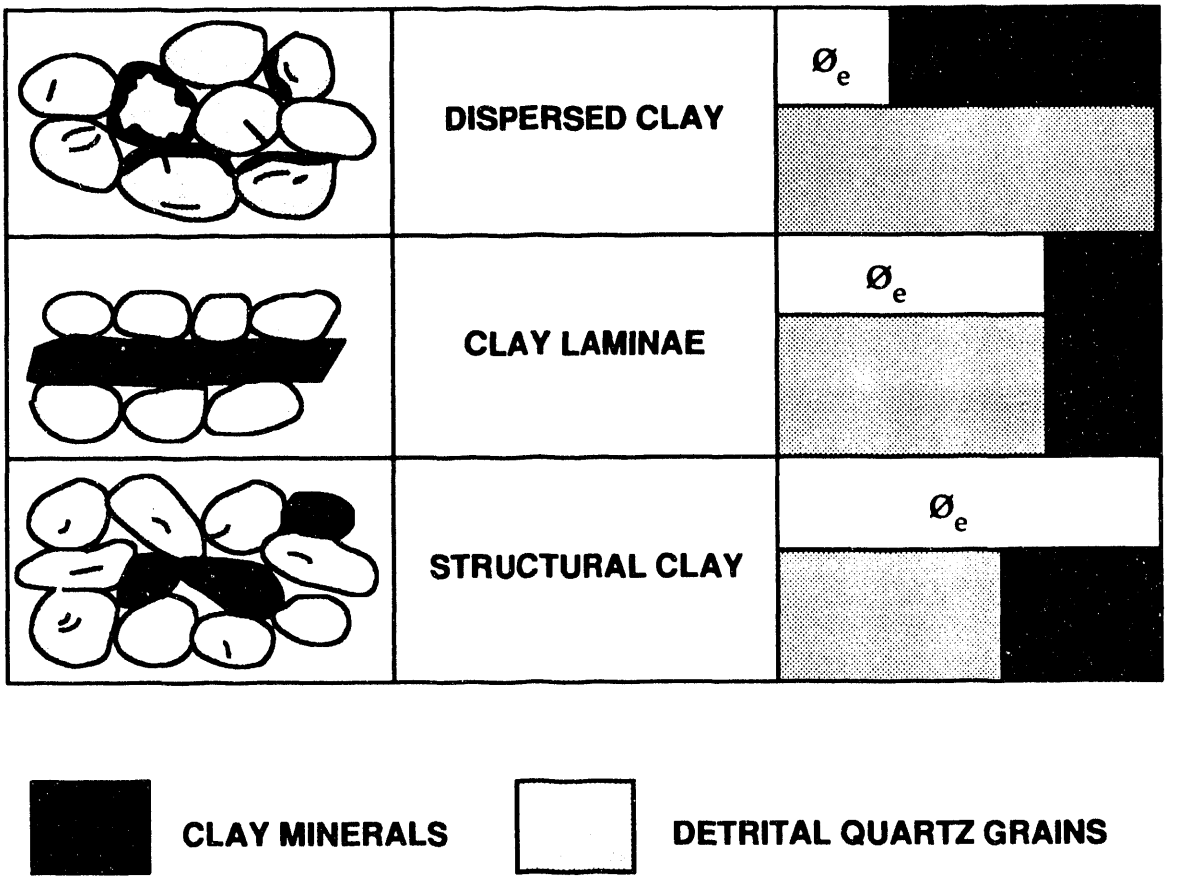

Figure 58.--Influence of clay-mineral distribution on effective porosity (ϕ_e) (modified from Frost and Fertl, 1981).

In core, the change from the lower permeability zone to the higher permeability zone corresponds with a transition from very fine-grained lower shoreface deposits with ripple laminae to fine-grained upper shoreface or foreshore deposits containing predominately low-angle crossbeds (fig. 44). Porosity is fairly constant throughout the reservoir interval, so the change in permeability is due to factors other than variation in the amount of pore-filling cement. Although permeability contrast in well PN3314 is discernible from commercial core analyses, high-pressure mercury porosimetry, which measures pore-throat size, provides a means of documenting factors controlling the permeability variation.

HIGH-PRESSURE MERCURY POROSIMETRY

Pore-throat size is a critical control on the distribution and producibility of hydrocarbons in a reservoir. High-pressure mercury porosimetry is the only effective means of quantitatively evaluating pore throats (Kopaska-Merkel and Friedman, 1989). Capillary pressure curves derived from mercury porosimetry can be used to determine several petrophysical parameters, including pore-throat size distribution, relationships between surface area and volume, porosity, recovery efficiency, oil-column height, height above free water, and reservoir-seal potential (Purcell, 1949; Dullien and Dhawan, 1974; Wardlaw, 1976; Jennings, 1987; Wardlaw and others, 1988; Kopaska-Merkel and Friedman,

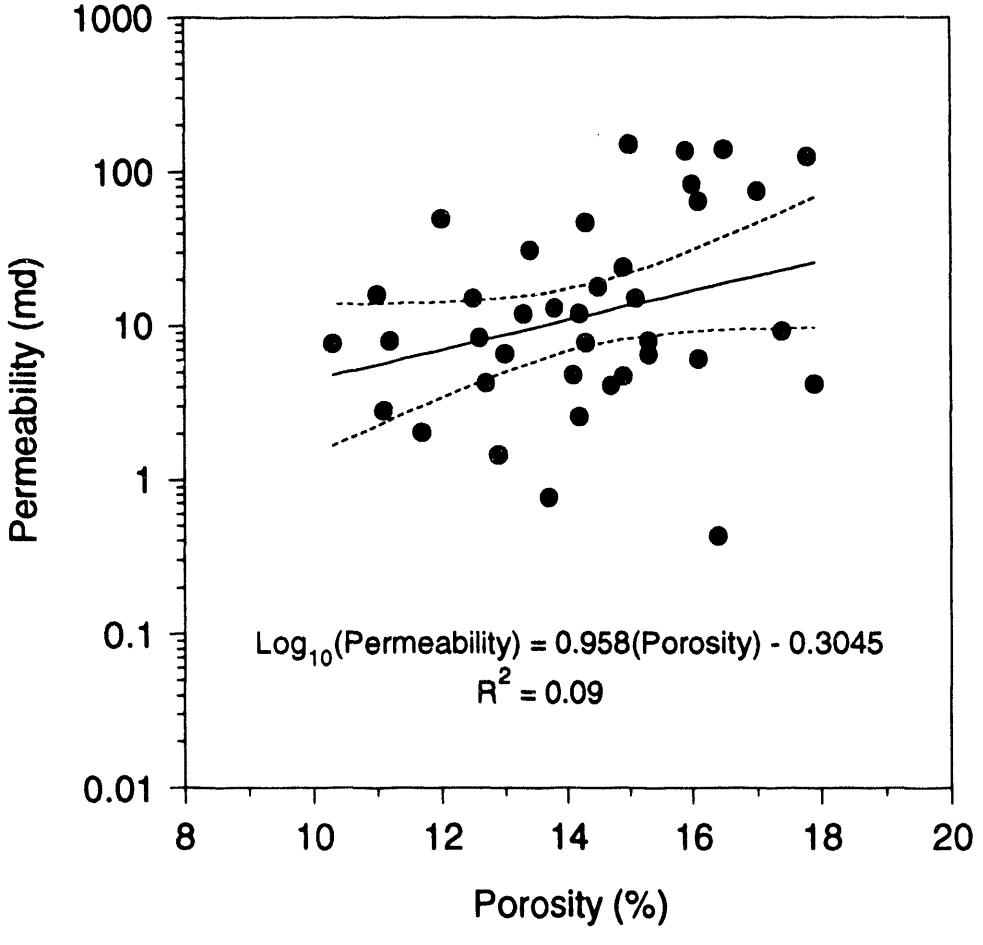

Figure 60.--Plot of porosity versus permeability for commercial core analyses from well PN3314, North Blowhorn Creek oil unit. The solid line is a linear regression line, and the dashed lines encase the 95 percent confidence interval. The regression equation and coefficient of determination (R^2) are at the bottom of the diagram.

sandstone in North Blowhorn Creek oil unit is 12 percent, using a lower cutoff of 6 percent for reservoir porosity. The geometric mean of permeability is 6.82 millidarcies, using a cutoff of 0.1 percent. Maximum porosity and permeability are 22 percent and 440 millidarcies, respectively. A crossplot of porosity versus air permeability for all data shows a roughly linear trend, but a weak correlation between the two parameters (R^2 = 0.52) (fig. 59). Data for individual wells have R^2 ranging from 0.09 (PN3314) to 0.83 (PN2999), and most are less than 0.5 (Kugler and Pashin, 1992). This indicates a weak relationship between porosity and permeability and a wide range of variation in the relationships among wells and a wide range of variation in these relationships among wells. In addition to interwell variation in porosity and permeability, permeability in reservoir sandstone within a single well may vary significantly.

In one of the most productive wells in North Blowhorn Creek oil unit (PN3314), commercial core analysis data indicate no relation exists between porosity and permeability in the reservoir interval (R^2 = 0.09) (fig. 60). Porosity varies minimally throughout the reservoir interval, but permeability is an order of magnitude or more higher in the upper part of the interval than in the lower part (fig. 61). Because the interval from which measurements were made is entirely within productive reservoir, this permeability contrast represents a heterogeneity that could have a marked effect on lateral sweep efficiency, through channeling, during enhanced recovery operations.

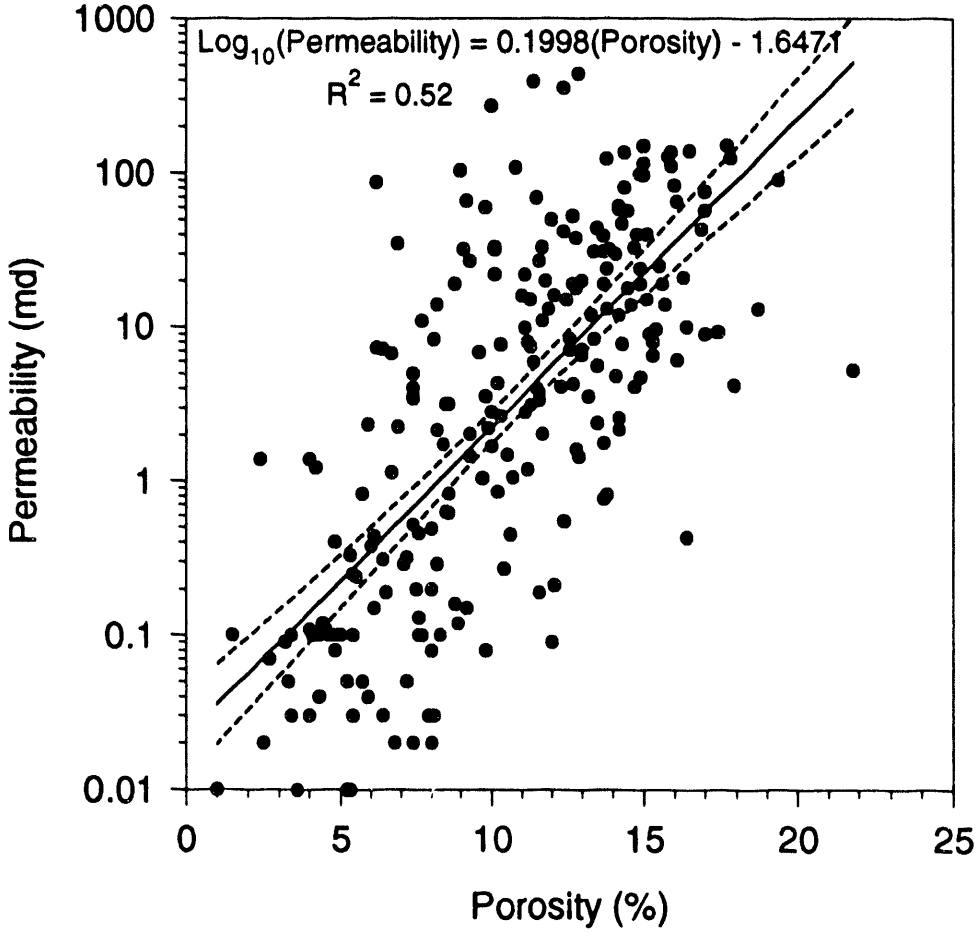

Figure 59.--Plot of porosity versus permeability for all commercial core analyses from North Blowhorn Creek oil unit. The solid line is a linear regression line, and the dashed lines encase the 95 percent confidence interval. The regression equation and coefficient of determination (R^2) are at the top of the diagram.

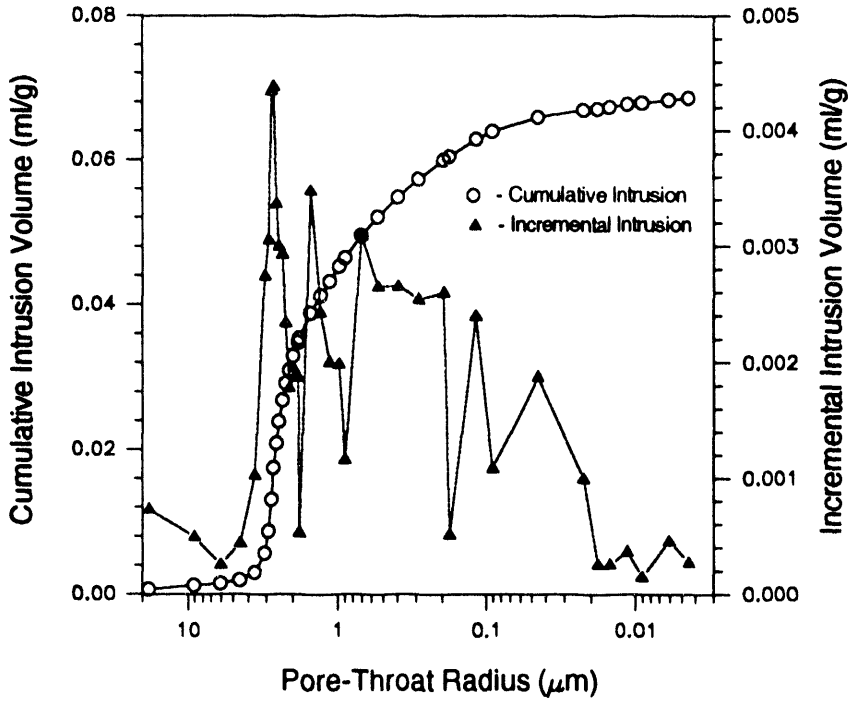

Figure 62.--Plot of pore-throat radius versus cumulative-intrusion volume and incremental-intrusion volume showing polymodal pore-throat size distribution (well PN3150, 2,371 ft, North Blowhorn Creek oil unit).

malized to maximum intrusion volume are directly related to the distribution of pore-throat sizes on incremental intrusion plots. Four distinct shapes of cumulative-intrusion curves can be recognized for Carter sandstone and associated sedimentary rocks (fig. 63). Curve A, which is convex with the steepest slope of the curve at a large pore-throat radius, is representative of the best quality reservoir in North Blowhorn Creek oil unit. Curve B is also convex, but the steepest slope is at a smaller pore-throat radius and the overall slope is gentler (fig. 63). The gentler slope indicates a polymodal distribution of pore-throat sizes. This curve shape also is representative of Carter sandstone. A gradation exists between curves A and B in the Carter reservoir at North Blowhorn Creek, due to variation in detrital grain size and variation in abundance of components that contribute to microporosity. The bimodal shape shown in curve C (fig. 63) is rare and generally indicates partially cemented transitional zones between pervasively carbonate-cemented sandstone and porous reservoir sandstone. Curve D is concave with the steepest slope at a small pore-throat size radius (fig. 63). This type of curve is representative of nonreservoir siltstone, pervasively carbonate-cemented zones, and sandstone in which all pores are filled with matrix.

Cumulative mercury-intrusion curves reveal that two factors can be related to permeability variation in well PN3314: (1) grain size and (2) microporosity (fig. 64). Fine grained sandstone in the upper, more permeable interval has median pore-throat radii between 3 and 7 μm, in contrast to median pore-throat radii of 0.3 to 2 μm in very fine-grained sandstone of the lower, less permeable interval (fig. 64). However, capillary-pressure data also show that grain-size variation is not the only factor responsible for the permeability contrast, because shapes of cumulative-intrusion curves differ between the two permeability intervals (fig. 65).

Cumulative mercury-intrusion curves for samples from the higher permeability interval have steeper slopes than those from the lower permeability interval. Incremental mercury-intrusion curves for individual samples from the two permeability zones show that the pore-throat size distribution in the upper, more permeable interval is unimodal (fig.

1989; Vavra and others, 1992). In mercury porosimetry, the volume of mercury intruded at a specific pressure is precisely related to the number of pore throats of corresponding size. Because of this relationship, plots of cumulative mercury-intrusion volume versus capillary pressure are equivalent to cumulative mercury intrusion versus pore-throat size. The equation used in this investigation to compute pore-throat size is: $(-4\gamma\cos(\theta))/p$, where γ is the interfacial angle (485 dynes/cm), θ is contact angle (130°), and p is pressure (psia). Pore-throat sizes determined by this equation are *effective* sizes because a cylindrical pore throat is assumed and surface irregularities are not taken into account. Refer to Kugler and Pashin (1992) for further discussion of procedures used in this investigation.

The most notable aspect of pore-throat radius versus incremental mercury-intrusion curves for Carter reservoir sandstone in North Blowhorn Creek oil unit is the polymodal distribution of pore-throat sizes (fig. 62). Typical Carter reservoir sandstone has a dominant pore-throat radius of 2 μm or more and several lesser modes at smaller pore-throat sizes. The dominant mode represents the size of pore throats between sand-size detrital grains. The other modes represent a range of variation in smaller pore throats between detrital grains, between clay particles in intrabasinal shale clasts, between dissolution pores in mud clasts, and between stacks of kaolinite crystals.

The shapes of curves of pore-throat radii plotted against cumulative mercury-intrusion volume nor-

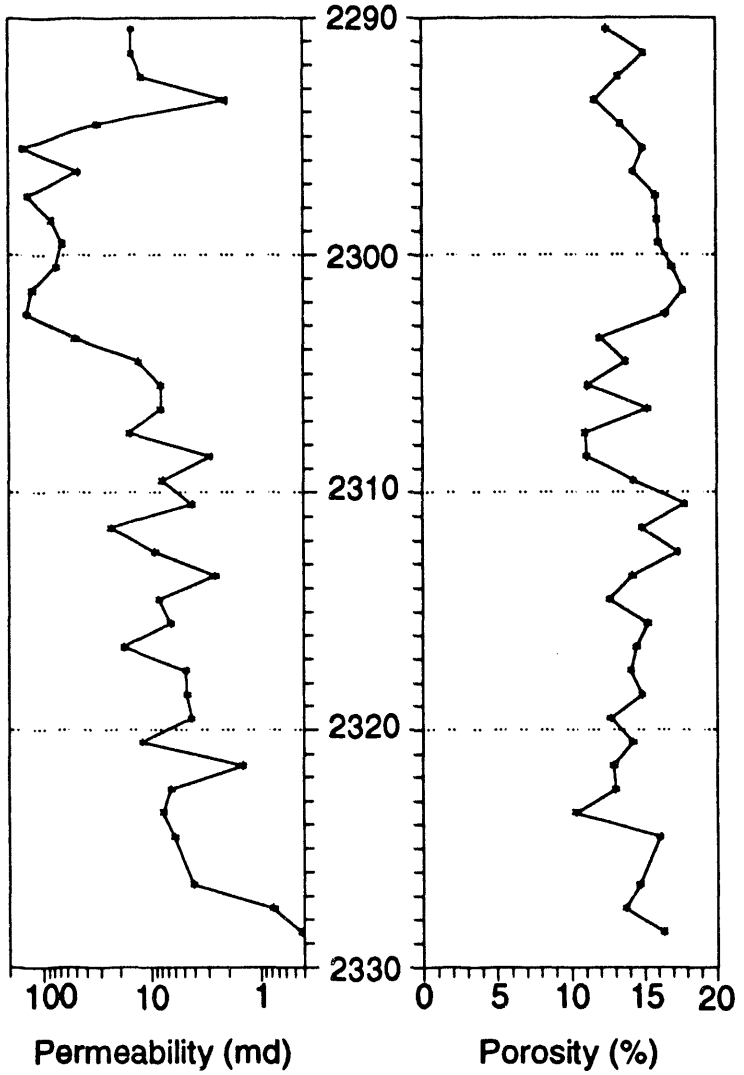

Figure 61.--Plot of permeability and porosity versus depth for well PN3314, North Blowhorn Creek oil unit.

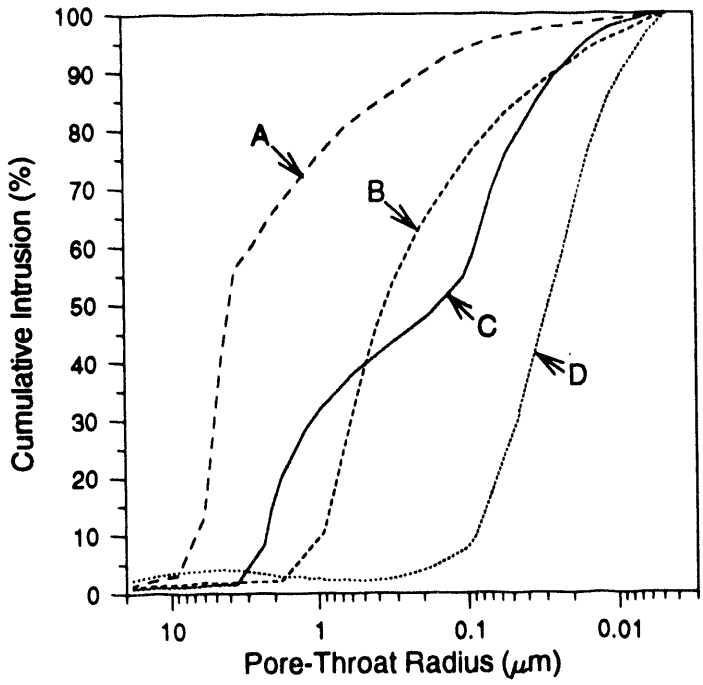

Figure 63.--Plot of pore-throat radius versus cumulative intrusion showing typical shapes of cumulative intrusion curves for Carter sandstone: (A) convex curve with large maximum pore-throat-size mode (well PN3314, 2,297 ft); (B) convex curve with smaller maximum pore-throat size mode (well PN3150, 2,34.5 ft; (C) stepped curve with bimodal pore-throat size distribution (well PN3160, 2,303.7 ft; and (D) concave curve with small pore-throat size mode (well PN3150, 2,350 ft).

65). In contrast, similar curves for samples from the lower, less permeable zone reflect polymodal distribution of pore-throat size (fig. 65). These plots show that the lower zone has more microporosity than the upper zone, but total porosity is similar because cumulative mercury-intrusion volume is the same for the two samples.

The difference between porosity calculated for maximum mercury-intrusion pressure (20,000 psia) and porosity at 1,000 psia indicates that microporosity is related to low permeability (fig. 66). The variation is subtle, but differential porosity for samples from the more permeable zone is consistently less than one percent, in contrast to the lower permeability zone where differential porosity is greater than one percent. The additional microporosity in this sandstone most likely is contained in fragmented clay drapes on ripple foresets, which form small-scale permeability barriers and baffles. Variation of pore-throat size and of the abundance of micropores together accounts for the weak correlation between porosity and permeability shown in figure 59.

Fine-grained sandstone, such as that near the top of the Carter reservoir, is scarce in North Blowhorn Creek oil unit, as well as in other unitized fields in the Black Warrior basin; most shoreface deposits in other wells consist of very fine-grained sandstone. Incremental mercury-intrusion curves for those other wells typically are polymodal with median pore throat radii between 0.7 and 2.0 μm (Kugler and Pashin, 1992). Although pore-throat size distribution in the North Blowhorn Creek reservoir reflects a combination of macroporosity and microporosity, petrographic data show that much of the microporosity is within aggregates of authigenic and detrital clay (Kugler and Pashin, 1992). These aggregates are the size of framework grains (structural clay of Frost and Fertl, 1981) and do not block pore throats as does dispersed clay.

However, anastomosing clay laminae and fragmented clay drapes on ripple foresets in shoreface

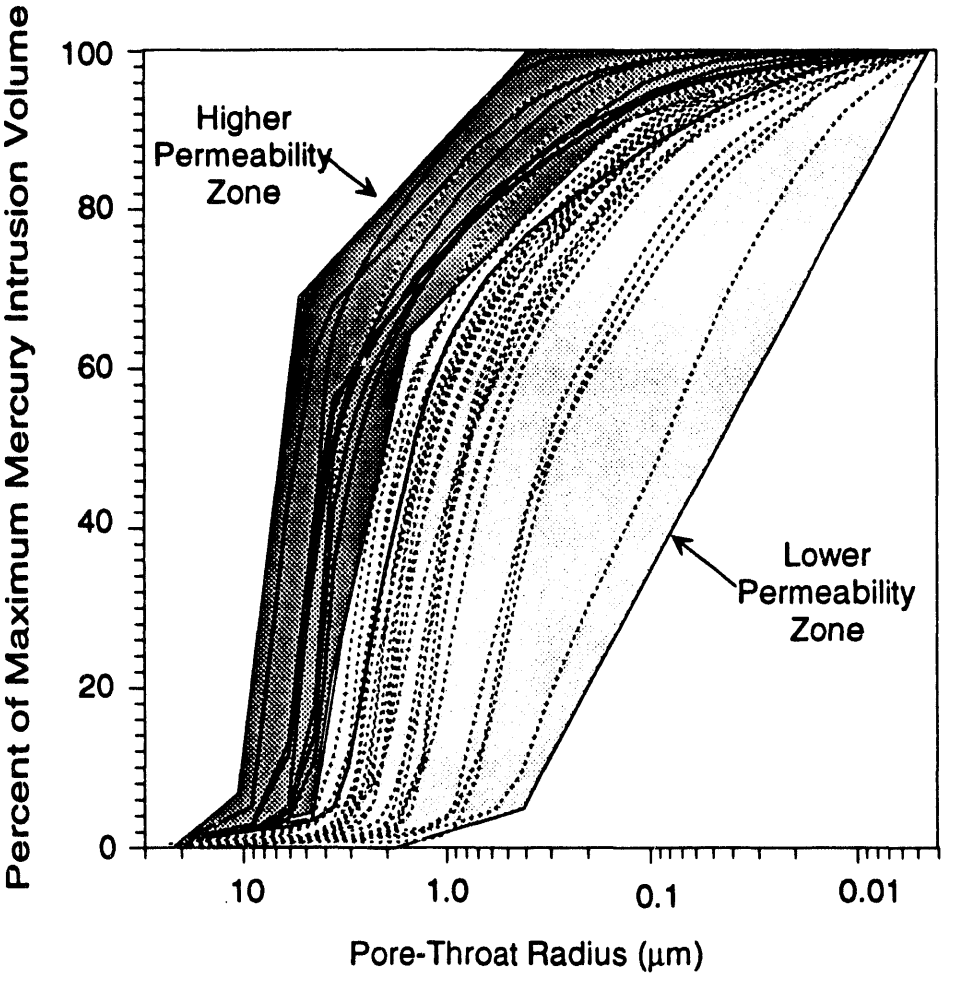

Figure 64.--Plot of pore-throat radius versus cumulative intrusion as a percent of maximum mercury intrusion volume for all data from well PN3314. Darkly shaded area encases curves from samples from the high permeability zone at the top of the reservoir. Lightly shaded area encases curves for samples from the underlying lower permeability zone.

sandstone also contain microporosity and disrupt the continuity of the interconnected pore system, thereby reducing permeability. In the central and southern parts of North Blowhorn Creek oil unit, some layers within the reservoir have median pore-throat size less than 1 μm. These intervals with small pore-throat sizes have a variety of origins. Most are thin ferroan dolomite/ankerite cemented zones, but others are within sandstone with concentrations of intrabasinal shale clasts and thin horizontal or anastomosing clay laminae. These small-scale permeability barriers, most of which likely only extend a few feet away from the well bore, give a false impression of segmentation of the reservoir. Indeed, nonreservoir backshore and shelf deposits, which typically have median pore-throat radii less than 0.1 μm (Kugler and Pashin, 1992) and are interbedded with reservoir sandstone in the southern part of the field, contribute much more significantly to segmentation of the reservoir.

Median pore-throat size in some clastic and carbonate reservoirs correlates with permeability (Kopaska-Merkel and others, 1993; Schatzinger and Sharma, 1993). Weak to no correlation was found between median pore-throat size and permeability in the Carter sandstone reservoir in North Blowhorn Creek oil unit. This lack of correlation is due, in part, to the relatively few paired permeability and capillary-pressure analyses available. However, weak correlation between the two parameters is

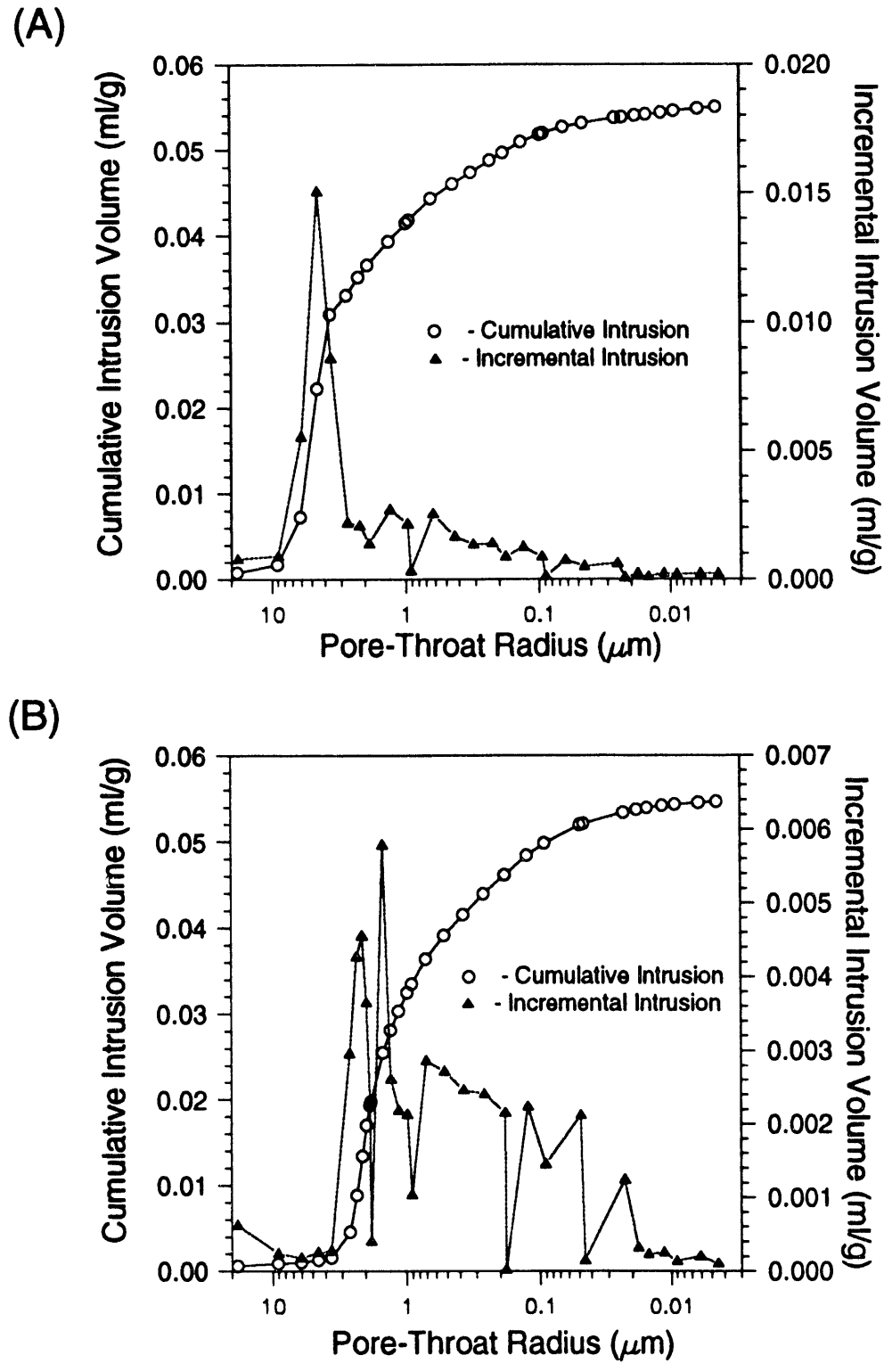

Figure 65.--Plots of pore-throat radius versus cumulative-intrusion volume and incremental-intrusion volume for well PN3314. (A) 2,297 ft. (B) 2,314 ft.

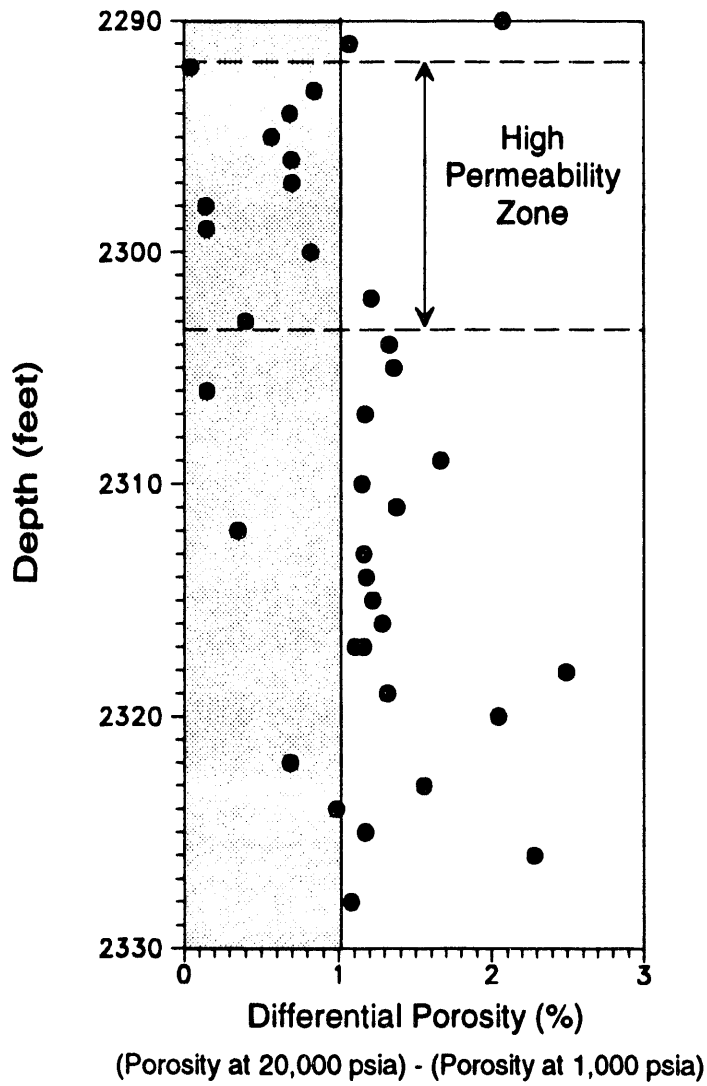

Figure 66.--Plot of differential porosity versus depth for well PN3314. Shaded area represents a difference of less than one percent between porosity calculated from the mercury intrusion volume at 20,000 psia and that calculated for the intrusion volume at 1,000 psia; differential porosity in the high permeability zone is less than one percent.

logical in light of the distribution of clays based on petrographic evidence. As described elsewhere, much of the detrital and authigenic kaolinite in the Carter reservoir fills grain size volumes rather than occupying intergranular pores and pore throats. This structural clay may not significantly alter the effective pore system, but contains water that adds to the total water saturation in the reservoir. However, the poor correlation between core analysis porosity and permeability suggests that authigenic clays influence the flow system in the sandstone at a microscopic scale by clogging some intergranular pores and pore throats.

Although capillary-pressure curves derived from high-pressure mercury porosimetry provide valuable information regarding microscopic-scale heterogeneity in oil reservoirs, this type of data is not commonly available and is expensive to acquire. An inexpensive alternative to capillary-pressure analysis was proposed by Pittman (1992), who developed a series of empirical equations for determination of pore-throat size distributions from routine porosity and uncorrected permeability measurements, such as those available as commercial core analyses. These equations produce pore-throat size distributions for mercury-intrusion volumes ranging from 10 to 75 percent saturation that are analogous to the mercury-intrusion curves presented elsewhere in this report As an example, the equation for the median pore throat size (50 percent intrusion) is: $\text{Log } r_{50} = 0.778 + 0.626\text{Log}(K) - 1.205\text{Log}(\phi)$, where r is pore-throat radius in μm, K is uncorrected permeability in millidarcies, and ϕ is porosity as percent. Additional equations for pore-throat size at successive 5 percent intrusion volumes are in Pittman (1992).

Pittman's technique was explored as a means of characterizing pore-throat size distribution in wells for which high-pressure mercury porosimetry data were not collected. Commercial core analyses data from three wells for which the most high-pressure mercury porosimetry data were available were used for this purpose. These wells include PN3150, PN3160, and PN3314 in North Blowhorn Creek oil unit. Plots of median pore-throat size distribution against depth for pore-throat sizes calculated from Pittman's equation are remarkably similar to those for median pore-throat sizes derived from high-pressure mercury porosimetry (figs. 67, 68, 69). In general, Pittman's technique results in slightly higher values than mercury porosimetry values. Nevertheless, results of this investigation suggest that Pittman's technique can be used to obtain pore-throat size distributions for wells for which capillary-pressure data are not available.

WELL-LOG DERIVED POROSITY AND WATER SATURATION

The third source of porosity data for this investigation was geophysical well logs. The major source of porosity data in the Black Warrior basin must be well logs, because of the paucity of core analyses. Individual reservoirs, including the Carter sandstone in North Blowhorn Creek oil unit for which there are 10 wells with core analyses, are both areally and stratigraphically undersampled with respect to porosity. North Blowhorn Creek oil unit, which has 50 production and injection wells, is even more undersampled with regard to the high-pressure mercury porosimetry data, although these data provide valuable constraints on interpretation of core analyses. Thus, correlating log-derived porosity to commercial core analyses and high-pressure mercury porosimetry data provides a means of increasing data density for petrophysical properties in North Blowhorn Creek oil unit. Indeed, this is the only means for acquiring porosity data in most oil fields in the Black Warrior basin.

The arithmetic mean of one-half foot by one-half foot (North Blowhorn Creek oil unit) and foot-by-foot (other fields) net pay, effective and total water saturation, and effective porosity were determined from digital well logs using a dual-water model for all wells in six of the most productive Carter sandstone fields, one Lewis field, one *Millerella* field, and one Gilmer field. These computations provided input data for calculation of original oil in place and other parameters for the TORIS database. Log-derived effective porosity of 6 percent and effective water saturation of 40 percent were used as pay cutoffs. Similar calculations were made for at least one well in each of the remaining oil fields in Alabama. Well logs from Mississippi fields were not modeled by the dual-water method due to lack of appropriate logs.

The frequency distribution for log-derived effective porosity for Carter sandstone with porosity greater than 6 percent in all 50 production and injection wells in North Blowhorn Creek oil unit is similar to that for the composite of core-analysis derived porosity for 10 cored wells (figs. 70, 71). The modes for porosity data from both sources are similar and occur at 12 to 15 percent. Additionally, both distributions are skewed toward low porosity. Cumulative percent curves in figures 70 and 71 show that more than 20 percent of porosity

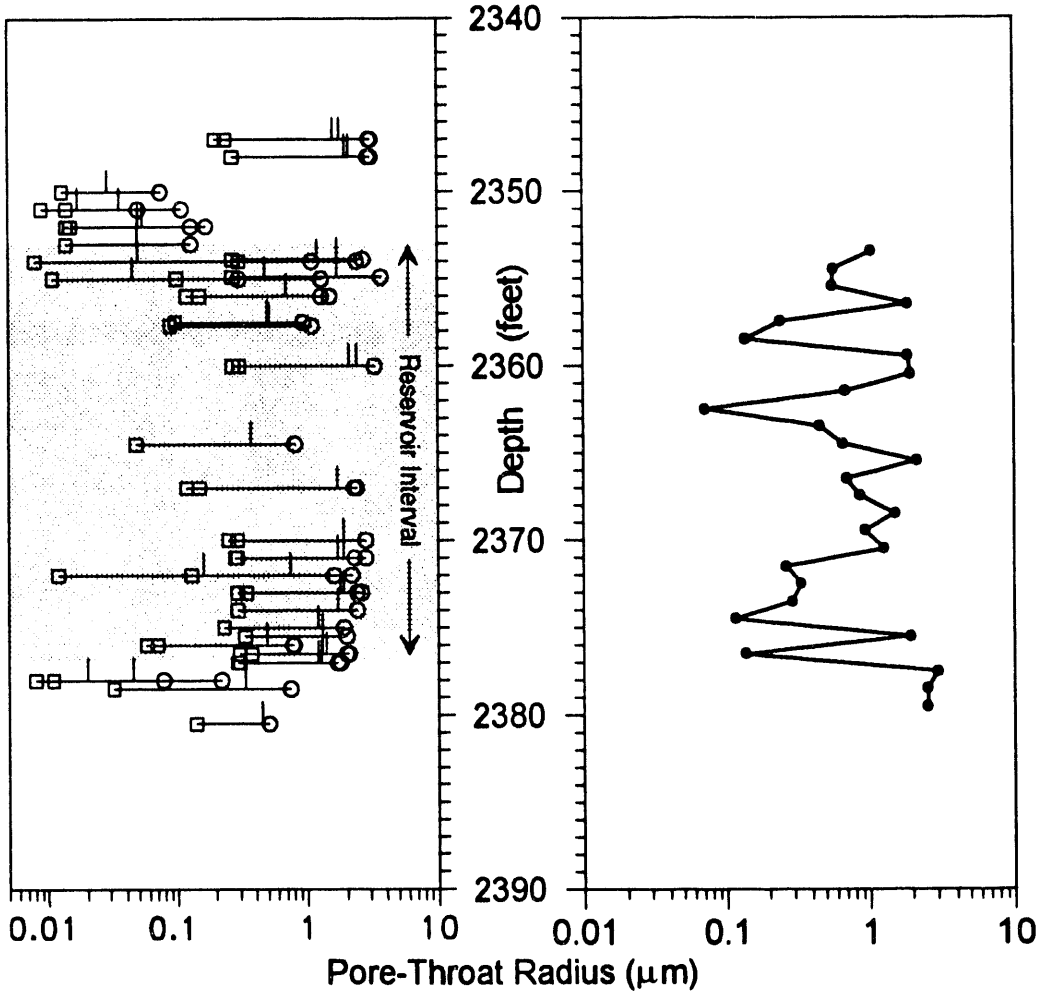

Figure 67.--Comparison of median pore-throat size determined by high-pressure mercury porosimetry (left) with that determined from commercial core analyses by Pittman's (1992) method (right) for well PN3150. Vertical lines in the plot on the left represent the median pore throat radius, open circles represent the pore-throat radius at the 16th percentile of cumulative mercury intrusion, and open boxes represent the pore-throat radius at the 84th percentile.

determined by both methods is between 6 and 9 percent. This is significant because a porosity cutoff of 9 percent was used in past calculations of original oil in place in North Blowhorn Creek oil unit (Docket No. 1-20-8340, State Oil and Gas Board of Alabama). It is reasonable to assume that sandstone with porosity between 6 and 9 percent contains oil that is extractable by improved or enhanced recovery techniques. If sandstone with porosity in this range is added to the pay section, the volume of oil in place would increase. This is discussed further in a subsequent section.

Similarities between frequency distributions for core-analysis and well-log derived porosity suggest the two methods are well calibrated. However, differences also exist between the two distributions. The lower three classes (6-9, 9-12, and 12-15 percent) account for more of total core-analysis porosity than of total well-log derived porosity (compare fig. 70 to fig. 71). Additionally, the 6 to 9 and 9 to 12 percent classes account for proportionately more of the porosity in the lower three classes in the core-analysis porosity histogram (fig. 71) than in the well-log derived porosity histogram (fig. 70). The

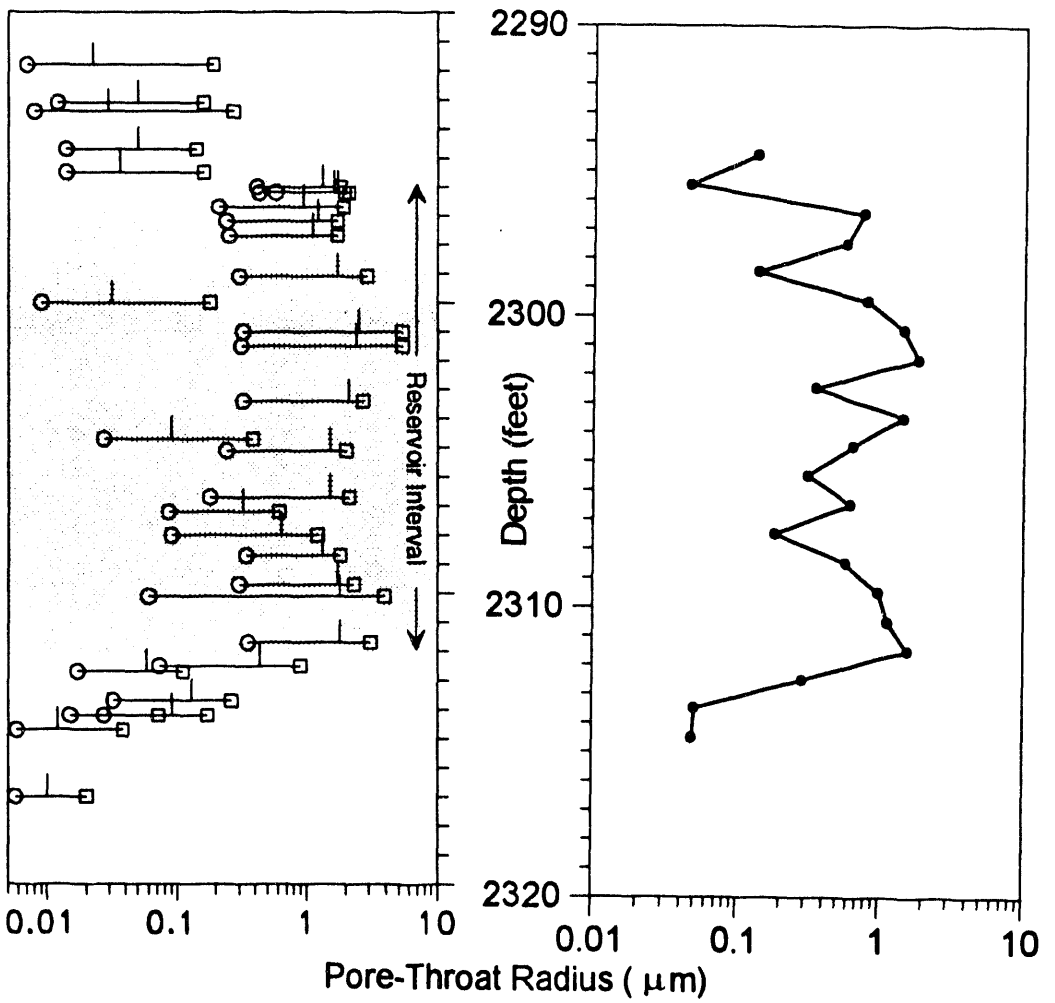

Figure 68.--Comparison of median pore-throat size determined by high-pressure mercury porosimetry (left) with that determined from commercial core analyses by Pittman's (1992) method (right) for well PN3160. Vertical lines in the plot on the left represent the median pore throat radius, open circles represent the pore-throat radius at the 16th percentile of cumulative mercury intrusion, and open boxes represent the pore-throat radius at the 84th percentile.

reason for this is related to the manner in which each type of porosity was determined. Commercial core analyses measure both effective porosity and an unknown amount of ineffective microporosity. Petrographic evidence and results of high-pressure mercury porosimetry show that microporosity within patches of detrital and authigenic kaolinite accounts for variable proportions of total porosity in the Carter reservoir. This microporosity, which contains bound water, does not contribute to the effective pore system, nor does it contain extractable oil. For this reason, the dual-water model was used in well-log analysis to determine effective water saturation by subtracting out the volume of immobile water bound between clay particles.

Relative to the pay cutoffs used in this investigation, reservoir-quality effective porosity occurs in Carter sandstone in all production and water-injection wells in North Blowhorn Creek oil unit (fig. 72). Generally, arithmetic-mean porosity for the pay interval is highest along the axis of the reservoir sandstone body. The highest values occur in two areas: (1) a narrow northern region which contains the highest porosity and (2) a wider, south-

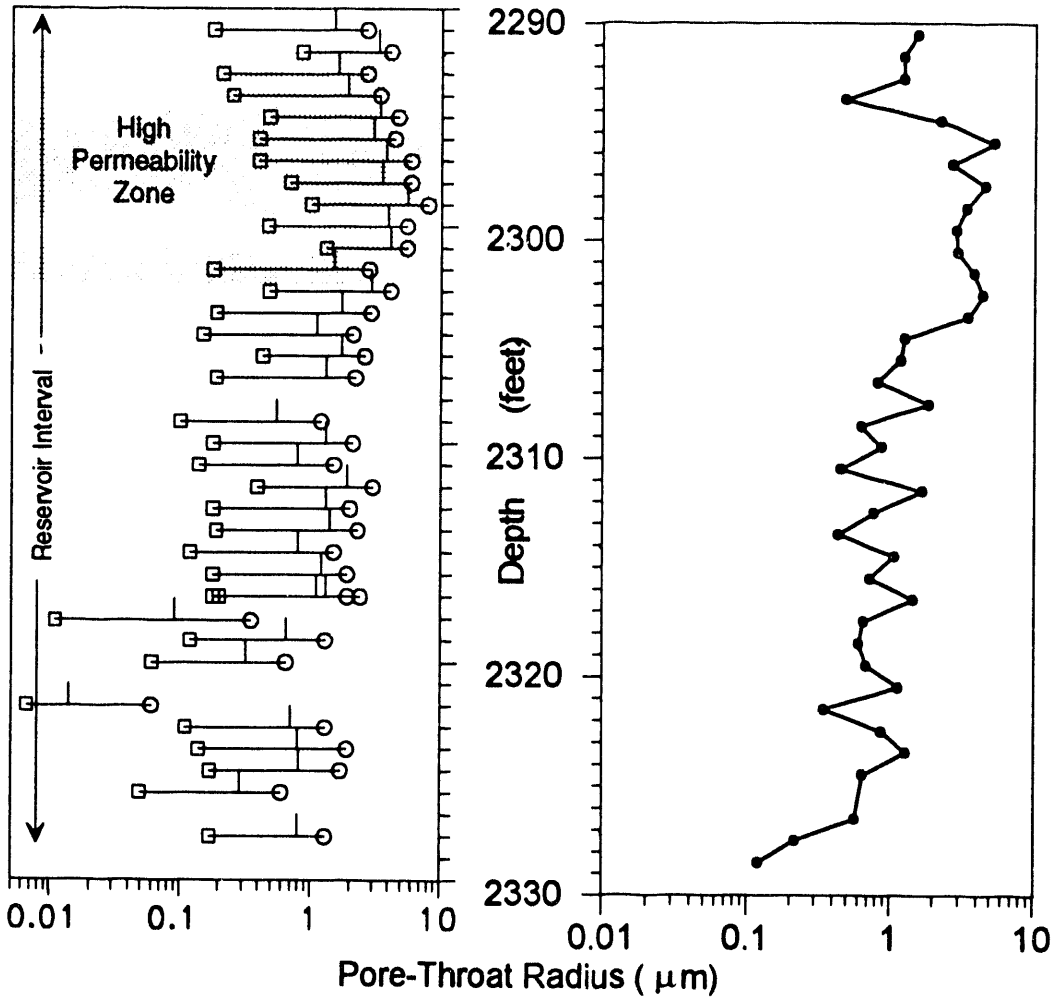

Figure 69.--Comparison of median pore-throat size determined by high-pressure mercury porosimetry (left) with that determined from commercial core analyses by Pittman's (1992) method (right) for well PN3314. Vertical lines in the plot on the left represent the median pore throat radius, open circles represent the pore-throat radius at the 16th percentile of cumulative mercury intrusion, and open boxes represent the pore-throat radius at the 84th percentile.

ern region with somewhat lower porosity. Although variation in mean porosity among wells is evident in figure 73, this two-dimensional view of a single parameter does not adequately describe factors affecting oil production related to heterogeneity in other reservoir properties. Net pay thickness also varies spatially within the North Blowhorn Creek oil unit reservoir (fig. 73), and patterns generally follow trends evident in the distribution of mean porosity (fig. 72). Again, two regions of maximum net pay are present, a northern and a southern region. Significantly, net pay thickness decreases substantially over short lateral distances along the northwestern margin of the northern region. Maximum net pay thickness in the southern region is equivalent to that in the northern region, although variation in net pay thickness is greater in the southern region (fig. 72).

Combining mean porosity with net pay as a product of these two parameters (porosity-feet) provides a method of assessing the fluid-storage capacity of the North Blowhorn Creek reservoir (fig. 74). As expected, general trends are similar to those displayed in individual maps for the two parameters.

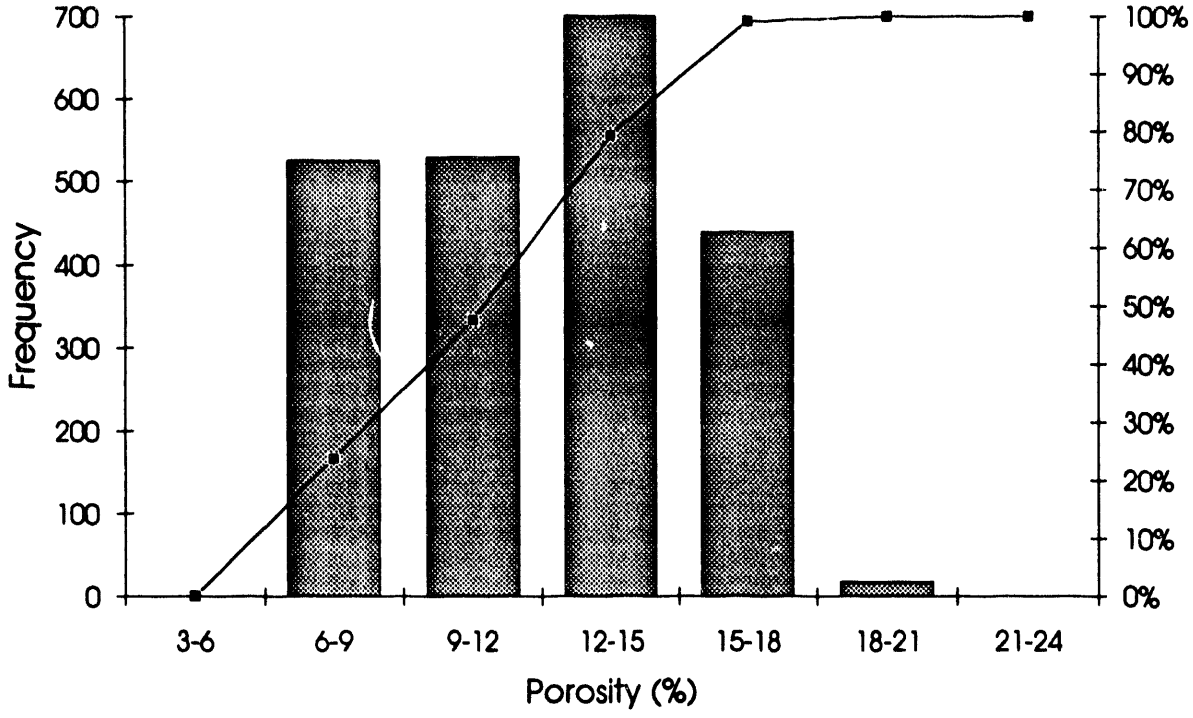

Figure 70.--Frequency histogram and cumulative-percent curve of well-log derived effective porosity for Carter sandstone in North Blowhorn Creek oil unit.

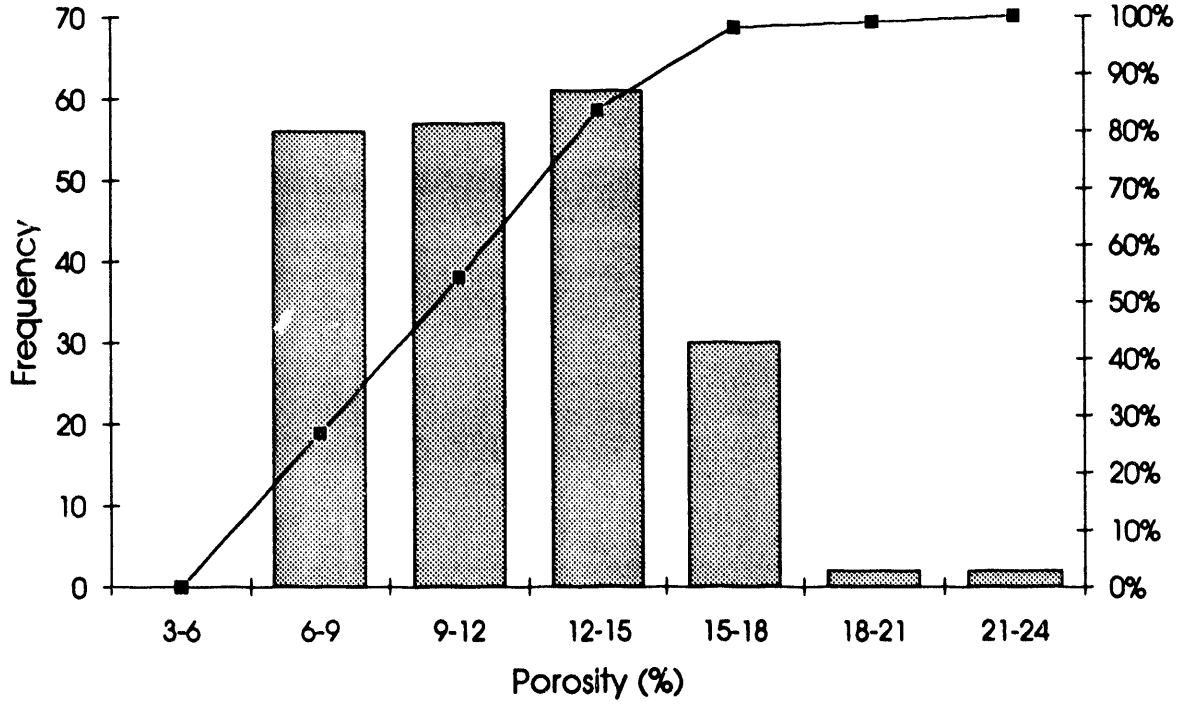

Figure 71.--Frequency histogram and cumulative-percent curve of core-analysis porosity for Carter sandstone in North Blowhorn Creek oil unit.

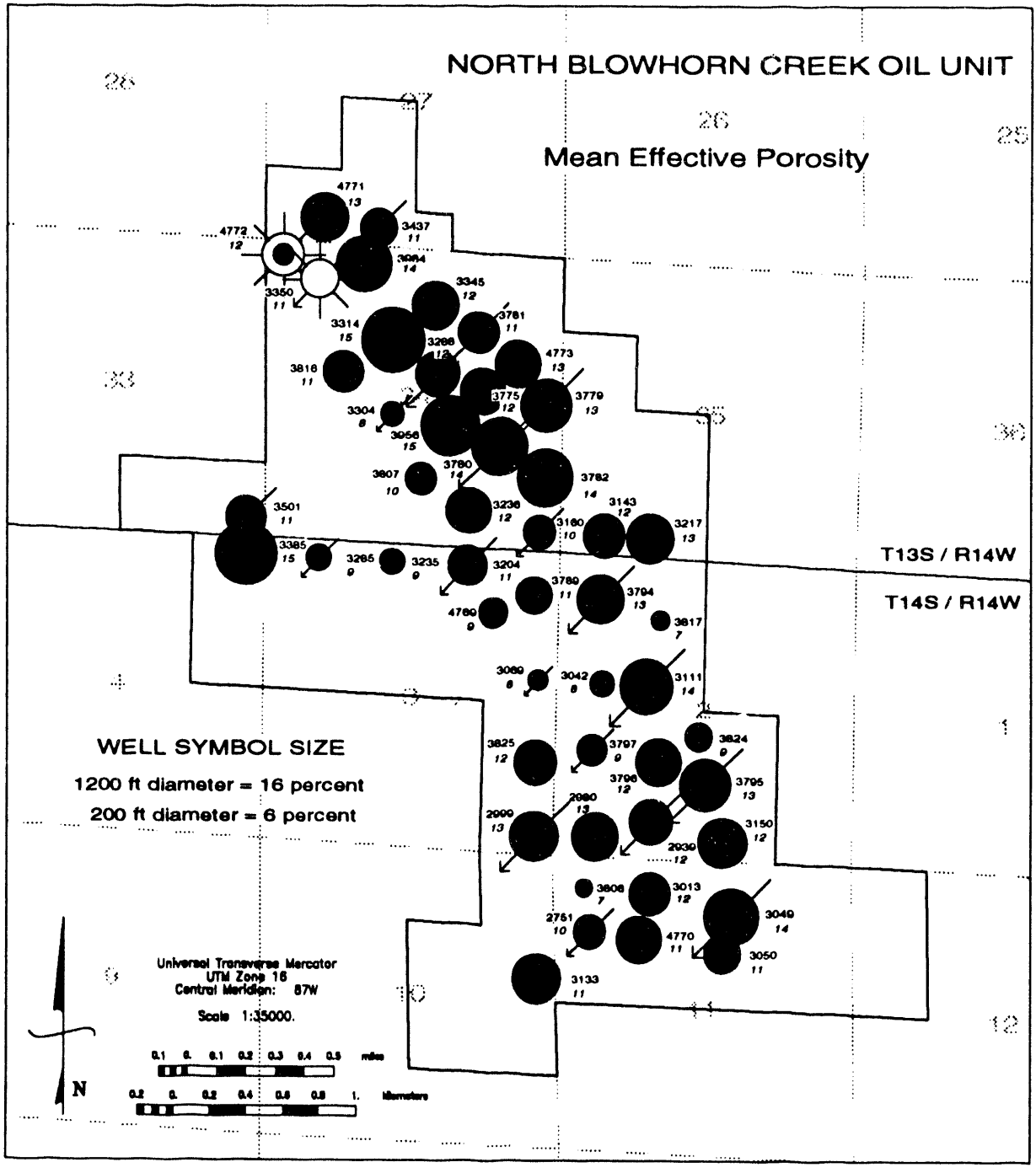

Figure 72.--Bubble map of mean effective porosity for Carter sandstone, North Blowhorn Creek oil unit. The size of well symbols is proportional to effective porosity. State Oil and Gas Board of Alabama permit numbers are adjacent to wells. Mean effective porosity, rounded to the nearest integer, is shown in italics below the permit numbers.

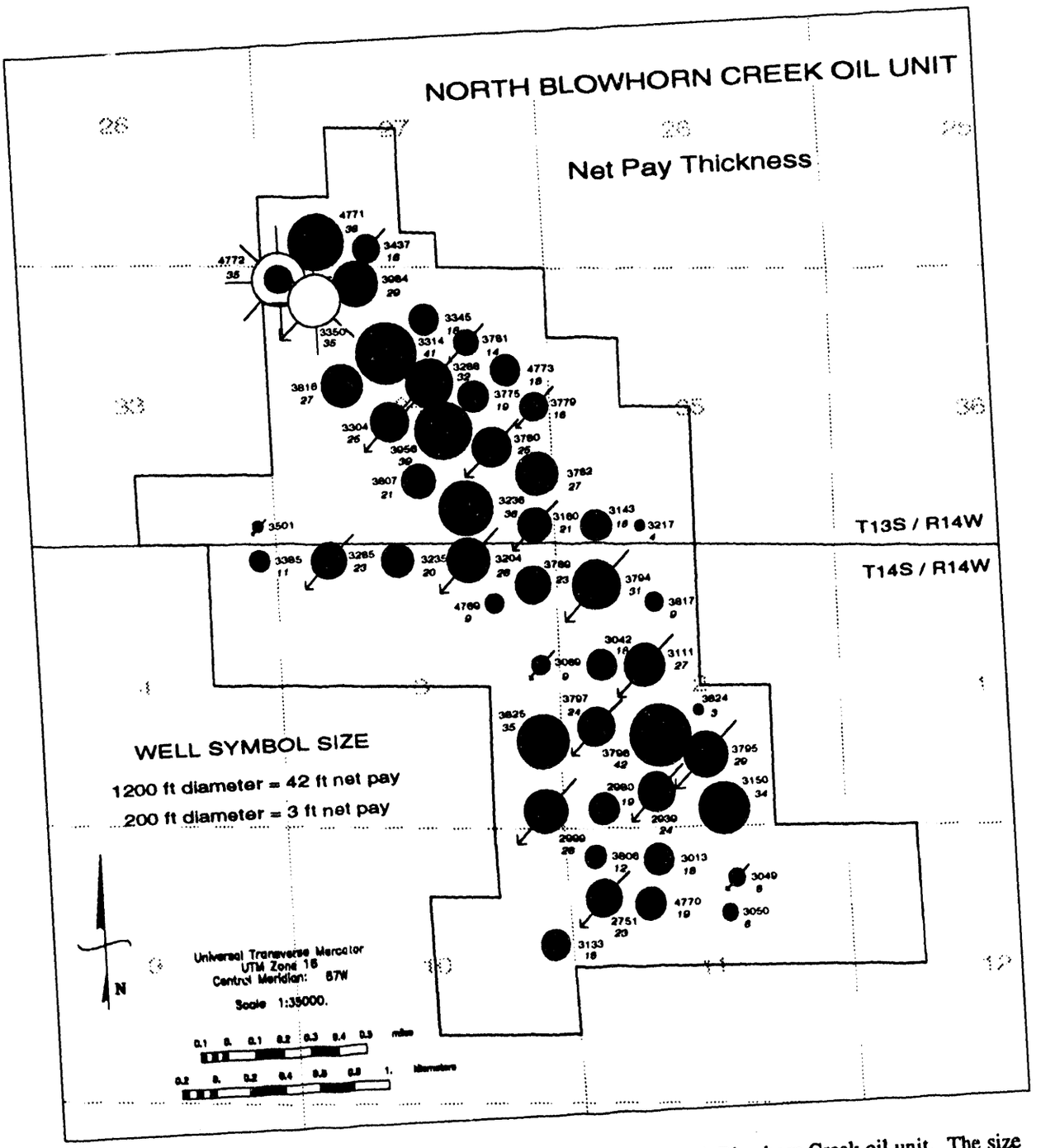

Figure 73.--Bubble map of net pay thickness for Carter sandstone in North Blowhorn Creek oil unit. The size of well symbols is proportional to net pay thickness. State Oil and Gas Board of Alabama permit numbers are adjacent to wells. Net pay thickness, rounded to the nearest integer, is shown in italics below the permit numbers.

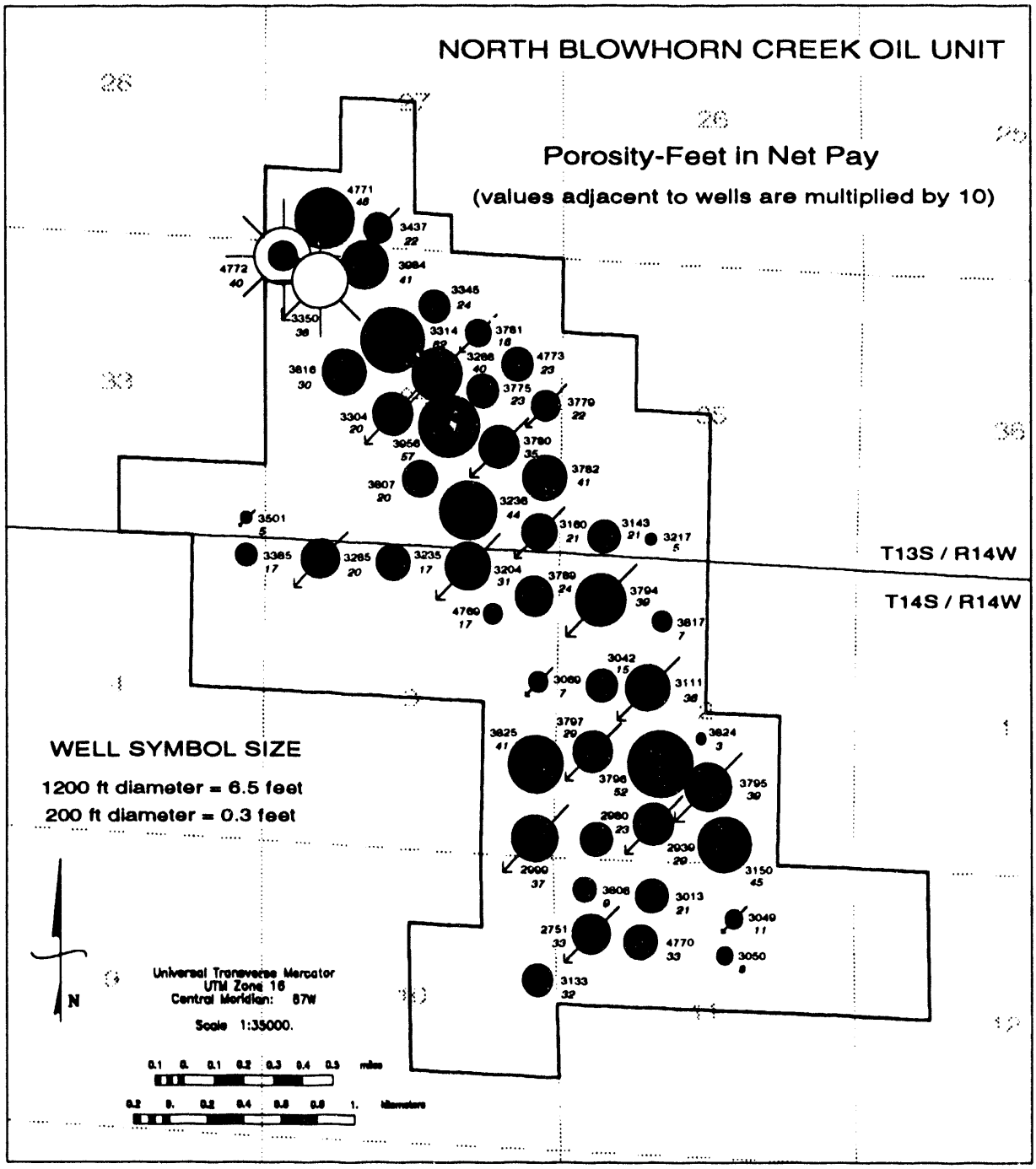

Figure 74.--Bubble map of pore volume (porosity x net pay thickness) for Carter sandstone in North Blowhorn Creek oil unit. The size of well symbols is proportional to pore volume. State Oil and Gas Board of Alabama permit numbers are adjacent to wells. Porosity-feet values, multiplied by 10 and rounded to the nearest integer, are shown in italics below permit numbers.

Maximum pore volume in the net pay section occurs in the northern region. However, this zone of maximum pore volume occurs in a much narrower band than is indicated on maps for the uncombined parameters (figs. 72, 73). The area with the highest pore volume in the southern region is broader and variability is greater than in the northern region (fig. 74).

The pore space in a reservoir commonly contains more than one type of fluid, and these fluids are not evenly distributed throughout the reservoir. In order to assess spatial variation in original oil saturation in the Carter reservoir in North Blowhorn Creek oil unit, total (Archie) and effective (dual-water model) water saturations were calculated (fig. 75). Effective water saturation was used to determine oil saturation (100% - % effective water saturation) for calculation of original oil in place for the TORIS database. The map in figure 75 shows the difference in water saturation calculated using the two techniques. Total water saturation is lowest in the northern part of the oil unit in the same wells that have the highest pore volume (compare to fig. 72). Petrographic evidence shows that clays are a less important component of sandstone in these wells than elsewhere in the reservoir. Total water saturation is highest in two areas: (1) the entire southwestern margin of the reservoir and (2) the southern part of the oil unit. Additionally, the ratio of effective to total water saturation is highest within these two regions (fig. 75). The reason for this is that sandstone in these regions contains a larger volume of clay with bound water. The distribution of water saturation shown in figure 75 emphasizes the importance of integrating petrographic observations with well-log analysis. If clays are not taken into account in log analysis, and Archie water saturations are used, determination of original oil in place would result in lower values than those determined using effective water saturation. Strategies for extracting additional oil through improved or enhanced recovery techniques also could be incorrectly influenced if the presence of clays is not acknowledged.

The product, effective porosity times net pay times oil saturation, when combined with reservoir area, is used to calculate original oil in place. A map of this product (fig. 76) clearly demonstrates the heterogeneous nature of the North Blowhorn Creek reservoir. This map indicates that the largest original volume of oil resides in the northern part of the oil unit. This oil mostly occurs along the axis of the reservoir where amalgamated sandstone lenses are thickest. The central part of the unit contains smallest volume of oil along the axis of the reservoir. Net pay thickness is low (fig. 73) and water saturation is high (fig. 75) in this region. The southern part of the unit contains a substantial, but sporadically distributed, volume of oil.

The distribution of porosity and fluid saturations in the North Blowhorn Creek reservoir has been treated two dimensionally, thus far, using average values for the pay interval in each well. However, stratigraphic, as well as areal, variation occurs in the reservoir. Structural cross sections of well-log derived effective-porosity profiles, containing the same wells as those used to develop the depositional model for North Blowhorn Creek oil unit (figs. 77 through 80) illustrate stratigraphic variation in porosity. Cross section A-A' (fig. 77) corroborates the distribution of high porosity along the axis of the reservoir sandstone body (figs. 72, 77). The thickest vertically contiguous section containing the two highest porosity classes (12 to 15 percent and >15 percent) occurs in wells in the northern half of the field. Thick sections containing these two porosity classes also occur in the southern part of the field. Wells with the highest porosity in the northern half of the field contain few intervals with porosity below 12 percent, whereas those in the southern half contain a higher proportion of lower porosity.

The porosity profiles are somewhat misleading because thin permeability barriers are not represented as very low porosity intervals, due to the resolution of well logging tools. For example, the lower half of the reservoir in well PN3314 contains alternating intervals of 12 to 15 percent and greater than 15 percent porosity. Core descriptions (fig. 44) show that these slightly lower porosity (12 to 15 percent) intervals, which are on the order of centimeters in thickness in the core, are completely carbonate-cemented shell accumulations. These cemented zones act as local barriers to vertical fluid flow and generally are not correlative from well to well.

Transverse cross sections (figs. 77 through 80) exhibit the greatest stratigraphic and areal variation in porosity. Cross-section B-B' (fig. 78), in the northern part of North Blowhorn Creek oil unit, shows the narrow, thick high-porosity zone along the reservoir axis in the northern part of the oil unit. Although reservoir thickness and porosity decrease to the east and west of well PN3314, porosity remains relatively high in the wells adjacent to well PN3314. Cross-section C-C' (fig. 79) reveals that porosity is both lower and much more variable in the central part of the unit. The reservoir becomes increasingly segmented west of the axis. Further to

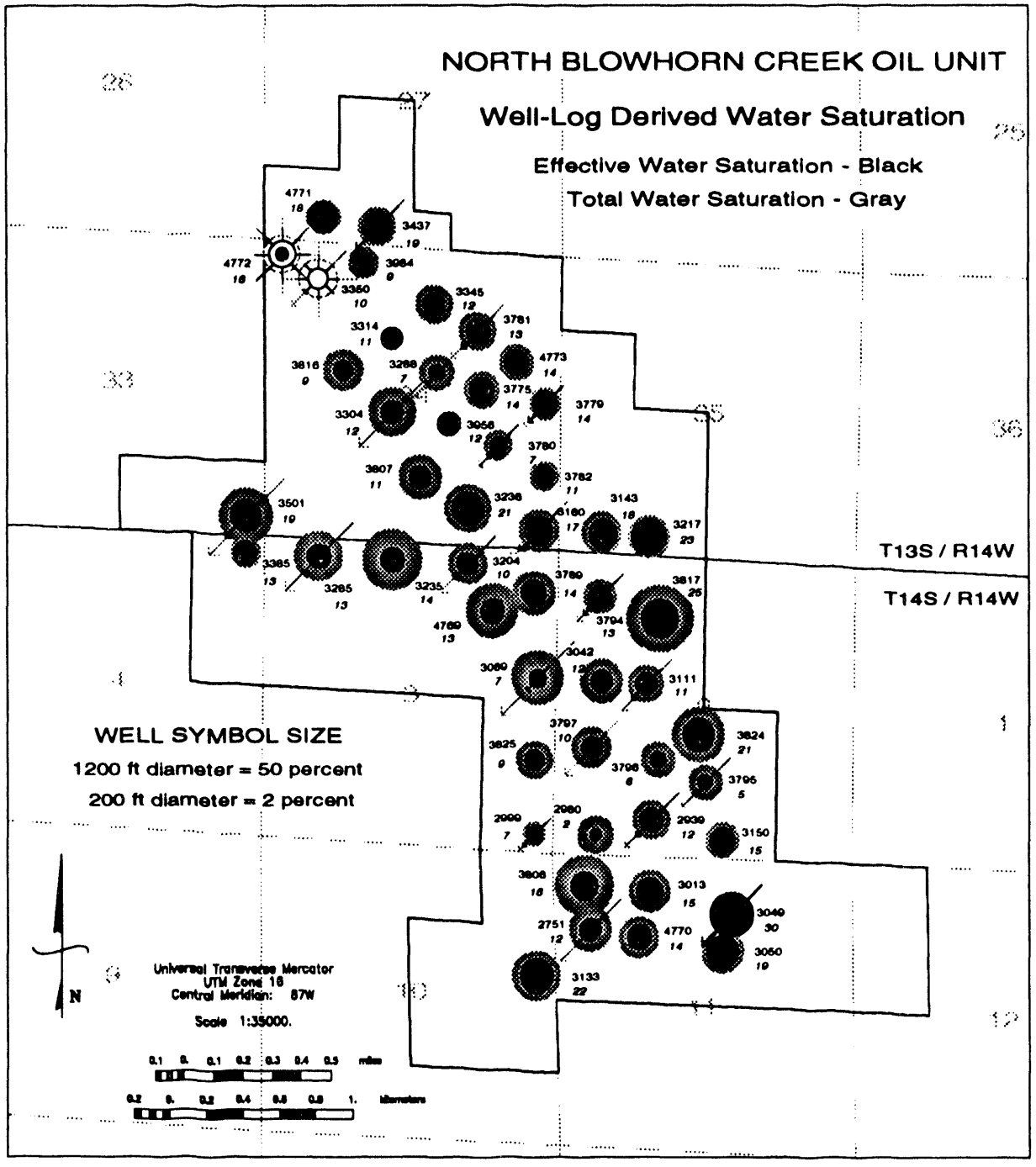

Figure 75.--Bubble map of effective and total water saturation for Carter sandstone, North Blowhorn Creek oil unit. The size of black well symbols is proportional to effective water saturation. The size of gray well symbols is proportional to total water saturation. State Oil and Gas Board of Alabama permit numbers are adjacent to wells. Effective water saturation, rounded to the nearest integer, is shown in italics below the permit numbers.

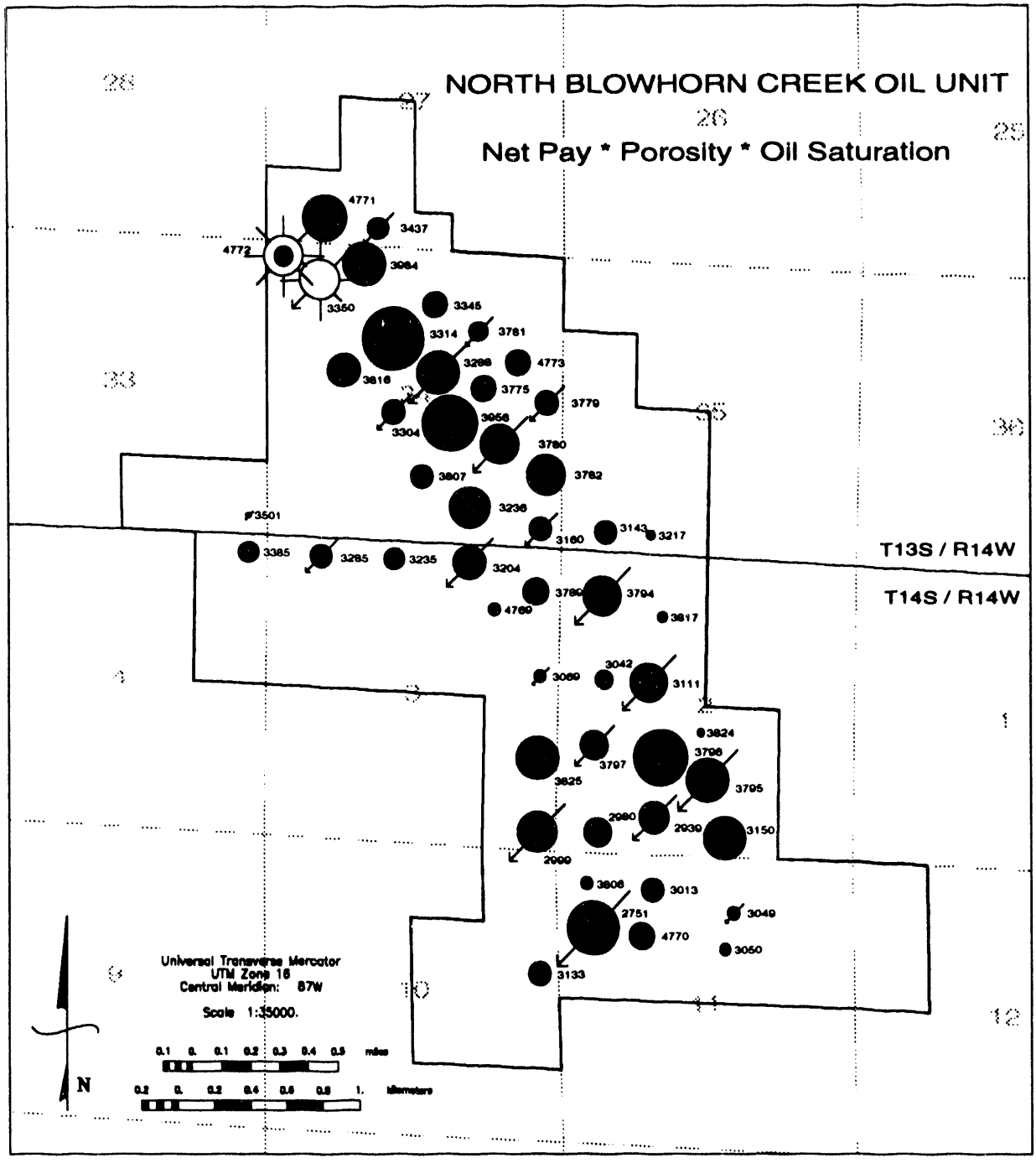

Figure 76.--Bubble map of the product, net pay times effective porosity times oil saturation for Carter sandstone, North Blowhorn Creek oil unit. The size of well symbols proportional to this product. State Oil and Gas Board of Alabama permit numbers are adjacent to wells.

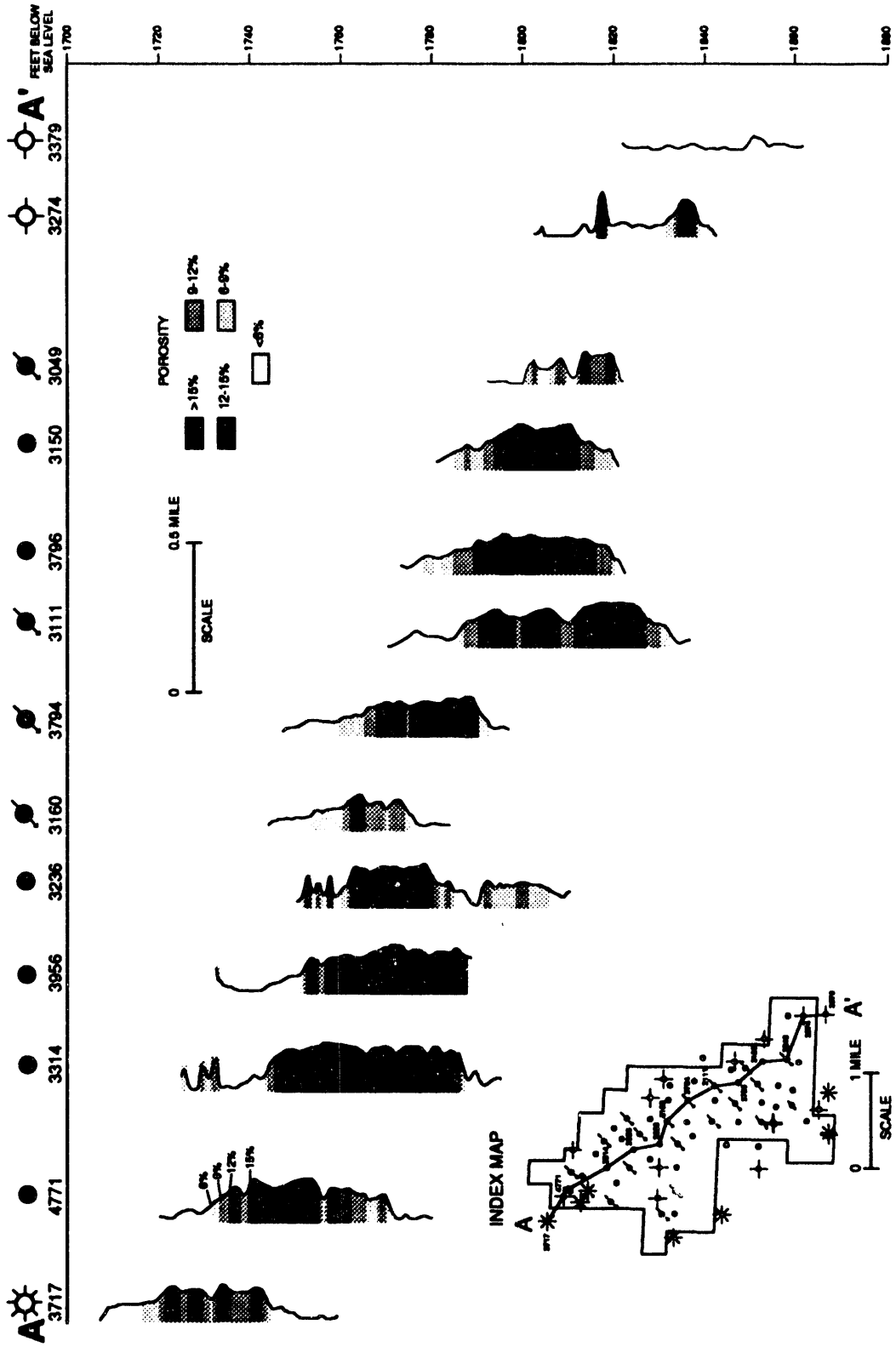

Figure 77.--Longitudinal structural cross-section A-A' of effective porosity profiles, Carter sandstone, North Blowhorn Creek oil unit.

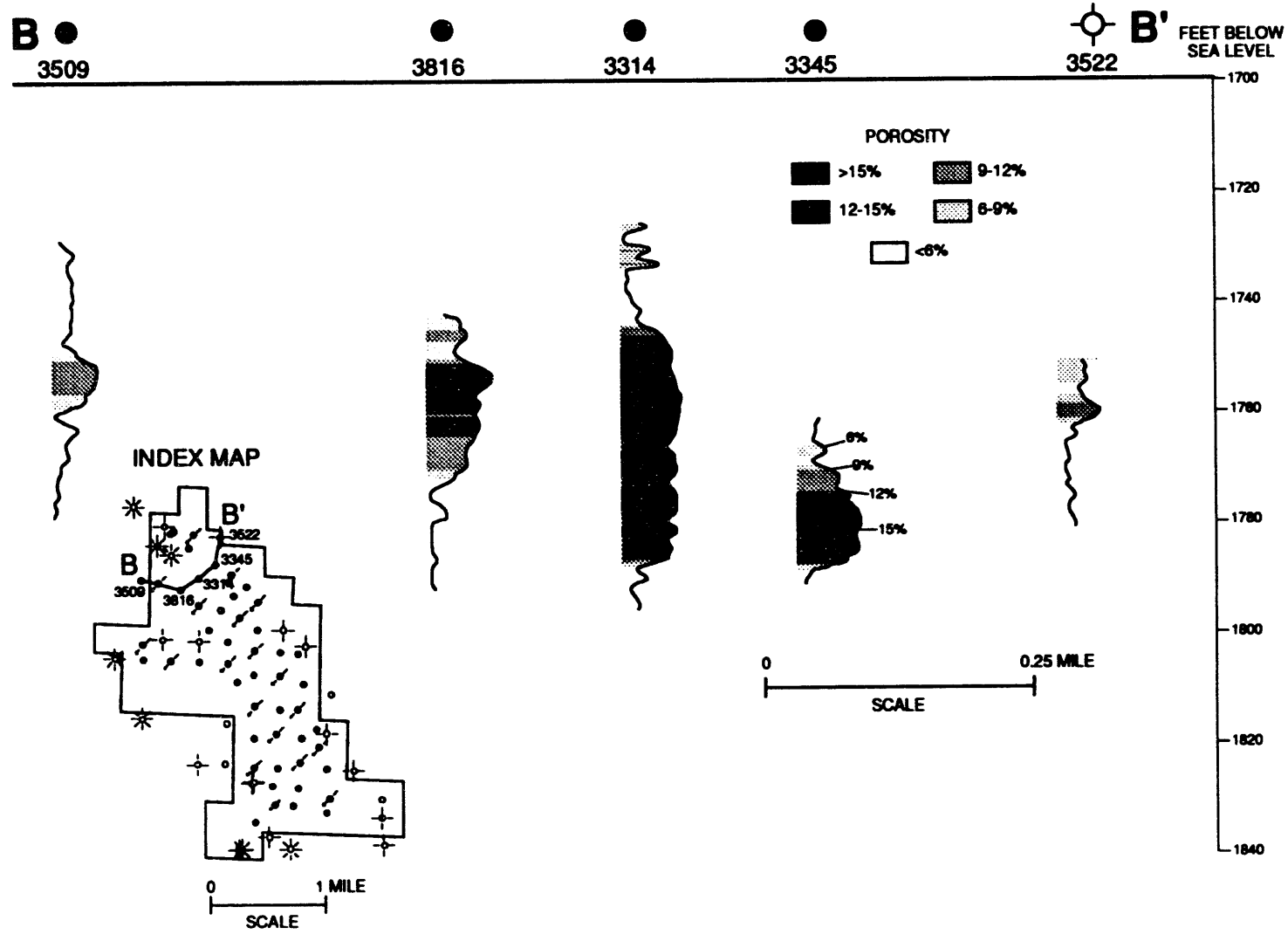

Figure 78.--Transverse structural cross-section B-B' of effective porosity profiles, Carter sandstone, North Blowhorn Creek oil unit.

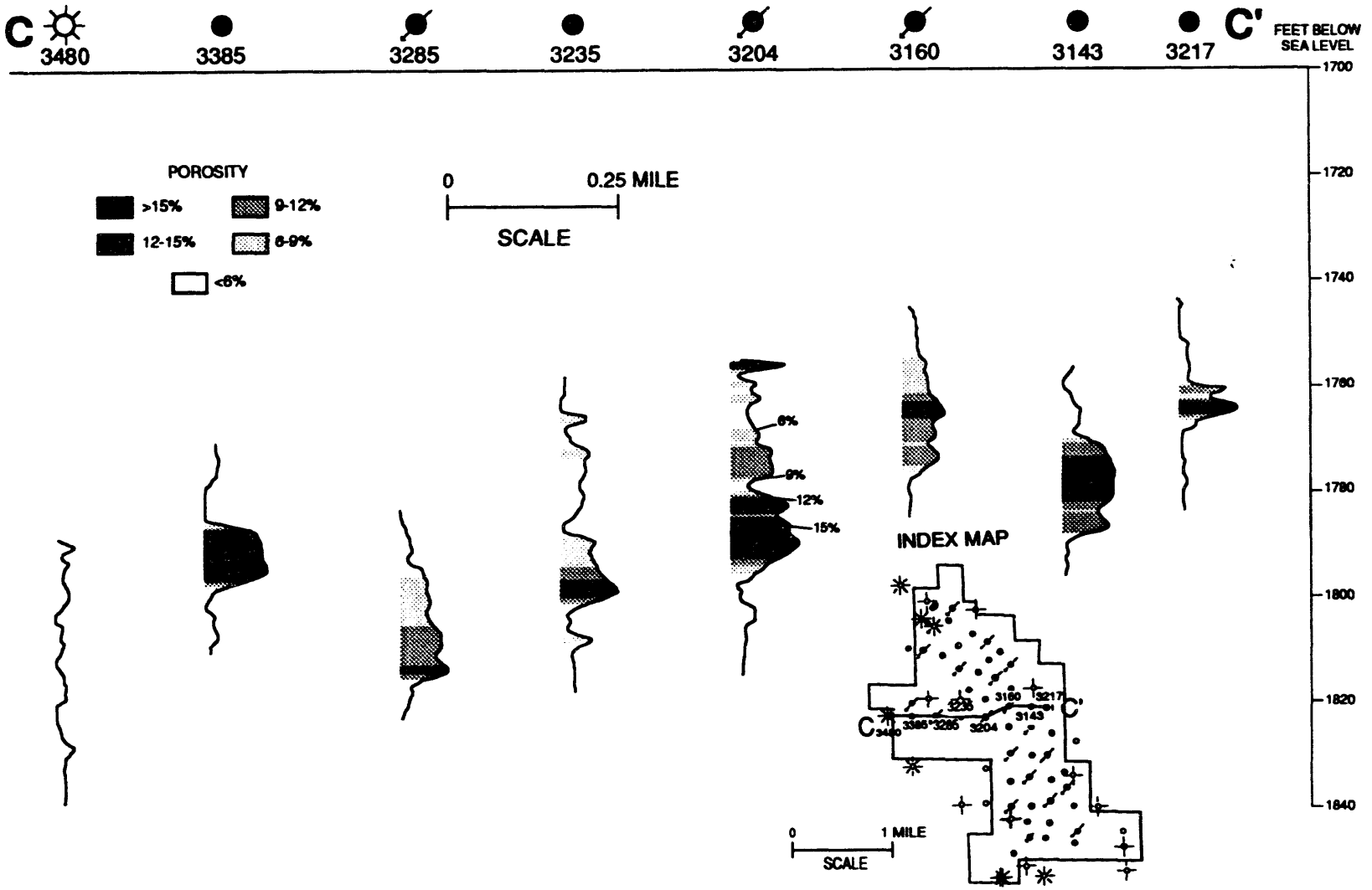

Figure 79.--Transverse structural cross-section C-C' of effective porosity profiles, Carter sandstone, North Blowhorn Creek oil unit.

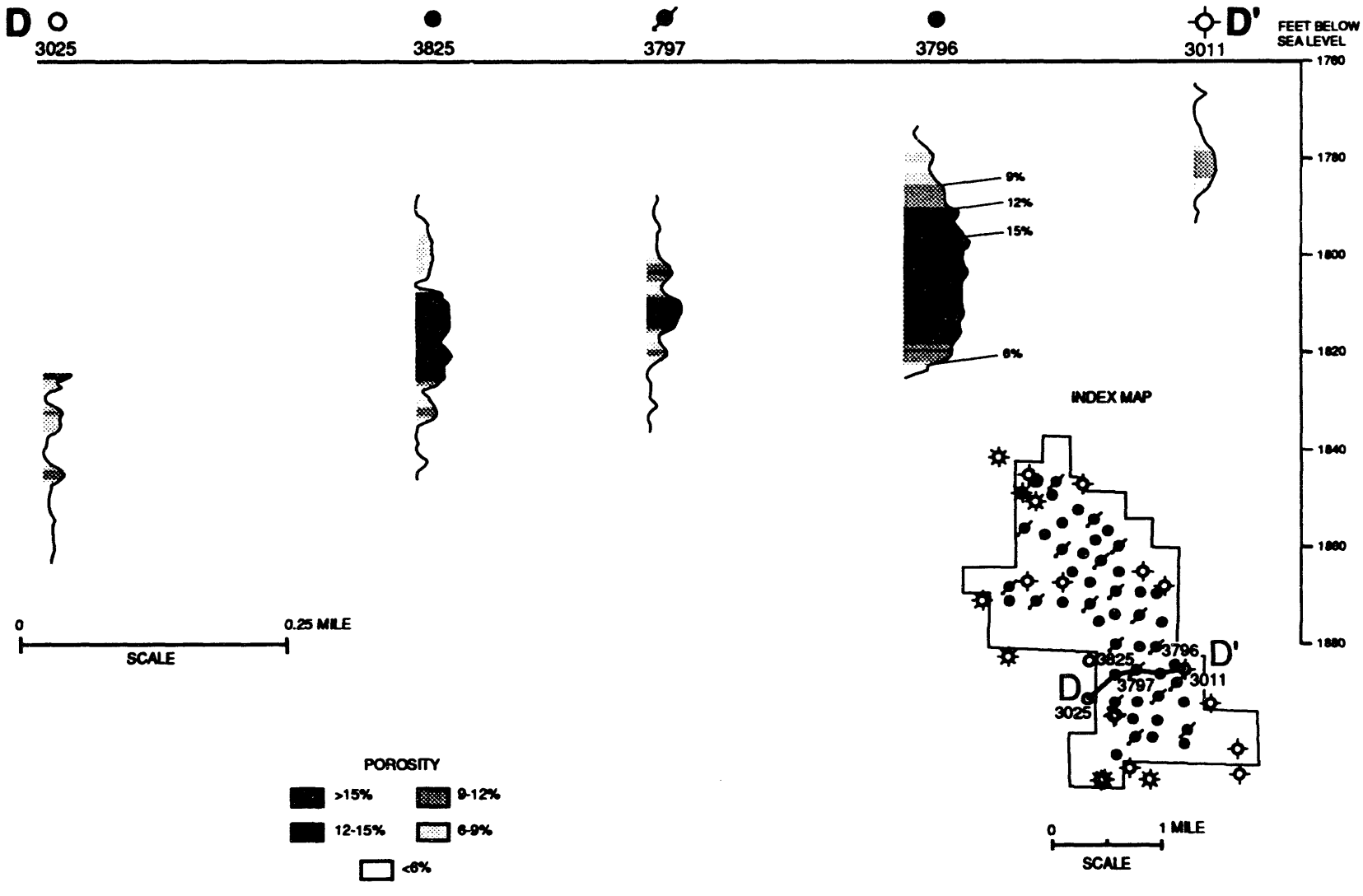

Figure 80.--Transverse structural cross-section D-D' of effective porosity profiles, Carter sandstone, North Blowhorn Creek oil unit.

the south and along the reservoir axis, well PN3796, in cross-section D-D' (fig. 80), contains a thick, continuous section of relatively high porosity. Again, segmentation of the reservoir increases west of the axis.

Variance, standard deviation, and the coefficient of variation are three ways to describe the variation of a parameter, such as porosity, about its mean. The coefficient of variation is simply standard deviation divided by the mean (Size, 1987). This parameter is not commonly used in statistical analysis, but it provides a readily determined and easily interpreted view of variation in comparison to other measures of statistical distribution because it takes both the mean and standard deviation into account. A map of coefficient of variance of effective porosity in the pay interval exhibits a distribution of porosity variation similar to that implicit in the porosity-profile cross sections. This pattern also is similar to that shown on the map of the product of net pay, mean effective porosity, and water saturation (fig. 81). That is, variation in porosity is lowest in the northern part of the unit and greatest along the western margin and at the southern end of the reservoir. Again, the reservoir is most homogeneous where clinoformal sandstone lenses are amalgamated. Porosity heterogeneity is greatest in segmented lenses and in backshore deposits.

In summary, North Blowhorn Creek oil unit can be divided areally into four zones with different reservoir characteristics, based on the areal and stratigraphic distribution of porosity water saturation, and pay thickness (fig. 82). Zone 1 contains the most-homogeneous, highest-quality reservoir. This zone occurs in the northern part of the unit where clinoformal sandstone lenses are amalgamated. Fluid flow in Zone 1 is favored along the reservoir axis. Zone 2 is a transitional zone between higher quality reservoir in Zones 1 and 3. The pay interval in Zone 2 is thin and has high water saturation. Zone 3 contains high-quality reservoir, but its distribution is sporadic. Sandstone lenses in Zone 3 are smaller than in zone 1. Moreover, these lenses are increasingly segmented toward the south and are oriented obliquely to the main reservoir axis at their distal ends. This results in complex fluid-flow patterns in Zone 3. Zone 4 contains the lowest quality and most heterogeneous reservoir sandstone. This zone consists of the distal ends of sandstone lenses and backshore deposits. The probability of uncontacted or unconnected compartments is greatest in this zone.

Depositional modeling, presented elsewhere in this report, indicates that reservoirs in other oil fields in the Black Warrior basin of Alabama are beach deposits consisting of clinoformal sandstone lenses similar to those in North Blowhorn Creek oil unit. Most of these fields either lack cores or have cores that were extracted from unrepresentative parts of the reservoir. Thus, petrophysical properties for these fields must be determined by well-log analysis. Well-log derived effective porosity in these fields is lower than that in North Blowhorn Creek oil unit. Porosity modes typically occur at 8 to 10 percent (figs. 83 through 86), in contrast to a mode of 12 to 15 percent for North Blowhorn Creek oil unit. Further, water saturation is anomalously low in North Blowhorn Creek oil unit compared to that in other oil fields (fig. 87). This suggests that sandstone in these other fields contains more detrital and authigenic clay. These factors, combined with a large reservoir size, explain why North Blowhorn Creek oil unit is the most productive field in the basin. These same factors also indicate that, despite similarities in depositional setting, caution should be exercised in using the North Blowhorn Creek reservoir as a direct analog for modeling heterogeneity and fluid flow in other reservoirs in the basin. Petrophysical properties for selected, unitized oil fields are discussed further in a subsequent section of this report.

PROBLEMS IN PREDICTION OF PETROPHYSICAL PROPERTIES IN INTERWELL REGIONS

Estimation of reservoir properties, including porosity and permeability, in unsampled, interwell areas is desirable for delineating flow units and for determination of hydrocarbon reserves. Estimation of permeability is particularly important because this parameter controls fluid flow. Permeability cannot be determined reliably by well-log analysis and typically is undersampled relative to porosity. Accurate prediction of undersampled or unsampled petrophysical properties is difficult to achieve for the Carter reservoir in North Blowhorn Creek oil unit. The main reason for this difficulty is the configuration of detrital and authigenic clay in Carter quartzarenite. The distribution of clay in the reservoir results in the weak correlation between porosity and permeability based on commercial core analysis data. Thus, permeability is difficult to predict from porosity. Further, the spatial correlation of petrophysical properties, such as porosity, within the reservoir in individual wells commonly is indeterminate.

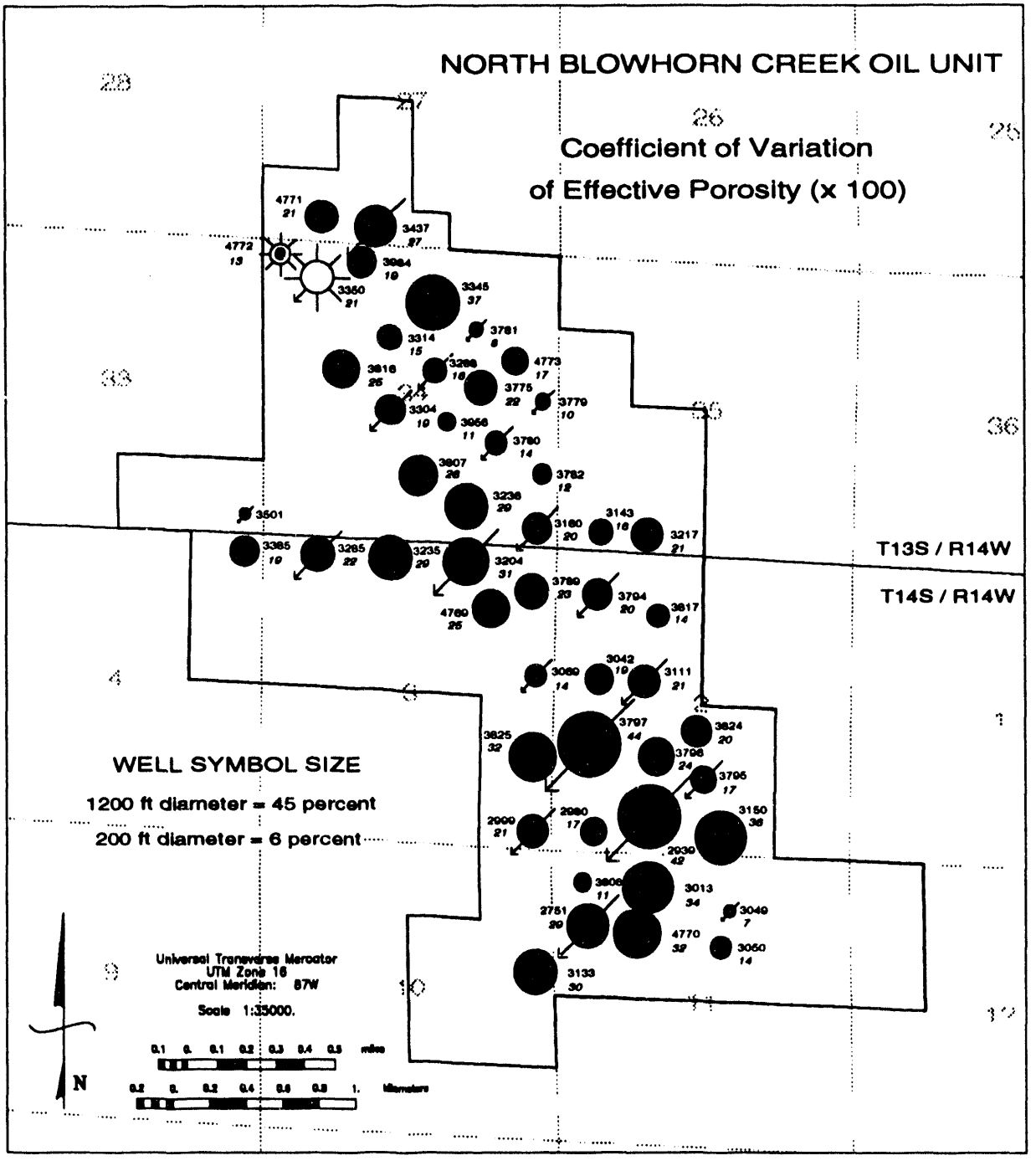

Figure 81.--Bubble map of coefficient of variation of effective porosity for Carter sandstone, North Blowhorn Creek oil unit. The size of well symbols is proportional to the coefficient of variation. State Oil and Gas Boad of Alabama permit numbers are adjacent to wells. The coefficient of variation is shown in italics below the permit numbers.

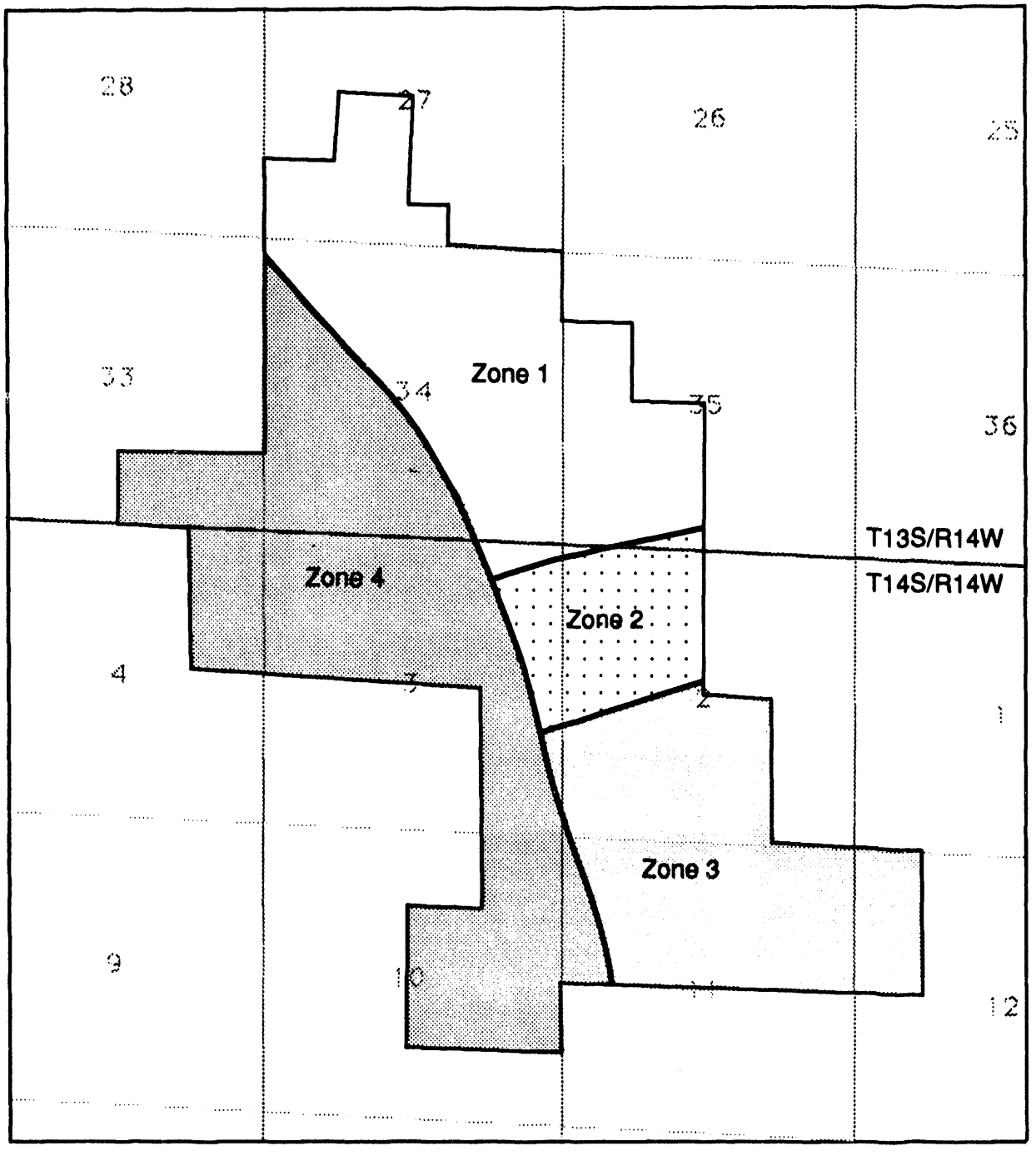

Figure 82.--Zones in Carter sandstone in North Blowhorn Creek oil unit with different reservoir characteristics.

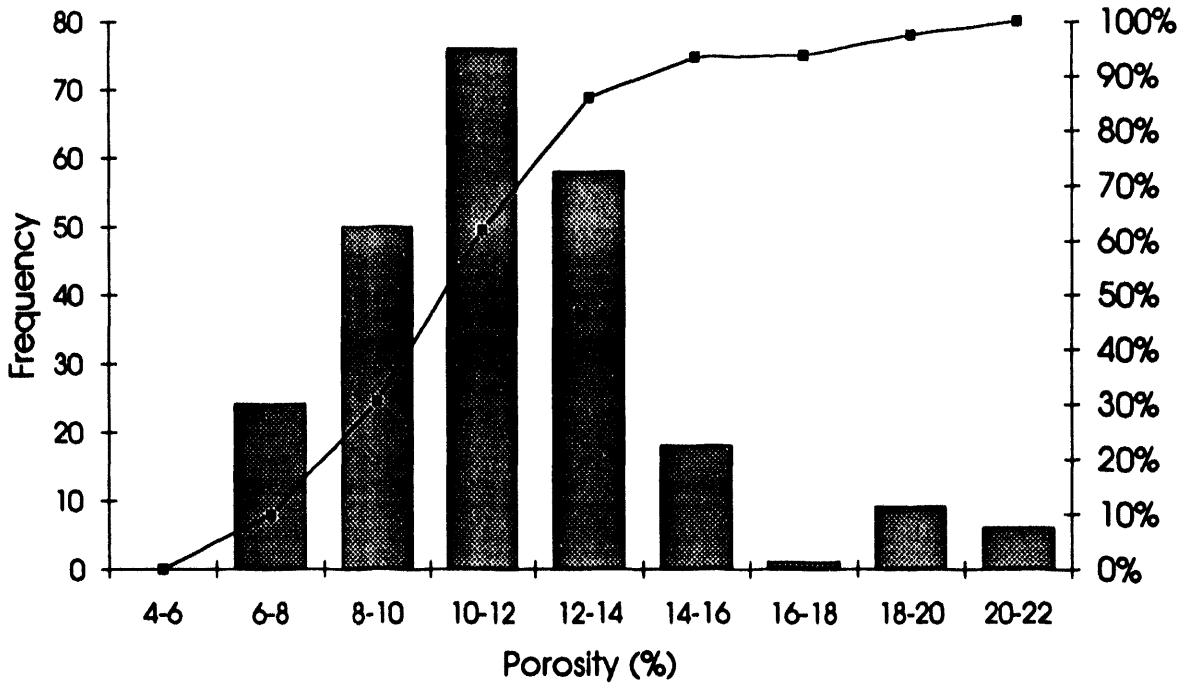

Figure 83.--Frequency histogram and cumulative-percent curve of well-log derived effective porosity for *Millerella* sandstone, Blowhorn Creek *Millerella* oil unit.

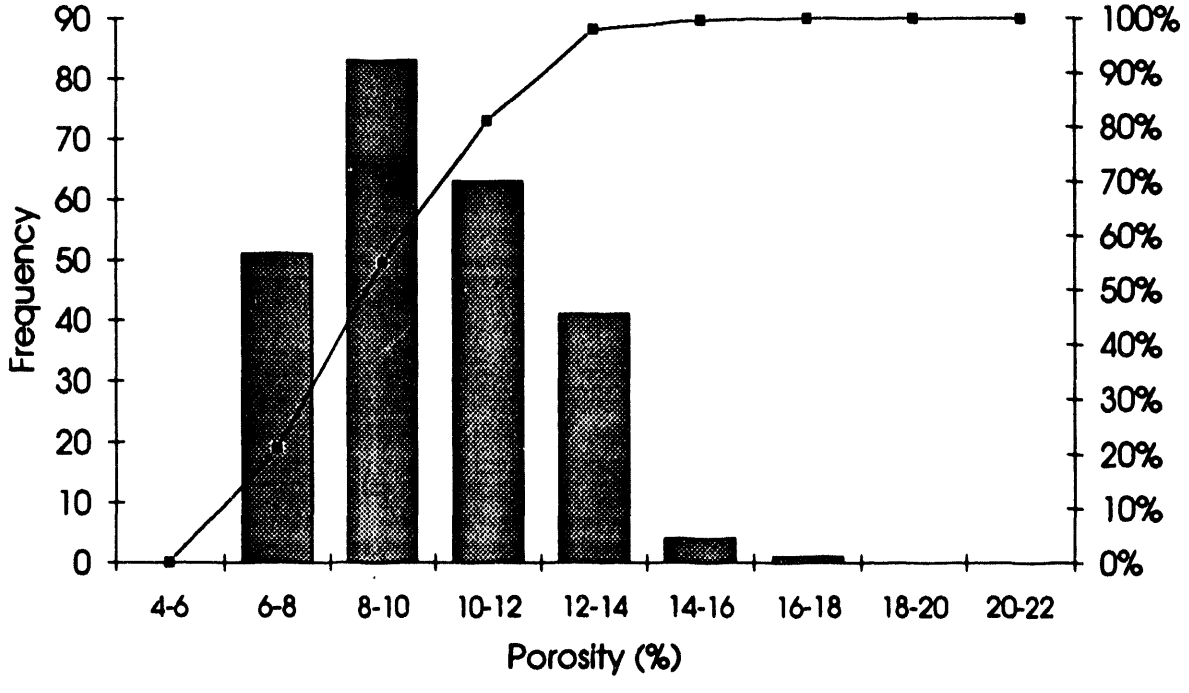

Figure 84.--Frequency histogram and cumulative-percent curve of well-log derived effective porosity for Carter sandstone, Central Fairview Carter sand oil unit.

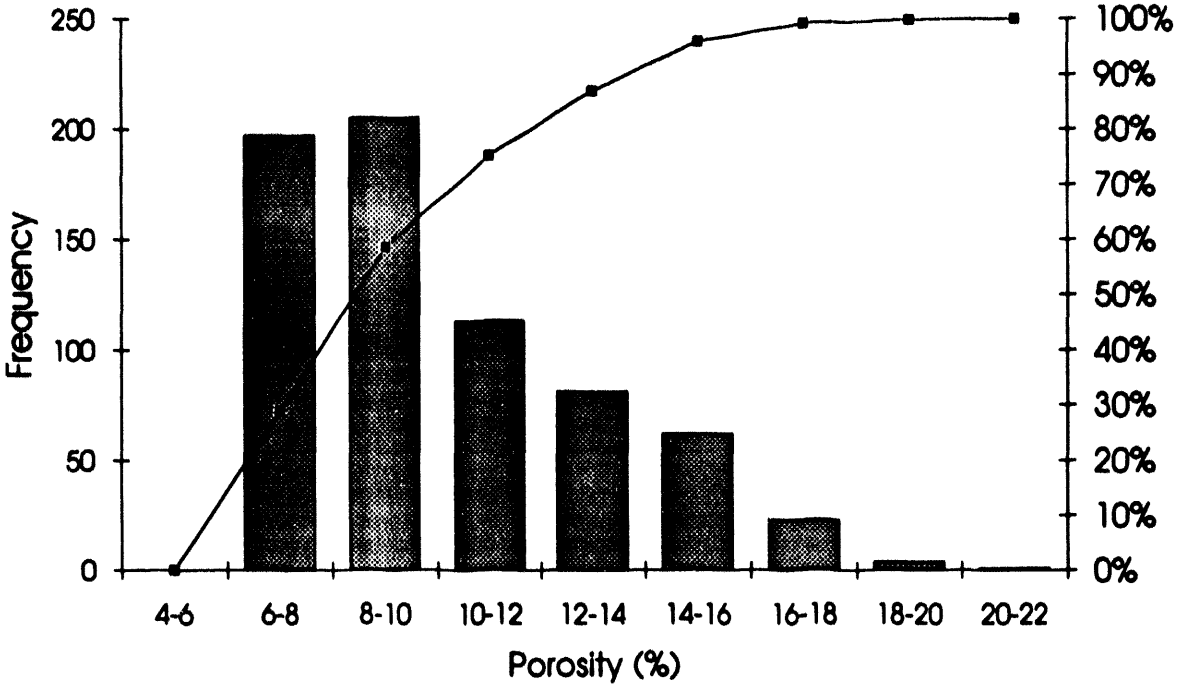

Figure 85.--Frequency histogram and cumulative-percent curve of well-log derived effective porosity for Carter sandstone, South Brush Creek oil unit.

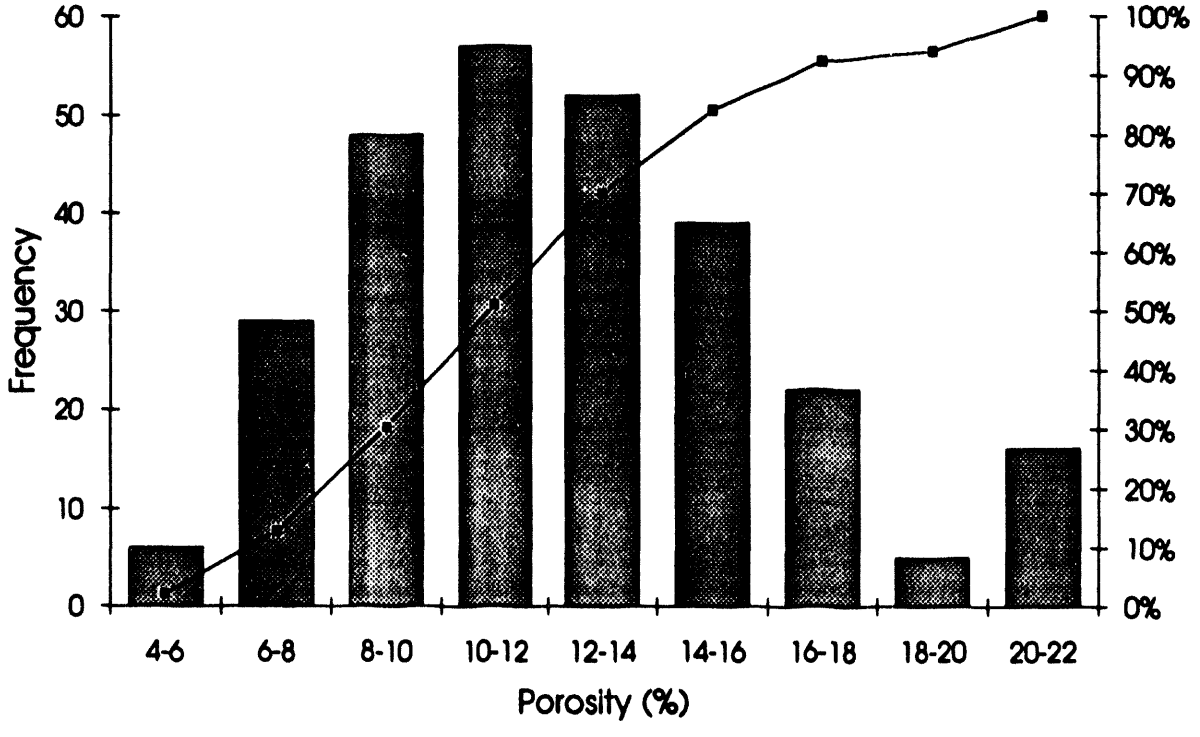

Figure 86.--Frequency histogram and cumulative-percent curve of well-log derived effective porosity for Carter sandstone, Wayside oil unit.

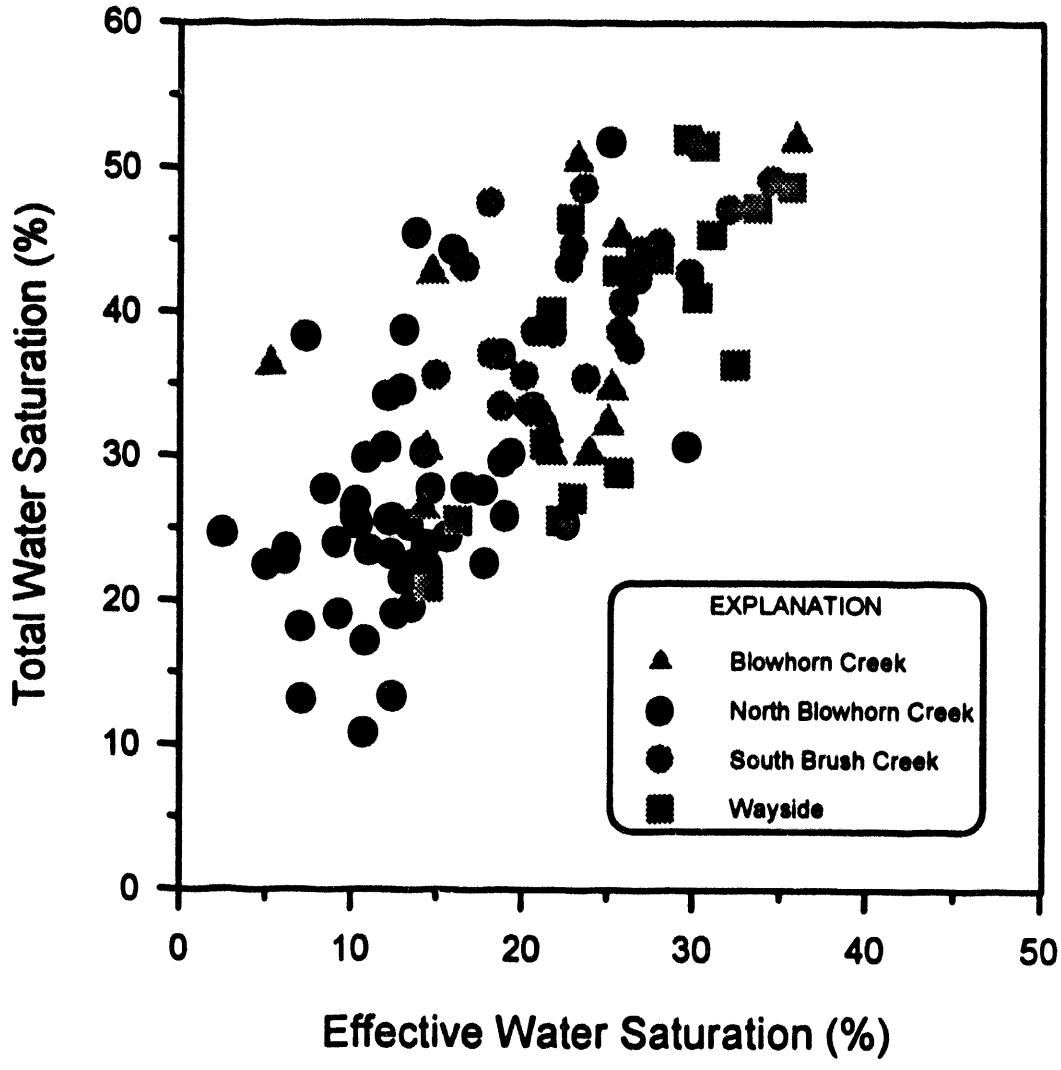

Figure 87.--Plot of effective water saturation versus total water saturation for selected Carter sandstone reservoirs.

Bubble maps have been used for presentation in this report because this type of map displays data values at the specific site of sampling. These maps, however, do not provide estimates of values between wells. Traditionally, contour maps are used to display the areal distribution of a parameter in interwell regions. Hand-drawn contours generally incorporate some degree of bias and may not be reproducible among different investigators. Moreover, interpolation of data values for interwell regions from hand-contoured maps typically has proven to be inadequate for providing input data for reservoir simulation. Computerized contouring generates reproducible maps, but not all contouring algorithms are suitable for accurate prediction of parameters in unsampled areas.

Geostatistical methods (Journel and Hijbregts, 1978; Isaaks and Srivastava, 1988) provide a promising means of estimating values of parameters for interwell regions. Geostatistics is a set of probabilistic methods that is used to estimate the

value of a regionalized variable, such as porosity, between sample sites. Geostatistical techniques have advantages over standard regression methods in that data values are honored at sample locations. Variography is a geostatistical method for analyzing the spatial variation of a parameter, such as porosity. Experimental variograms (fig. 88) describe this variation as a function of distance for a particular data set. The semivariance of different pairs of samples at increasing intervals of distance commonly increases until a separation in distance between points is reached beyond which no further increase occurs. The variogram is modeled by fitting a curve through the data points. Three aspects of the model are important. First, the variogram model may not originate at zero semivariance due to small-scale heterogeneity. This is referred to as the nugget. Second, the distance beyond which semivariance does not change is the range. This is the distance beyond which no spatial correlation exists. Third, the semivariance at the range is the sill.

The semivariogram model is used to provide input data for kriging, which estimates values between sample points and can be used to produce contour maps. Additional geostatistical methods, such as cokriging (Isaaks and Srivastava, 1988) can be used to predict values for an undersampled parameter on the basis of its correlation with a more extensively sampled parameter. For example, permeability typically is an undersampled parameter relative to porosity, which is readily determined by a variety of methods. If a correlation exists between porosity and permeability, cokriging can be used to estimate permeability. Kriging techniques have been criticized because they tend to produce unrealistically smooth spatial distributions of estimated parameters. As a result, a variety of other techniques for estimating parameters in interwell regions have been explored, including conditional hierarchical simulation, turning-band methods, annealing, fractal geometry, and fuzzy probability.

Geostatistical analysis can be used to make estimates of a parameter in one, two, or three dimensions, providing sufficient well density exists. Most oil fields in the Black Warrior basin of Alabama contain few wells and, therefore, have insufficient

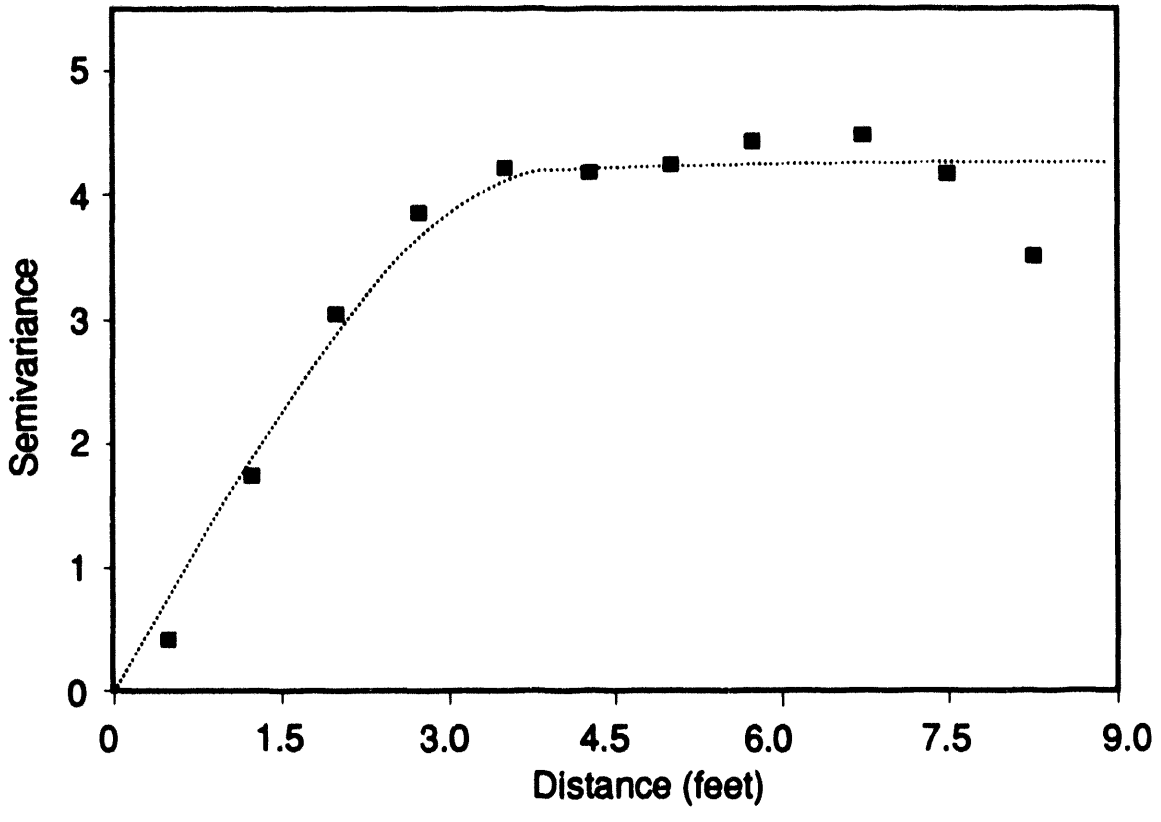

Figure 88.--Example of a modeled experimental semivariogram for Carter sandstone in North Blowhorn Creek oil unit (well PN3437, spherical model, negget = 0, sill = 4.2, range = 4.0).

data density for geostatistical evaluation. The Carter sandstone in North Blowhorn Creek oil unit, and perhaps in South Brush Creek oil unit, is the only reservoir in the Black Warrior basin of Alabama with appropriate data density for modeling. In addition to the small number of wells typical of Black Warrior basin oil fields, cores are rarely extracted. Moreover, the few cores that exist for fields outside of North Blowhorn Creek oil unit are not necessarily representative of reservoirs in those fields. Again, only North Blowhorn Creek oil unit has a sufficient number of cores to provide input data for geostatistical modeling.

One-dimensional geostatistical analysis of the vertical porosity distribution in 50 wells in North Blowhorn Creek oil unit, using Geo-EAS (Englund, 1988), a public-domain software package, gave indeterminate results. Four types of data were modeled using one dimensional variography: (1) raw neutron porosity curves; (2) raw porosity density curves; (3) cross-plot porosity; and (4) dual-water model derived effective porosity. Variograms also were prepared for selected wells using different sample spacing. Most variograms have no nugget effect, implying that little variability exists below the smallest sample spacing. Ranges of 2 to 12 feet are typical for variograms that could be modeled (fig. 88). However, more than one-half of the variograms constructed for wells in North Blowhorn Creek could not be modeled (fig. 89), and some that could be modeled have significant hole effects. Wells with uninterpretable variograms are dispersed throughout North Blowhorn Creek oil unit. These variograms for Carter sandstone are similar in structure to those modeled by Gould and others (1993). However, modeling was not pursued further because the variograms for Carter sandstone exhibit significant proportional effects (Isaaks and Srivastava, 1989), which imply strong local variation. This precludes two- and three-dimensional modeling of vertical porosity variation in interwell regions in North Blowhorn Creek oil unit. Therefore, additional consideration needs to be given to the structure of porosity data for Carter sandstone in North Blowhorn Creek oil unit before interwell porosity distribution can be determined accurately and permeability can be estimated by methods such as cokriging. Methods of estimating petrophysical

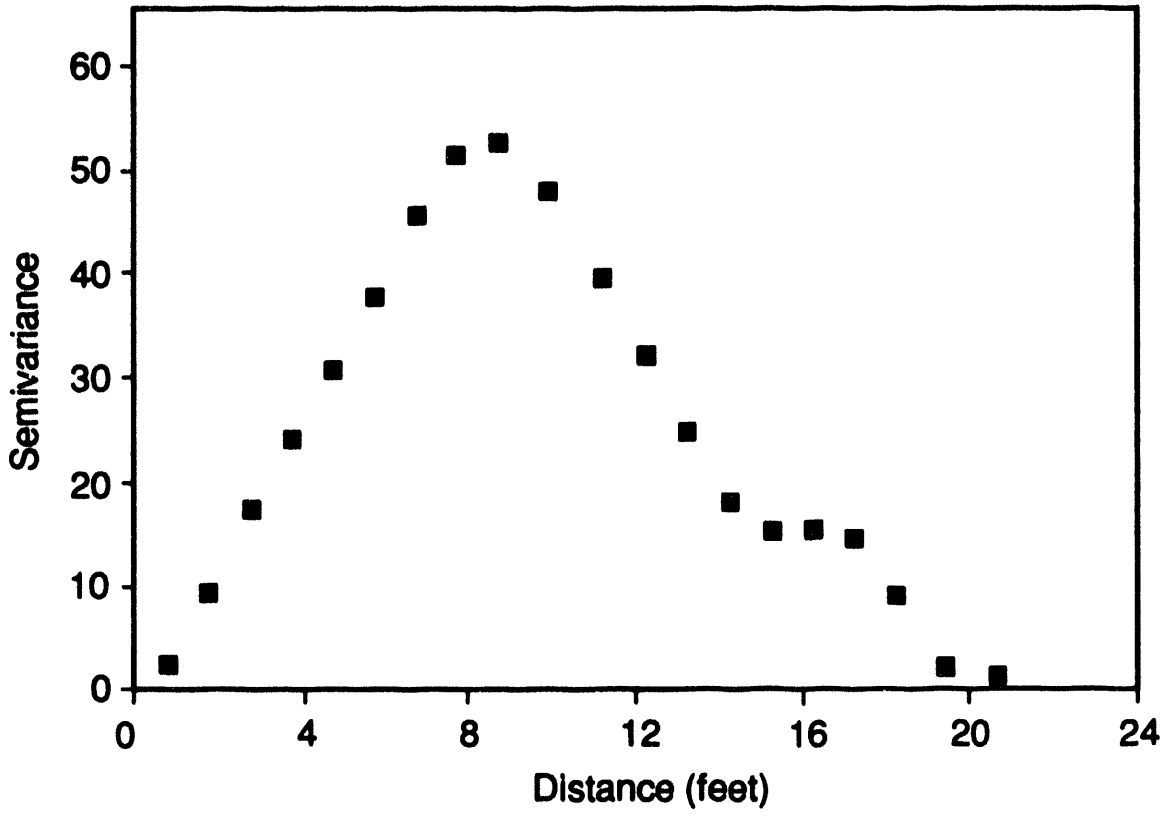

Figure 89.--Example of an experimental semivariogram for Carter sandstone in North Blowhorn Creek oil unit that could not be modeled (well PN3437).

properties in interwell regions of North Blowhorn Creek oil unit continue to be explored.

The weak correlation between porosity and permeability in Carter sandstone and the indeterminate results of one-dimensional geostatistical analysis are surprising for two reasons. First, reservoirs in quartzarenite commonly have higher reservoir quality than those in more lithic or feldspathic sandstone because deleterious effects of diagenesis are less significant in quartzarenite owing to the mechanical and chemical stability of the detrital framework. Second, hydrocarbon reservoirs in barrier and strandplain sandstone generally are among the least heterogeneous clastic reservoirs (Finley and others, 1988; Ambrose and others, 1991). Carter sandstone reservoirs, however, differ from those reservoirs used to establish heterogeneity ranking based on depositional environment. Indeed, delta-destructive strandplain deposits, such as the Carter sandstone, are largely undocumented in the literature.

In contrast to the widespread beach-barrier systems that are the basis of commonly used reservoir heterogeneity models (for example, Sharma and others, 1990a, b; Ambrose and others, 1991; Schatzinger and others, 1992), Carter reservoirs are composed of localized, clinoformal sandstone lenses. Moreover, Carter beach systems were muddier than beach systems used as the basis of these reservoir models. Thus, more detrital clay was present in the Carter at the time of deposition. The abundance of clay minerals further increased during burial diagenesis. It is the relatively unpredictable distribution of both detrital and authigenic clay within reservoir sandstone that renders spatial quantification of petrophysical properties in North Blowhorn Creek oil unit difficult. Problems encountered in prediction of petrophysical properties in North Blowhorn Creek oil unit are further compounded in other Black Warrior basin oil fields because available data are fewer and reservoir sandstone in these fields typically is muddier than that in the North Blowhorn Creek reservoir.

OVERVIEW OF BLACK WARRIOR BASIN OIL PRODUCTION

The search for oil and gas in the Black Warrior basin of Alabama began in the early 1900's (Masingill, 1991). In 1909, a test well drilled for coal in Fayette County encountered oil shows at a depth of less than 500 feet. By 1917, more than 40 wells had been drilled in the basin, primarily for gas, but it would take more than 60 years from the initial show before commercial quantities of oil were found. In 1970, the discovery of the East Detroit oil field in Carter sandstone at depths of 1,782 to 1,798 feet marked the first oil discovery in the Black Warrior basin of Alabama. As of 1990, 123 fields in Alabama produced conventional hydrocarbons and coal-bed methane in the basin (Masingill, 1991). By July 1992, the Black Warrior basin in Alabama had produced 9.2 million barrels of oil and 523.9 billion cubic feet of gas.

Of the hydrocarbon-producing fields in the Black Warrior basin of Alabama, 26 are designated as oil fields or oil units for production from 33 pools (table 7). However, some of the designated oil fields are no longer active. Currently, nine fields containing 11 oil pools have been abandoned (table 7). Oil fields in Alabama typically are developed on a 40- or 80-acre spacing and no requirement for the minimum distance between wells (table 7).

The 26 designated oil fields and units produced 7,478,179 barrels of oil as of July 1992. An additional 932,420 barrels were produced from gas fields and wells outside the 26 fields that are now abandoned. Seven Mississippian sandstone units produce oil in Alabama, including Carter, Coats, Chandler, Gilmer, Lewis, *Millerella*, and Sanders sandstones. Of these, Carter sandstone has produced more than 90 percent of the oil from the designated oil fields and units (figs. 4, 90). Eighteen of the 26 fields have produced oil from Carter sandstone (fig. 91), and North Blowhorn Creek oil unit has produced 5.1 million barrels, or approximately two-thirds of that oil (fig. 5). South Brush Creek oil unit is the only other field in the Black Warrior basin to have produced more than one million barrels of oil. Five Carter sandstone fields have been unitized for pressure maintenance and waterflood or gas injection. *Millerella* sandstone is the next most productive Mississippian reservoir in Alabama. *Millerella* (eight fields and units) and Lewis (three fields) sandstones are the next most productive Mississippian reservoirs in Alabama (fig. 92). Maximum production from *Millerella* and Lewis oil fields is in the range of two to three hundred thousand barrels of oil (fig. 93). Most *Millerella* production is from Blowhorn Creek and Mud Creek oil units, both of which are currently under waterflood. Mt. Zion oil field produces the most Lewis oil; no Lewis fields have been unitized.

The Mississippi part of the Black Warrior basin has 17 active oil fields that produced 1,110,747 barrels of oil, as of December 1991, from 29 Mississippian sandstone pools. Oil is produced in

Table 7.--Characteristics of oil fields in the Black Warrior basin of Alabama.

Field	Pool	Date field established	Required Spacing (acres)	Number of producing wells	Status	Unit shape	Distance from unit lines (in ft)	Distance between wells (in ft)
Beaver Creek	Carter	6/24/68	80	1	Producing	2 contiguos governmental 1/4 1/4 sections	330	no requirement
Binion Creek	Coats	4/25/85	40	0	P&A	contiguous	330	no requirement
Binion Creek	Lewis	4/25/85	40	0	P&A	contiguous	330	no requirement
Blakely Creek	Carter	7/30/82	40	1	Producing	contiguous	330	no requirement
Blowhorn Creek	Carter	9/07/79	80	0	P&A	contiguous	330	no requirement
Blowhorn Creek	Millerella	7/11/80	80, except in unitized area	6	Producing	contiguous	330 (prod. wells) 50 (inj. wells)	no requirement
Bluff	Upper Carter	7/03/84	80	4	Producing	contiguous	330	no requirement
Bluff	Lower Carter	12/19/85	80	1	Producing	contiguous	330	no requirement
Bluff	Gilmer	10/10/85	80	4	Producing	contiguous	330	no requirement
Bluff	Millerella	10/10/85	80	0	P&A	contiguous	330	no requirement
Cains Ridge	Millerella	12/16/86	80	1	Producing	contiguous	330	no requirement
Central Bluff	Millerella	8/16/84	40	0	P&A	contiguous	330	no requirement
Chicken Swamp Branch	Lewis	11/01/89	80	1	Producing	2 contiguous governmental 1/4 1/4 sections	330	no requirement
Coal Fire Creek	Carter	4/03/87	80	0	P&A	contiguous	330	no requirement
Cooper Creek	Millerella	4/23/86	40	1	Producing	contiguous	330	no requirement
East Detroit	Carter	12/18/70	40	3	Producing	governmental 1/4 1/4 section	330	660
Fairview	Carter	8/27/74	40, except in unitized area	13	Producing	governmental 1/4 1/4 section	330	no requirement
Henson Springs	Carter	10/29/75	40	0	P&A	governmental 1/4 1/4 section	660 with a 150 foot tolerance	no requirement
McCracken Mountain	Millerella	11/04/77	40	0	P&A	contiguous	330	660
Mt Zion	Lewis	12/18/87	80	3	Producing	2 contiguous governmental 1/4 1/4 sections	330	no requirement
Mud Creek	Millerella	9/11/87	unitized	2	Producing	contiguous	330	no requirement
North Blowhorn Creek	Carter	6/11/80	unitized	31	Producing	2 contiguous governmental 1/4 1/4 sections	330	no requirement
North Bluff	Millerella	7/03/84	80	0	P&A	contiguous	330	no requirement
North Fairview	Carter	9/06/83	40	3	Producing	contiguous	330	no requirement
Sand Springs	Carter	4/06/77	40	0	P&A	governmental 1/4 1/4 section	330	no requirement
South Brush Creek	Carter	6/26/85	unitized	12	Producing	2 contiguous governmental 1/4 1/4 sections	330	no requirement
Southeast Detroit	Carter	10/10/86	40	1	Producing	governmental 1/4 1/4 section	330	no requirement
Star	Chandler	4/11/84	40	0	P&A	contiguous	330	no requirement
Star	Carter	4/17/85	80	1	Producing	2 adjacent governmental 1/4 1/4 sections	330	no requirement
Wayside	Carter	5/23/85	unitized	13	Producing	contiguous	330	no requirement
West Brush Creek		9/11/87	80	2	Producing	2 adjacent governmental 1/4 1/4 sections	330	no requirement
Yellow Creek	Carter	12/20/84	80	1	Producing	2 adjacent governmental 1/4 1/4 sections	330	no requirement
Yellow Creek	Sanders	12/20/84	80	3	Producing	2 adjacent governmental 1/4 1/4 sections	330	no requirement

Mississippi from Mississippian Abernathy, Carter, Evans Lewis, Rea, and Sanders sandstones. Approximately 75 percent of oil production from the 17 Mississippi fields is from Lewis sandstone, and 58 percent of total production is from a single Lewis sandstone pool in Maple Branch field.

Standard well stimulation procedures in the Black Warrior basin of Alabama include acidization and hydraulic fracturing. Acidization is designed to remove blocking agents, such as drilling mud, calcium carbonate, and other material on the wellbore face and in the immediate vicinity of the wellbore. Acid treatments are designed to eliminate near wellbore damage prior to fracturing and to lower the pressure required to break down the formation during the fracturing process. Typical acid treatments use 500 to 2,000 gallons of 7.5 to 15 percent hydrochloric acid, containing corrosion inhibitors, iron sequestiant agents, clay stabilizers, and ball sealers. The solution is displaced into the formation using a 2 percent potassium chloride solution. After an appropriate period of time, the well is flowed to clean up the formation and remove spent acid. After the acid treatment, wells typically are hydraulically fractured through tubing, using a two-component water-based gel system. Fracture treatments are

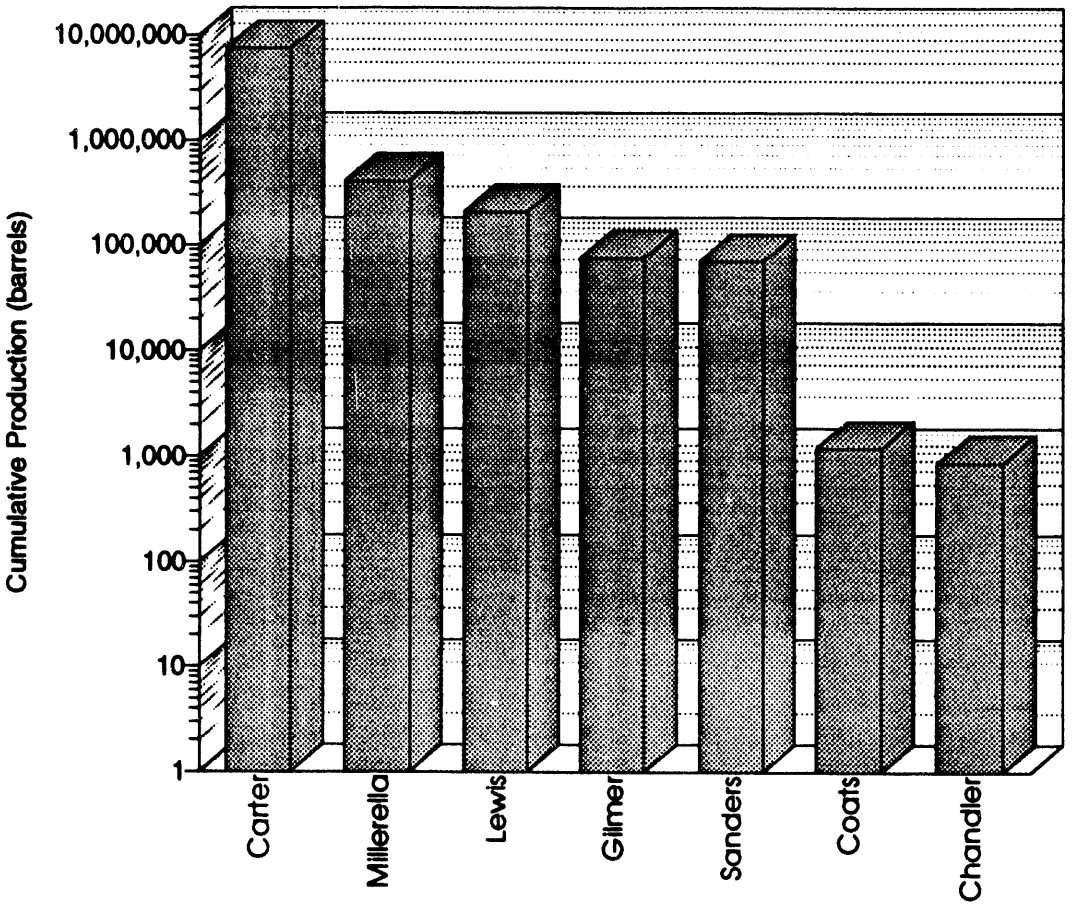

Figure 90.--Bar chart of cumulative oil production for reser oir units in the Black Warrior basin of Alabama, as of July 1992.

designed to initiate and propagate fractures that are approximately 300 feet in length with a width of 0.3 inch at the wellbore.

IMPROVED-RECOVERY PROJECTS IN THE BLACK WARRIOR BASIN OF ALABAMA

As of July 1992, seven oil fields producing from Carter or *Millerella* sandstone have been partially or completely unitized for the purpose of increasing the ultimate recovery of oil in the Black Warrior basin of Alabama (table 8). These unitized fields currently are under waterflood or a combination of waterflood and gas injection; no tertiary recovery projects are active in the Black Warrior basin of Alabama. However, a microbial enhanced recovery project is planned for the southern part of North Blowhorn Creek oil unit (Gulf Coast Oil World, 1992). The unitized oil fields in Alabama include Blowhorn Creek *Millerella* oil unit, Central Fairview Carter sand oil unit, Mud Creek oil unit, North Blowhorn Creek oil unit, South Fairview Carter sand oil unit, South Brush Creek oil unit, and Wayside oil unit. Five of these oil units produce from Carter sandstone, and two units produce from *Millerella sandstone*. The size of waterflood projects ranges from North Blowhorn Creek oil unit, with 30 production wells and 20 water injection wells, to Mud Creek oil unit with 2 production wells and 1 water injection well. Five-spot or peripheral waterflood patterns are used over the entire productive area in the largest units. Smaller units have too few wells for standard waterflood patterns. The location of water injection wells in these units is

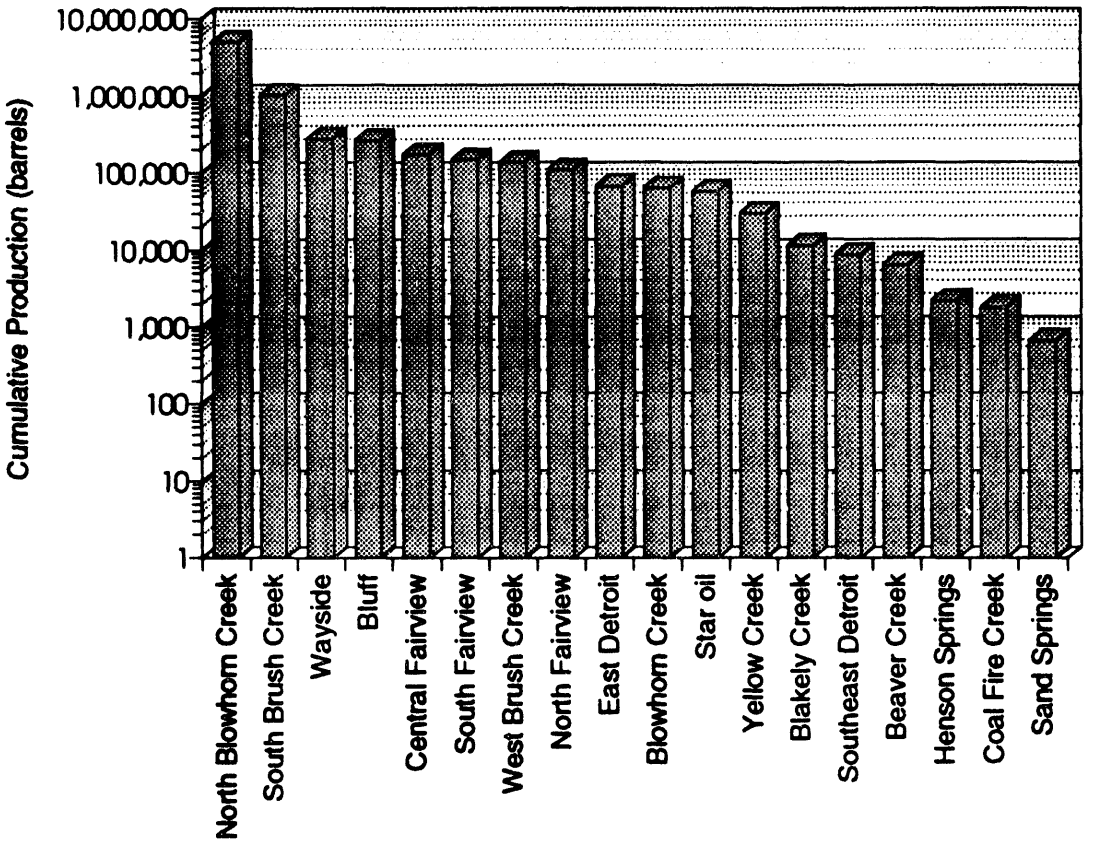

Figure 91.--Bar chart of cumulative oil production from Carter sandstone fields in the Black Warrior basin of Alabama, as of July 1992.

designed to enhance recovery from specific wells. Total oil production from these fields ranges from 64,151 to 5,100,000 barrels. Salient features of the seven unitized fields are discussed in this section. Production prior to and after unitization for each unitized field is shown in figure 94.

BLOWHORN CREEK *MILLERELLA* OIL UNIT

The Blowhorn Creek oil field was discovered in 1979 with the drilling of the Jones 26-3 no. 1 (PN2690) well by Pruet Production Co., Hughes & Hughes, and Warrior Drilling and Engineering Co. The discovery well was perforated in Carter sandstone from 2,473 to 2,488 feet and initially tested 168 barrels of 35.4° API oil and 135 Mcf of gas per day on a 48/64 inch choke with a flowing tubing pressure of 100 psig. A pressure-volume-temperature (PVT) study of a subsurface fluid sample from the discovery well shows that the reservoir fluid existed as a saturated liquid under original reservoir conditions of 1,192 psia and 90° F. Bubble point pressure for the reservoir was 1,335 psia. Additional reservoir data are in table 9. The trapping mechanism in Blowhorn Creek *Millerella* oil unit is stratigraphic due to pinchout of *Millerella* sandstone.

The field was developed on an 80-acre spacing and six production wells produced 202,445 barrels of oil and 693,435 Mcf of gas prior to unitization in May 1987. The drive mechanism for the reservoir is solution gas. Initially the gas-oil ratio was 1,000 SCF/Bbl, but the ratio increased to over 6,000 SCF/Bbl in 1982 as reservoir pressure declined. Reservoir pressure declined from the original 1,192 psia in 1979 to 138 psia in 1985. Oil production had reached a maximum of 8,000 barrels per month in September 1980 and declined rapidly to approximately 500 barrels of oil per month prior to

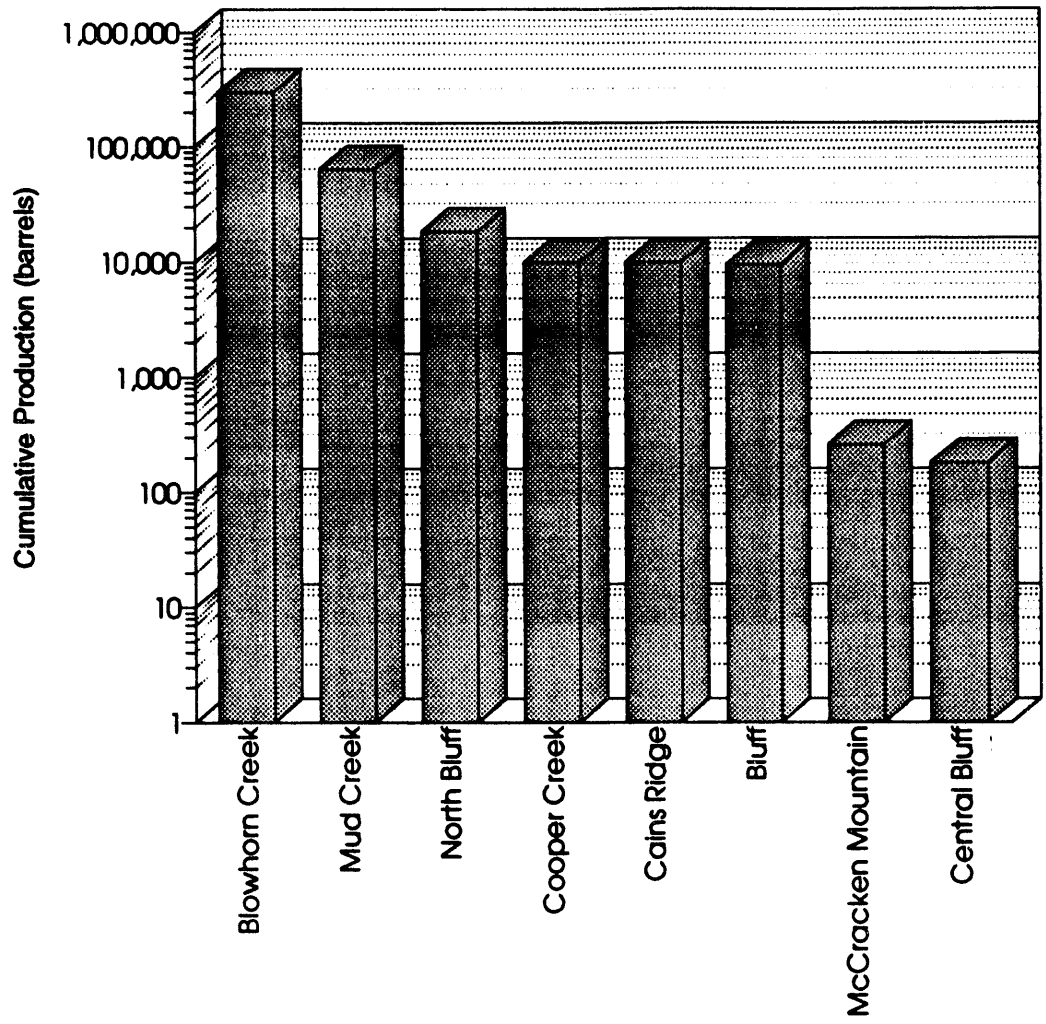

Figure 92.--Bar chart of cumulative oil production from *Millerella* sandstone fields in the Black Warrior basin of Alabama, as of July 1992.

unitization (fig. 95). A waterflood project was initiated after the field was unitized on May 1, 1987. Initially the unitized field consisted of three injection wells and 6 production wells. From March 1989 through August 1992 three additional water injection wells were completed. Water injection began in September 1987 and a total of 1,337,839 barrels of fresh water were injected through July 1992.

Of the present producing wells in the unit, the greatest amount of oil has been extracted through wells PN2690 and PN2933 prior to unitization (fig. 96). Well PN2878 (now plugged and abandoned), which is shown as productive in figure 96, produced from Carter, rather than *Millerella* sandstone; wells PN2937 and PN3081 penetrate *Millerella* limestone (fig. 43). The location of injection wells does not correspond to a standard waterflood pattern, but is designed to increase production from these two wells (fig. 96). Well PN10192 is a new water injection well that went online in August 1992 to increase production from well PN3098. Breakthrough of injection water has occurred only in well PN2690 (fig. 97). This breakthrough does not necessarily suggest channeling of fluids through high permeability zones because water has been injected into the reservoir from wells surrounding well PN2690 for a longer period of time than for well PN2933. The location of the two most productive wells does not correspond to areas with highest net pay thickness (fig. 98). Effective water

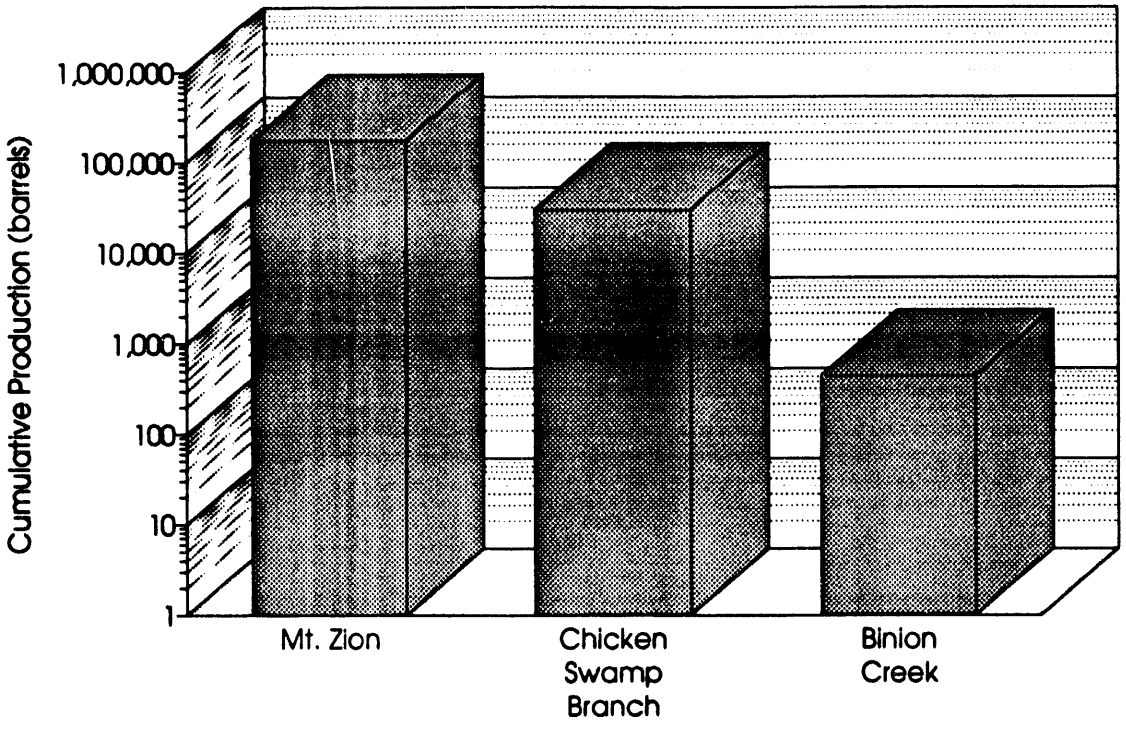

Figure 93.--Bar chart of cumulative oil production from Lewis sandstone fields in the Black Warrior basin of Alabama, as of July 1992.

saturation differs between the two wells (fig. 99), although log-derived effective porosity is similar (fig. 100). Average effective water saturation is lower and average effective porosity is higher in well PN2690. Log-derived effective porosity cross sections (figs. 101, 102) reveal that porosity generally is lower and water saturation is higher in Blowhorn Creek *Millerella* oil unit than in North Blowhorn Creek oil unit. However, the vertical distribution of porosity is more homogeneous. Sandstone distribution, petrophysical properties, and production patterns indicate that Blowhorn Creek *Millerella* oil unit should have fewer production problems related to thief zones and uncontacted or unconnected compartments than other units, such as South Brush Creek and Wayside oil units.

The productive area of the *Millerella* sandstone is approximately 436 acres. Original oil in place, volumetrically determined by the operator (Docket No. 4-2-879, State Oil and Gas Board of Alabama) is 2,448,425 stock tank barrels of oil, using a 9 percent porosity cutoff for pay, with estimated primary oil recovery of 220,358 stock tank barrels. The operator anticipates ultimate recovery from the waterflood to be 734,528 stock tank barrels. The effects of water injection were realized in June 1990 as oil production increased sharply (fig. 95). This increase in oil production also coincides with a significant increase in water production, indicating breakthrough. Cumulative production through July 1992 from the Blowhorn Creek *Millerella* oil unit is 301,866 stock tank barrels of oil and 819,293 Mcf of gas. Currently, the unit contains 4 producing wells, 6 water injection wells, and 2 plugged and abandoned wells.

CENTRAL AND SOUTH FAIRVIEW CARTER SAND OIL UNITS

Two parts of the Fairview oil field have been unitized as Central Fairview oil unit and South Fairview oil unit. The Fairview oil field was discovered in 1971 by Skelton Operating Co., Inc., with the drilling of the Vista Mae Gilmer No. 1 well (PN1968). An initial test for the discovery well produced 160 barrels of 22.8° API oil and 438 Mcf of gas per day on a 32/64-inch choke with a flowing

Table 8.--Characteristics of unitized oil fileds in the Black Warrior basin.

Field	Type Unitization	Effective Date of Unitization	Fluids Injected	Date of Injection	Number of Production wells	Number of Injection wells	Production prior to Unitization (BBLS)	Production after Unitization (BBLS)	Total Production (BBLS)
Blowhorn Creek Millerella oil unit	Partial	5/01/87	Fresh Water	9/87	10	6	202,445	85,261	287,706
Central Fairview oil unit	Partial	8/01/89	Fresh Water	6/90	6	3	163,091	6,172	169,263
Mud Creek Millerella oil unit	Fieldwide	2/02/90	Fresh Water	10/90	2	1	36,651	27,500	64,151
North Blowhorn Creek oil unit	Fieldwide	2/01/83	Fresh Water	8/83	31	19	601,036	4,510,118	5,111,154
South Brush Creek oil unit	Fieldwide	1/01/89	Fresh Water & Salt Water	4/89	12	10	621,387	416,359	1,037,746
South Fairview Carter oil unit	Partial	3/02/90	Fresh Water	10/90	5	1	126,849	24,236	151,085
Wayside oil unit	Partial	5/01/88	Fresh Water, Salt Water, & Casing Head Gas	5/88	18	9	144,371	138,579	282,950

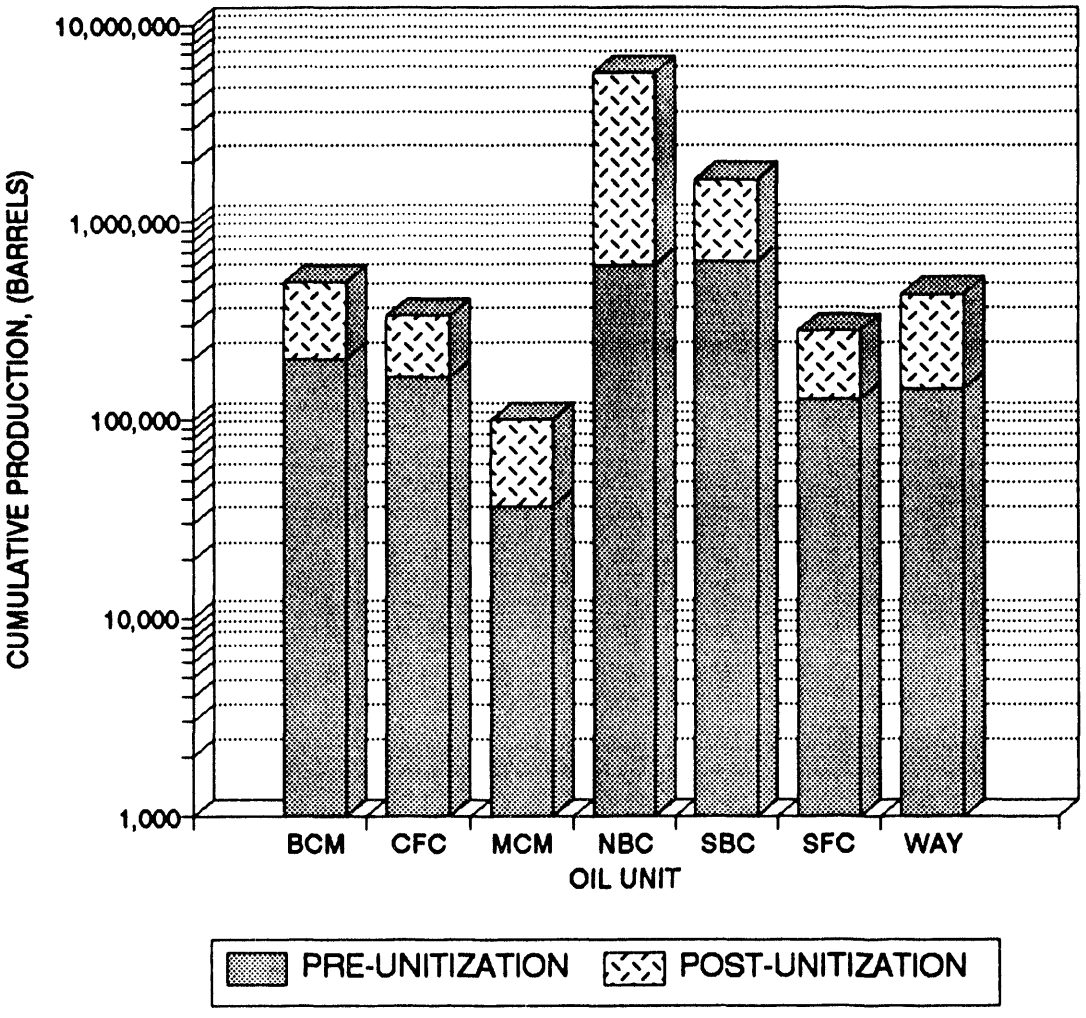

Figure 94.--Bar chart showing pre- and post-unitization oil production from unitized fields in the Black Warrior basin of Alabama, as of July 1992. BCM = Blowhorn Creek *Millerella* oil unit. CFC = Central Fairview Carter oil unit. MCM = Mud Creek *Millerella* oil unit. NBC = North Blowhorn Creek oil unit. SBC = South Brush Creek oil unit. SFC = South Fairview Carter oil unit. WAY = Wayside oil unit.

tubing pressure of 540 psig. Production was from Carter sandstone through perforations from 2,430 to 2,440 feet. As the field was developed, it became evident that two lobes of Carter sandstone exist within the oil field boundaries. By 1981, 15 wells had been drilled in Fairview oil field, 10 penetrating the northern lobe, and 5 penetrating the southern lobe. A pressure-volume-temperature study of a recombined sample of separator oil and gas indicated that fluid contained in the Carter sandstone in the northern lobe existed as a saturated liquid at the initial reservoir conditions of 1,113 psia and 84°F. A gas cap was thought to occur in the northern portion of this lobe and was subsequently verified by high gas-oil ratios for wells completed in that area. Additional fluid properties are listed in table 9. On August 1, 1989, the northern lobe was unitized and designated as the Central Fairview Carter Sand oil unit. Water injection began in June 1990. Three wells were converted to water injection wells and six wells remained as producers. The operator estimated original oil in place for the northern lobe to

Table 9.-- Reservoir fluid properties of select fields in the Black Warrior basin.

FIELD	INITIAL RESERVOIR PRESSURE (PSIA)	BUBBLE POINT PRESSURE (PSIA)	SOLUTION GAS-OIL RATIO (SCF/STB)	OIL GRAVITY API	INITIAL OIL VISCOSITY (cp)	OIL VISCOSITY @ Pb (cp)	FORMATION VOLUME FACTOR (Rbl/STB)
BLOWHORN CREEK "MILLERELLA" OIL UNIT	1192	1335	306	35.4	1.4		1.312
CENTRAL FAIRVIEW OIL UNIT	1113	1113	240	34	4.45	4.45	1.125
FAIRVIEW OIL FIELD	1113	1113	240	34	4.45	4.45	1.125
MT ZION	2010	1739	558	41.4	0.734	0.721	1.263
MUD CREEK OIL UNIT	1701	1701	585	41	0.84	0.84	1.292
NORTH BLOWHORN CREEK OIL UNIT	1190	1154	302	32.5	2.55	2.52	1.154
NORTH FAIRVIEW OIL FIELD	995	924	218	30	3	3	1.119
SOUTH BRUSH CREEK OIL UNIT	1164	1164	330	37	1.45	1.45	1.16
SOUTH FAIRVIEW OIL UNIT	N/A	N/A	N/A	N/A	N/A	N/A	N/A
WAYSIDE OIL UNIT	1020	1020	201	34	4.96	4.96	1.107
YELLOW CREEK "CARTER" SAND	N/A	N/A	N/A	N/A	N/A	N/A	N/A
YELLOW CREEK "SANDERS" SAND	1854	1854	N/A	41	N/A	N/A	1.241

N/A - Not available

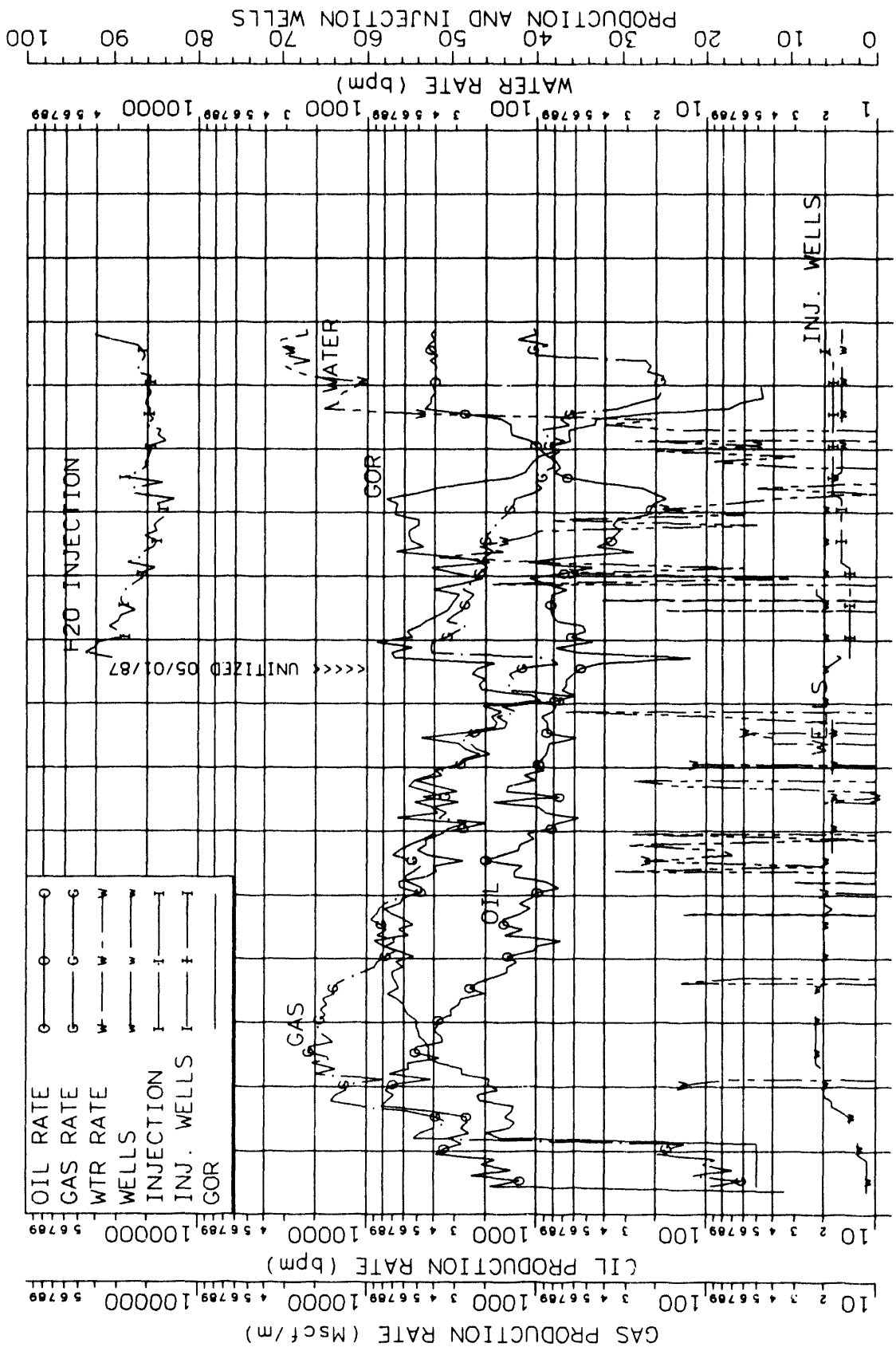

Figure 95.–Production plot for Blowhorn Creek *Millerella* oil unit.

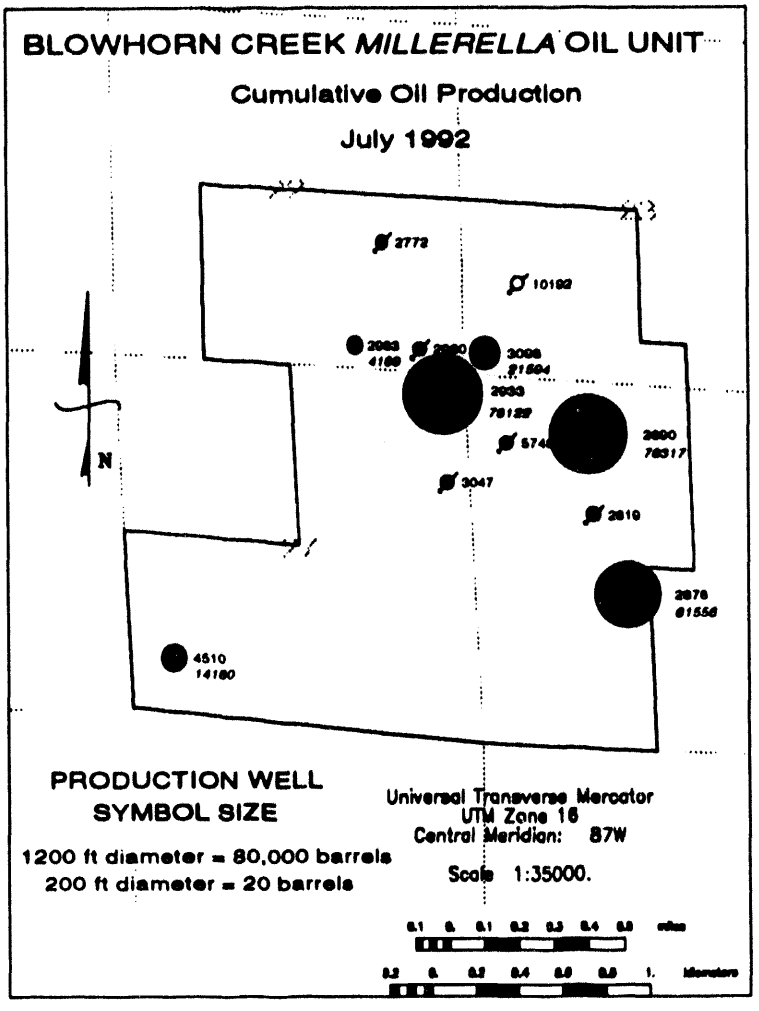

Figure 96.--Bubble map of cumulative oil production from Blowhorn Creek *Millerella* oil unit, as of July 1992. The size of well symbols are proportional to oil production. State Oil and Gas Board of Alabama permit numbers are adjacent to wells. The volume of oil produced is shown in italics adjacent to production wells.

be 1,612,795 stock tank barrels with estimated primary recovery of 162,369 stock tank barrels, using a 9 percent porosity cutoff for pay (Docket No. 12-15-889B, State Oil and Gas Board of Alabama). As of July 1992, 202,572 barrels of fresh water have been injected into the Central Fairview Carter Sand oil unit (fig. 103). Effects of waterflooding have not been realized to date, and results have been disappointing. Cumulative production through July 1992 was 175,685 barrels of oil and 364,384 Mcf of gas; only 6,172 barrels of oil and 22,224 Mcf of gas have been produced since unitization.

The southern lobe of Carter sandstone in the Fairview oil field was unitized on March 2, 1992, and designated as the South Fairview Carter Sand oil unit. Fresh water injection began in October 1990. This lobe is bisected by two east-west faults that trend perpendicularly to the strike of the reservoir. Effects of water injection were realized approximately seven months after initiation of the waterflood program, as indicated by a sharp increase in oil production and decrease in the gas-oil ratio during midyear 1992 (fig. 104). The productive area of the South Fairview Carter Sand oil unit is

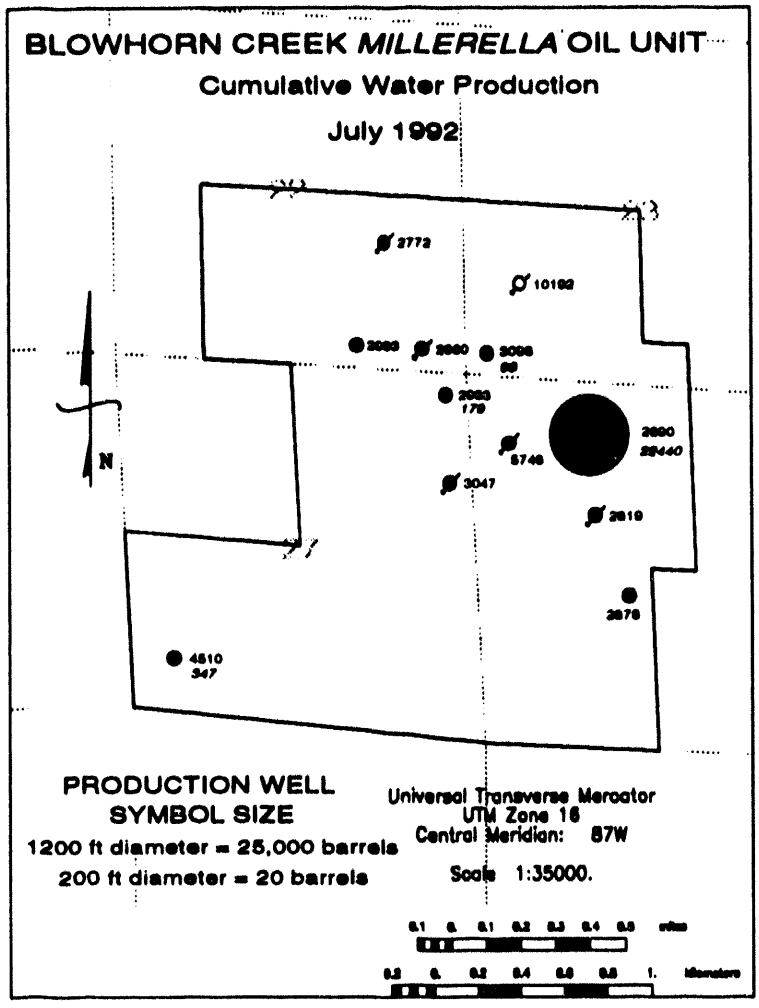

Figure 97.--Bubble map of cumulative water production from Blowhorn Creek *Millerella* oil unit, as of July 1992. The size of well symbols is proportional to water production. State Oil and Gas Board of Alabama permit numbers are adjacent to wells. The volume of water produced is shown in italics adjacent to production wells.

approximately 333 surface acres. Original oil in place, volumetrically calculated by the operator (Docket No. 12-15-897A, State Oil and Gas Board of Alabama) is 2,180,170 stock tank barrels, using a 9 percent porosity cutoff for pay. Estimated primary recovery is 156,992 stock tank barrels of oil and anticipated secondary recovery is 497,079 stock tank barrels. Cumulative production through July 1992 was 151,085 barrels of oil and 103,706 Mcf of gas; 24,236 barrels of oil, 15,192 Mcf of gas, and 44 barrels of water have been produced since unitization. As of July 1992, 167,177 barrels of water had been injected into the reservoir in South Fairview Carter Sand oil unit.

MUD CREEK *MILLERELLA* OIL UNIT

The Mud Creek oil unit was discovered by Anderman Smith Operating Company in 1987 with the drilling of the Thomas 6-7 well (PN5249). An initial test on the discovery well produced 195 barrels of oil and 169 Mcf of gas per day on a 12/64-inch choke with 600 psig flowing tubing pressure. Production was from the *Millerella* sandstone

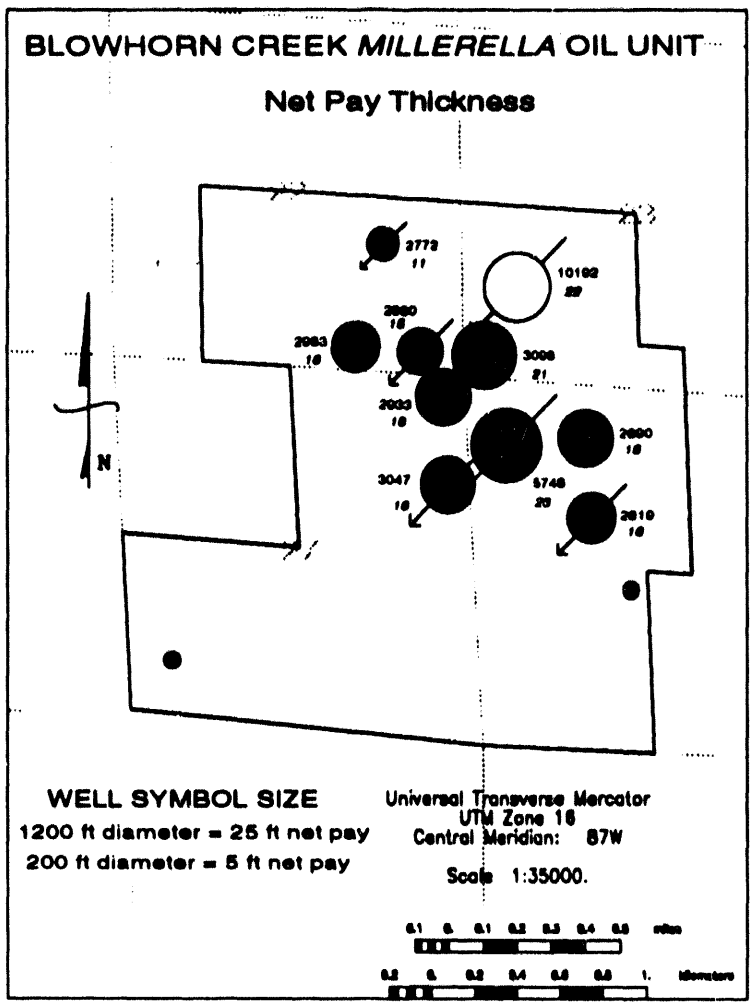

Figure 98.--Bubble map of net pay thickness for *Millerella* sandstone in Blowhorn Creek *Millerella* oil unit. The size of well symbols is proportional to net pay thickness. State Oil and Gas Board of Alabama permit numbers are adjacent to wells. The net pay thickness, rounded to the nearest integer, is shown in italics below the permit numbers.

through perforations from 4,185 to 4,196 feet. Initial reservoir pressure and temperature for the *Millerella* sandstone were 1,701 psia and 110° F, respectively. No pressure-volume-temperature study was performed, but bubble point pressure is expected to be the same as the discovery pressure. Additional reservoir fluid properties are in table 9. The drive mechanism for the reservoir is solution gas. An initial gas cap was suspected along the top of the sandstone in the Thomas 6-16 well (PN5323) because of a rapid increase in the gas-oil ratio in the well.

The field was developed on 80-acre units and two additional production wells were completed by February 1988. Reservoir pressure declined rapidly from 1,701 psia at the time of discovery of the field to 1,258 psia in July 1988. As a result, the field was unitized and a pressure maintenance program was initiated with a waterflood project. The Thomas 6-16 well (PN5323) was converted to a water injection well and injection began in October 1990 (fig. 105). As of July 1992, 72,782 barrels of water had been injected into the reservoir.

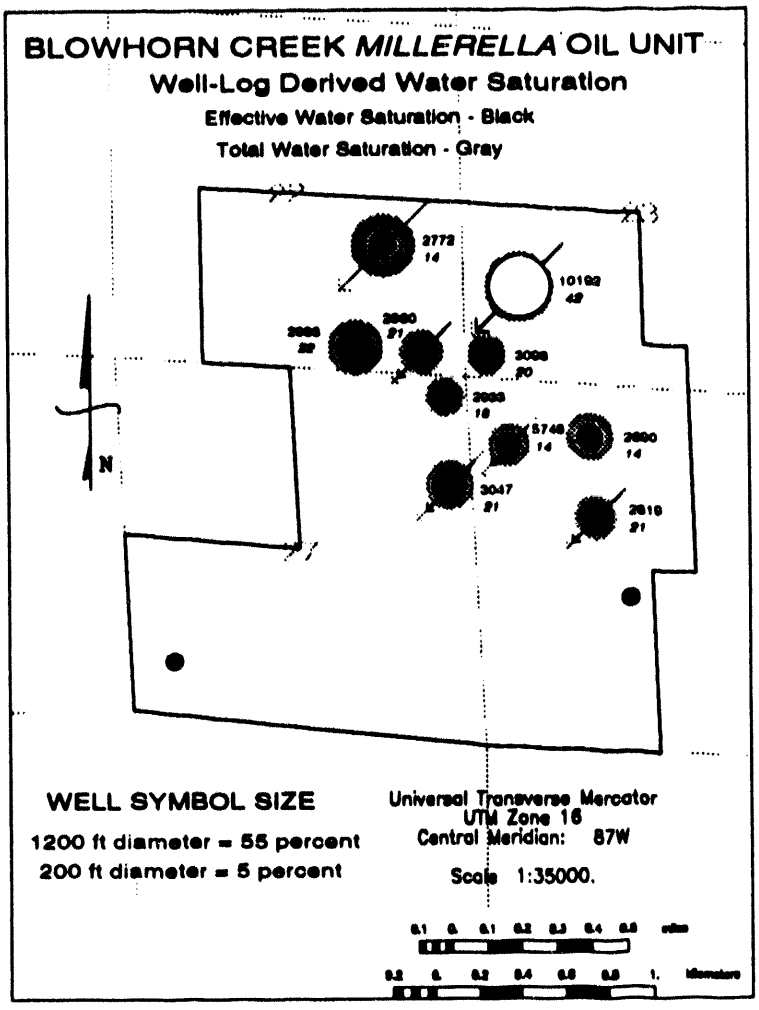

Figure 99.–Bubble map of effective and total water saturation in *Millerella* sandstone, Blowhorn Creek *Millerella* oil unit. The size of black well symbols is proportional to effective water saturation. The size of gray well symbols is proportional to total water saturation. State Oil and Gas Board of Alabama permit numbers are adjacent to wells. Effective water saturation, rounded to the nearest integer, is shown in italics below the permit numbers.

The productive area for the reservoir in the Mud Creek *Millerella* oil unit is estimated by the operator to be 226 acres. Volumetrically determined original oil in place, estimated by the operator, is 618,500 stock tank barrels, using a 9 percent porosity cutoff for pay (Docket No. 12-14-895, State Oil and Gas Board of Alabama). Estimated primary recovery is 30,925 stock tank barrels of oil and anticipated ultimate production is anticipated to be 129,885 stock tank barrels of oil. Cumulative production from Mud Creek oil unit through July 1992 is 64,151 barrels of oil and 197,849 Mcf of gas, and 3,790 barrels of water.

NORTH BLOWHORN CREEK OIL UNIT

North Blowhorn Creek oil unit was discovered by Warrior Drilling and Engineering Company, Inc. in 1979 with the drilling of the Gordon No. 11-5 well (PN2751), which initially flowed 342 barrels of 32.5° API oil and 1,090 Mcf of gas per day on a

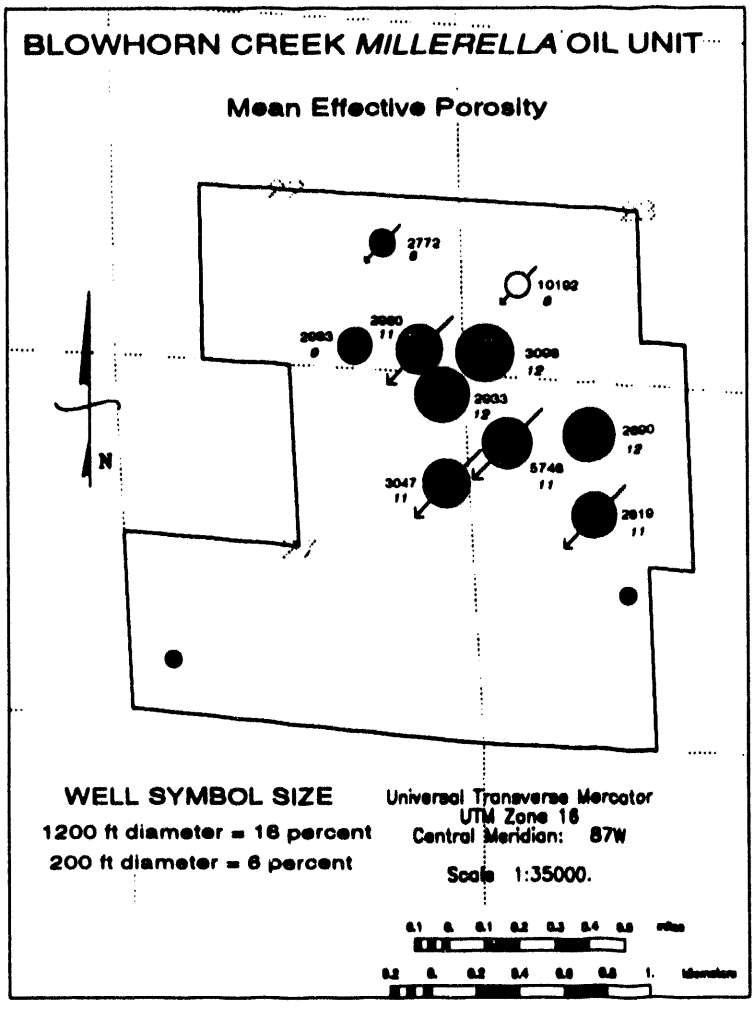

Figure 100.--Bubble map of effective porosity in *Millerella* sandstone, Blowhorn Creek *Millerella* oil unit. The size of well symbols is proportional to effective porosity. State Oil and Gas Board of Alabama permit numbers are adjacent to wells. Mean effective porosity, rounded to the nearest integer, is shown in italics below the permit numbers.

16/64-inch choke with a flowing tubing pressure of 740 psig. Carter sandstone production in this well was from perforations between 2,285 and 2,294 feet. Structural dip of the top of the Carter sandstone is 25 to 60 ft/mi. The Carter sandstone in North Blowhorn Creek oil unit is contiguous with the Carter reservoir in the adjacent Armstrong Branch gas field, to the northwest (Bearden, 1984, 1985; Epsman, 1987). The updip limit of the oil reservoir at North Blowhorn Creek oil unit is defined by the oil/gas contact at -1,724 feet. The updip limit of the Armstrong Branch gas field is defined by pinchout of porous Carter sandstone. Thus, the trapping mechanism for the combined North Blowhorn Creek oil unit/Armstrong Branch gas field is stratigraphic, defined by pinchout of Carter sandstone (Bearden, 1985).

Development of the field began shortly after completion of the discovery well. The field was developed on 80-acre units. The original fluid in the North Blowhorn Creek oil unit reservoir was a saturated oil with an original bubble point pressure of 1,115 psia. The primary drive mechanism for the reservoir was solution gas. Additional reservoir

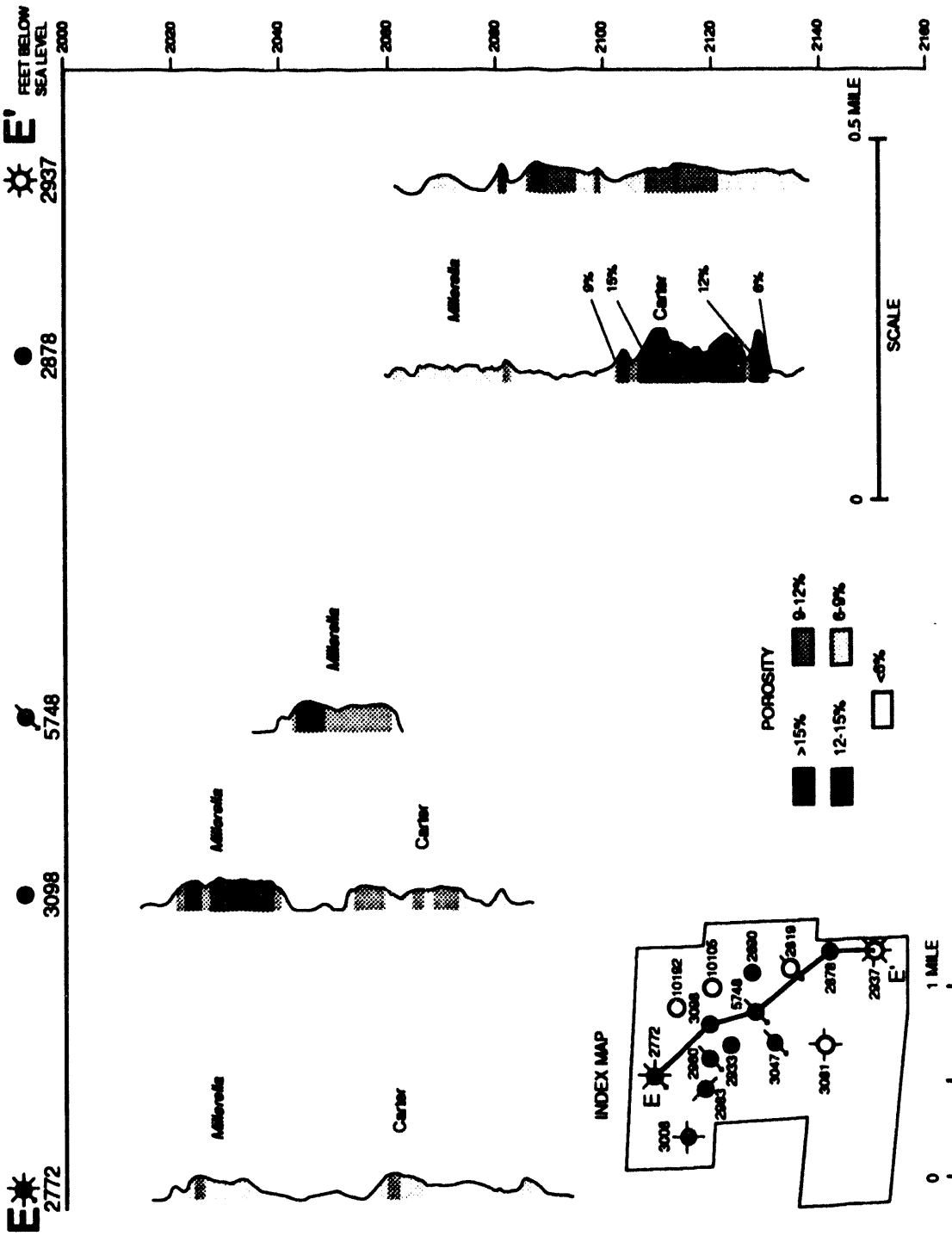

Figure 101.--Structural cross-section E-E' of effective porosity profiles, Carter sandstone, Blowhorn Creek *Millerella* oil unit.

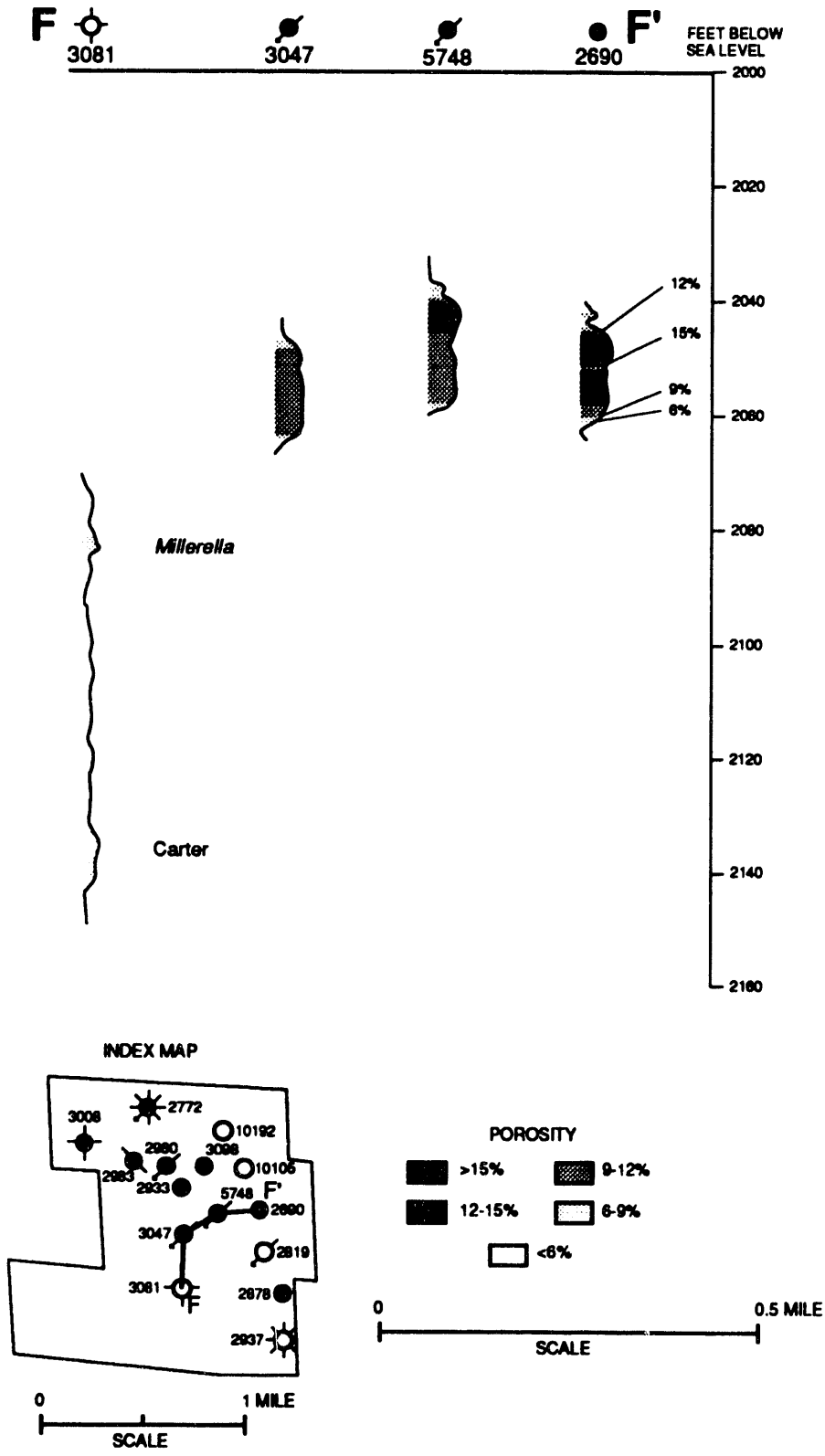

Figure 102.--Structural cross-section F-F' of effective porosity profiles, Carter sandstone, Blowhorn Creek *Millerella* oil unit.

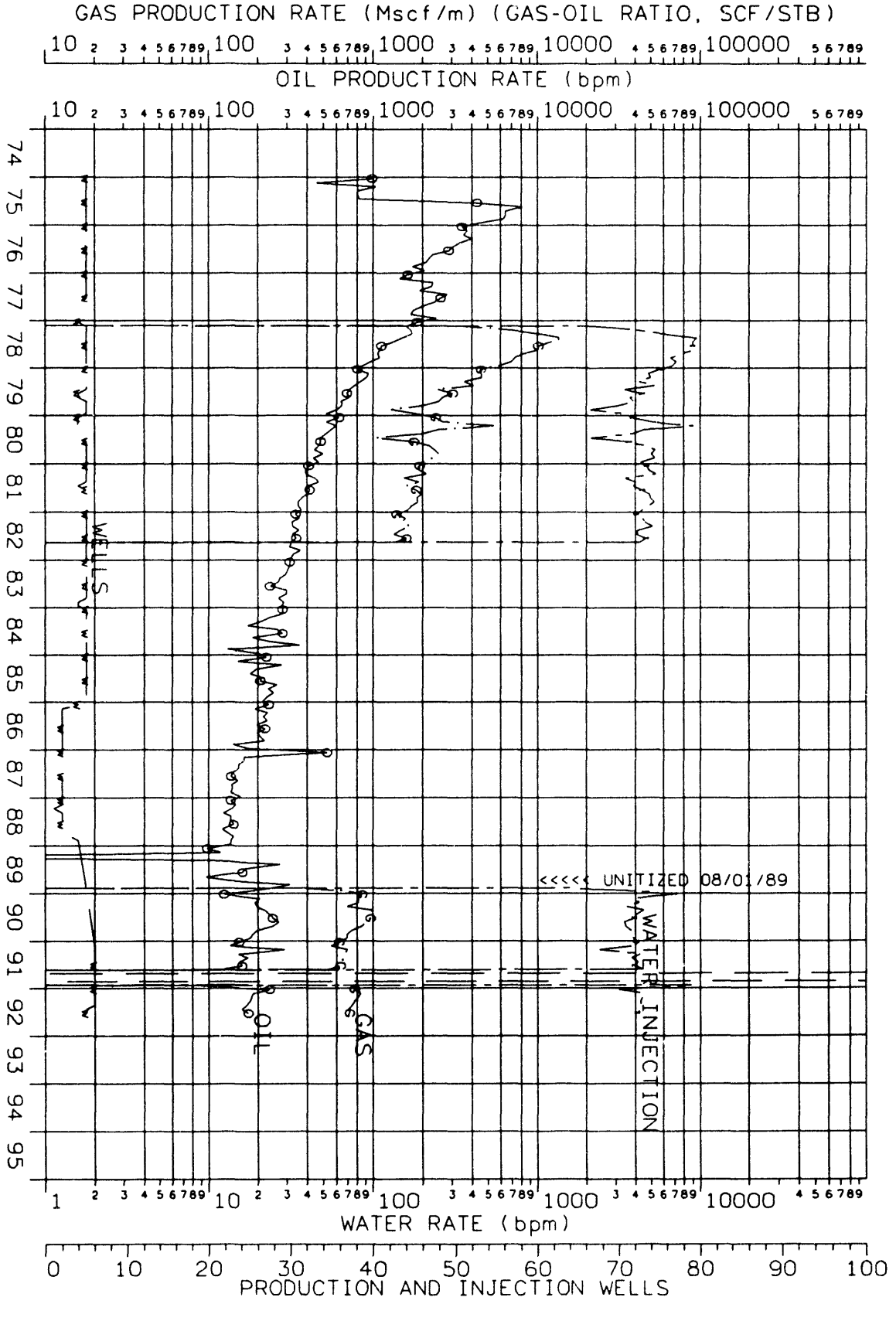

Figure 103.--Production plot for Central Fairview Carter sand oil unit.

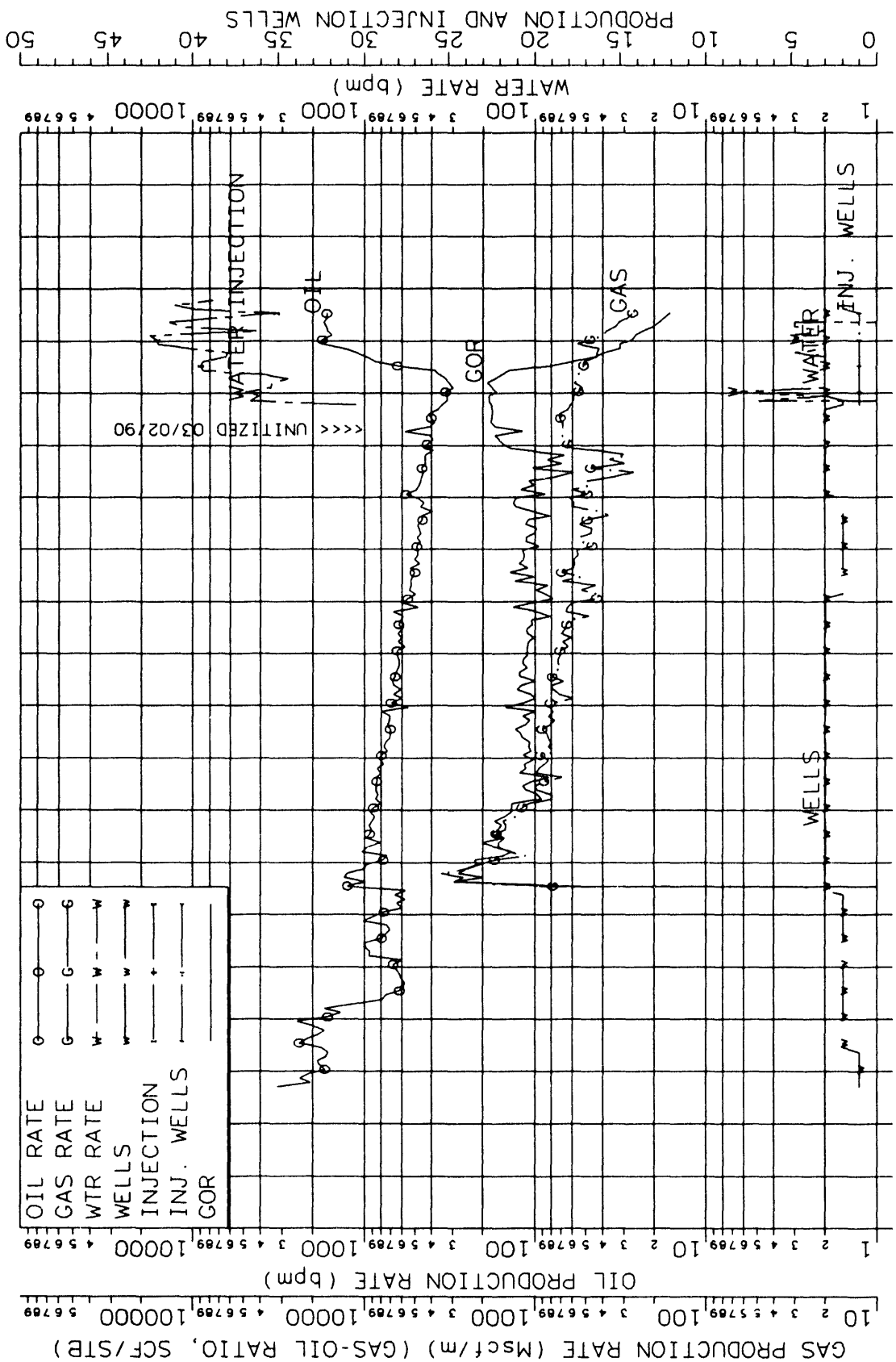

Figure 104.--Production plot for South Fairview Carter sand oil unit.

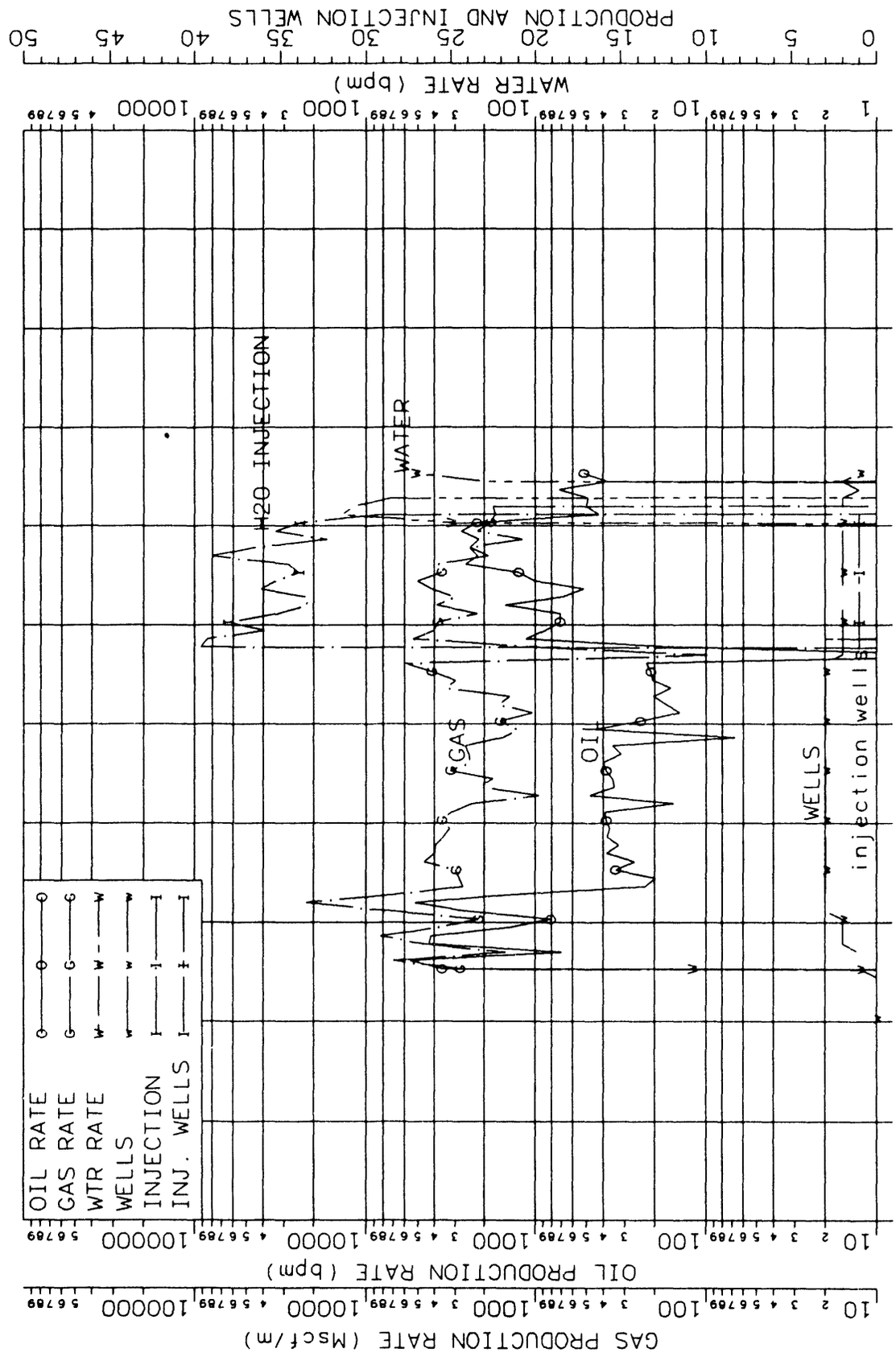

Figure 105.--Production plot for Mud Creek *Millerella* oil unit.

fluid properties are listed in table 9. As reservoir pressure declined, sucker rod pumping equipment was installed on wells. Production prior to unitization and waterflood totaled 601,007 barrels of oil, 888 MMcf of gas, and 887 barrels of water.

North Blowhorn Creek oil field was unitized on February 1, 1983, and waterflood operations were initiated. Wells PN3350 and PN3437, in the northern part of the unit, were converted to water injection wells in June 1983 and used for a pilot injectivity test to verify compatibility of injection water with formation fluids. These wells were also used to form a water block to prevent migration of gas and oil between the adjacent Armstrong Branch gas field and North Blowhorn Creek oil unit. Water injection began in the rest of the unit in November 1983. Well PN3501 was converted to a water injection well in September 1992. Injection water is supplied by two fresh water source wells completed in the Pottsville Formation. The original 80-acre development of the field facilitated conversion of existing production wells to injection wells and limited the necessity of additional infill wells. A 5-spot pattern was used to flood the unit. An increase in oil production and a decrease in the gas-oil ratio due to water injection occurred approximately six months after initiation of injection (fig. 106). The peak oil production rate of 86,341 barrels of oil per month occurred in 1985, two and one-half years after the waterflood began. Although production from wells in North Blowhorn Creek oil unit began at approximately the same time and injection was initiated within a five-month period, per well cumulative production differs significantly throughout the unit (fig. 107). The most productive wells are in the northern half of the unit. Well PN3782 has produced the most oil, 39,2759 barrels of oil as of September 1992. This pattern of production closely corresponds to sandstone distribution patterns defined in the depositional model and also correlates well with the distribution of parameters derived from well-log analysis. Production is consistently the highest where Carter sandstone lenses are amalgamated. Although productive wells are present in the southern part of the unit, where spit arms segment, the distribution of the most productive wells is scattered relative to that in the northern part. Wells along the southwestern margin of the unit are less productive, particularly well PN3385. Backshore deposits and the distal ends of spit arms are prevalent in this area.

More water has been injected into the Carter reservoir in the southern part of the unit during waterflood operations than in the northern part (fig. 108). Further, more water has been produced in the southern part of the unit (fig. 109). Only small amounts of water were produced prior to unitization, although water-production records are incomplete for this time. Thus, water production shown in figure 109 represents injection water produced after breakthrough. By January 1986, breakthrough had occurred in four wells in the northern part of the unit and eight wells in the southern part. Well PN3314 has produced the most water in the northern part of the field (fig. 108). Data presented elsewhere show that the upper part of the Carter reservoir in well PN3314 has permeability an order of magnitude or more higher than that in the lower part of the reservoir. This higher permeability occurs in foreshore sandstone lenses that parallel the strike of the reservoir body. Thus, a high-permeability conduit may exist between well PN3314 and adjacent injection wells along the reservoir axis. The existence of this conduit is supported by petrophysical evidence. This could result in lowering sweep efficiency of the waterflood in the lower, less permeable zone, resulting in bypass of some producible oil.

Reasons for the pattern of water production in the southern part of the unit are less apparent than those for well PN3314 because cores were not extracted from wells in appropriate locations. However, sweep efficiency of the waterflood likely is lower in this part of the unit because of fractures and channeling through high permeability zones. Well PN2980 was the first well to produce water as a result of breakthrough of injection water, and breakthrough generally occurred earlier, with larger quantities of produced water, in the southern part of the unit. Well PN2980 has produced an anomalously large amount of water compared to other wells in its vicinity. This implies that water injected in surrounding wells may have been captured by and channeled through a natural fracture network. If this is the case, producible oil would be bypassed in the vicinity of well PN2980. Channeling of injected water likely also occurred between other injection and production wells in the southern part of the unit. However, this fluid channeling may be related more to permeability contrasts within the reservoir sandstone, related to depositional processes and diagenesis, than to fractures. Thus, the pattern of oil production and water injection and production indicates a higher degree of heterogeneity in the Carter reservoir in the southern part of North Blowhorn Creek oil unit. The injection radius for cumulative water injection through December 1992 emphasizes the degree of reservoir heterogeneity and

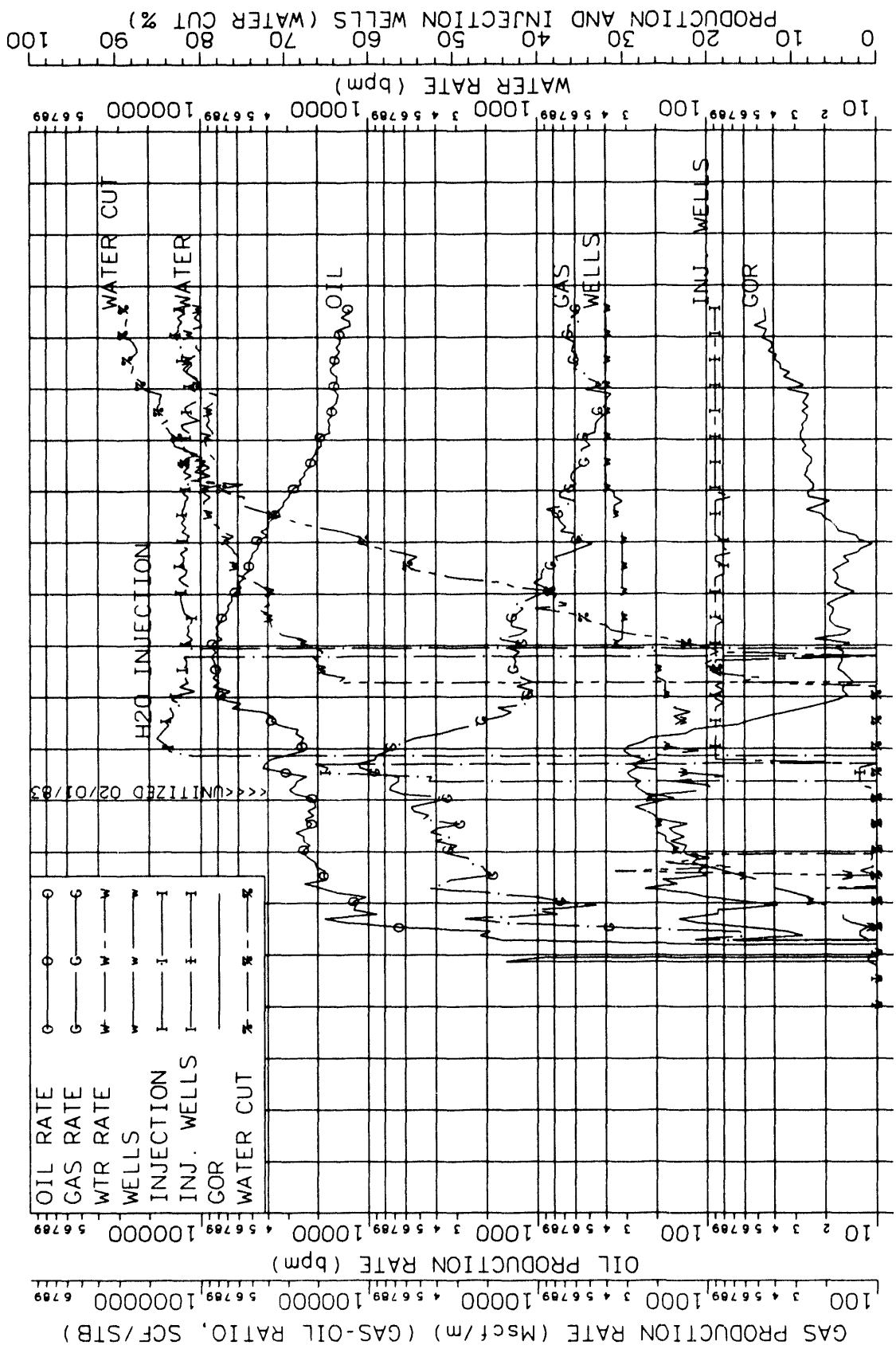

Figure 106.--Production plot for North Blowhorn Creek oil unit.

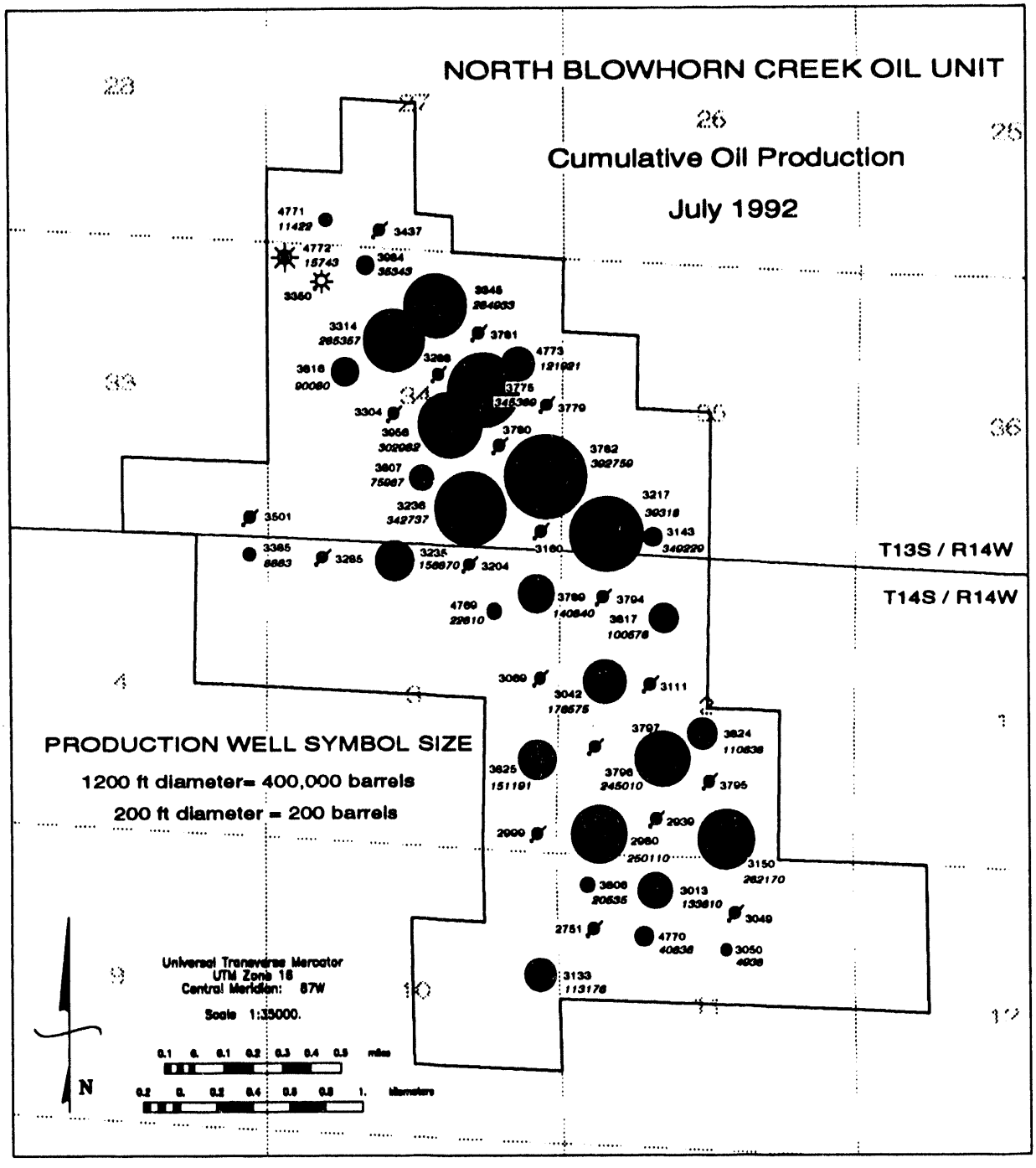

Figure 107.--Bubble map of cumulative oil production from Carter sandstone in North Blowhorn Creek oil unit, as of July 1992. The size of well symbols is proportional to oil production. State Oil and Gas Board of Alabama permit numbers are adjacent to all wells. The volume of oil produced is shown in italics adjacent to production wells.

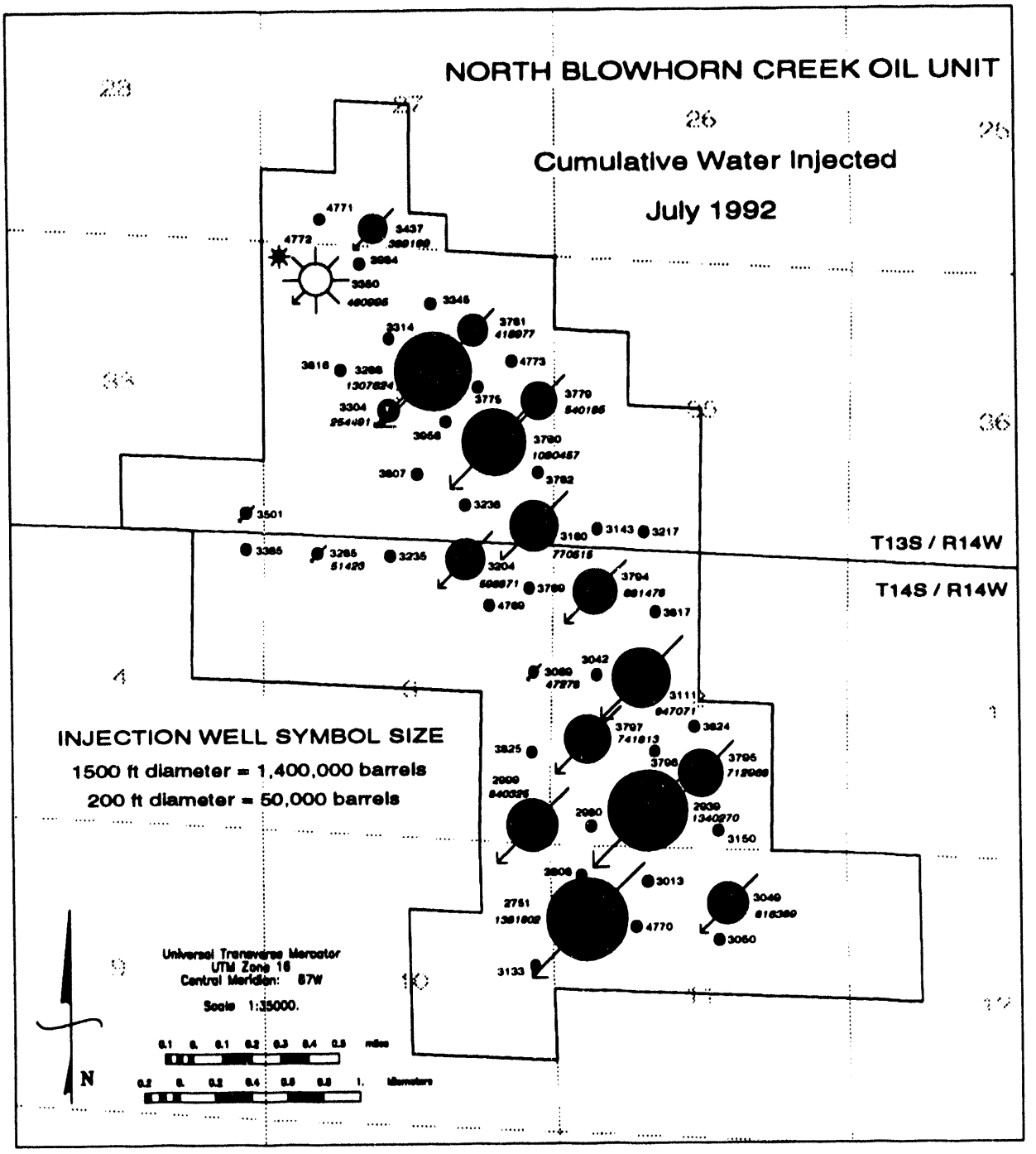

Figure 108.--Bubble map showing cumulative volume of water injected into the Carter sandstone reservoir in North Blowhorn Creek oil unit, as of July 1992. The size of well symbols is proportional to the amount of water injected. State Oil and Gas Board of Alabama permit numbers are adjacent to all wells. The volume of water injected is shown in italics adjacent to injection wells.

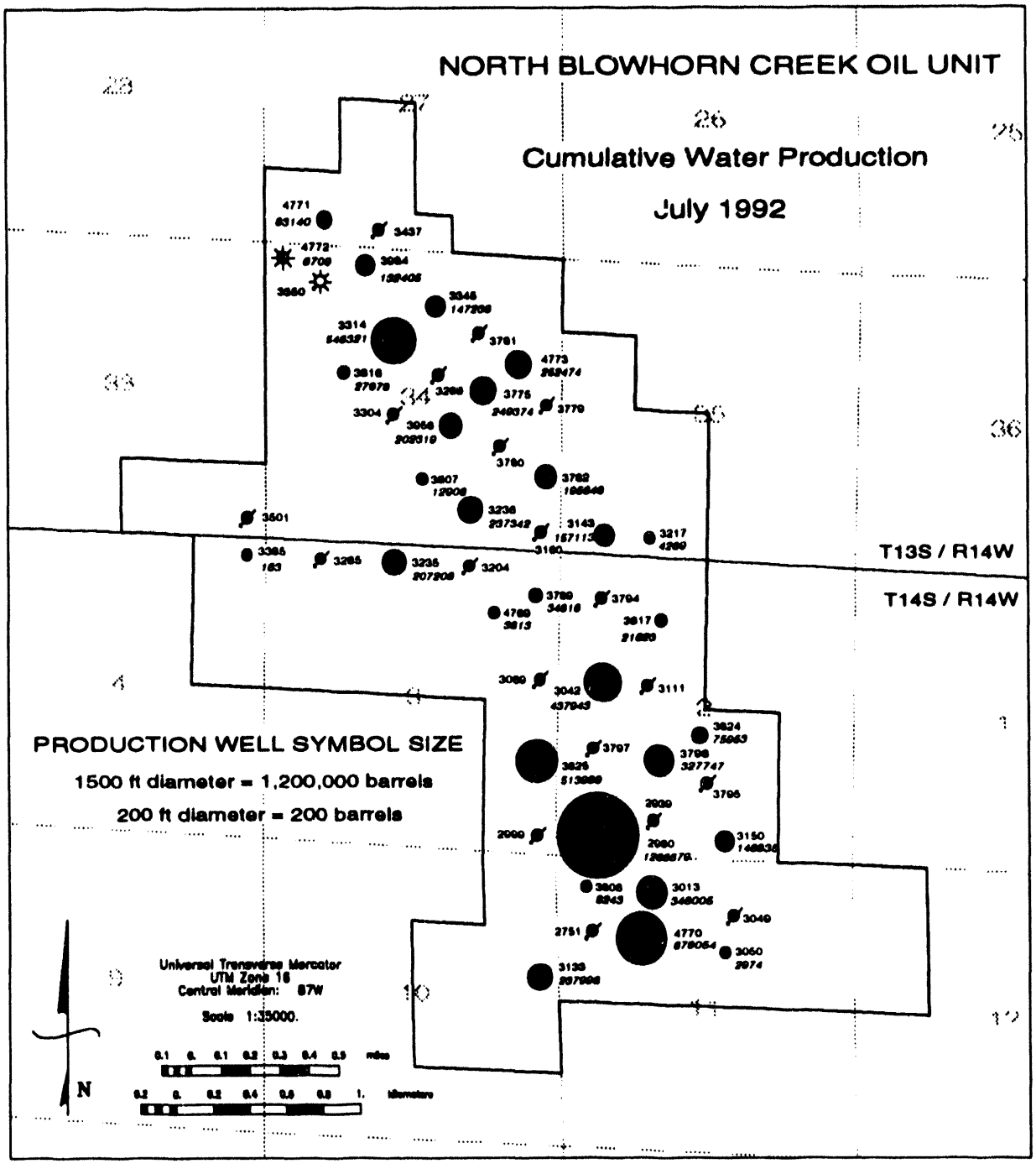

Figure 109.--Bubble map of cumulative water production in North Blowhorn Creek oil unit, as of July 1992. The size of well symbols is proportional to water production. State Oil and Gas Board of Alabama permit numbers are adjacent to all wells. The volume of water produced is shown in italics adjacent to production wells.

fluid channeling (fig. 110). Radii shown in figure 110 were calculated assuming a homogeneous reservoir with 100 percent sweep efficiency. Based on these simple assumptions, the map indicates that only a few wells should have achieved breakthrough or are close to breakthrough. This, of course, differs from actual injected water production patterns (fig. 109).

One notable aspect of development of North Blowhorn Creek oil unit is that the same five-spot pattern of injectors and producers was used throughout the unit. In effect, the pattern consists of alternating rows of injectors and producers. This pattern appears suitable for the northern part of the field where the axis of amalgamated sandstone lenses coincides with the strike of the reservoir sandstone body. However, in the southern part of the field, diverse orientation of sandstone lenses occurs as the spit arms segment and curve toward the southwest. Thus, in this part of the unit, the orientation of zones of maximum permeability likely varies considerably. Parts of the sandstone lenses are continuations, along the same strike, of those in the northern part of the unit (see fig. 52). However, the distal ends of the spit arms are oriented oblique or perpendicular to this strike. The pattern of injectors in this part of the unit may be less appropriate than that in the northern part. Infill wells, adjustment of the configuration of existing producers and injectors, or enhanced recovery techniques may provide a more suitable pattern for increasing production or for contacting bypassed oil in the southern part of North Blowhorn Creek oil unit.

As of July 1992, 5,111,154 barrels of oil and 2,893,093 Mcf of gas had been produced from the Carter reservoir in North Blowhorn Creek oil unit. This accounts for approximately two-thirds of all oil produced from fields in the Black Warrior basin of Alabama examined in this investigation. Oil production for the entire unit decreased in mid-1986 as a result of breakthrough of injection water (fig. 106). Production increased slightly at the beginning of 1991 (fig. 106) owing to installation of new pumping equipment and pigging of production lines.

As of July 1992, 13,190,929 barrels of water have been injected into the Carter reservoir, and 0.34 barrels of oil have been produced for each barrel of oil injected. Original oil in place, calculated by the operator (Docket No. 1-20-8340, State Oil and Gas Board of Alabama). was determined to be 15,683,528 stock tank barrels of oil. The operator estimated primary recovery to be 9 percent and the anticipated ultimate recovery under secondary recovery to be 30 percent of original oil in place. Using the operator's estimate of original oil in place, the unit has produced 32.5 percent of that value to date.

Original oil in place in North Blowhorn Creek oil unit, calculated for this investigation, differs significantly from that determined in the past. Values determined in this study are nearly one and one-half times as high (21.6 million reservoir barrels) as those previously reported in dockets on file with the State Oil and Gas Board of Alabama. There are several reasons for this difference. Calculations in the past have assumed a higher porosity cutoff of 9 percent for North Blowhorn Creek oil unit, as well as for the other units examined in this investigation. A 6 percent cutoff was used in this investigation. This lower value was chosen because it is believed that this porosity more appropriately reflects the pore volume containing extractable oil in Black Warrior basin fields. Additionally, some past calculations used porosity and water saturation values determined from only one "representative" well in each field. Values from this one well were then generalized over the entire area planimetered on net pay maps. In this investigation, data for all wells in each field were utilized. Further, oil saturation was determined from well-log derived effective water saturation, using a dual-water model, rather than the Archie equation. This was done because petrographic and petrophysical data collected in this investigation indicate that microporosity in detrital and authigenic clay is an important component of total porosity in the reservoirs. The effect of using effective water saturation, rather than total (or Archie) water saturation, is to increase the estimate of the volume of the effective pore system occupied by oil by subtracting out the water that is bound in micropores between clay particles.

Currently, a feasibility study is being performed to determine the effectiveness of a microbial flood in the North Blowhorn Creek oil unit (Gulf Coast Oil World, 1992). The purpose of this project is to use microbes to plug the most porous zones in the reservoir in an effort to extract bypassed oil from less porous and permeable horizons. The project uses inorganic nutrient sources to stimulate microbes, rather than standard sources such as molasses. A pilot project will be performed in the southern end of the reservoir to monitor success before applying the method fieldwide. If the pilot project is successful, future plans call for drilling two infill well, potentially resulting in recovery of an additional 9 percent of the original oil in place.

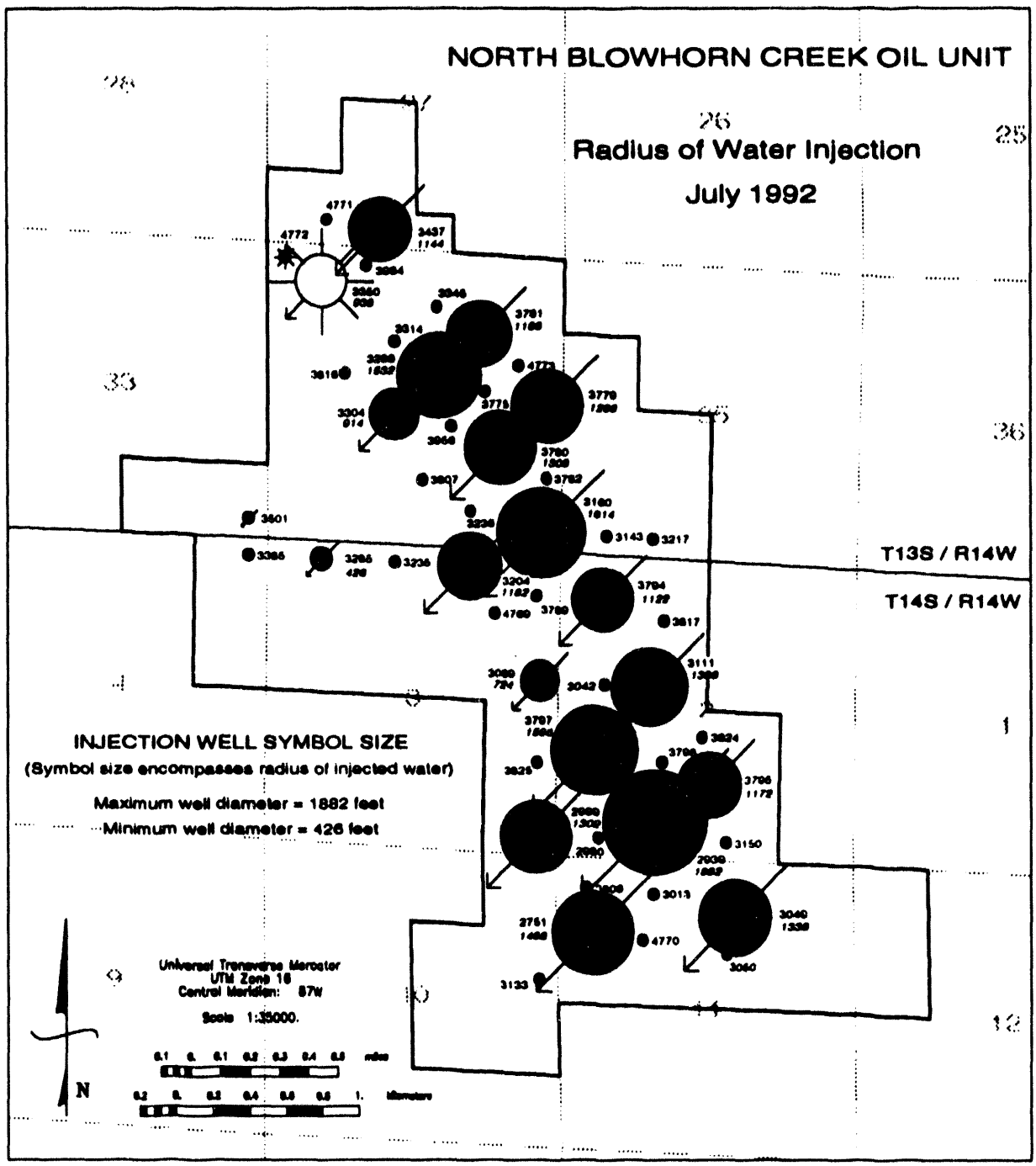

Figure 110.--Bubble map showing water injection radius in North Blowhorn Creek oil unit, as of July 1992. The size of well symbols is proportional to injection radius. State Oil and Gas Board of Alabama permit numbers are adjacent to all wells. The diameter of water injection is shown in italics adjacent to injection wells.

SOUTH BRUSH CREEK OIL UNIT

The South Brush Creek oil unit was discovered in 1984 with the drilling of the Weyerhaeuser 33-3 no. 1 (PN4322) well by Alagasco Energy Co., Inc. Initial test for the discovery well produced 422 barrels of 37° API oil and 235 Mcf of gas per day on an open choke with a flowing tubing pressure of 250 psig. Production was from Carter sandstone through perforations from 2,600 to 2,623 feet. The field was developed on 80-acre units and 14 wells produced 621,287 barrels of oil, 1,167 MMcf of gas and 5,740 barrels of water prior to unitization. The primary drive mechanism in the reservoir is solution gas, and fluid contained in the reservoir existed as saturated oil with a bubble-point pressure equal to the original reservoir pressure of 1,164 psia. Additional reservoir fluid properties for South Brush Creek oil unit are listed in Table 9. The trapping mechanism in South Brush Creek oil unit is a combination stratigraphic-structural trap, resulting from updip pinchout of porous and permeable Carter sandstone across an anticlinal nose (Moore and Kugler, 1990).

Reservoir pressure declined rapidly after production began. As a result, the field was unitized on January 1, 1989 in order to initiate a waterflood program. Development plans called for a 5-spot waterflood pattern that required drilling of three production wells and three injection wells and the conversion of seven existing production wells to water injection. This was completed in March 1990. An increase in oil production occurred approximately 18 months after initiation of water injection (fig. 111). A peak oil production rate of 22,831 barrels of oil per month occurred in January 1992, two years after water injection began. The most productive well in South Brush Creek oil unit is well PN4322, in the northwestern part of the unit. Cumulative oil production decreases toward the southeast corner of the unit (fig. 112). Breakthrough of injection water has occurred in three wells, PN4322, PN4802, and PN7055 (fig. 113). Part of the reason for lower production and the lack of breakthrough in the southeastern part of the field is due to the placement of injection wells. The distribution of cumulative oil production in South Brush Creek oil unit does not correlate well with net pay thickness (fig. 114). For example, net pay is close to maximum values in well PN4884, which has been much less productive than well PN4322. Well PN4322 has a smaller net pay thickness. Therefore, other factors influence production. Well PN4322 has among the highest effective porosity and lowest effective water saturation in the unit (figs. 115, 116). Effective water saturation generally is higher in the southeastern part of the unit. Although total water saturation is relatively high throughout the reservoir, effective water saturation varies substantially (fig. 116). This suggests that microporosity and irreducible water saturation in detrital and authigenic clay exert greater control on production patterns in South Brush Creek oil unit than in North Blowhorn Creek oil unit.

Cross sections of log-derived effective porosity (figs. 117, 118) also show the general decrease in porosity from the northwest corner of the unit toward the south and southeast. The highest porosity typically occurs near the top of the reservoir sandstone, but there are several exceptions where thin, high porosity zones occur in the middle of the reservoir and lower porosity occurs near the top, including wells PN4682 and PN7056 (fig. 117). The depositional model, presented elsewhere in this report, shows that upper high porosity zone in these wells has been removed by erosion. This difference in the stratigraphic position of high porosity, and presumably high permeability, zones in adjacent production and injection wells affects the efficiency of the waterflood. For example, well PN6275 has the thickest interval of high porosity of the wells along the lines of cross section (fig. 117). Prior to and within the first year of waterflood, oil production from this well was the highest in the unit (fig. 119). However, production did not increase substantially after waterflooding began, relative to other wells in the unit. This low cumulative production is due, in part, to the shorter period of time this well has been producing compared to surrounding wells. However, one of the adjacent water injection wells, PN4682, provides further clues to the reason for lower production. This well has low porosity throughout the section with nonreservoir rock segmenting the reservoir (fig. 113). The highest porosity in this well is near the middle of the section, not near the top. Thus, water from the injection well may not flow through permeable intervals in contact with the high porosity zone in PN6275. The lack of breakthrough of injection water in well PN6275 further indicates that the upper, high porosity zone is unconnected with well PN4682. In contrast, well PN7056 has been producing for a shorter period of time than well PN6275, but has been more productive because the middle porosity zone is connected.

The productive area, as defined by the operator, is 597 surface acres. The operator estimated volumetrically calculated original oil in place to be 7,555,555 stock tank barrels, using a 9 percent

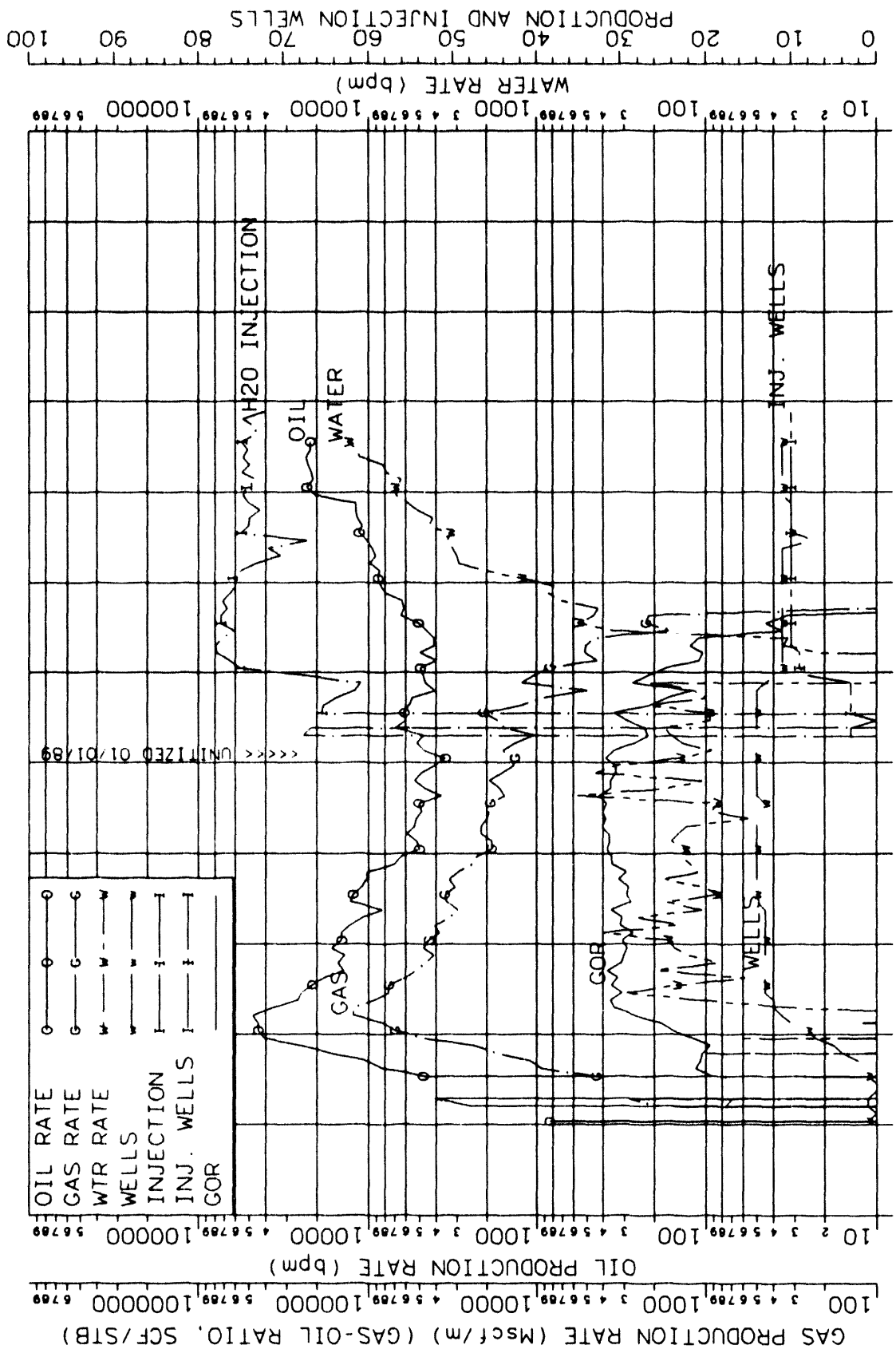

Figure 111.--Production plot for South Brush Creek oil unit.

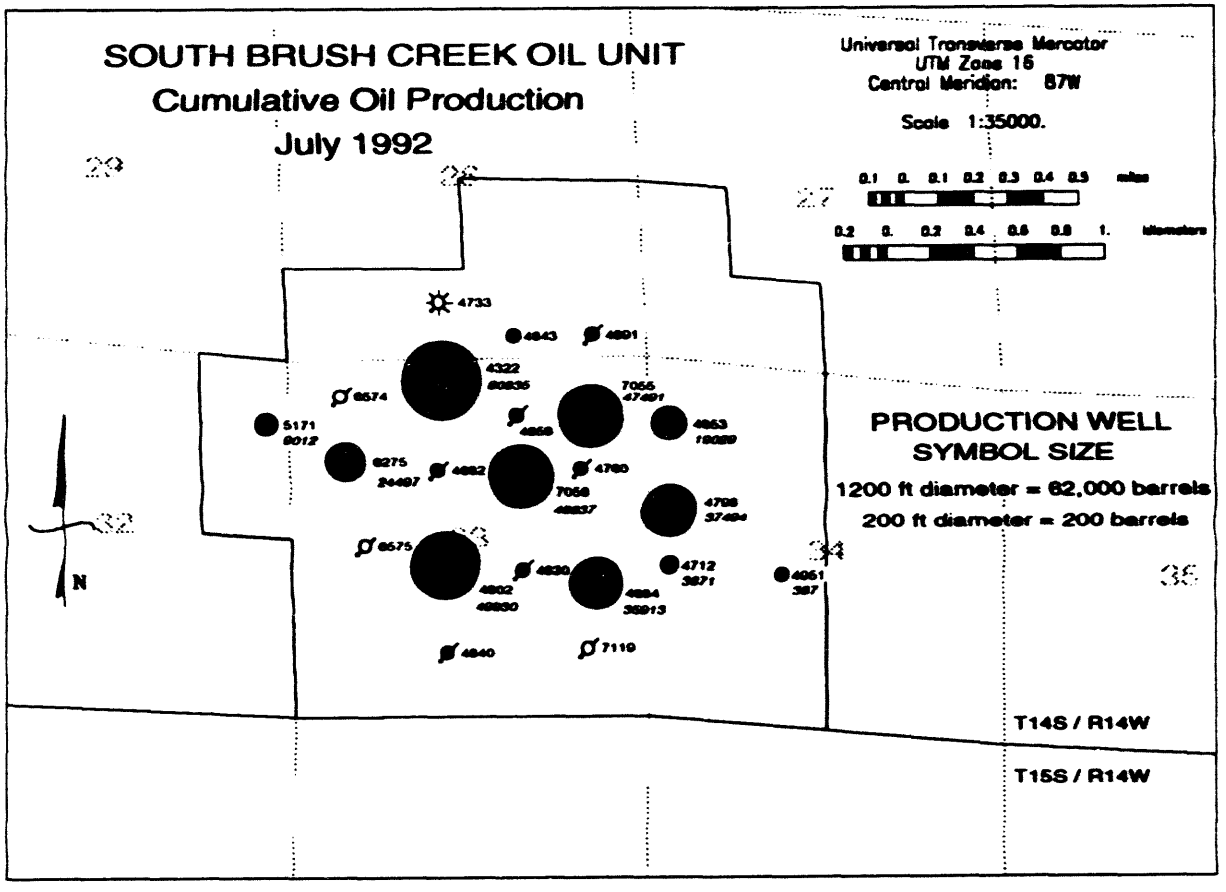

Figure 112.--Bubble map of cumulative oil production in South Brush Creek oil unit, as of July 1992. The size of well symbols is proportional to oil production. State Oil and Gas Board of Alabama permit numbers are adjacent to all well.. The volume of oil produced is shown in italics adjacent to production wells.

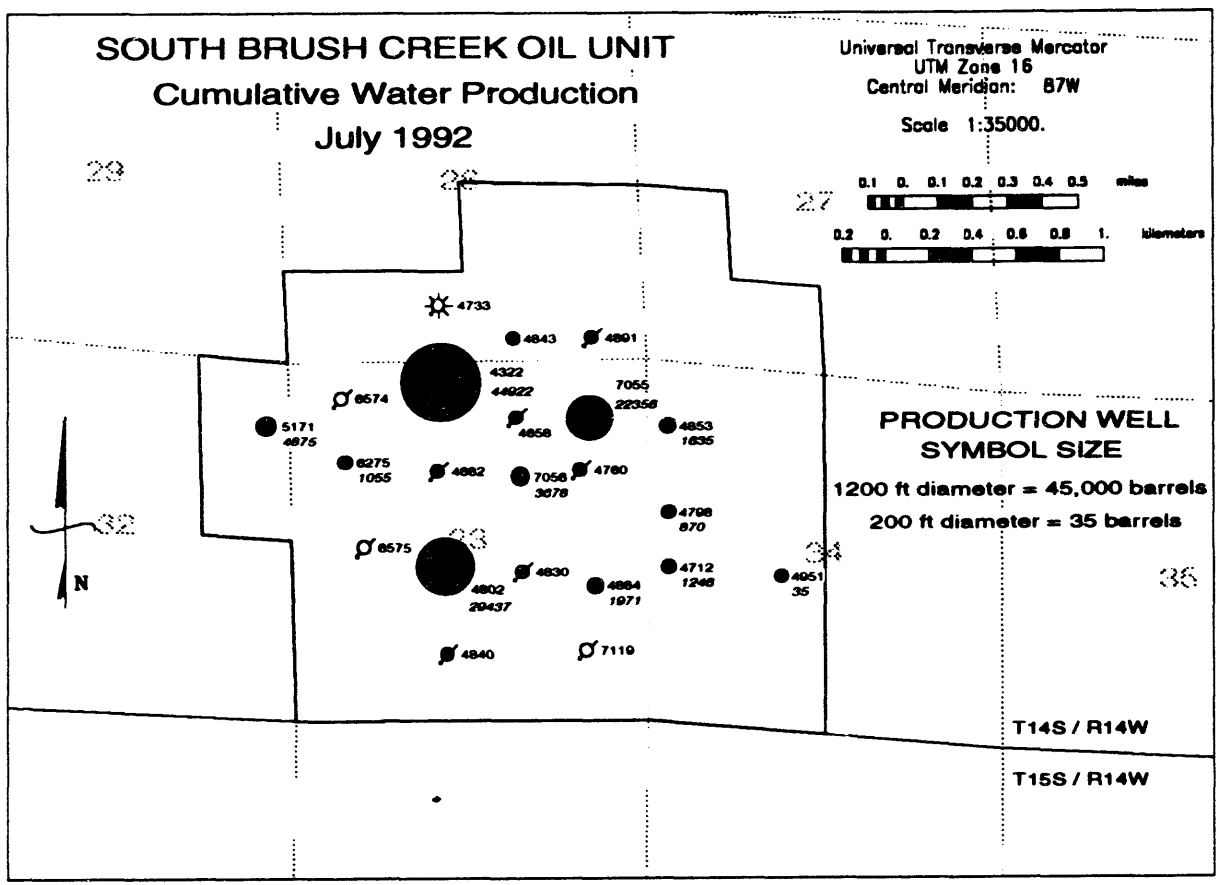

Figure 113.--Bubble map of cumulative water production in South Brush Creek oil unit, as of July 1992. The size of well symbols is proportional to water production. State Oil and Gas Board of Alabama permit numbers are adjacent to all wells. The volume of water produced is shown in italics adjacent to production wells.

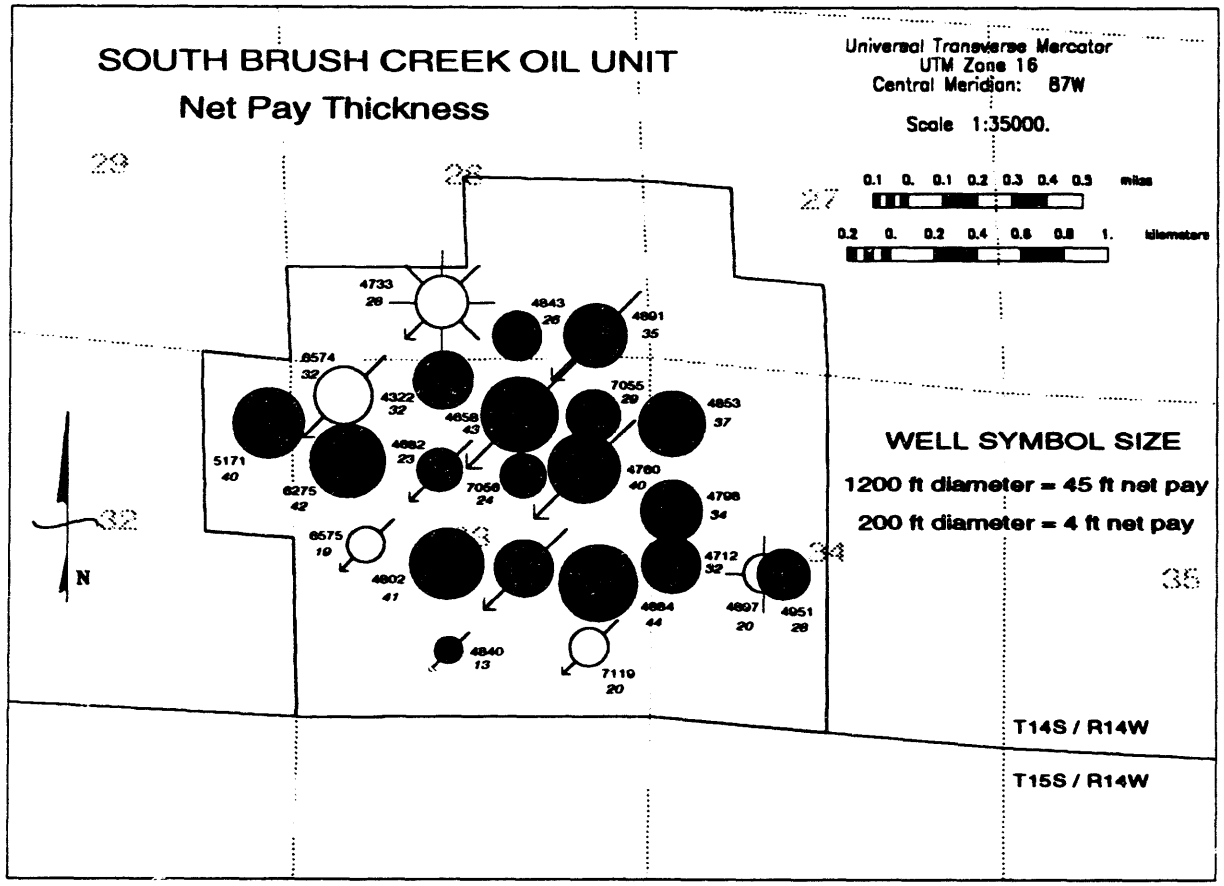

Figure 114.--Bubble map of net pay thickness in Carter sandstone, South Brush Creek oil unit. The size of well symbols is proportional to net pay thickness. State Oil and Gas Board of Alabama permit numbers are adjacent to all wells. The net pay thickness, rounded to the nearest integer, is shown in italics below the permit numbers.

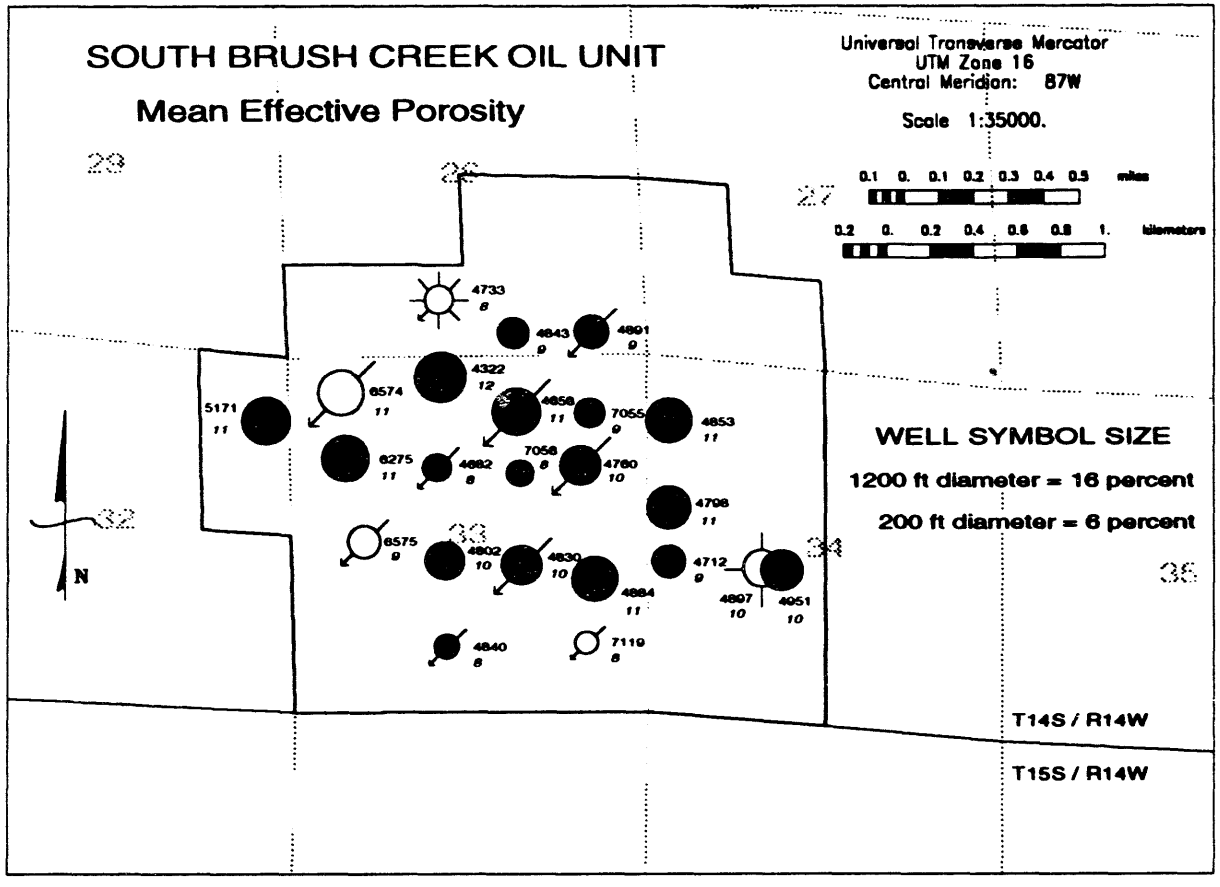

Figure 115.--Bubble map of effective porosity in Carter sandstone, South Brush Creek oil unit. The size of well symbols is proportional to effective porosity. State Oil and Gas Board of Alabama permit numbers are adjacent to all wells. Mean effective porosity, rounded to the nearest, is shown in italics below the permit numbers.

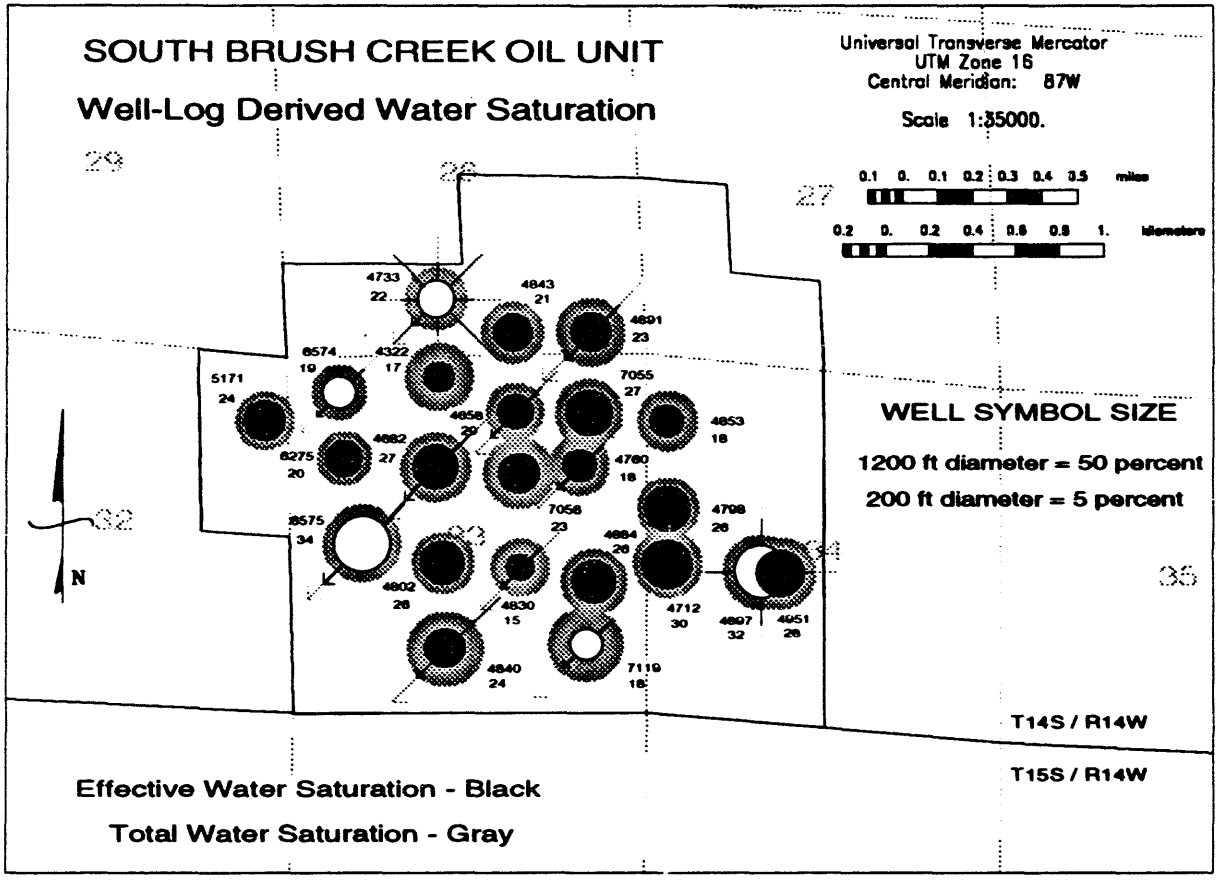

Figure 116.--Bubble map of effective and total water saturation in Carter sandstone, South Brush Creek oil unit. The size of black well symbols is proportional to effective water saturation. The size of gray well symbols is proportional to total water saturation. State Oil and Gas Board of Alabama permit numbers are adjacent to all wells. Effective water saturation, rounded to the nearest integer, is shown in italics below the permit numbers.

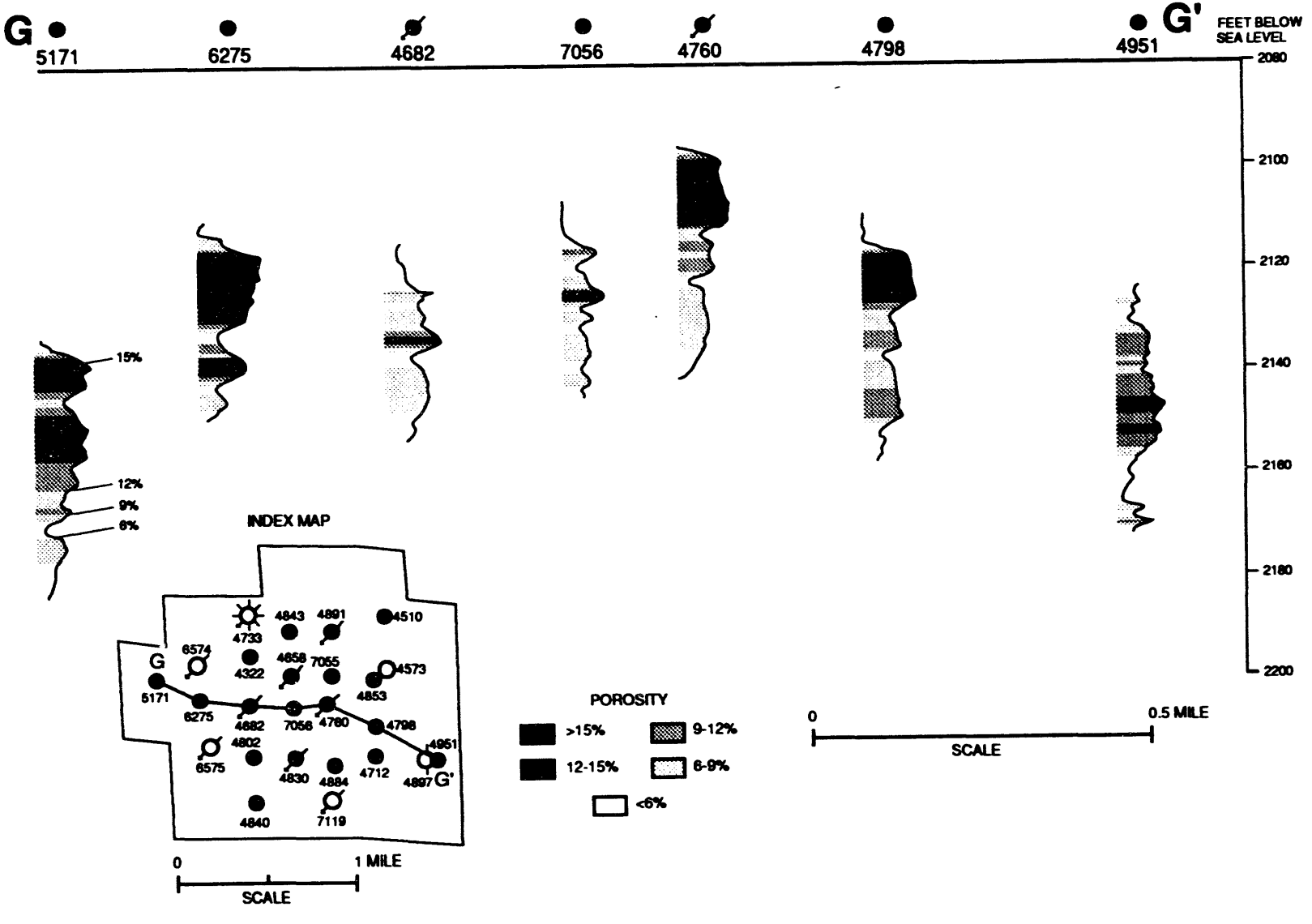

Figure 117.--Structural cross-section G-G' of effective porosity profiles, Carter sandstone, South Brush Creek oil unit.

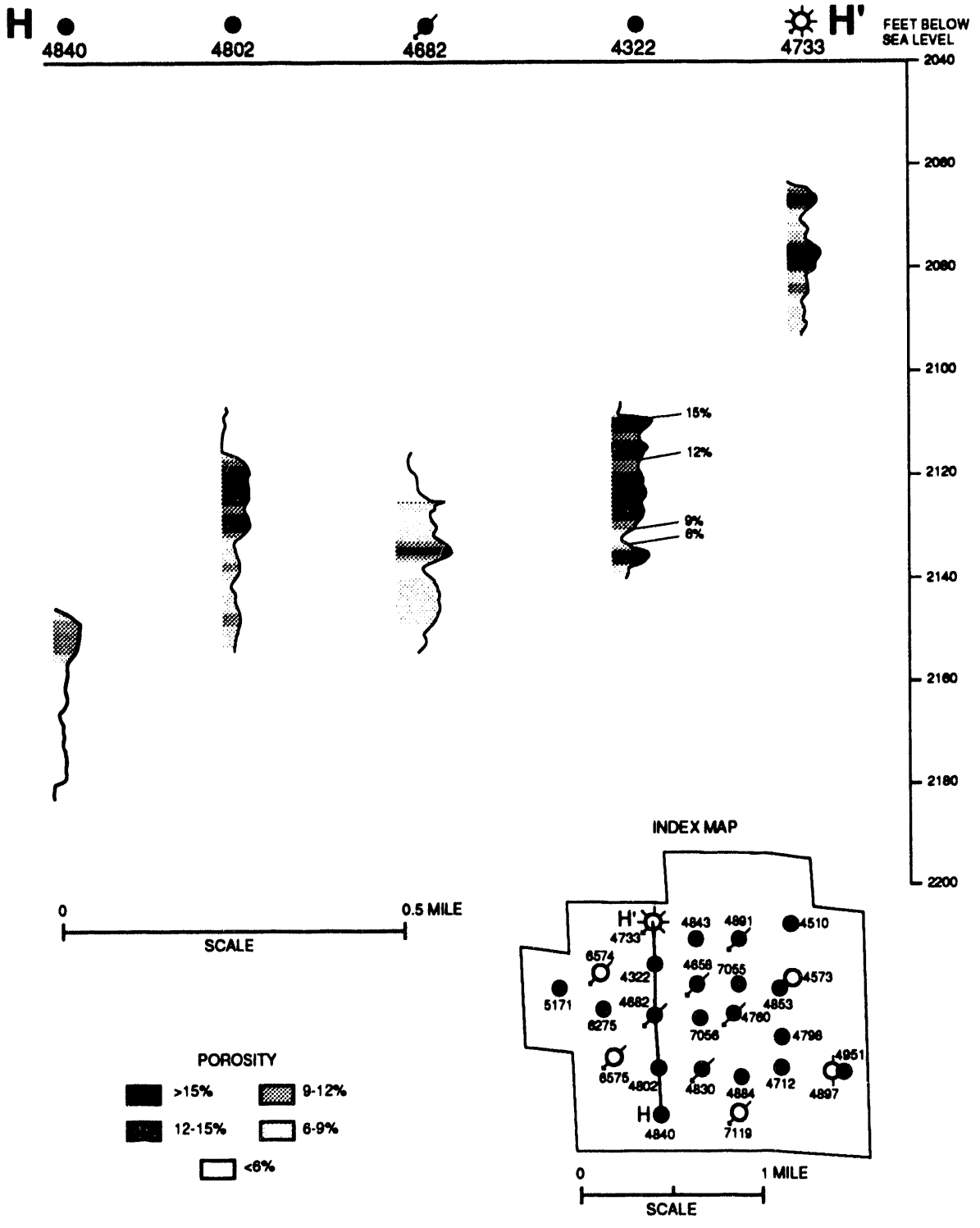

Figure 118.--Structural cross-section H-H' of effective porosity profiles, Carter sandstone, South Brush Creek oil unit.

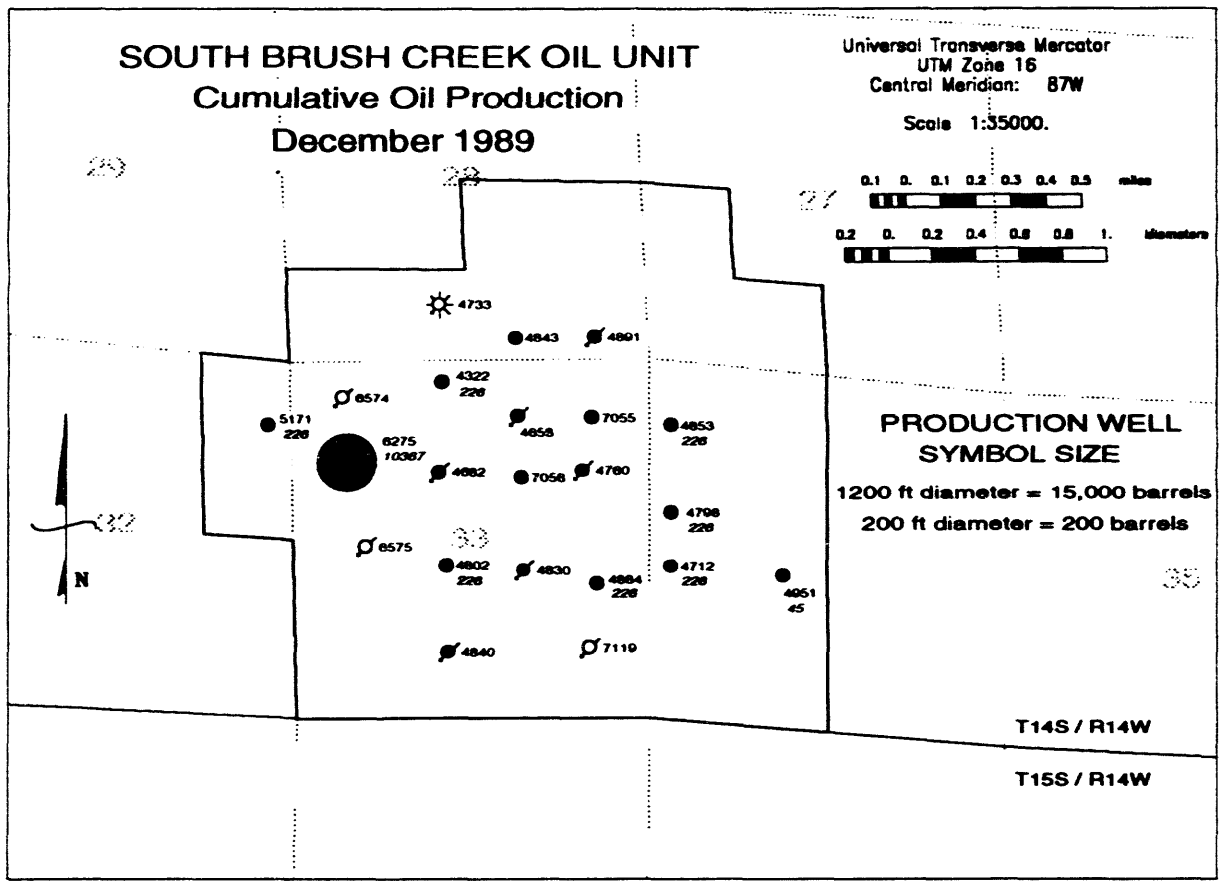

Figure 119.--Bubble map of cumulative oil production in South Brush Creek oil unit one year after unitization (December 1989). The size of well symbols is proportional to oil production. State Oil and Gas Board of Alabama permit numbers are adjacent to all wells. The volume of oil produced is shown in italics adjacent to production wells.

porosity cutoff for pay (Docket No. 11-4-8819, State Oil and Gas Board of Alabama). Primary recovery was estimated to be 680,000 stock tank barrels. Ultimate recovery from secondary recovery operations is estimated to be 1,360,000 stock tank barrels. As of July 1992, South Brush Creek oil unit produced 1,037,746 barrels of oil and 1,810,578 Mcf of gas, making the unit the second largest producer of oil in the Black Warrior basin of Alabama.

WAYSIDE OIL UNIT

The Wayside oil field was discovered by Charles L. Cherry and Associates, Inc., in 1985 with the drilling of the Junior Atkinson 3-6 no. 1 well (PN4465). Initial tests produced 45 barrels of 34.1° API gravity oil per day and a trace of gas on a 16/64-inch choke with a flowing tubing pressure of 50 psig. Production was from Carter sandstone through perforations from 2,157 to 2,161 feet. The trapping mechanism in the field is stratigraphic, resulting from pinchout of Carter sandstone. A subsurface fluid sample from the discovery well indicated the reservoir fluid was saturated with a bubble point equal to the original reservoir pressure of 1,020 psia. The drive mechanism for the reservoir is a combination of solution gas and gas cap expansion. A free water zone is present in the southeastern part of the reservoir but encroachment is negligible. Additional reservoir fluid properties are in table 9. Structural dip on top of the Carter sandstone is 100 ft/mi toward the south-southwest. The trapping mechanism for the reservoir in Wayside oil unit is stratigraphic, resulting from pinchout of Carter sandstone. Cumulative production from Wayside oil field prior to unitization was 144,271 barrels of oil and 212,365 Mcf of gas.

The need for a secondary recovery program in Wayside field was evident because of a rapid decrease in reservoir pressure and production (fig. 120). The field was unitized in May 1988, and a crestal gas flood to maintain pressure, combined with a peripheral waterflood, was initiated. Casinghead gas produced from the Wayside oil unit is mixed with gas produced from the Lewis sandstone and is injected into the crest of the reservoir in well PN4586. The original unitization plan called for drilling two infill production wells, converting an existing producer to a gas injection well, converting two producing wells to water injection wells, and drilling one new water injector. Ultimately, the field contained 7 oil-producing wells, 10 water injection wells, and one gas injection well. Of the two infill producers originally proposed, one is now a water injection well (PN5731) and the other has not been highly productive (PN5733, fig. 121) because the well penetrates a thin Carter pay section (fig. 122). Furthermore, well PN5733 is not associated with nearby water injectors; there is a gap in the distribution of water injectors south of PN5733 (fig. 121). A total of 411,404 barrels of water and 173,032 Mcf of gas were injected into the reservoir through July 1992. At present 0.34 barrels of oil are produced for every barrel of water injected. With the exception of well PN4591, a response in wells within the oil unit from water and gas injection has not yet occurred (fig. 123). Injected water may be bypassing parts of the reservoir.

The most productive well in Wayside oil unit both prior to and subsequent to gas injection and waterflood is well PN4788 (fig. 121). Carter sandstone in this well has the thickest pay section in the unit (fig. 122). Generally, the pay section in production wells in Wayside oil unit is thin compared to that in the most productive Carter oil fields. Mean effective porosity in the pay section is relatively uniform throughout much of the unit (fig. 124), but the highest porosity intervals are in the western part of the unit (figs. 125, 126). As expected, total water saturation is highest in the southern part of the unit (fig. 127), nearest the oil-water contact, and decreases updip toward the oil-gas contact in the northern part of the unit.

The productive area of Carter sandstone in Wayside oil unit is approximately 691 acres. The unit operator volumetrically estimated original oil in place to be 2,922,810 stock tank barrels of oil, using a 9 percent porosity cutoff for pay (Docket No. 3-10-8819, State Oil and Gas Board of Alabama). Primary recovery was estimated to be 233,825 stock tank barrels, and anticipated ultimate recovery is 818,389 stock tank barrels. Currently, the unit contains 8 production wells, 9 injection wells, and 2 shutin wells. Cumulative production from Wayside oil unit through July 1992 is 282,950 stock tank barrels of oil, 423,249 Mcf of gas, and 15,748 barrels of water.

DISCUSSION: HETEROGENEITY IN BLACK WARRIOR BASIN OIL RESERVOIRS

Reservoir heterogeneity is the spatial variability in engineering parameters in the porous rock making up a reservoir (Goggin, 1988). Heterogeneity in

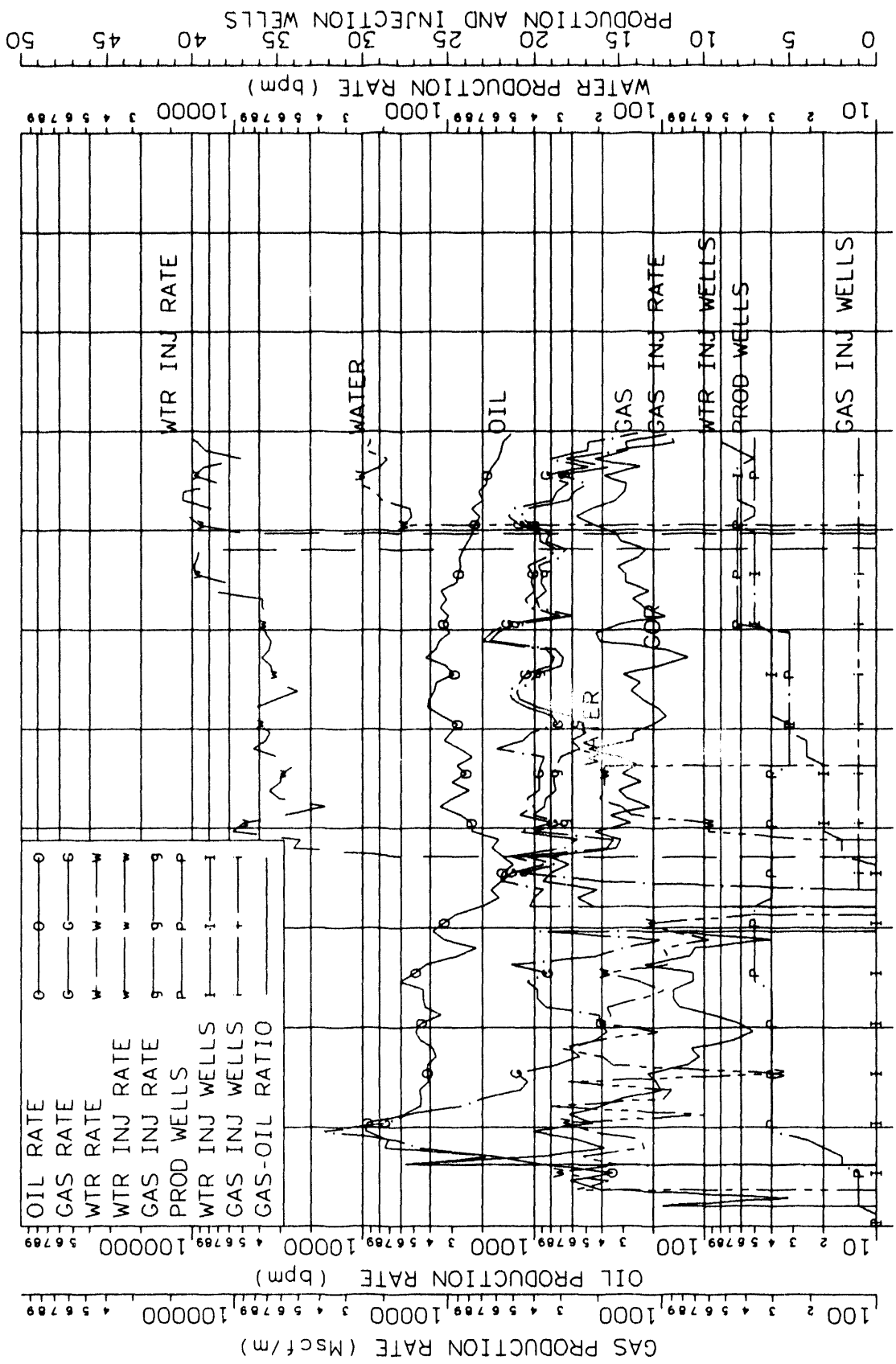

Figure 120.–Production plot for Wayside oil unit.

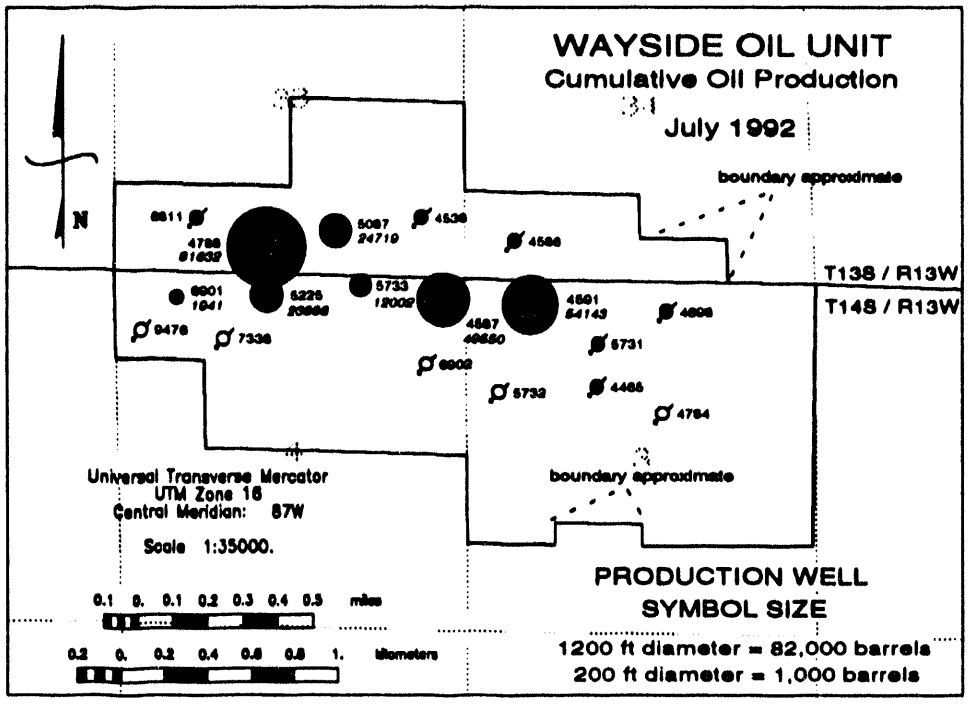

Figure 121.--Bubble map of cumulative oil production in Wayside oil unit, as of July 1992. The size of well symbols is proportional to oil production. State Oil and Gas Board of Alabama permit numbers are adjacent to wells. The volume of oil produced is shown in italics adjacent to production wells.

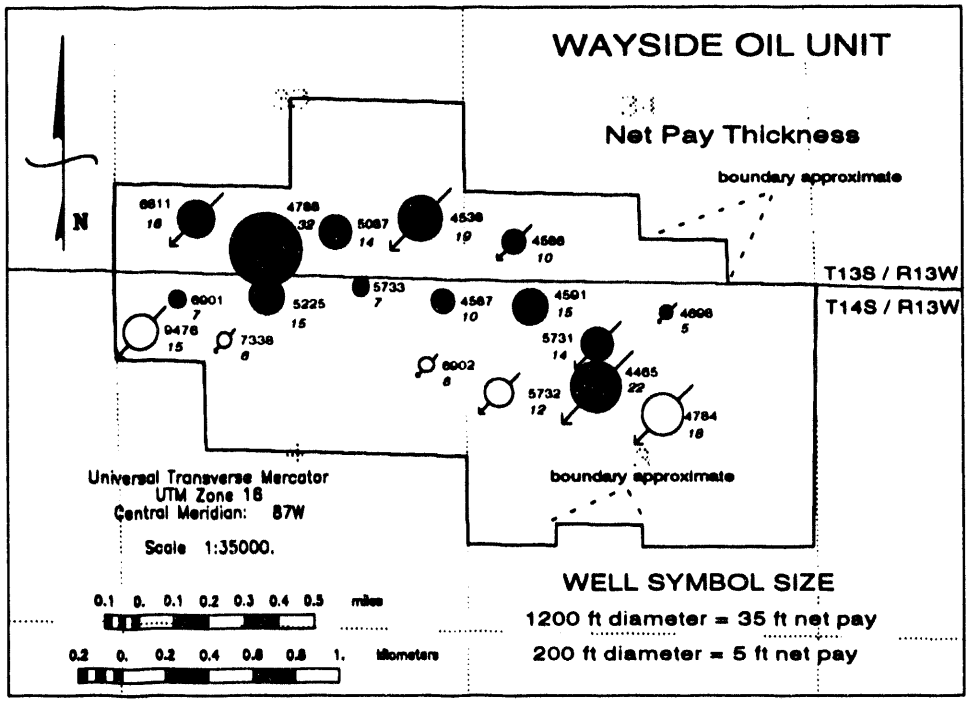

Figure 122.--Bubble map of net pay thickness in Carter sandstone, Wayside oil unit. The size of well symbols is proportional to net pay thickness. State Oil and Gas Board of Alabama permit numbers are adjacent to wells. The net pay thickness, rounded to the nearest integer, is shown in italics below permit numbers.

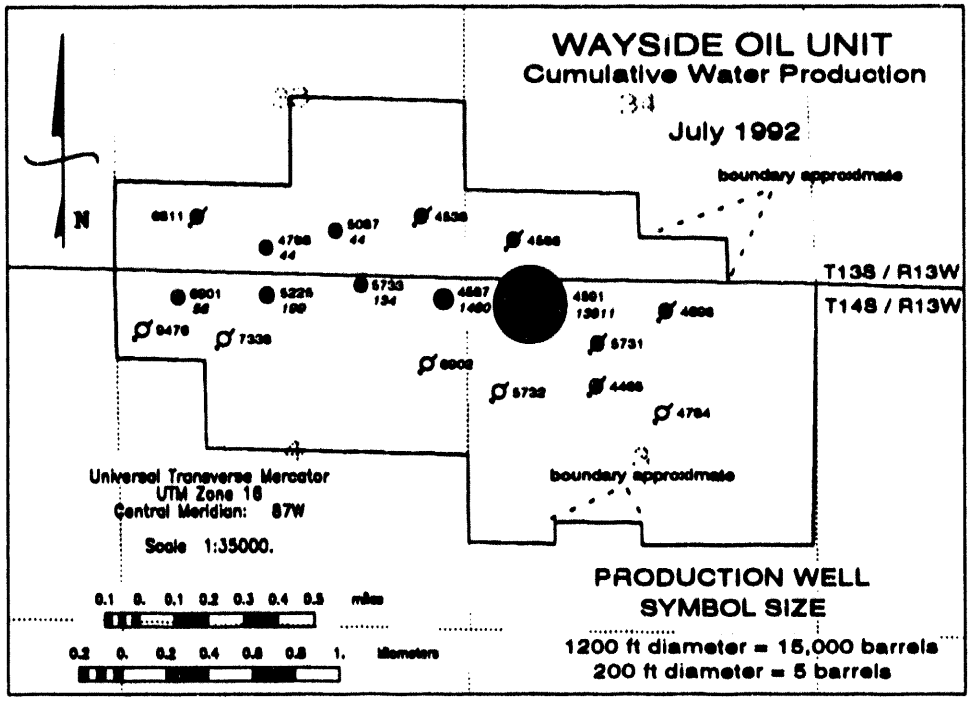

Figure 123.--Bubble map of cumulative water production in Wayside oil unit, as of July 1992. The size of well symbols is proportional to water production. State Oil and Gas Board of Alabama permit numbers are adjacent to wells. The volume of water produced is shown in italics adjacent to production wells.

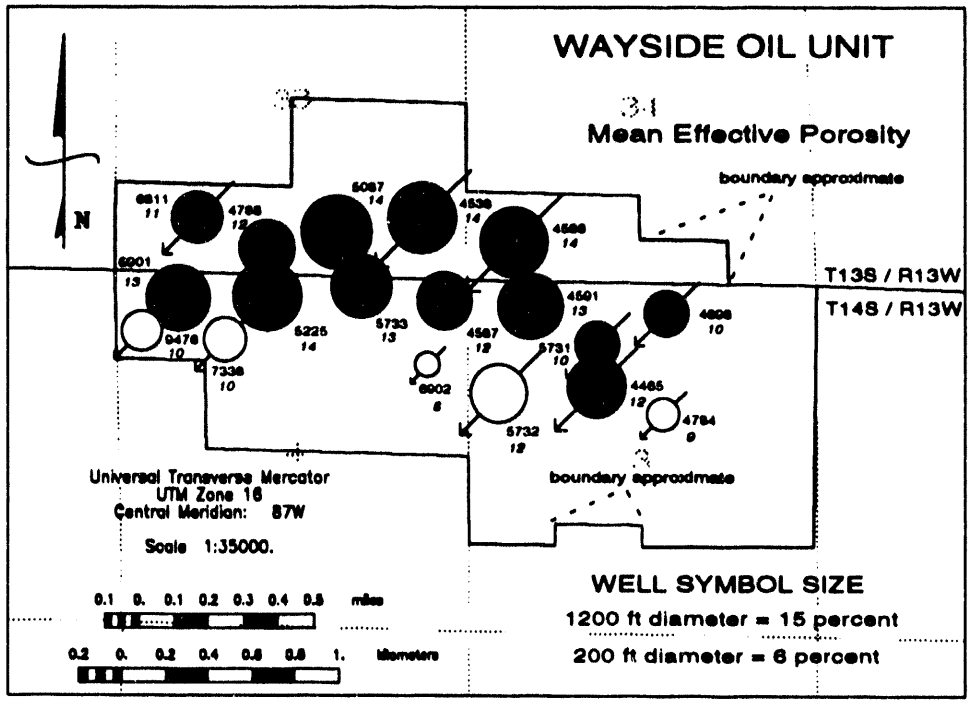

Figure 124.--Bubble map of effective porosity in Carter sandstone, Wayside oil unit. The size of well symbols is proportional to effective porosity. State Oil and Gas Board of Alabama permit numbers are adjacent to wells. Mean effective porosity, rounded to the nearest integer, is shown in italics below the permit numbers.

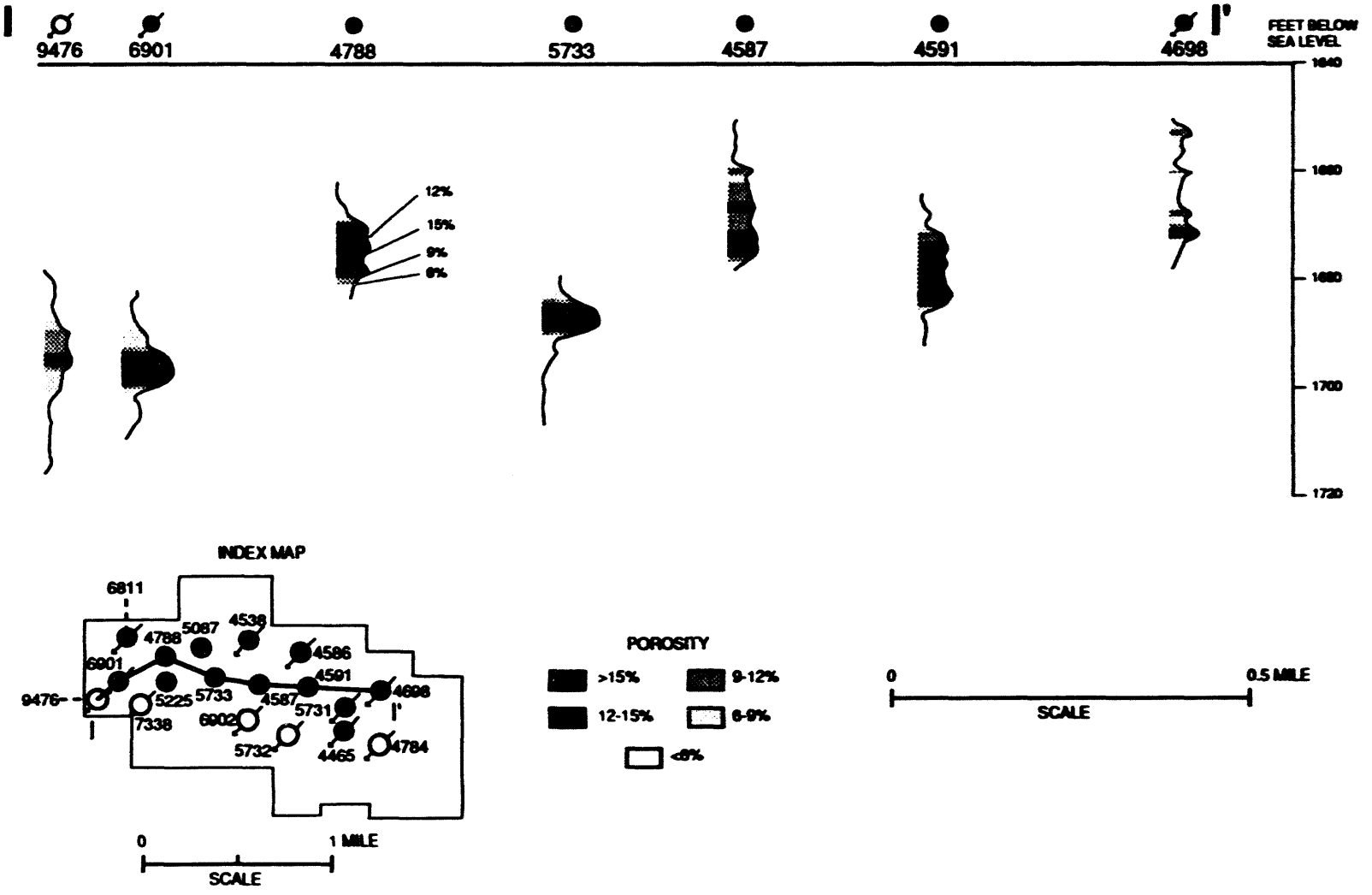

Figure 125.--Structural cross-section I-I' of effective porosity profiles, Carter sandstone, Wayside oil unit.

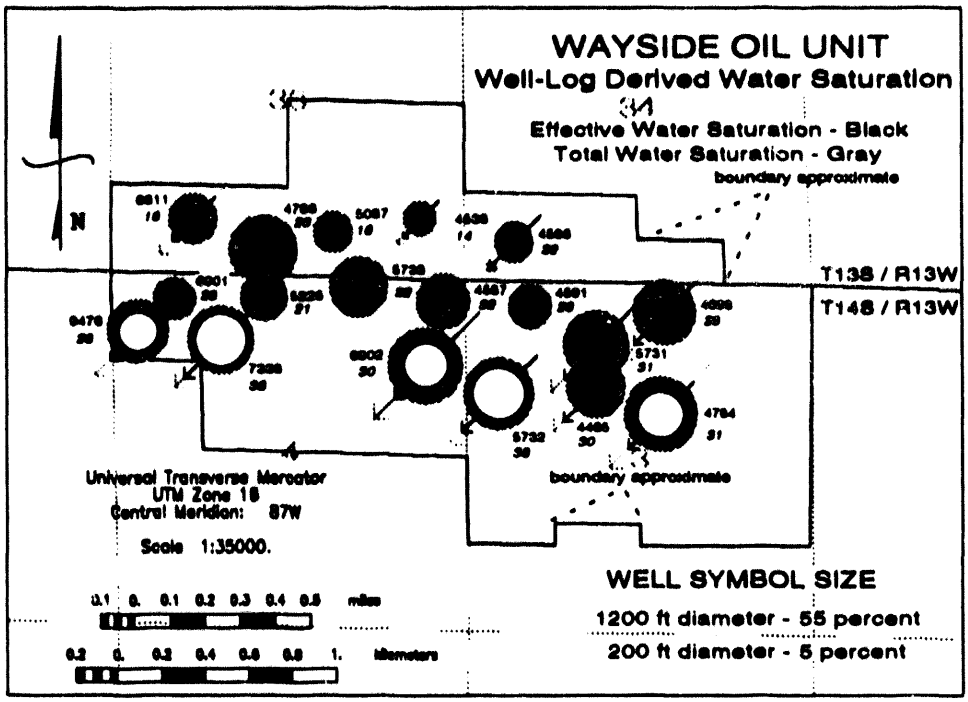

Figure 127.--Bubble map of effective and total water saturation in Carter sandstone, Wayside oil unit. The size of black well symbols is proportional to effective water saturation. The size of gray well symbols is proportional to total water saturation. State Oil and Gas Board of Alabama permit numbers are adjacent to wells. Effective water saturation, rounded to the nearest integer, is shown in italics below the permit numbers.

hydrocarbon reservoirs is the cumulative result of numerous geological factors, including depositional processes (wind, water, and biologic activity), tectonic and structural processes (basin evolution, subsidence, faulting, folding), and post-depositional processes (compaction, diagenesis, thermal maturation, fluid composition). Detailed knowledge of factors controlling reservoir heterogeneity is crucial to the success of enhanced recovery projects. Lack of sufficient knowledge of the spatial distribution of permeability, porosity, and fluids can result in bypassing of hydrocarbons in uncontacted compartments or channeling of injected and produced fluids, and ultimately can result in premature abandonment of producing fields (Tyler and Finley, 1991).

Heterogeneity is scale dependent, reflecting the diverse geological processes that define a hydrocarbon reservoir (Goggin, 1988). Further, as field development progresses from primary recovery to various types of improved recovery, heterogeneity becomes increasingly important at smaller scales (Jackson and others, 1993). Controls on reservoir heterogeneity, therefore, are discussed in this section in terms of their scale dependence, using a classification scheme modified from Moore and Kugler (1990) (fig. 6). This heterogeneity scheme is similar to other commonly used classifications (for example, Lake and others, 1991; Hurst, 1993). Scales of heterogeneity include megascopic, macroscopic, mesoscopic, and microscopic features of a reservoir (fig. 6).

In addition to these four commonly utilized scales of heterogeneity, an additional category, the gigascopic scale, was found to be particularly useful during the course of this investigation. Gigascopic heterogeneity incorporates those features encompassing several producing fields in a reservoir unit to entire sedimentary basins. Megascopic heterogeneity is the reservoir, namely a body of

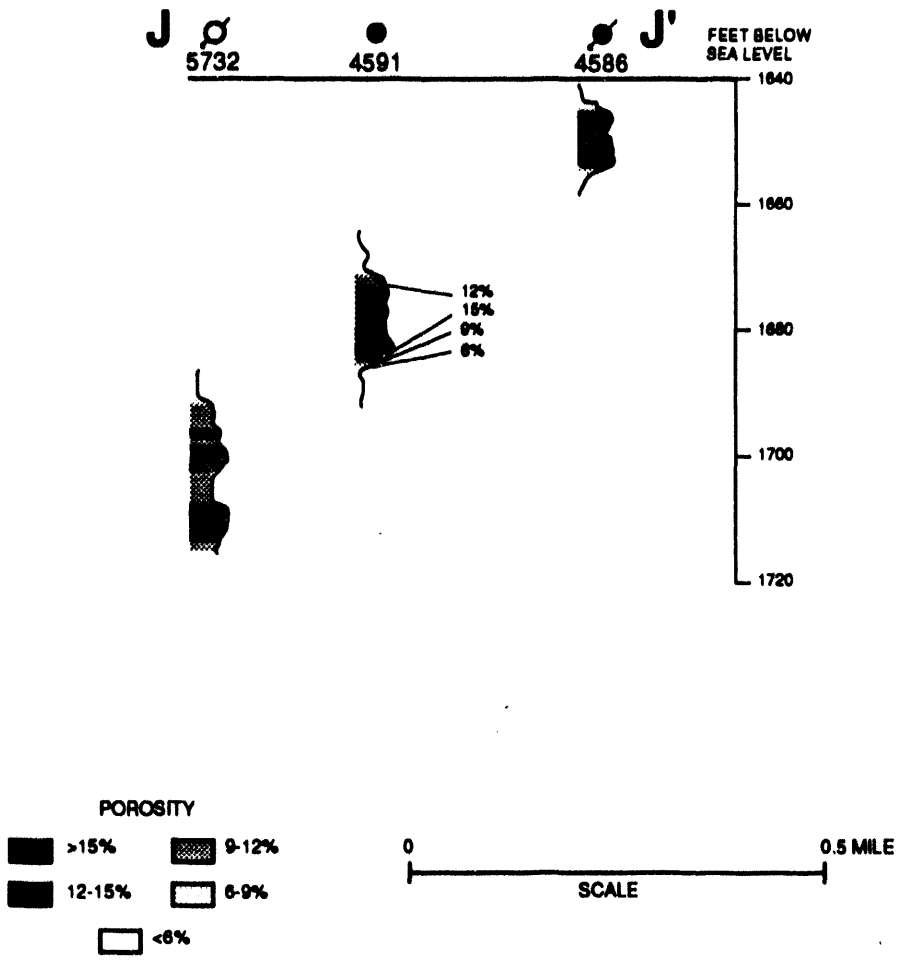

Figure 126.--Structural cross-section J-J' of effective porosity profiles, Carter sandstone, Wayside oil unit.

permeable reservoir rock surrounded by impermeable nonreservoir rock (fig. 6). Macroscopic heterogeneity represents features that restrict fluid flow and occur among two or more wells. Mesoscopic heterogeneity represents features that occur at an interwell to borehole scale. Microscopic heterogeneity occurs at the scale of pores and pore throats.

GIGASCOPIC HETEROGENEITY

Previous investigations of hydrocarbon producibility have emphasized microscopic- to megascopic-scale heterogeneity in single producing reservoirs. Fields where these studies have been conducted generally are larger and are in an advanced state of development compared to oil fields in the Black Warrior basin. Furthermore, these fields have a longer history of data acquisition, have more cores, and have denser well spacing over larger areas than the Black Warrior basin. In basins lacking closely spaced wells and cores, reservoirs are characterized most effectively in terms of the regional geological framework. Gigascopic investigations, therefore, are critical to understanding reservoir architecture and predicting heterogeneity in underdeveloped oil reservoirs.

At this scale, the Black Warrior basin can be characterized as an intricate system of source and reservoir rocks. Oil-prone source rocks are near the base of the section in the Chattanooga and Floyd shales. Lewis, Evans, and Hartselle sandstone accumulated mainly north of the area of major source-rock deposition, whereas the Carter sandstone, the most productive oil reservoir in the basin, was among the first units deposited above the oil-prone Floyd Shale. The upper Parkwood Formation contains the youngest oil reservoirs in the basin and represents a major change in style of the basin fill. Upper Parkwood and younger strata contain mainly gas-prone kerogen, including coal. Whereas reservoir-quality quartzarenite was dominant through Carter deposition, moreover, nonreservoir litharenite became increasingly abundant during upper Parkwood deposition.

MEGASCOPIC HETEROGENEITY

At the megascopic scale, sandstone-body geometry and thickness varies significantly within and among reservoirs throughout the stratigraphic succession in the basin, owing to differences in depositional systems and the position of individual reservoirs within these systems. Lewis, Evans, and Hartselle sandstones are part of the cratonic succession and were deposited in beach and shelf (Lewis), wave-dominated deltaic (Evans), and barrier-strandplain (Hartselle) systems. Carter, *Millerella*, Coats, and Gilmer sandstone reservoirs are all deltaic and are part of the orogenic basin fill. The Carter sandstone is part of the first major deltaic system, and the best oil reservoirs accumulated as part of a destructive, shoal-water delta system that prograded onto a carbonate bank margin. The Gilmer sandstone consists of clinoformal sandstone bodies containing intermixed quartzarenite and litharenite, whereas the Coats sandstone consists of a widespread, fining-upward, quartzarenite-litharenite sequence deposited in deltaic environments above a lowstand surface of erosion.

Carter and *Millerella* sandstone were deposited as part of a muddy, delta-destructive strandplain. These reservoirs do not fit well into existing heterogeneity classifications, such as that used in the TORIS database, because muddy strandplains are not recognized in these classifications. Although similar systems are well known in modern settings, muddy strandplains are not well documented in the ancient record. Although Carter sandstone can be classified as a barrier shoreface reservoir in the TORIS database, Carter sandstone bodies are smaller and muddier than those reservoirs generally placed in this category. Heterogeneity crucial to field planning and production may not be appropriately emphasized by broad categorization in a heterogeneity classification. In addition, categories used in heterogeneity classifications are not mutually exclusive. For example, a strandplain can be part of a delta, as is the case with the Carter reservoirs, or part of an interdeltaic bight, as are the modern cheniers of the Gulf Coast.

Furthermore, remarkable diversity exists in the geometry of Carter and *Millerella* sandstone bodies within the 100 square-mile area that accounts for most oil production in the Black Warrior basin. In effect, each field is different, reflecting evolution of the delta-destructive strandplain, from cuspate beaches to spits and, in turn, to crescentic tidal barriers. This diversity limits use of individual fields as direct analogs for determining megascopic heterogeneity. Thus, potential effects of megascopic heterogeneity on implementing improved recovery projects must be determined on a field-by-field basis.

MACROSCOPIC HETEROGENEITY

A fundamental result of this investigation is the recognition that Carter and *Millerella* reservoirs consist of imbricate, clinoformal sandstone lenses. This reservoir architecture differs significantly from that determined by the layer-cake stratigraphic approaches typically used for Black Warrior basin reservoirs. Use of the layer-cake approach for Carter and *Millerella* reservoirs could result in incorrect representation of flow units because uncontacted or unconnected compartments may be modeled as connected units.

The size and arrangement of sandstone lenses differs substantially among Black Warrior basin oil fields, resulting in inhomogeneous reservoirs at the macroscopic scale. In the northern part of North Blowhorn Creek oil unit, for example, Carter sandstone contains amalgamated shoreface and foreshore sandstone lenses that form a single, strike-oriented flow unit near the depositionally downdip margin of the reservoir. In depositionally updip parts of the reservoir, facies changes are pronounced, resulting in reduced reservoir quality as separate lenses of reservoir sandstone merge into poorer quality backshore facies. This results in facies anisotropy that favors flow along the axis of the sandstone body.

In addition to the geometry of sandstone lenses, the degree of preservation of those lenses influences reservoir heterogeneity at the macroscopic scale. The Carter reservoir in North Blowhorn Creek oil unit, for example, is a well-preserved delta-destructive spit system. In South Brush Creek oil unit, by comparison, the sandstone lenses are truncated by an exposure surface. In Blowhorn Creek and Wayside oil units, moreover, the lenses are truncated by tidal channels and inlets. In Blowhorn Creek oil unit, truncation separates Carter and *Millerella* reservoirs into a series of unconnected compartments.

Diagenesis and the distribution of formation fluids further affect flow characteristics within sandstone lenses. Diagenesis helps confine flow along the axis of reservoirs because the margins of Carter sandstone bodies typically are cemented by carbonate minerals. Interstitial clay also retards flow and is most common in backshore and shelf deposits. Indeed, most stratigraphic traps in the Black Warrior basin have a significant diagenetic component. The importance of the distribution of formation fluids is especially apparent in Wayside oil unit, where the oil-saturated zone is mainly in muddy backshore deposits and the gas-saturated zone is in the highest quality shoreface and foreshore deposits.

MESOSCOPIC HETEROGENEITY

Mesoscopic heterogeneity, which occurs at the interwell to wellbore scale, is mainly a product of facies anisotropy. Within individual reservoirs, the importance of interwell heterogeneity varies considerably. For example, in the northern part of North Blowhorn Creek oil unit facies parallel the sandstone body axis and generally extend between wells (Zone 1, fig. 82). In this region, interwell heterogeneity is of limited concern. However, in the southern part of the unit (Zone 3, fig. 82), where imbricate sandstone lenses decrease in size, interwell heterogeneity is pronounced parallel to the axis of the sandstone body. Bedform distribution within reservoir sandstone also contribute to facies anisotropy. Shoreface and foreshore bars represented by high-angle crossbeds probably prograded shoreward only a few tens of feet but may extend hundreds or even thousands of feet along depositional strike.

Grain-size variation results in subtle heterogeneity that may significantly affect sweep efficiency. Fine-grained sandstone is sparse in the reservoirs and likely is not laterally extensive. However, this sandstone is more permeable and contains less clay than the surrounding very fine-grained sandstone and thus contains larger, better-connected pore throats. High permeability in fine-grained sandstone forms thief zones through which fluids are channeled. As a result, fluids may not be efficiently swept from the adjacent reservoir. Production patterns combined with core analyses indicate that thief zones are especially well developed in North Blowhorn Creek oil unit.

Features resulting in heterogeneity at the wellbore or core scale include thin, individual to anastomosing groups of stylolitized clay laminae, cross laminae, grain-size variations within laminae, intrabasinal shale chips, and kaolinite- and carbonate-cemented horizons. Convergence of anastomosing clay laminae and clay drapes on ripple foresets increases tortuosity of flow and impounds minor amounts of oil in ripple-laminated sandstone during improved-recovery operations. Grain-size variation within individual laminae in low-angle planar-crossbedded sandstone may result in slight differences in permeability. However, results of high-pressure mercury porosimetry indicate that median pore-throat size is relatively uniform throughout the reservoir (Kugler and Pashin, 1992), indicating

these differences have limited effect on recovery. Shell accumulations cemented with ferroan dolomite/ankerite form discontinuous baffles and barriers to fluid flow. Detrital grain-size clay and larger shale rip-up clasts dispersed throughout the reservoir decrease permeability disproportionately to their abundance in the reservoirs.

MICROSCOPIC HETEROGENEITY

Microscopic heterogeneity occurs at the scale of pores and pore throats. Although Carter and *Millerella* sandstone is quartzarenite deposited in high-energy environments, the quality of the reservoir is affected by detrital and authigenic clays, mainly kaolinite. Clays are present throughout the reservoir and contribute to polymodal pore and pore-throat size distributions.

The pore system consists of diagenetically modified, effective, interconnected macropores between detrital framework grains and ineffective micropores among detrital and authigenic clays. Secondary pores formed by carbonate-cement dissolution did not enhance the effective pore system significantly. Dissolution of aluminosilicate framework grains also contributed little to the effective pore system because reaction products of dissolution of detrital feldspar were redistributed as authigenic kaolinite. The distribution of clays in Carter and *Millerella* reservoirs results in lower permeability than is characteristic of the larger beach-barrier deposits used as the basis of reservoir heterogeneity models.

Clay minerals in Carter sandstone have high surface area to volume ratios and contain immobile water, which affects calculation of effective porosity and water saturation from well logs. Well-log interpretations should acknowledge the presence of both structural and dispersed clay in the reservoirs in order to avoid misinterpretation of pay thickness, reserve volume, and connectivity of flow units.

SUMMARY AND CONCLUSIONS

Although oil production in the Black Warrior basin of Alabama is declining, additional oil may be produced through improved recovery strategies, such as waterflooding, chemical injection, strategic well placement, and infill drilling. High-quality characterization of reservoirs in the Black Warrior basin is necessary to utilize advanced technology to recover additional oil and to avoid premature abandonment of fields. This report documents controls on the distribution and producibility of oil from heterogeneous Carboniferous reservoirs in the Black Warrior basin of Alabama. This is the final summary report for DOE contract number FG22-90BC14448, entitled "Characterization of Sandstone Heterogeneity in Carboniferous Reservoirs for Increased Recovery of Oil and Gas from Foreland Basins."

The first part of the report summarizes the structural and depositional evolution of the Black Warrior basin and establishes the geochemical characteristics of hydrocarbon source rocks and oil in the basin. This second part characterizes facies heterogeneity and petrologic and petrophysical properties of Carter and *Millerella* sandstone reservoirs. This is followed by a summary of oil production in the Black Warrior basin and an evaluation of seven improved-recovery projects in Alabama. In the final part, controls on the producibility of oil from sandstone reservoirs are discussed in terms of a scale-dependent heterogeneity classification.

The Black Warrior basin is a foreland basin that formed by tectonic loading of the Alabama promontory during late Paleozoic Appalachian-Ouachita orogenesis. The sedimentary sequence in the basin records the tectonic evolution of the Alabama promontory as well as major climatic changes. Hydrocarbon source and reservoir rocks in the basin range in age from Devonian through Pennsylvanian. From Late Devonian through Middle Mississippian time, the Black Warrior basin was part of the passive margin of the Ouachita embayment. During this time, organic-rich Chattanooga Shale, phosphatic and glauconitic Maury Shale, siliceous micrite of the Fort Payne Chert, and skeletal calcarenite of the Tuscumbia Limestone were deposited.

Foreland-basin development began at the start of the Chesterian epoch. As an orogenic forebulge formed, the lowstand wedge of the Lewis cycle was deposited. Deposition of the Lewis was followed by the Evans and Hartselle cycles. These cycles comprise southwest-dipping clinoformal sequences that contain shelf, deltaic, and beach-barrier deposits derived from cratonic sources. The Evans and Hartselle cycles represent the onset of load-related subsidence adjacent to the Ouachita orogen. Deposition of clinoformal parasequences continued after deposition of these cycles, culminating with formation of the prograding Bangor carbonate platform-ramp system. During deposition of the Bangor, starved-basin conditions persisted in the southwestern part of the basin and are represented by the organic-rich Floyd Shale, the major source rock in the basin. The

Bangor platform-ramp system significantly influenced localization of the most prolific oil reservoirs in the Black Warrior basin.

As Bangor deposition ended, deep-water deltaic sediment of the lower Parkwood Formation filled the starved basin. This deltaic system ultimately prograded onto the carbonate bank, resulting in deposition of a destructive, shoal water deltaic system, represented by the Carter sandstone. The most productive hydrocarbon reservoirs in the basin are part of this shoal-water delta system, which formed as the receiving basin shallowed along the bank margin. The lower Parkwood Formation records a reversal of the southwest paleoslope that prevailed earlier in basin evolution and thus represents the first succession to enter the basin from sources in the Ouachita orogen.

Marine transgression occurred in middle Parkwood time, following deposition of Carter sandstone, as *Millerella* limestone accumulated in a carbonate platform-ramp system. Deposition of *Millerella* sandstone marked continued destruction of the Carter delta plain. After this phase, the remaining parts of the starved basin filled with deltaic sediment. Subsidence and continued filling of the foreland basin with deltaic sediment continued as the upper Parkwood Formation was deposited. Clinoformal Gilmer sandstone represents highstand progradation of deltaic sediment at the start of upper Parkwood deposition, whereas the aggradational Coats sandstone represents transgressive modification of the deltaic system. The Pottsville Formation unconformably overlies the Parkwood and Bangor Formations and signals the onset of the Alleghanian orogeny. Pottsville deposition was characterized by fluvial and deltaic sedimentation adjacent to the orogenic belts and by mesotidal shelf and beach sedimentation seaward of the fluvial-deltaic systems.

Vitrinite reflectance of the Mary Lee coal group in the lower Pottsville Formation reveals that thermal maturity in the Black Warrior basin increases from northwest to southeast. Vitrinite reflectance values increase from 0.62 percent near the top of the Pottsville Formation to 1.12 percent in the Chattanooga Shale in a well near the margin of the Bangor carbonate platform. Deeper in the basin, to the southwest, vitrinite reflectance values also show an increase with depth, from 0.74 percent in the upper Pottsville Formation to 1.61 percent in Lewis shale. Burial history and time/temperature index modeling indicate that conditions suitable for liquid hydrocarbon generation occurred between 290 and 200 MA. Near the margin of the Bangor carbonate platform, shale beneath the Carter sandstone is within the liquid hydrocarbon window but below peak generation potential. Deeper in the basin, the same units are near the upper limit of liquid hydrocarbon generation.

Results of total organic carbon and Rock-Eval pyrolysis analyses indicate that sufficient quantities of type II kerogen occur in Chattanooga and Floyd shales for these units to serve as oil source rocks. Because of volume considerations and proximity to the most productive Carter and *Millerella* sandstone reservoirs, the Floyd Shale is considered to be the primary source for oil in the basin. API gravity of oil in Carter sandstone increases systematically from northeast to southwest from 22° to 44°, paralleling an increase in depth of burial. Chemical analyses of oil show that most contain a high percent of saturated hydrocarbons relative to aromatic hydrocarbons and asphaltenes, indicating that minimal biodegradation has occurred.

Carter and *Millerella* oil reservoirs present the best opportunity for understanding reservoir heterogeneity in the Black Warrior basin because these units are the most productive in the basin, have the closest well spacing, and have the most available cores. All Carter cores contain the same tripartite sequence of lithofacies, including from bottom to top: (1) shale-and-siltstone facies; (2) sandstone facies; and (3) variegated facies. These facies are interpreted to represent storm-dominated shelf deposits, shoreface and foreshore deposits, and backshore deposits, respectively. Beach deposits of Carter sandstone developed on a muddy strandplain during destruction of the lower Parkwood deltaic system. Although lithofacies vary little among Carter and *Millerella* fields, stratigraphic architecture varies considerably and is a primary source of heterogeneity. This diversity in geometry of beach systems from lobate bodies in the southwest to thin, isolated lenses in the northeast records systematic evolution of the strandplain and exceptional preservation of the paleogeographic framework of the shoal-water delta.

Carter sandstone in North Blowhorn Creek oil unit represents a spit-type beach system, composed of imbricate, clinoformal sandstone lenses that decrease in size and segment toward the southeastern terminus of the reservoir. In contrast to the elongate geometry of the North Blowhorn Creek spit complex, Carter sandstone in Wayside oil unit occurs as a localized, arcuate body that accumulated at the distal edge of the shoal-water delta system. The lobate, coarsening upward Carter sandstone in South Brush Creek oil unit reflects deposition at the distal

edge of a constructive, wave-dominated delta complex. The Carter reservoir in Blowhorn Creek oil unit is a continuation of that in South Brush Creek oil unit and was deposited at the distalmost edge of the constructive, wave-dominated delta system. The Carter reservoir in Bluff oil field is part of a string of beach systems that formed after abandonment of the North Blowhorn Creek spit complex and is the most heterogeneous Carter-*Millerella* oil field in the basin, containing several uncontacted or poorly contacted oil compartments.

Millerella sandstone bodies were deposited during the latest stage of delta destruction as carbonate deposition was reestablished. The *Millerella* reservoir in Blowhorn Creek oil unit differs from the other beach systems and represents part of a delta-destructive shoal massif. In Bluff oil unit, *Millerella* sandstone exhibits a backstepping relation relative to Carter sandstone bodies and represents development of a small beach above a tidal inlet as the deltaic strandplain was inundated.

Carter sandstone in North Blowhorn Creek oil unit is dominantly very fine to fine-grained, moderately well-sorted quartzarenite. Despite the quartzose nature of Carter sandstone, reservoirs in North Blowhorn Creek and other fields are heterogeneous, owing not only to imbricate, clinoformal sandstone lenses and associated facies changes, but also to the presence of intrabasinal framework grains and to diagenesis. Volumetrically important authigenic minerals in Carter sandstone are quartz, kaolinite, and a variety of carbonate minerals, including nonferroan and ferroan calcite, ferroan dolomite/ankerite, and siderite. The distribution of diagenetic components in North Blowhorn Creek oil unit is directly related to depositional facies, but the present composition of authigenic minerals, and the nature of compactional features, resulted from burial diagenesis. Carbonate cemented zones along the margins of the reservoir and in the vicinity of shell accumulations form baffles and barriers to fluid flow. Pressure-solution seams also form effective barriers to flow and mark the lower limit of oil stained sandstone in several cores. Wispy microstylolites associated with small-scale sedimentary structures and deformed rip-up clasts increase tortuosity of fluid flow.

The pore system in Carter sandstone consists of effective macropores between framework grains and ineffective micropores between detrital and authigenic clay particles. The effective pore system was not enhanced significantly by dissolution of aluminosilicate framework grains because products of dissolution are redistributed locally kaolinite. Further, authigenic carbonate minerals occlude all pores only in the vicinity of shell accumulations, suggesting that secondary porosity formed by dissolution of carbonate cement is not widespread. Dispersed and laminated clay have the most detrimental effects on reservoir properties.

Owing to the presence of detrital and authigenic clays, only a weak correlation exists between porosity and permeability ($R^2 = 0.52$) in the Carter reservoir in North Blowhorn Creek oil unit. Moreover, because Carter sandstone was deposited on a muddy strandplain, porosity and permeability are lower than that in beach-barrier sequences that have been used as models for reservoir heterogeneity. Capillary pressure data indicate that pore-throat size distributions typically are polymodal, reflecting the mixture of macropores and micropores in Carter sandstone. Pore-throat size distributions determined by empirical methods that utilize commercial core analysis data are similar to distributions determined by high-pressure mercury porosimetery, suggesting that capillary-pressure data can be derived from routine core analyses of Carter and other Black Warrior basin reservoirs. Local, order-of-magnitude variation in permeability occurs in some wells in upper shoreface and foreshore sandstone due to grain size differences. These grain size variations affect sweep efficiency during waterflood because fluids are channeled through the high-permeability zones.

Because of the scarcity of cores in the Black Warrior basin, porosity and other petrophysical parameters must be determined by well-log analysis. The distribution well-log derived parameters, including mean effective porosity, porosity-feet, total and effective water saturation, and the product, effective porosity times net pay thickness times effective water saturation, demonstrates that the Carter sandstone reservoir in North Blowhorn Creek oil unit is heterogeneous. However, prediction of the distribution of these reservoir properties in interwell regions by routine geostatistical methods is difficult because of the relatively unpredictable distribution of both detrital and authigenic clay.

Based on evaluation of petrophysical parameters, North Blowhorn Creek oil unit can be divided areally into four zones with different reservoir characteristics. The spatial distribution of these zones closely corresponds to the depositional architecture of the reservoir. The highest quality reservoir occurs in the northern part of the unit, where clinoformal sandstone lenses are amalgamated. Fluid flow in this northern zone is favored along the reservoir axis. The southern part

of the unit also contains high quality reservoir. Sandstone lenses in this zone, however, are segmented and smaller than those in the northern zone. In addition, the lenses are oriented obliquely to the axis of the sandstone body. Flow patterns are more irregular in this zone than in the northern zone. A transitional zone with lower quality reservoir occurs along the reservoir axis between the northern and southern zones. A fourth zone, with the lowest quality reservoir, occurs in the depositionally updip areas. This zone is dominated by backshore deposits. The probability of uncontacted or unconnected compartments is greatest in this zone.

Although depositional modeling indicates that Carter and *Millerella* sandstone reservoirs in other fields also are beach deposits consisting of similar clinoformal sandstone lenses similar to those in North Blowhorn Creek oil unit, these reservoirs were deposited in smaller, muddier, less well-preserved beach systems and contain more detrital and authigenic clay. These differences explain why North Blowhorn Creek oil unit is the most productive field in the basin. These same factors also suggest that, despite similarities in depositional setting, caution should be used in application of the North Blowhorn Creek reservoir as a direct analog for modeling fluid flow and heterogeneity in other reservoirs of the basin.

Oil production in the Black Warrior basin of Alabama declined after reaching a peak in 1985. As of July 1992, the basin produced 9.2 million barrels of oil; 7.5 million barrels of this oil have been extracted from the 26 designated oil fields and units. Seven Mississippian sandstone units produce oil in Alabama, including Carter, Coats, Chandler, Gilmer, Lewis, *Millerella*, and Sanders sandstones. Of these units, the Carter sandstone has produced more than 90 percent of the oil extracted from designated oil fields and units. Two-thirds of that oil has been extracted from the Carter sandstone reservoir in North Blowhorn Creek oil unit. South Brush Creek oil unit is the only other Carter field that has produced more than one million barrels of oil. The second and third most productive reservoir units in the Alabama part of the Black Warrior basin are the *Millerella* and Lewis sandstones.

In order to sustain or increase oil production in the Alabama part of the Black Warrior basin, five Carter and two *Millerella* sandstone oil fields have been unitized for waterflood, gas injection, or a combination of the two processes. No tertiary or enhanced recovery operations currently are active in the basin. Unitized fields, as of July 1992, include Blowhorn Creek *Millerella*, Central Fairview Carter, North Blowhorn Creek, Mud Creek *Millerella*, South Brush Creek, South Fairview Carter, and Wayside oil units. The success of these projects has been variable.

Oil and water production patterns in North Blowhorn Creek oil unit correlate well with the zones determined by depositional modeling and evaluation of petrophysical parameters. Most oil has been extracted along the axis of the reservoir in the northern zone. Patterns of oil production in the southern zone are more variable reflecting both segmentation of sandstone lenses and changes in orientation of the lenses. Although water injection began at approximately the same time throughout the unit, breakthrough is more widespread in the southern zone. Channeling of fluids through high-permeability thief zones or through fractures is likely to have resulted in bypassing of some producible oil in North Blowhorn Creek oil unit, particularly in the southern zone. Similar factors affect the efficiency of improved-recovery projects in other unitized fields. In addition, erosional truncation of part of the upper Carter sandstone in South Brush Creek oil unit resulted in segmentation of the reservoir.

Because the geological processes that form a sandstone reservoir operate at a variety of scales, heterogeneity in petrophysical and other engineering properties in the reservoir also is scale-dependent. Knowledge of controls on reservoir heterogeneity at smaller scales becomes increasingly important as field development progresses. Heterogeneity in the Black Warrior basin is discussed in terms of a scale-dependent classification that acknowledges gigascopic, megascopic, macroscopic, mesoscopic, and microscopic features of reservoirs. Carter and *Millerella* reservoirs do not fit well into existing heterogeneity classifications, such as that used in the TORIS database, or into commonly used reservoir models for beach-barrier systems. Moreover, Carter reservoirs represent diverse beach systems in a small area, so each field needs to be characterized individually. For these reasons, investigators of reservoir heterogeneity need to evaluate carefully the sedimentologic, structural, and diagenetic characteristics of individual sandstone bodies to gain the fullest understanding of controls on oil production and the methods that can best be applied to improve recovery.

ACKNOWLEDGMENTS

Dudley Rice and Jerry Clayton (U.S. Geological Survey) provided geochemical analyses of source rocks and oils.

REFERENCES CITED

Aigner, Thomas, and Reineck, H.-E., 1982, Proximality trends in modern storm sands from the Helgoland Bight (North Sea) and their implications for basin analysis: Senckenbergiana Maritima, v. 14, p. 183-215.

Ambrose, W.A., Tyler, Noel, and Parsley, M.J., 1991, Facies heterogeneity, pay continuity, and infill potential in barrier-island, fluvial, and submarine-fan reservoirs: examples from the Texas Gulf Coast and Midland basin, *in* Miall, A.D. and Tyler, Noel, eds., The three-dimensional facies architecture of terrigenous clastic sediments and its implications for hydrocarbon discovery and recovery: SEPM (Society for Sedimentary Geology), concepts in Sedimentology and Paleontology, v. 3, p. 13-21.

Andronaco, Peter, 1986, Lithofacies, depositional environments, and cyclicity of the Bangor Limestone in Blount County, north-central Alabama: Tuscaloosa, Alabama, University of Alabama, unpublished Master's thesis, 250 p.

Asquith, G.B., 1989, Log evaluation of shaley sandstone: a practical guide: Tulsa, Oklahoma, American Association of Petroleum Geologists Continuing Education Series #31, 59 p.

Barnett, R.L., Moore, H.E., Jr., Kugler, R.L., Hall, D.R., and Pashin, J.C., 1991, Characterization of oil pools in Carboniferous reservoirs, Black Warrior basin, Alabama: Alabama Geological Survey, U.S. Department of Energy contract no. DE-FG22-90BC14448, Draft topical report, 263 p.

Bat, D.T., 1987, A subsurface facies analysis of distribution, depositional environments, and diagenetic overprint of the Evans and Lewis sandstone units in north Mississippi and northwestern Alabama: Stillwater, Oklahoma State University, unpublished Master's thesis, 225 p.

Bearden, B.L., 1984, Hydrocarbon trapping mechanisms in the Carter sandstone (Upper Mississippian) in the Black Warrior basin, Fayette and Lamar Counties, Alabama: Tuscaloosa, University of Alabama, unpublished Master's thesis, 195 p.

___1985, Hydrocarbon trapping mechanisms in the Carter sandstone (Upper Mississippian) in the Black Warrior basin of Alabama: State Oil and Gas Board of Alabama Oil and Gas Report 9, 50 p.

Bearden, B.L., and Mancini, E.A., 1985, Petroleum geology of the Carter sandstone (Upper Mississippian) in the Black Warrior basin of Alabama: American Association of Petroleum Geologists Bulletin, v. 69, p. 361-377.

Berner, R.A., 1981, A new geochemical classification of sedimentary environments: Journal of Sedimentary Petrology, v. 51, p. 359-365.

Beaumont, Christopher, Quinlan, G.M., and Hamilton, Juliet, 1987, The Alleghanian orogeny and its relationship to the evolution of the eastern interior, North America: Canadian Society of Petroleum Geologists Memoir 12, p. 425-445.

___1988, Orogeny and stratigraphy: numerical models of the Paleozoic in the eastern interior of North America: Tectonics, v. 7, p. 389-416.

Boothroyd, J.C., 1985, Tidal inlets and tidal deltas, *in* Davis, R.A., Jr., ed., Coastal sedimentary environments (2nd ed.): New York, Springer-Verlag, p. 445-532.

Bradley, D.C., 1991, Flexural extension of the upper continental crust in collisional foredeeps: Geological Society of America Bulletin, v. 103, p. 1416-1438.

Burdick, D.W., and Strimple, H.L., 1982, Genevievian and Chesterian crinoids of Alabama: Alabama Geological Survey Bulletin 121, 277 p.

Butts, Charles, 1926, The Paleozoic rocks, *in* Adams, G.I., Butts, C., Stephenson, L.W., and Cooke, C.W., Geology of Alabama: Alabama Geological Survey Special Report 14, p. 41-230.

Byers, C.W., 1977, Biofacies patterns in euxinic basins: a general model: Society of Economic Paleontologists and Mineralogists Special Publication 25, p. 5-17.

Cecil, C.B., 1990, Paleoclimate controls on stratigraphic repetition of chemical and siliciclastic rocks: Geology, v. 18, p. 533-536.

Chesnut, D.R., 1988, Stratigraphic analysis of the Carboniferous rocks of the central Appalachian basin: Lexington, Kentucky, University of Kentucky, unpublished Doctoral dissertation, 297 p.

Clavier, C., Coates, G., and Bumanoir, J., 1984, Theoretical and experimental bases for the dual-water model for interpretation of shaley sands: The Society of Petroleum Engineers Journal, v. 24, no. 2, p. 153-168.

Cleaves, A.W., 1981, Resource evaluation of Lower Pennsylvanian (Pottsville) depositional systems of the western Warrior coal field, Alabama and Mississippi: Jackson, Mississippi Mineral Re-

sources Institute Final Technical Report no. 81-1, 125 p.

___1983, Carboniferous terrigenous clastic facies, hydrocarbon producing zones, and sandstone provenance, northern shelf of Black Warrior basin: Gulf Coast Association of Geological Societies Transactions, v. 33, p. 41-53.

Cleaves, A.W., and Bat, D.T., 1988, Terrigenous clastic facies distribution and sandstone diagenesis, subsurface Lewis and Evans format units (Chester Series), on the northern shelf of the Black Warrior basin: Gulf Coast Association of Geological Societies Transactions, v. 38, p. 177-186.

Cleaves, A.W., and Broussard, M.C., 1980, Chester and Pottsville depositional systems, outcrop and subsurface, in the Black Warrior basin of Mississippi and Alabama: Gulf Coast Association of Geological Societies Transactions, v. 30, p. 49-60.

Clifton, H.E., 1976, Wave-formed sedimentary structures - a conceptual model: SEPM Special Publication 24, p. 126-148.

Conant, L.C., and Swanson, V.E., 1961, Chattanooga Shale and related rocks of central Tennessee and nearby areas: U.S. Geological Survey Professional Paper 357, 91 p.

Davidson-Arnott, R.G.D., and Greenwood, B., 1976, Facies relationships on a barred coast, Kouchibougac Bay, New Brunswick, Canada: SEPM Special Publication 24, p. 149-168.

Davis, R.A., Fox, W.T., Hayes, M.O., and Boothroyd, J.C., 1972, Comparison of ridge and runnel systems in tidal and non-tidal environments: Journal of Sedimentary Petrology, v. 42, p. 413-421.

Davis, R.A., Jr., Andronaco, Margaret, and Gibeaut, J.C., 1989; Formation and development of a tidal inlet from a washover fan, west-central Florida coast, U.S.A: Sedimentary Geology, v. 65, p. 87-94.

Dickinson, W.R., 1977, Paleozoic plate tectonics and the evolution of the Cordilleran continental margin, *in*, Stewart, J.H., Stephens, C.H., and Fritsche, A, E., eds., Paleozoic Paleogeography of the Western United States: Los Angeles, Society of Economic Paleontologists and Mineralogists Pacific Section, p. 137-155.

DiGiovanni, Marcel, Jr., 1984, Stratigraphy and depositional environments of the lower Pride Mountain Formation (Upper Mississippian) in the Colbert County area, northwest Alabama: Tuscaloosa, University of Alabama, unpublished Master's thesis, 144 p.

Dominguez, J.M.L., and Wanless, H.R., 1991, Facies architecture of a falling sea-level strandplain, Doce River coast, Brazil, *in* Swift, D.J.P., and others, eds., Shelf Sand and Sandstone Bodies: International Association of Sedimentologists Special Publication 14, p. 259-281.

Drahovzal, J.A., 1967, The biostratigraphy of Mississippian rocks in the Tennessee valley, *in* Smith, W.E., ed., A field guide to Mississippian sediments in northern Alabama and south-central Tennessee: Alabama Geological Society, 5th Annual Field Trip Guidebook, p. 10-24.

Dullien, F.A.L., and Dhawan, G.K., 1974, Characterization of pore structure by a combination of quantitative photomicrography and mercury porosimetry: Journal of Colloid and Interface Science, v. 47, p. 337-349.

Eble, C.F., and Gillespie, W.H., 1989, Palynology of selected coal beds from the central and southern Appalachian basin: correlation and stratigraphic implications, *in* Characteristics of the mid-Carboniferous boundary and associated coal-bearing rocks in the Appalachian basin: 28th International Geological Congress Guidebook T352, p. 61-66.

Eble, C.F., Gillespie, W.H., and Henry, T.W., 1991, Palynology, paleobotany, and invertebrate paleontology of Pennsylvanian coal beds and associated strata in the Warrior and Cahaba coal fields, *in* Mississippian-Pennsylvanian tectonic history of the Cahaba synclinorium: Alabama Geological Society Guidebook, 28th Annual Field Trip, p. 119-132.

Elliott, T., 1986, Siliciclastic shorelines, *in* Reading, H.G., ed., Sedimentary Environments and Facies (2nd ed.): Oxford, Blackwell Scientific Publications, p. 155-188.

Elphick, R.Y., 1990, A spreadsheet model of finding Rw from the SP: Geobyte, v. 5, p. 39-42.

Engman, M.A., 1985, Depositional systems in the lower part of the Pottsville Formation, Black Warrior basin, Alabama: Tuscaloosa, Alabama, University of Alabama, unpublished Master's thesis, 250 p.

Englund, Evan, 1988, Geo-EAS (Geostatistical Environmental Assessment Software) User's Guide: Las Vegas, Nevada, U.S. Environmental Protection Agency, p. 1-1 - 17.3.

Epsman, M.L., 1987, Subsurface geology of selected oil and gas fields in the Black Warrior basin of Alabama: Alabama Geological Survey Atlas 21, 255 p.

Ettensohn, F.R., 1980, An alternative to the barrier-shoreline model for deposition of Mississippian

and Pennsylvanian rocks in northeastern Kentucky: Geological Society of America Bulletin, v. 91, part 1, p. 130-135, part 2, p. 934-1056.

___1985a, Controls on the development of Catskill Delta complex basin-facies: Geological Society of America Special Paper 201, p. 65-77.

___1985b, Controls on the development of Catskill Delta complex basin-facies: Geological Society of America Special Paper 201, p. 65-77.

___1986, The Mississippian-Pennsylvanian transition along I-64, northeastern Kentucky: Geological Society of America Centennial Field Guide—Southeastern Section, p. 37-41.

___1990, Flexural interpretation of relationships between Ordovician tectonism and stratigraphic sequences, central and southern Appalachians, U.S.A., *in*, Barnes, C.R., and Williams, S.H., eds., Advances in Ordovician Geology: Geological Survey of Canada Paper 90-9, p. 213-224.

Ettensohn, F.R., and Barron, L.S., 1981, Depositional model for the Devonian-Mississippian black shales of North America: a paleogeographic-paleoclimatic approach, *in* Roberts, T.G., ed., Geological Society of America Cincinnati '81 Field Trip Guidebooks, v. II: Economic Geology, Structure, p. 344-357.

Ettensohn, F.R., Fulton, L.P., and Kepferle, R.C., 1979, Use of scintillometer and gamma-ray logs for correlation and stratigraphy in homogeneous black shales: Geological Society of America Bulletin., v. 90, part II, p. 828-849.

Evamy, B.D., 1963, The application of a chemical staining technique to study of dedolomitization: Sedimentology, v. 2, p. 164-170.

Fairbridge, R.W., 1980, The estuary: its definition and geodynamic cycle, *in* Olausson, E., and Cato, I., eds., Chemistry and Biogeochemistry of Estuaries: New York, John Wiley and Son, p. 1-36.

Ferm, J.C., Ehrlich, R., and Neathery, T.L., 1967, A field guide to Carboniferous detrital rocks in northern Alabama: Guidebook, 1967 Coal Division Field Trip, Geological Society of America, 101 p.

Ferm, J.C., and Weisenfluh, G.A., 1989, Evolution of some depositional models in Late Carboniferous rocks of the Appalachian coal fields: International Journal of Coal Geology, v. 12, p. 259-292.

Finley, R.J., Fisher, W.L., Seni, S.J., Ruppel, S.C., White, W.G., Ayers, W.B., Jr., Dutton, S.P., Jackson, M.L.W., Banta, Nancy, Kuuskraa, V.A., McFall, K.S., Godec, M., and Jennings, T.V., 1988, An assessment of the natural gas resource base of the United States: The University of Texas at Austin, Bureau of Economic Geology, Report of Investigations No. 179, 69 p.

Fisher, D.R., 1987, Regional diagenesis of the Tuscumbia Limestone (Meramecian, Mississippian) in northern Alabama and northeastern Mississippi: Tuscaloosa, Alabama, University of Alabama, unpublished Master's thesis, 248 p.

Folk, R.L., 1980, Petrology of Sedimentary Rocks: Austin, Texas, Hemphill Publishing Company, 182 p.

Frost, E., and Fertl, W.H., 1981, Integrated core and log analysis concepts in shaley clastic reservoirs: The Log Analysts, v. 32, no. 2, p. 3-16.

Gastaldo, R.A., Demko, T.M., and Liu, Y., eds., 1991, Carboniferous coastal environments and paleocommunities of the Mary Lee coal zone, Marion and Walker Counties, Alabama: Geological Society of America Southeastern Section Guidebook, Field Trip 6, Alabama Geological Survey Guidebook Series 3-6, 139 p.

Goggin, D.J., 1988, Geologically sensible modeling of permeability patterns in an eolian sandstone sequence: Page Sandstone, northern Arizona: University of Texas at Austin, upublished Ph.D. dissertation, 417 p.

Gould, H.R., and McFarlan, E., 1959, Geological history of the chenier plain, southwestern Louisiana: Gulf Coast Association of Geological Societies Transactions, v. 9, p. 261-270.

Gould, G.E., Green, D.W., Willhite, G.P, Phares, R.A., and Walton, A.W., 1993, Reservoir description and modeling of the Pen field, Graham County, Kansas, *in* Linville, Bill, Burchfield, T.E., and Wesson, T.C., eds., Reservoir characterization III: Tulsa, Oklahoma, Pennwell Publishing Company, p. 715-744.

Gulf Coast Oil World, 1992, DOE picks six Gulf Coast fields for EOR sampling: Gulf Coast Oil World, June, 1992, p. 17-18.

Gutschick, R.C., and Sandberg, C.A., 1983, Mississippian continental margins of the conterminous United States: Society of Economic Paleontologists and Mineralogists Special Publication 33, p. 79-96.

Haldorsen, H.H., and Damsleth, E., 1993, Challenges in reservoir characterization: American Association of Petroleum Geologists Bulletin, v. 77, p. 541-551.

Hale-Ehrlich, W.S., and Coleman, J.L., Jr., 1993, Ouachita-Appalachian juncture: a Paleozoic transpressional zone in the Southeastern U.S.A.: American Association of Petroleum Geologists Bulletin, v. 77, p. 552-568.

Ham, W.E., and Wilson, J.L., 1967, Paleozoic epeirogeny and orogeny in the central United States: American Journal of Science, v. 265, p. 332-407.

Harland, W.B., Cox, A.V., Llewellyn, P.G., Pickton, C.A.G., Smith, A.G., and Walters, R., 1982, A geologic time scale: Cambridge, Cambridge University Press, 131 p.

Hayes, M.O., 1967, Hurricanes as geological agents: case studies of Hurricane Carla, 1961, and Cindy, 1963: Texas Bureau of Economic Geology Report of Investigations 61, 54 p.

___1979, Barrier island morphology as a function of wave climate and tidal regime, *in* Leatherman, S.P., ed., Barrier Islands—From the Gulf of St. Lawrence to the Gulf of Mexico: New York, Academic Press, p. 1-27.

Heckel, P.H., and Witzke, B.J., 1979, Devonian world paleogeography determined from distribution of carbonate and related lithic, paleoclimatic indicators: Special Papers in Paleontology 23, p. 99-123.

Higginbotham, D.R., 1986, Regional stratigraphy, environments of deposition, and tectonic framework of Mississippian clastic rocks between the Tuscumbia and Bangor Limestones in the Black Warrior basin of Alabama and Mississippi: Gulf Coast Association of Geological Societies Transactions, v. 36, p. 161-169.

Hine, A.C., Wilber, R.J., and Neumann, A.C., 1981, Carbonate sand-bodies along contrasting shallow-bank margins facing open seaways: American Association of Petroleum Geologists Bulletin, v. 65, p. 261-290.

Hines, R.A., Jr., 1988, Carboniferous evolution of the Black Warrior foreland basin, Alabama and Mississippi: Tuscaloosa, Alabama, University of Alabama, unpublished Doctoral dissertation, 231 p.

Hitchon, B., 1984, Geothermal gradients, hydrodynamics, and hydrocarbon occurrences, Alberta, Canada: American Association of Petroleum Geologists Bulletin, v. 68, p. 713-743.

Hobday, D.K., 1974, Beach and barrier island facies in the Upper Carboniferous of northern Alabama: Geological Society of America Special Paper 148, p. 209-224.

Holmes, J.W., 1981, The depositional environment of the Mississippian Lewis sandstone in the Black Warrior basin of Alabama: Tuscaloosa, University of Alabama, unpublished Master's thesis, 172 p.

Horsey, C.A., 1981, Depositional environments of the Pennsylvanian Pottsville Formation in the Black Warrior basin of Alabama: Journal of Sedimentary Petrology, v. 51, p. 799-806.

Howard, R.O., Jr., 1990, Petrology of hardbottom rocks, Mississippi-Alabama-Florida continental shelf: Tuscaloosa, University of Alabama, unpublished Master's thesis, 172 p.

Hughes, S.B., and Meylan, M.A., 1988, Petrology and hydrocarbon reservoir potential of Mississippian (Chesterian) sandstone, Black Warrior basin, Mississippi: Gulf Coast Association of Geological Societies Transactions, v. 38, p. 167-176.

Hurst, Andrew, 1993, Sedimentary flow units in hydrocarbon reservoirs: Some shortcomings and a case for high-resolution permeability data, *in* Flint, S.S. and Bryant, I.D., eds., The geological modelling of hydrocarbon reservoirs and outcrop analogues: International Association of Sedimentologists, Special Publication No. 15, p. 191-204.

Hurst, Andrew, and Archer, J.S., 1986, Sandstone reservoir description: An overview of the role of geology and mineralogy: Clay Minerals, v. 21, p. 769-780.

Isaaks, E.H., and Srivastava, R.M., 1989, Applied geostatistics: Oxford, Oxford University Press, 561 p.

Jackson, Susan, Chang, M.M., and Tham, Min, 1993, Data requirements and acquisition for reservoir characterization: Bartlesville, Oklahoma, U.S. Department of Energy, Fossil Energy Report NIPER-615, 26 p.

Jennings, J.B., 1987, Capillary pressure techniques: application to exploration and development geology: American Association of Petroleum Geologists Bulletin, v. 71, p. 1196-1209.

Jennings, J.R., and Thomas, W.A., 1987, Fossil plants from Mississippian-Pennsylvanian transition strata in the southern Appalachians: Southeastern Geology, v. 27, p. 207-217.

Johnson, J.G., 1971, Timing and coordination of orogenic, epeirogenic, and eustatic events: Geological Society of America Bulletin, v. 82, p. 3263-3298.

Journel, A.G., and Hijbregts, C.J., 1978, Mining geostatistics: London, Academic Press, 600 p.

Kopaska-Merkel, D.C., 1991, Analytical procedure and experimental design for geological analysis of reservoir heterogeneity using mercury porosimetry: Alabama Geological Survey Circular 153, 29 p.

Kopaska-Merkel, D.C., and Friedman, G.M., 1989, Petrofacies analysis of carbonate rocks: example from Lower Paleozoic Hunton Group of Okla-

homa and Texas: American Association of Petroleum Geologists Bulletin, v. 73, p. 1289-1306.

Kopaska-Merkel, D.C., Hall, D.R., Mann, S.D., and Tew, B.H., 1993, Reservoir characterization of the Smackover Formation in southwest Alabama: Bartlesville, Oklahoma, U.S. Department of Energy, Fossil Energy Report DOE/BC/14425-7, 124 p.

Kugler, R.L., and Pashin, J.C., 1992, Reservoir heterogeneity in Carter sandstone, North Blowhorn Creek oil unit and vicinity, Black Warrior basin, Alabama: Bartlesville, Oklahoma, U.S. Department of Energy, Fossil Energy Report DOE/BC/14448-9, 92 p.

Lake, L.W., Carroll, H.B., Jr., and Wesson, T.C., eds., 1991, Reservoir characterization II: Orlando, Florida, Academic Press, Inc., 726 p.

Levine, J.R., and Telle, W.R., 1991, Coal rank in the Cahaba coal field and surrounding areas, and their significance, *in* Mississippian-Pennsylvanian tectonic history of the Cahaba Synclinorium, Thomas, W.A., and Osborne, W.E., eds.: Guidebook for the 28th Annual Field Trip of the Alabama Geological Society, p. 99-117.

Lopatin, N.V., 1971, Temperature and time as geologic factors in coalification (in Russian): Izv. Akad. Nauk SSSR, Seriya geolgicheskaya, no. 3, p. 95-106.

Mack, G.H., James, W.C., and Thomas, W.A., 1981, Composition of Carboniferous sandstones associated with southern Appalachian-Ouachita orogen: American Association of Petroleum Geologists Bulletin, v. 65, p. 1444-1456.

Mack, G.H., Thomas, W.A., and Horsey, C.A., 1983, Composition of Carboniferous sandstones and tectonic framework of southern Appalachian-Ouachita orogen: Journal of Sedimentary Petrology, v. 54, p. 1444-1456.

Majorowicz, J.A., and Jessop, A.M., 1981, Regional heat flow patterns in the western Canadian sedimentary basin: Tectonophysics, v. 74, p. 209-238.

Maples, C.G., and Waters, J.A., 1987, Redefinition of the Meramecian/Chesterian boundary (Mississippian): Geology, v. 15, p. 647-651.

Masingill, J.H., 1989, The petroleum industry in Alabama, 1988: State Oil and Gas Board of Alabama , Oil and Gas Report 3-L, 100 p.

___1991, The petroleum industry in Alabama, 1990: State Oil and Gas Board of Alabama, Oil and Gas Report 3-N, 117 p.

McBride, E.F., 1984, Rules of sandstone diagenesis related to reservoir quality: Gulf Coast Association of Geological Societies Transactions, v. 34, p. 137-139.

McCalley, Henry, 1896, Report on the valley regions of Alabama, Part I. On the Tennessee Valley region: Alabama Geological Survey Special Report 8, 436 p.

___1900, Report on the Warrior coal basin: Alabama Geological Survey Special Report 10, 327 p.

McCubbin, D.G., 1982, Barrier-island and strandplain facies: American Association of Petroleum Geologists Memoir 31, p. 137-139.

Mellen, F.F., 1947, Black Warrior basin, Alabama and Mississippi: American Association of Petroleum Geologists Bulletin, v. 31, p. 1801-1816.

Miesfeldt, M.A., 1985, Facies relationships between the Parkwood and Bangor formations in the Black Warrior basin: Tuscaloosa, Alabama, University of Alabama, unpublished Master's thesis, 149 p.

Miller, J.A., 1975, Facies characteristics of Laguna Madre wind-tidal flats, *in* Ginsburg, R.N., ed., Tidal deposits: a casebook of recent examples and fossil counterparts: New York, Springer-Verlag, p. 67-73.

Moore, H.E., and Kugler, R.L., 1990, Determination of reservoir heterogeneity in the Mississippian Carter sandstone to improve hydrocarbon recovery in oil fields in the Black Warrior basin: Alabama Department of Economic and Community Affairs, Contract 1STE89 06, 291 p.

Moore, R.C., 1944, Correlation of Pennsylvanian formations of North America: Geological Society of America Bulletin, v. 55, p. 657-706.

Morton, R.A., and Donaldson, A.C., 1973, Sediment distribution and evolution of tidal deltas along a tide-dominated shoreline, Washapreague, Virginia: Sedimentary Geology, v. 10, p. 285-299.

Mozley, P.S., 1989, Relation between depositional environment and the elemental composition of early diagenetic siderite: Geology, v. 17, p. 704-706.

Mozley, P.S., and Wersin, Paul, 1992, Isotopic composition of siderite as an indicator of depositional environment: Geology, v. 20, p. 817-820.

Mozley, P.S., and Carothers, W.W., 1992, Elemental and isotopic composition of siderite in the Kuparuk Formation, Alaska: effect of microbial activity and water/sediment interaction on early pore-water chemistry: Journal of Sedimentary Petrology, v. 62, p. 681-692.

Nix, M.A., 1986, Facies within the lower part of the Parkwood Formation in the Black Warrior basin

of Mississippi and Alabama: Appalachian Basin Industrial Associates Fall Program, v. 11, p. 93-107.

___1991, Facies and facies relationships of the lower part of the Parkwood Formation in the Black Warrior basin of Mississippi and Alabama: Tuscaloosa, University of Alabama, unpublished Master's thesis, 362 p.

Oliver, J.M., 1988, Structural geology of part of the Black Warrior basin in Alabama and Mississippi: Tuscaloosa, Alabama, University of Alabama, unpublished Master's thesis, 174 p.

Pashin, J.C., 1991, Regional analysis of the Black Creek-Cobb coalbed-methane target interval, Black Warrior basin, Alabama: Alabama Geological Survey Bulletin 145, 127 p.

Pashin, J.C., and Ettensohn, F.R., 1987, An epeiric shelf-to-basin transition: Bedford-Berea sequence, northeastern Kentucky and south-central Ohio: American Journal of Science, v. 287, p. 893-926.

Pashin, J.C., Osborne, W.E., and Rindsberg, A.K., 1991, Outcrop characterization of sandstone heterogeneity in Carboniferous reservoirs, Black Warrior basin, Alabama: Bartlesville, Oklahoma, U.S. Department of Energy Fossil Energy Report DOE/BC/14448-6, 126 p.

Pashin, J.C., and Kugler, R.L., 1992, Delta-destructive spit complex in Black Warrior basin: facies heterogeneity in Carter sandstone (Chesterian), North Blowhorn Creek oil unit, Lamar County, Alabama: Gulf Coast Association of Geological Societies Transactions, v. 42, p. 305-325.

Pashin, J.C., and Carroll, R.E., 1993, Origin of the Pottsville Formation (Lower Pennsylvanian) in the Cahaba synclinorium of Alabama: genesis of coalbed reservoirs in a synsedimentary foreland thrust system: Tuscaloosa, Alabama, The University of Alabama, 1993 International Coalbed Methane Symposium Proceedings, p. 623-637.

Penland, Shea, and Boyd, R., 1985, Barrier island arcs along abandoned Mississippi River deltas: Marine Geology, v. 63, p. 197-233.

Pittman, E.D., 1992, Relationship of porosity and permeability to various parameters derived from mercury injection-capillary pressure curves for sandstone: American Association of Petroleum Geologists Bulletin, v. 76, p. 191-198.

Purcell, W.R., 1949, Capillary-pressures -- their measurement using mercury and the calculation of permeability therefrom: Petroleum Transactions, American Institute of Mining, Metallurgical, and Petroleum Engineers, v. 186, p. 39-48.

Reineck, H-E., and Singh, I.B., 1980, Depositional sedimentary environments, with reference to terrigenous clastics (2nd ed.): New York, Springer-Verlag, 549 p.

Rheams, K.F., and Neathery, T.L., 1988, Characterization and geochemistry of Devonian oil shale, north Alabama, northwest Georgia, and south-central Tennessee (a resource evaluation): Alabama Geological Survey Bulletin 128, 214 p.

Rice, C.L., 1984, Sandstone units of the Lee Formation and related strata in eastern Kentucky: U.S. Geological Survey Professional Paper 1151-G, 53 p.

Rich, J.L., 1951a, Three critical environments of deposition and criteria for the recognition of rocks deposited in each of them: Geological Society of America Bulletin, v. 62, p. 481-533.

___1951b, Probable fondo origin of Marcellus-Ohio-New Albany-Chattanooga bituminous shales: American Association of Petroleum Geologists Bulletin, v. 35, p. 2017-2040.

Rich, Mark, 1980, Carboniferous calcareous foraminifera from northeastern Alabama, south-central Tennessee, and northwestern Georgia: Cushman Foundation for Foraminiferal Research Special Publication, v. 18, 84 p.

Robertson Research (U.S.), Inc., 1985, Oil generation in the Black Warrior basin, Alabama: a geochemical study: Kingwood, Texas, 328 p.

Rodgers, John, 1950, Mechanics of Appalachian folding as illustrated by the Sequatchie anticline, Tennessee and Alabama: American Association of Petroleum Geologists Bulletin, v. 34, p. 672-681.

Ruppel, S.C., 1979, Conodonts from the Lower Mississippian Fort Payne and Tuscumbia Formations of northern Alabama: Journal of Paleontology, v. 53, p. 55-70.

Sclater, J.G., and Cristie, P.A.F., 1980, Continental stretching: an explanation of the post-mid-Cretaceous subsidence of the central North Sea basin: Journal of Geophysical Research, v. 85, p. 3711-3739.

Schatzinger, R.A., Szpakiewicz, M.J., Jackson, S.R., Chang, M.M., Sharma, Bijon, and Tham, M.K., 1992, Integrated geological-engineering model of Patrick Draw field and examples of similarities and differences among various shoreline barrier systems: Bartlesville, Oklahoma, U.S. Department of Energy, Fossil Energy Report NIPER-575, 146 p.

Schatzinger, R.A., and Sharma, Bijon, 1993, Structural and sedimentological features that control fluid distribution and movement, *in* Jackson, Susan, ed., Integration of the geological/engineering model with production performance for Patrick Draw field, Wyoming: Bartlesville, Oklahoma, U.S. Department of Energy, Fossil Energy Report NIPER-634, p. 53-84.

Schmoker, J.W., and Halley, R.B., 1982, Carbonate porosity versus depth: a predictable relation for south Florida: American Association of Petroleum Geologists Bulletin, v. 66, p. 2561-2570.

Scotese, C.R., 1990, Atlas of Phanerozoic plate tectonic reconstructions: International Lithosphere Program (IUGG-IUGS), Paleomap Project Technical Report 10-90-1, 54 p.

Scott, G.L., 1978, Deposition, facies patterns, and hydrocarbon potential of Bangor Limestone (Mississippian), northern Black Warrior basin, Alabama and Mississippi: Mississippi Geological Society Guidebook, 17th Annual Field Trip, p. 34-54.

Sharma, Bijon, Honarpour, M.M., Szpakiewicz, M.J., and Schatzinger, R.A., 1990a, Critical heterogeneities in a barrier island deposit and their influence on various recovery processes: SPE Formation Evaluation, v. 5, p. 103-112.

Sharma, Bijon, Honarpour, M.M., Jackson, S.R., Schatzinger, R.A., and Tomutsa, L., 1990b, Determining the productivity of a barrier island sandstone deposit from integrated facies analysis: SPE Formation Evaluation, v. 5, p. 413-420.

Sharma, Bijon, Chang, M.M., and Szpakiewicz, M.J., 1993, The effect of salinity variations on oil saturation calculations from wireline logs at Patrick Draw field, *in* Jackson, Susan, ed., Integration of the geological/engineering model with production performance for Patrick Draw field, Wyoming: Bartlesville, Oklahoma, U.S. Department of Energy, Fossil Energy Report NIPER-634, p. 41-52.

Shepard, B.K., 1979, Petrography and environment of deposition of the Carter sandstone (Mississippian) in the Black Warrior basin of Alabama and Mississippi: Tuscaloosa, University of Alabama, unpublished Master's thesis, 196 p.

Shepard, N.K., 1985, Geothermal history of the plateau province of northern Alabama: New Orleans, Louisiana, Tulane University, unpublished Master's thesis, 79 p.

Size, W.B., 1987, Use of representative samples and sampling plans in describing geologic variability and trends, *in* Size, W. B., ed., Use and abuse of statistical methods in the earth sciences: New York, Oxford University Press, International Association of Mathematical Geology Studies in Mathematical Geology no. 1, p. 3-20.

Sloss, L.L., 1963, Sequences in the cratonic interior of North America: Geological Society of America Bulletin, v. 74, p. 93-114.

___1988, Tectonic evolution of the craton in Phanerozoic time, *in* Sloss, L.L., ed., Sedimentary cover -- North American craton: Geological Society of America, The Geology of North America, v. D-2, p. 25-51.

Stapor, F.W., and Cleaves, A.W., 1992, Mississippian (Chesterian) sequence stratigraphy in the Black Warrior basin: Pride Mountain Formation (lowstand wedge) and Hartselle Sandstone (transgressive systems tract): Gulf Coast Association of Geological Societies Transactions, v. 42, p. 683-696.

Stapor, F.W., Mathews, T.D., and Lindfors-Kearns, F.E., 1991, Barrier-island progradation and Holocene sea-level history in southwest Florida: Journal of Coastal Research, v. 7, p. 815-838.

Szabo, M.W., Osborne, W.E., and Copeland, C.W., 1988, Geologic map of Alabama: Alabama Geological Survey Special Map 220.

Szpakiewicz, M.J., 1993, The importance and application of hydrogeochemical techniques to reservoir characterization, *in* Jackson, Susan, ed., Integration of the geological/engineering model with production performance for Patrick Draw field, Wyoming: Bartlesville, Oklahoma, U.S. Department of Energy, Fossil Energy Report NIPER-634, p. 13-40.

Szpakiewicz, M.J., Schatzinger, R.A, Jackson, Susan, Sharma, Bijon, Cheng, A, and Honarpour, M., 1991, Selection and initial characterization of a second barrier island reservoir system and refining of methodology for characterization of shoreline barrier reservoirs -- Topical report: Bartlesville, Oklahoma, U.S. Department of Energy, Fossil Energy Report NIPER-484, p. 170.

Telle, W.R., Thompson, D.A., Lottman, L.K., and Malone, P.G., 1987, Preliminary burial - thermal history investigations of the Black Warrior basin: Implications for coalbed methane and conventional hydrocarbon development: Proceedings, Coalbed Methane Symposium, p. 37-49.

Thomas, W.A., 1968, Contemporaneous normal faults on flanks of Birmingham anticlinorium, central Alabama: American Association of Petroleum Geologists Bulletin, v. 52, p. 2123-2136.

___1972a, Mississippian stratigraphy of Alabama: Alabama Geological Survey Monograph 12, 121 p.

___1972b, Regional Paleozoic stratigraphy in Mississippi between Appalachian and Ouachita Mountains: American Association of Petroleum Geologists Bulletin, v. 56, p. 81-106.

___1973, Southwestern Appalachian structural system beneath the Gulf Coastal Plain: American Journal of Science, v. 273-A, p. 372-390.

___1974, Converging clastic wedges in the Mississippian of Alabama: Geological Society of America Special Paper 148, p. 187-207.

___1976, Evolution of the Appalachian-Ouachita continental margin: Journal of Geology, v. 84, p. 323-342.

___1977, Evolution of Appalachian-Ouachita salients and recesses from reentrants and promontories in the continental margin: American Journal of Science, v. 277, p. 1233-1278.

___1985a, The Appalachian-Ouachita connection: Paleozoic orogenic belt at the southern margin of North America: Annual Review of Earth and Planetary Sciences, v. 13, p. 175-199.

___1985b, Northern Alabama sections, *in* Woodward, N.B., ed., Valley and Ridge thrust belt: balanced structural sections, Pennsylvania to Alabama: University of Tennessee Department of Geological Sciences, Studies in Geology 12, p. 54-60.

___1988, The Black Warrior basin, *in* Sloss, L.L., ed., Sedimentary cover - North American craton: Geological Society of America, The Geology of North America, v. D-2, p. 471-476.

___1991, The Appalachian-Ouachita rifted margin of southeastern North America: Geological Society of America Bulletin, v. 103, p. 415-431.

Thomas, W.A., Ferrill, B.A., Allen, J.L., Osborne, W.E., and Leverett, D.E., 1991, Synorogenic clastic-wedge stratigraphy and subsidence history of the Cahaba synclinorium and the Black Warrior foreland basin, *in* Thomas, W.A., and Osborne, W.E., eds., Mississippian-Pennsylvanian tectonic history of the Cahaba synclinorium: Alabama Geological Society Guidebook, 28th Annual Field Trip, p. 37-39.

Thomas, W.A., and Mack, G.H., 1982, Paleogeographic relationship of a Mississippian barrier-island and shelf-bar system (Hartselle Sandstone) in Alabama to the Appalachian-Ouachita orogenic belt: Geological Society of America Bulletin, v. 93, p. 6-19.

Thomas, W.A., and Neathery, T.L., eds., 1982, Appalachian thrust belt in Alabama: tectonics and sedimentation: Tuscaloosa, Alabama, Geological Society of America Guidebook, Geological Society of America Annual Meeting, New Orleans, Louisiana, 78 p.

Thomas, W.A., Smith, W.E., and Bicker, A.R., 1979, The Mississippian and Pennsylvanian (Carboniferous) Systems in the United States—Alabama and Mississippi: U.S. Geological Survey Professional Paper 1110-I, 45 p.

Thompson, W.O., 1937, Original structures of beaches, bars, and dunes: Geological Society of America Bulletin, v. 48, p. 723-752.

Tyler, Noel, and Finley, R.J., 1991, Architectural controls on the recovery of hydrocarbons from sandstone reservoirs, *in* Miall, A.D. and Tyler, Noel, eds., The three-dimensional facies architecture of terrigenous clastic sediments and its implications for hydrocarbon discovery and recovery: SEPM (Society for Sedimentary Geology), Concepts in Sedimentology and Paleontology, v. 3, p. 1-5.

United States Geological Survey (USGS) and American Association of Petroleum Geologists (AAPG), 1976, Geothermal gradient map of North America: U.S. Geological Survey, Scale 1:500,000, 2 sheets.

van Andel, Tj.,H., and Curray, J.R., 1960, Regional aspects of modern sedimentation in northern Gulf of Mexico and similar basins and paleogeographic significance, *in* Shepard, F.P., Phleger, F.B., and van Andel, Tj., H., eds., Recent Sediments, Northwest Gulf of Mexico: Tulsa, Oklahoma, American Association of Petroleum Geologists, p. 345-364.

van Beek, J.L., and Koster, E.A., 1972, Fluvial and estuarine sediments exposed along the Oude Mass (The Netherlands): Sedimentology, v. 19, p. 237-256.

Vavra, C.L., Kaldi, J.G., and Sneider, R.M., 1992, Geological applications of capillary pressure: a review: American Association of Petroleum Geologists Bulletin, v. 76, p. 840-850.

Viele, G.W., and Thomas, W.A., 1989, Tectonic synthesis of the Ouachita orogenic belt, *in* Hatcher, R.D., Thomas, W.A., and Viele, G.W, eds., The Appalachian-Ouachita Orogen in the United States: Geological Society of America, The Geology of North America, v. F-2, p. 695-728.

Wanless, H.R., 1975, Appalachian region, *in* McKee, E.D., and Crosby, E.J., coordinators, Paleotectonic investigations of the Pennsylvanian System in the United States: U.S. Geological Survey Professional Paper 853, part 1, p. 17-62.

END DATE

7-1-94